

February 2017

## Biogeochemical processing of greenhouse gases (methane and nitrous oxide) in meromictic lakes



**Supervisor:** Alberto V. Borges

Fleur Roland

Dissertation presented for the degree of PhD

# Biogeochemical processing of greenhouse gases (methane and nitrous oxide) in meromictic lakes

Fleur Roland

**Supervisor:** Alberto V. Borges

**Members of the Examination**

**Committee:**

Prof. Jean-Pierre Thomé

Prof. Jean-Pierre Descy

Dr. Frédéric Guérin

Dr. Célia Joaquim-Justo

Dr. François Darchambeau

Dr. Cédric Morana

Dissertation presented for the  
degree of PhD

February 2017

## Acknowledgments

---

A chapter of my life is now closing with the redaction of these acknowledgments. Already four years, full of emotion. If I'm now writing these words, it is thanks to two persons who particularly involved.

First, my promoter Alberto V. Borges, who welcomed me in his lab five years ago, for my master thesis. I have learnt so much from you, I'm still learning, and I will learn a lot more. I sincerely think I could not have had a better supervisor. Your door was always opened, and I'm really grateful for all you have done for me. Ne sachant pas traduire cette expression en anglais, je vais l'écrire en français: j'espère pouvoir un jour t'arriver à la cheville d'un point de vue scientifique.

The second person I want to thank is François Darchambeau, who was the promoter of my master thesis and who supervised the beginning of my thesis. François, I would not be here without you for many reasons. You helped me to write my FRIA project, you taught me the field work, and you were always available for all my (sometimes stupid) questions. You were there for the worst moment of my life, and also for the best one. More than a colleague, you became a friend. François, just thank you.

My field campaigns would not have been feasible without the support of the Eagles project. Many thanks to Jean-Pierre Descy, who welcomed me on the project. I think I will always remember our first meet, on Lake Kivu, in 2012. I would have passed hours and hours to listen your stories. Also, many thanks to the Kivu team of February 2012 for all the nice moments. Special thanks to Cédric Morana, for your availability and your motivation, and to Marc Llorós, who is always ready to help. Also, I thank Wim Thiery for the data of precipitations reported in Figure 24.

Many thanks to Bruno Leporcq, Marc-Vincent Commarieu and Sandro Petrovic for their help in the samplings. Marc and Sandro, I am sure you will always remember your frozen fingers and your muscles sore by the effort. Marc, I also thank you for all the hours passed for the manufacturing of our homemade sampler for Kabuno Bay. Also, field campaigns on Lake Kivu would not have been possible without the support of the local team. I thank Boniface Kaningini, Pascal Isumbisho, Georges Alunga, Fabrice Muvundja, Silas, Djoba and Pascal Masilya (Institut Pédagogique de Bukavu) for the logistic support, and providing the meteorological data. Many thanks to the team of the Observatoire Volcanologique de Goma (OVG) for their involvement in sampling. I also thank the Rwanda Energy Company for the access to their platform in Gisenyi. Also, I would like to thank all the persons involved

in the laboratory work: Bo Thamdrup and his team (in particular Laura Bristow, Dina Holmgaard Skov and Heidi Grøn Jensen), Steven Bouillon, Jean-Pierre Thomé and Renzo Biondo.

I would also like to thank all the other members of the Chemical Oceanography Unit for their good mood (sometimes) and their passion for life (always). Bruno, Willy, Marie, Gaëlle, Fanny, Gersande and Thibault, thank you for all the good moments shared. I particularly thank Thibault Lambert for the elaboration of the Figure 16.

Many thanks to the team of the "Otaries Club", from Maffle, for the access to the Lake Dendre, for their help in sampling and simply for their kindness. Thanks to the divers of the former stone quarry "La Gombe" in Esneux for testing our experimental material.

This thesis received financial support from the Fonds National de la Recherche Scientifique (FNRS) and the Belgian Science Policy (BELSPO).

Afin qu'ils puissent me lire, j'écris ces derniers remerciements en français. Je tiens à remercier toute ma famille, soutien indéfectible dans tous les moments de doute, qui n'ont pas du tout été nombreux ! Merci à tous pour l'oreille attentive que vous m'avez prêtée. Un merci particulier à Jonathan, maître de la patience, qui a dû supporter non pas une femme enceinte, mais une thésarde en fin de thèse enceinte ! Mon petit Mathéo, peut-être un jour t'intéresseras-tu à la science, et peut-être seras-tu alors intéressé par lire ce livre. J'espère que tu verras entre les lignes à quel point le lac Kivu a été une incroyable expérience pour ta maman, et que cela te donnera l'envie de vivre tes propres aventures. Enfin, je dédie ce travail à mon papa, qui, j'en suis certaine, aurait été très fière de sa petite fille.

## Summary

---

During this study, we focused on the biogeochemical cycles of carbon and nitrogen in two tropical lakes, Lake Kivu and one of its bays, Kabuno Bay, located on the border between the Democratic Republic of the Congo and Rwanda, and a small temperate lake located in a limestone quarry in Belgium (Lake Dendre). Seasonal and inter-annual variations in methane ( $\text{CH}_4$ ) and nitrous oxide ( $\text{N}_2\text{O}$ ) fluxes to the atmosphere in Lake Kivu were calculated based on the concentrations of these two elements measured monthly for almost two consecutive years. These data show that Lake Kivu is a low  $\text{CH}_4$  emitter throughout the year (mean of  $86 \mu\text{mol m}^{-2} \text{d}^{-1}$ ), in proportion to the high levels of  $\text{CH}_4$  present in its deep waters, and alternates between a source and a sink of  $\text{N}_2\text{O}$ . The oxidation of  $\text{CH}_4$  has been proposed to explain these low emissions to the atmosphere. This study concentrated particularly on the detection of the anaerobic oxidation of  $\text{CH}_4$  (AOM) within the water column and on the identification of the potential electron acceptors: nitrate ( $\text{NO}_3^-$ ), nitrite ( $\text{NO}_2^-$ ), sulfate ( $\text{SO}_4^{2-}$ ), iron (Fe) and manganese (Mn). Significant levels of AOM, up to 16 and  $75 \mu\text{mol m}^{-2} \text{d}^{-1}$ , were found in the water column of Lake Kivu and Kabuno Bay, respectively, but the identification of the potential electron acceptors is not so obvious. At Kabuno Bay, which is considered as a ferruginous basin, Fe seems to be the most likely electron acceptor, since  $\text{NO}_3^-$ ,  $\text{NO}_2^-$  and Mn concentrations are very low, and the sulfur cycle seems to be not really developed. Despite the high concentrations of  $\text{SO}_4^{2-}$  measured in oxic waters (up to  $600 \mu\text{mol L}^{-1}$ ), concentrations of sulfide ( $\text{HS}^-$ ) remained very low in anoxic waters ( $<1 \mu\text{mol L}^{-1}$ ), suggesting a poor occurrence of  $\text{SO}_4^{2-}$  reduction. In Lake Kivu, the main electron acceptor is most likely  $\text{SO}_4^{2-}$  in view of the high concentrations recorded (up to  $225 \mu\text{mol L}^{-1}$ ) compared to the concentrations of the other elements ( $\text{NO}_3^-$ :  $<10 \mu\text{mol L}^{-1}$ ,  $\text{NO}_2^-$   $<1.5 \mu\text{mol L}^{-1}$ , Mn and Fe total  $<15 \mu\text{mol L}^{-1}$ ), and high  $\text{HS}^-$  concentrations (up to  $120 \mu\text{mol L}^{-1}$  at 80 m depth) suggesting the occurrence of significant  $\text{SO}_4^{2-}$  reduction. However, some vertical profiles observed in the rainy season, which showed that AOM levels were higher in the  $\text{NO}_3^-$  accumulation zone, suggest that  $\text{NO}_3^-$  could be an electron acceptor for AOM, but at a low extent.  $\text{NO}_3^-$  concentrations were mostly too low to explain the AOM rates observed, and competition with other processes is most likely too high. Indeed, during this study, we also highlighted the occurrence of denitrification, the dissimilatory reduction of  $\text{NO}_3^-$  to ammonium ( $\text{NH}_4^+$ ) (DNRA) and the anaerobic oxidation of  $\text{NH}_4^+$  (Anammox), which compete for substrates. Finally, since Lake Dendre shares some characteristics with Lake Kivu (ie mainly they are both meromictic and have high  $\text{CH}_4$  concentrations in their anoxic waters), we also measured  $\text{CH}_4$  oxidation within the water column and put in evidence AOM rates up to  $14 \mu\text{mol L}^{-1} \text{d}^{-1}$ . Despite these high oxidation rates, Lake Dendre was a large emitter of  $\text{CH}_4$  for the atmosphere.  $\text{SO}_4^{2-}$  was likely the primary electron acceptor, but high concentrations of  $\text{NO}_3^-$  (up to  $80 \mu\text{mol L}^{-1}$ ) suggest that they could

also be used for AOM, since AOM coupled to denitrification is thermodynamically much more favorable than the AOM coupled to the reduction of  $\text{SO}_4^{2-}$ .

## Résumé

---

Durant cette étude, nous nous sommes intéressés aux cycles biogéochimiques du carbone et de l'azote au sein de deux lacs tropicaux, le lac Kivu et l'une de ses baies, la baie de Kabuno, situés à la frontière entre la République Démocratique du Congo et le Rwanda, et un petit lac tempéré localisé dans une ancienne carrière de calcaire en Belgique (le lac de la Dendre). Les variations saisonnières et interannuelles des flux de méthane ( $\text{CH}_4$ ) et de protoxyde d'azote ( $\text{N}_2\text{O}$ ) vers l'atmosphère au niveau du lac Kivu ont été calculées sur base des concentrations en ces deux éléments mesurées mensuellement pendant presque deux années consécutives. Ces données ont montré que le lac Kivu est un faible émetteur de  $\text{CH}_4$  durant toute l'année (moyenne de  $86 \mu\text{mol m}^{-2} \text{j}^{-1}$ ), proportionnellement aux quantités élevées de  $\text{CH}_4$  présentes dans ses eaux profondes, et alterne entre une source et un puits de  $\text{N}_2\text{O}$ . L'oxydation du  $\text{CH}_4$  a été proposée pour expliquer ces faibles émissions vers l'atmosphère. Cette étude s'est particulièrement concentrée sur la mise en évidence de l'oxydation anaérobique du  $\text{CH}_4$  (AOM) au sein de la colonne d'eau, et sur l'identification des accepteurs potentiels d'électrons: nitrate ( $\text{NO}_3^-$ ), nitrite ( $\text{NO}_2^-$ ), sulfate ( $\text{SO}_4^{2-}$ ), fer (Fe) et manganèse (Mn). Des taux significatifs d'AOM, jusque  $16$  et  $75 \mu\text{mol m}^{-2} \text{j}^{-1}$ , ont été mis en évidence dans la colonne d'eau du lac Kivu et de la baie de Kabuno, respectivement, mais l'identification des accepteurs potentiels d'électrons n'est pas si évidente. Au niveau de la baie de Kabuno, qui est considérée comme un bassin ferrugineux, le Fe semble être l'accepteur d'électrons le plus probable, étant donné que les concentrations en  $\text{NO}_3^-$ ,  $\text{NO}_2^-$  et Mn sont très faibles, et que le cycle du soufre ne semble pas très développé. En effet, en dépit des fortes concentrations en  $\text{SO}_4^{2-}$  mesurées dans les eaux oxiques (jusque  $600 \mu\text{mol L}^{-1}$ ), les concentrations en sulfure d'hydrogène ( $\text{HS}^-$ ) sont restées très faibles dans les eaux anoxiques ( $< 1 \mu\text{mol L}^{-1}$ ), suggérant une faible réduction des  $\text{SO}_4^{2-}$ . Au niveau du lac Kivu, le principal accepteur d'électron est très probablement les  $\text{SO}_4^{2-}$  au vu des fortes concentrations enregistrées (jusque  $225 \mu\text{mol L}^{-1}$ ) comparativement aux concentrations des autres éléments ( $\text{NO}_3^-$ :  $< 10 \mu\text{mol L}^{-1}$ ;  $\text{NO}_2^-$   $< 1.5 \mu\text{mol L}^{-1}$ ; Mn et Fe total  $< 15 \mu\text{mol L}^{-1}$ ), et des concentrations en  $\text{HS}^-$  élevées (jusqu'à  $120 \mu\text{mol L}^{-1}$  à 80 m de profondeur), suggérant que la réduction des  $\text{SO}_4^{2-}$  puisse être un processus significatif. Toutefois, certains profils verticaux observés en saison humide, qui montrent que les taux d'AOM étaient plus élevés dans la zone d'accumulation des  $\text{NO}_3^-$ , suggèrent que les  $\text{NO}_3^-$  pourraient servir d'accepteurs d'électrons pour l'AOM, mais à une faible mesure. Les concentrations en  $\text{NO}_3^-$  étaient la plupart du temps trop faibles pour expliquer les taux observés, et de plus la compétition avec d'autres processus est très probablement trop forte. En effet, durant cette étude, nous avons également mis en évidence l'occurrence de la dénitrification, la réduction dissimilative des  $\text{NO}_3^-$  vers l'ammonium ( $\text{NH}_4^+$ ) (DNRA) et l'oxydation anaérobique de l' $\text{NH}_4^+$  (Anammox), qui entrent en compétition pour les substrats. Enfin, au vu des caractéristiques que partagent le lac de la Dendre et

le lac Kivu (i.e principalement méromicticité et fortes concentrations en CH<sub>4</sub> dans les eaux anoxiques), nous avons également mesuré l'oxydation du CH<sub>4</sub> au sein de la colonne d'eau, avec des taux maximum d'AOM de 14 μmol L<sup>-1</sup> j<sup>-1</sup>. Malgré ces taux d'oxydation élevée, le lac de la Dendre est un gros émetteur de CH<sub>4</sub> pour l'atmosphère. Les SO<sub>4</sub><sup>2-</sup> sont très probablement le principal accepteur d'électrons, mais les concentrations élevées en NO<sub>3</sub><sup>-</sup> (jusque 80 μmol L<sup>-1</sup>) suggèrent qu'ils pourraient également servir pour l'AOM, étant donné que l'AOM couplée à la dénitrification est thermodynamiquement bien plus favorable que l'AOM couplée à la réduction des SO<sub>4</sub><sup>2-</sup>.



## Outline

---

Chapter 1: Introduction.....	1
<b>1.1 The global methane cycle</b> .....	1
<b>1.2 Anaerobic methane oxidation in waters and biogeochemical processes associated</b> .....	3
1.2.1 <i>Anaerobic methane oxidation coupled to sulfate reduction</i> .....	4
1.2.2 <i>Anaerobic methane oxidation coupled to Fe and Mn reduction</i> .....	5
1.2.3 <i>Anaerobic methane oxidation coupled to nitrate reduction</i> .....	5
<b>1.3 Importance of freshwaters in CH<sub>4</sub> cycle</b> .....	7
<b>1.4 Description of the study sites</b> .....	8
1.4.1 <i>Lake Kivu</i> .....	8
1.4.2 <i>Kabuno Bay</i> .....	10
1.4.3 <i>The Dendre Lake</i> .....	11
<b>1.5 Objectives and outlines of the thesis</b> .....	11
Chapter 2: Nitrous oxide and methane seasonal variability in the epilimnion of a large tropical meromictic lake (Lake Kivu, East-Africa).....	13
<b>2.1 Abstract</b> .....	13
<b>2.2 Introduction</b> .....	13
<b>2.3 Material and methods</b> .....	15
2.3.1 <i>Study site</i> .....	15
2.3.2 <i>Physico-chemical parameters and sampling</i> .....	15
2.3.3 <i>Water column chemical analyses</i> .....	16
2.3.4 <i>CH<sub>4</sub> and N<sub>2</sub>O flux calculations</i> .....	16
2.3.5 <i>Schmidt Stability Index calculations</i> .....	16
<b>2.4 Results</b> .....	17
<b>2.5 Discussion</b> .....	20
Chapter 3: Anaerobic methane oxidation in an East African great lake (Lake Kivu).....	28
<b>3.1 Abstract</b> .....	28
<b>3.2 Introduction</b> .....	29
<b>3.3 Material and methods</b> .....	30
3.3.1 <i>Sampling sites</i> .....	30
3.3.2 <i>Physico-chemical parameters and sampling</i> .....	30
3.3.3 <i>Chemical analyses</i> .....	30
3.3.4 <i>CH<sub>4</sub> oxidation and production, NO<sub>3</sub><sup>-</sup> and SO<sub>4</sub><sup>2-</sup> consumption and Mn<sup>2+</sup> production rates calculations</i> .....	33

3.3.5	<i>N</i> stable isotope labelling experiments .....	34
3.3.6	Pigment analysis.....	35
<b>3.4</b>	<b>Results</b> .....	<b>36</b>
3.4.1	<i>Physico-chemical characteristics of the water column</i> .....	36
3.4.2	<i>Microbial process rate measurements</i> .....	38
<b>3.5</b>	<b>Discussion</b> .....	<b>40</b>
<b>3.6</b>	<b>Conclusions</b> .....	<b>48</b>
Chapter 4: Anaerobic methane oxidation in a ferruginous tropical lake (Kabuno Bay, East Africa) .....		
		50
<b>4.1</b>	<b>Abstract</b> .....	<b>50</b>
<b>4.2</b>	<b>Introduction</b> .....	<b>50</b>
<b>4.3</b>	<b>Material and methods</b> .....	<b>52</b>
4.3.1	<i>Sampling and physico-chemical parameters</i> .....	52
4.3.2	<i>Chemical analyses</i> .....	53
4.3.3	<i>CH<sub>4</sub> oxidation and production rates calculations</i> .....	56
4.3.4	<i>Pigment analyses</i> .....	56
<b>4.4</b>	<b>Results</b> .....	<b>57</b>
4.4.1	<i>Physico-chemical parameters and CH<sub>4</sub> concentrations</i> .....	57
4.4.2	<i>CH<sub>4</sub> oxidation and production rates</i> .....	57
4.4.3	<i>Potential electron acceptors concentrations</i> .....	59
<b>4.5</b>	<b>Discussion</b> .....	<b>60</b>
Chapter 5: Denitrification, anaerobic ammonium oxidation and dissimilatory nitrate reduction to ammonium in an East African Great Lake (Lake Kivu) .....		
		67
<b>5.1</b>	<b>Abstract</b> .....	<b>67</b>
<b>5.2</b>	<b>Introduction</b> .....	<b>67</b>
<b>5.3</b>	<b>Material and methods</b> .....	<b>69</b>
5.3.1	<i>Sampling sites</i> .....	69
5.3.2	<i>Physico-chemical parameters and sampling</i> .....	70
5.3.3	<i>N</i> stable isotope labeling experiments .....	70
5.3.4	<i>Water-column chemical analyses</i> .....	71
<b>5.4</b>	<b>Results and discussion</b> .....	<b>72</b>
5.4.1	<i>Physico-chemical parameters and Lake Kivu vertical structure description</i> .....	72
5.4.2	<i>Denitrification, anammox and DNRA without H<sub>2</sub>S added</i> .....	75
5.4.3	<i>Denitrification, anammox and DNRA with H<sub>2</sub>S added</i> .....	81
5.4.4	<i>Natural rates</i> .....	83
5.4.5	<i>Spatial heterogeneity</i> .....	85

5.5	<b>Conclusion</b> .....	86
Chapter 6: Emission and oxidation of methane in a meromictic, eutrophic and temperate lake (Dendre, Belgium).....		
6.1	<b>Abstract</b> .....	87
6.2	<b>Introduction</b> .....	87
6.3	<b>Material and methods</b> .....	89
6.3.1	<i>Physico-chemical parameters and sampling</i> .....	89
6.3.2	<i>CH<sub>4</sub> oxidation measurements and water column chemical analyses</i> .....	89
6.3.3	<i>CO<sub>2</sub>, CH<sub>4</sub> and N<sub>2</sub>O fluxes calculations</i> .....	91
6.4	<b>Results</b> .....	91
6.4.1	<i>Physico-chemical parameters</i> .....	91
6.4.2	<i>CH<sub>4</sub> oxidation</i> .....	93
6.4.3	<i>CH<sub>4</sub>, N<sub>2</sub>O and CO<sub>2</sub> fluxes</i> .....	95
6.5	<b>Discussion</b> .....	95
Chapter 7: General discussion, conclusions and perspectives .....		
7.1	<b>Comparison between two tropical lakes and a temperate lake</b> .....	104
7.1.1	<i>Are the systems reliable models of their respective category?</i> .....	105
7.1.2	<i>Are three lakes comparable?</i> .....	106
7.2	<b>Why studying small environments such as Lake Dendre?</b> .....	109
7.3	<b>On the problem of the AOM electron acceptors</b> .....	110
7.4	<b>Conclusions and perspectives</b> .....	112
Bibliography.....		114
List of publications (peer-reviewed) .....		130



---

## Chapter 1: Introduction

---

### 1.1 The global methane cycle

Methane (CH<sub>4</sub>) is the second most abundant long-lived greenhouse gas in the atmosphere, with global emission estimated to 550 Tg CH<sub>4</sub> yr<sup>-1</sup> (IPCC, 2013). Although this emission is much lower than anthropogenic carbon dioxide (CO<sub>2</sub>) emission, CH<sub>4</sub> impact on global warming is 34 times higher on a 100-year time frame than CO<sub>2</sub> (IPCC, 2013). CH<sub>4</sub> has a short residence time in the atmosphere (10 years), meaning that alleviating CH<sub>4</sub> emissions could represent an efficient option for mitigation of climate change.

CH<sub>4</sub> concentrations in the atmosphere increased from 722 ppb in 1750 to 1803 ppb in 2011, most likely due to human activities (IPCC, 2013). There are different sources of CH<sub>4</sub> for the atmosphere, which can be grouped into three categories: biogenic (due to microbial activity: wetlands, termites, oceans, rice fields, ruminants, landfills and sewage treatment), thermogenic (fossil fuel) and pyrogenic (biomass burning) (Conrad, 2009;Kirschke et al., 2013). About 53 % of the total CH<sub>4</sub> emissions are natural, and 47 % are anthropogenic (Saunio et al., 2016). Total anthropogenic CH<sub>4</sub> emissions have been recently estimated to 346 Tg CH<sub>4</sub> yr<sup>-1</sup> for the decade 2003-2012 (Saunio et al., 2016). The human activities leading to CH<sub>4</sub> emission are the production and use of fossil fuels, agriculture and ruminants, landfills and sewage, and incomplete biomass burning. Table 1 reports the anthropogenic and natural CH<sub>4</sub> sources, and the part of each sector in total CH<sub>4</sub> emission. The two highest anthropogenic sources are the domestic ruminants and the production and use of fossil fuels (coal, oil, natural gas and shale gas), which contribute for 31 and 23 % of the anthropogenic sources, respectively. The wetlands represent the major natural sources of CH<sub>4</sub> for the atmosphere, with emission estimated to 185 Tg CH<sub>4</sub> yr<sup>-1</sup>, i.e. 25 % of the total CH<sub>4</sub> emission. CH<sub>4</sub> production in wetlands is biogenic, that is due to microbial activity. More than 70 % of the total CH<sub>4</sub> produced (natural and anthropogenic) are biogenic. CH<sub>4</sub> production, also called methanogenesis, is a biogeochemical process mainly occurring in anoxic environments and performed by methanogenic Archaea. Currently, 6 orders of methanogenic Archaea have been identified: *Methanomicrobiales*, *Methanosarcinales*, *Methanocellales*, *Methanobacteriales*, *Methanococcales* and *Methanopyrales* (Borrel et al., 2011). They use different metabolic pathways to degrade organic matter and produce CH<sub>4</sub>: hydrogenotrophic (CO<sub>2</sub> reduction), acetoclastic (acetate fermentation) or methylotrophic (methyl groups' reduction) methanogenesis (Borrel et al., 2011). Hydrogenotrophic methanogenesis (performed by the six orders of methanogenic Archaea) is the most widespread pathway in oceans, while acetoclastic methanogenesis (only performed by the *Methanosarcinales*) is mostly encountered in freshwater sediments (Whiticar et al., 1986;Borrel et al.,

2011). Also, acetoclastic methanogenesis is the dominant pathway of CH<sub>4</sub> production in landfills (Hackley et al., 1996), and is theoretically responsible for 70% of the CH<sub>4</sub> production in rice fields (Conrad, 1999; Krüger et al., 2001). However, in natural rice fields, this proportion is strongly influenced by temperature or by the presence of other elements, such as NO<sub>3</sub><sup>-</sup>, NO<sub>2</sub><sup>-</sup>, Fe or SO<sub>4</sub><sup>2-</sup> (Conrad, 1999). On the contrary, in ruminants' rumen and termites' gut, methanogens mostly use H<sub>2</sub> and CO<sub>2</sub> to produce CH<sub>4</sub> (Hungate, 1967; Brauman et al., 1992).

<b>Table 1: Anthropogenic and natural CH<sub>4</sub> emissions (in Tg CH<sub>4</sub> yr<sup>-1</sup>) and their contribution in total CH<sub>4</sub> emissions (in %), and CH<sub>4</sub> sinks (in Tg CH<sub>4</sub> yr<sup>-1</sup>) (Saunois et al., 2016).</b>		
<b>SOURCES</b>		
	CH <sub>4</sub> emission (Tg CH <sub>4</sub> yr <sup>-1</sup> )	Contribution (%)
<b>Anthropogenic sources</b>		
<b>Fossil fuels</b>	<b>121</b>	<b>16</b>
Coal mining	41	6
Oil and natural gas sectors	79	11
<b>Agriculture and waste</b>	<b>195</b>	<b>26</b>
Livestock	106	14
Waste management	59	8
Rice fields	30	4
<b>Biomass and biofuel burning</b>	<b>30</b>	<b>4</b>
Biomass burning	18	2
Biofuel burning	12	2
<b>Sub-total</b>	<b>346</b>	<b>47</b>
<b>Natural sources</b>		
<b>Wetlands</b>	<b>185</b>	<b>25</b>
<b>Inland freshwaters</b>	<b>122</b>	<b>17</b>
Lakes	76	10
Reservoirs	19	3
Rivers and streams	27	4
<b>Geological sources</b>	<b>52</b>	<b>7</b>
Termites	9	1
Wild ruminants	10	1
<b>Marine sources</b>	<b>14</b>	<b>2</b>
Geological sources	12	2
Non geological sources	2	<1
<b>Terrestrial permafrost and hydrates</b>	<b>1</b>	<b>&lt;1</b>
<b>Sub-total</b>	<b>393</b>	<b>53</b>
<b>TOTAL</b>	<b>739</b>	<b>100</b>
<b>SINKS</b>		
	Tg CH <sub>4</sub> yr <sup>-1</sup>	
<b>OH oxidation</b>	<b>454-617</b>	
<b>Stratospheric loss</b>	<b>16-84</b>	
<b>Tropospheric oxidation with Cl</b>	<b>13-37</b>	
<b>Soil uptake</b>	<b>9-47</b>	
<b>TOTAL</b>	<b>492-785</b>	

For a long time, it was commonly assumed that methanogenesis was a strictly anaerobic process, but the well-known "oceanic CH<sub>4</sub> paradox" raised numerous questions. Whether CH<sub>4</sub> is produced in anoxic sediments and waters, how to explain the ubiquitous CH<sub>4</sub> oversaturation of oxic superficial waters in oceans? Karl and Tilbrook (1994) suggested that CH<sub>4</sub> was produced in anoxic micro-environments within anaerobic particles (aggregates and fecal pellets). Later, Karl et al. (2008) suggested that CH<sub>4</sub> was produced as a by-product of methylphosphonate decomposition in phosphate-depleted waters, and Metcalf et al. (2012) supported that study by identifying Archaea capable to produce significant quantities of methylphosphonate in marine waters. Very recently, Repeta et al. (2016) directly showed that organic matter from North Pacific is rich in phosphonates, and that their oxic bacterial degradation leads to CH<sub>4</sub> production. Aerobic CH<sub>4</sub> production was also directly measured in the water column of temperate lakes, and was demonstrated to be linked with phytoplankton activity (Grossart et al., 2011; Bogard et al., 2014; Tang et al., 2014; Tang et al., 2016). The authors suggested that phytoplankton could produce methylated compounds (such as dimethylsulfoniopropionate (DMSP) or dimethyl sulfide (DMS)), used by aerobic methanogens to produce CH<sub>4</sub>. Numerous studies specifically focused on CH<sub>4</sub> production from DMSP (Damm et al., 2008; Damm et al., 2010; Zindler et al., 2013; Damm et al., 2015) or DMS (Florez-Leiva et al., 2013). They put in correlation CH<sub>4</sub> production and phytoplankton bloom, and showed that CH<sub>4</sub> and DMSP or DMS concentrations were inversely correlated. However, further studies are still required to really elucidate the mechanisms involved in aerobic CH<sub>4</sub> production.

Atmospheric CH<sub>4</sub> sinks compensate the CH<sub>4</sub> sources, so the resulting residual that corresponds to the increase in the atmosphere is in fact one order of magnitude lower than total sources. The first CH<sub>4</sub> sink is its oxidation by the hydroxyl radical (OH), in the troposphere, which represents 90 % of the sinks (Ehhalt, 1974; Saunio et al., 2016). The other sinks are photochemistry in the stratosphere and in the marine boundary layer, and oxidation in soils (Allan et al., 2007; Curry, 2007; Dutaur and Verchot, 2007; Thornton et al., 2010).

## **1.2 Anaerobic methane oxidation in waters and biogeochemical processes associated**

CH<sub>4</sub> can be produced by methanogenesis in the anoxic bottom layers (sediments or water columns) of aquatic systems. Once produced, CH<sub>4</sub> travels towards the atmosphere by diffusion, ebullition or plant-mediated transport. During this transport, CH<sub>4</sub> can be aerobically or anaerobically oxidized by methanotrophs. Aerobic CH<sub>4</sub> oxidation uses oxygen (O<sub>2</sub>) as electron acceptor. It is performed by methanotrophic bacteria and is a very effective CH<sub>4</sub> consumer. From a thermodynamic point of view, O<sub>2</sub> is the most effective electron acceptor (Figure 1; Burgin et al., 2011). However, CH<sub>4</sub>

oxidation can be performed in anoxic conditions with other electron acceptors: nitrate ( $\text{NO}_3^-$ ), nitrite ( $\text{NO}_2^-$ ), iron (Fe), manganese (Mn) and sulfate ( $\text{SO}_4^{2-}$ ).

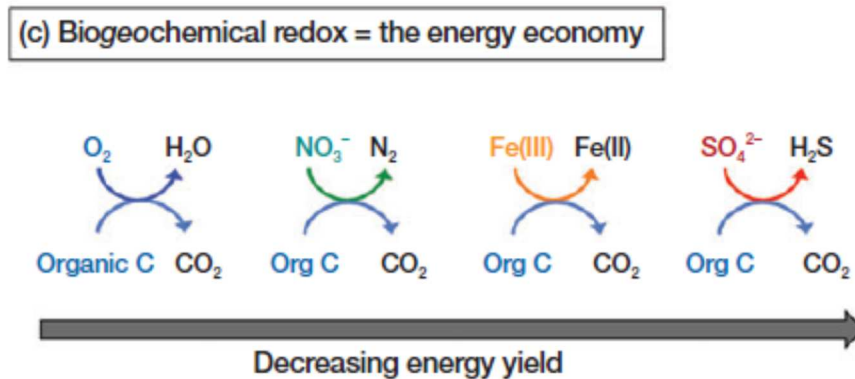


**Figure 1:** Ranking of the different potential electron acceptors for AOM, according to their energy yield. From Burgin et al. (2011).

### 1.2.1 Anaerobic methane oxidation coupled to sulfate reduction

Although the energy yield strongly influences the electron acceptors used for anaerobic  $\text{CH}_4$  oxidation (AOM), the availability of these ones is the primary factor determining the occurrence of the different processes. In marine environments,  $\text{SO}_4^{2-}$  concentrations are very high compared with the other elements, what explains that AOM coupled with  $\text{SO}_4^{2-}$  reduction (S-DAMO) is the major AOM pathway. It has been demonstrated in various marine systems, such as for examples in the sediments from Kattegat and Skagerrak (Iversen and Jørgensen, 1985), in the Hydrates Ridge sediments (Boetius et al., 2000), in the Black Sea sediments (Jørgensen et al., 2001) and water column (Durisch-Kaiser et al., 2005) or in the seeps and vents from Eel River Basin (Orphan et al., 2004). AOM in marine sediments is a very effective process, since it is estimated that without it, the  $\text{CH}_4$  reaching the atmosphere would be higher of 10-60 % (Conrad, 2009). Even if S-DAMO is mainly encountered in marine environments, it has also been demonstrated in freshwater environments, such as in the water column of Lake Plußsee (Eller et al., 2005). S-DAMO is performed by a consortium of  $\text{SO}_4^{2-}$ -reducing bacteria and anaerobic methanotrophic archaea (ANME) related to the orders *Methanosarcinales* and *Methanomicrobiales* (Hinrichs et al., 1999; Hinrichs and Boetius, 2003) (Figure 2A).

In freshwater environments,  $\text{SO}_4^{2-}$  concentrations are usually too low to be responsible for significant S-DAMO rates, justifying why AOM in lakes has been firstly assumed to be negligible compared with aerobic  $\text{CH}_4$  oxidation (Rudd et al., 1974). However, the other three potential electron



acceptors, Fe, Mn and  $\text{NO}_3^-$  can be found in higher concentrations in freshwater environments, and can thus contribute significantly to AOM.

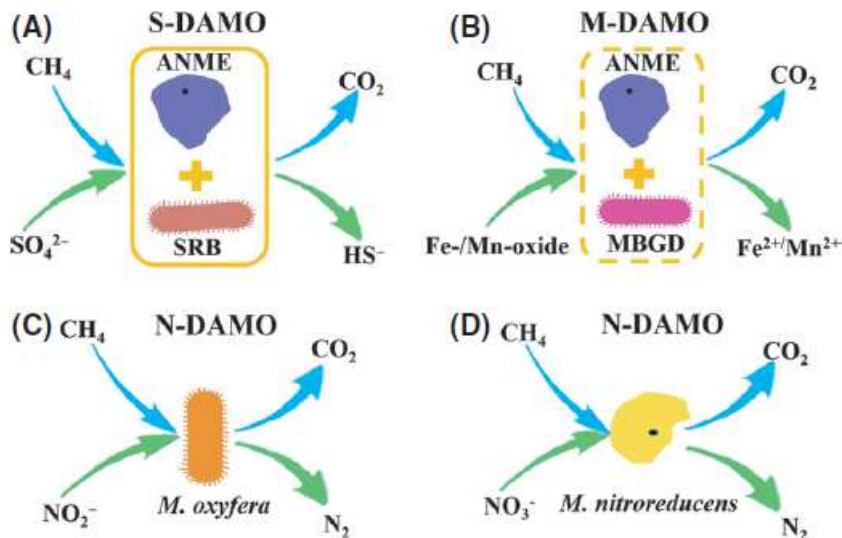


**Figure 2:** The three pathways of AOM with the different potential electron acceptors. (A) Sulfate-dependent AOM (S-DAMO), performed by a consortium of ANME and  $\text{SO}_4^{2-}$ -reducing bacteria (SRB); (B) Metals-dependent AOM, performed by a consortium of ANME and a bacteria affiliated to Marine Benthic Group D (MBGD); (C) and (D) Nitrate-dependent AOM (N-DAMO), performed either by a bacteria alone (*Candidatus Methyloirabilis oxyfera*) or by an archaea alone (*Candidatus Methanoperedens nitroreducens*). From Cui et al. (2015).

### 1.2.2 Anaerobic methane oxidation coupled to Fe and Mn reduction

AOM coupled with metals (Fe and Mn) reduction (M-DAMO) is still a poorly-known process. It is supposed to occur in some ferruginous freshwater environments like Lake Matano (Crowe et al., 2011), Lake Kinneret (Sivan et al., 2011) and the Danish Lake Ørn (á Norði et al., 2013), or in marine sediments (Beal et al., 2009). Its global significance is still unknown, but it is supposed to be potentially significant for coastal marine AOM, since high Fe and Mn concentrations can be provided by rivers (Beal et al., 2009; Cui et al., 2015). Organisms responsible for M-DAMO are not fully identified, but it is supposed to be performed by a consortium of ANME and a bacteria affiliated to Marine Benthic Group D (Beal et al., 2009; Cui et al., 2015; Figure 2B).

### 1.2.3 Anaerobic methane oxidation coupled to nitrate reduction

AOM coupled to  $\text{NO}_3^-$  or  $\text{NO}_2^-$  reduction (N-DAMO) is thermodynamically highly favorable (Table 2). It has been demonstrated for the first time by Raghoebarsing et al. (2006) in an enrichment

culture. Since, it has been widely put in evidence in other cultures (Ettwig et al., 2008;Ettwig et al., 2009;Hu et al., 2009;Ettwig et al., 2010;Hu et al., 2011;Luesken et al., 2011;Kampman et al., 2012), in substrates-enrichment experiments (Haroon et al., 2013;á Norði and Thamdrup, 2014) or in radiotracer experiments (Deutzmann and Schink, 2011). Although these experiments have often been conducted with natural materials, N-DAMO has never been measured in natural conditions, and its broader significance is thus still unknown. N-DAMO was firstly supposed to be performed by a consortium between an archaea ANME and a denitrifying bacteria NC10 (Raghoebarsing et al., 2006;Hu et al., 2009), but it has been shown later that it could also be performed by the bacteria without archaea (Ettwig et al., 2009;Ettwig et al., 2010; Figure 2C). More recently, Haroon et al. (2013) also showed that some archaea were capable to perform N-DAMO without any bacterial partner (Figure 2D).

**Table 2:** The four different pathways of AOM, their equation and their free Gibbs Energy (kJ mol<sup>-1</sup>) (Cui et al., 2015).

AOM coupled with	Equation	Free Gibbs Energy (ΔG°)
<i>Denitrification</i>	$5\text{CH}_4 + 8\text{NO}_3^- + 8\text{H}^+ \rightarrow 5\text{CO}_2 + 4\text{N}_2 + 14\text{H}_2\text{O}$	-765
	$3\text{CH}_4 + 8\text{NO}_2^- + 8\text{H}^+ \rightarrow 3\text{CO}_2 + 4\text{N}_2 + 10\text{H}_2\text{O}$	-928
<i>Mn reduction</i>	$\text{CH}_4 + 4\text{MnO}_2 + 7\text{H}^+ \rightarrow \text{HCO}_3^- + 4\text{Mn}^{2+} + 5\text{H}_2\text{O}$	-556
<i>Fe reduction</i>	$\text{CH}_4 + 8\text{Fe}(\text{OH})_3 + 15\text{H}^+ \rightarrow \text{HCO}_3^- + 8\text{Fe}^{2+} + 21\text{H}_2\text{O}$	-270
<i>SO<sub>4</sub><sup>2-</sup> reduction</i>	$\text{CH}_4 + \text{SO}_4^{2-} \rightarrow \text{HCO}_3^- + \text{HS}^- + \text{H}_2\text{O}$	-17

### 1.2.3.1 Denitrification

N-DAMO is thus the coupling between CH<sub>4</sub> oxidation and denitrification. Denitrification is an anaerobic process of NO<sub>3</sub><sup>-</sup> reduction to N<sub>2</sub>, which can use different electron donors. The most commonly encountered is heterotrophic denitrification, which simply uses organic matter. But denitrification can also be chemolithotrophic, with CH<sub>4</sub> (=N-DAMO), sulfur compounds, Fe or hydrogen as electron donors (Kirchman et al., 2008). Denitrification produces N<sub>2</sub>O as intermediate, a very potent greenhouse gas, whose impact on global warming is 298 times higher than CO<sub>2</sub> on a 100-year time frame (IPCC, 2013). Due to its global importance, denitrification has been widely studied and has been observed in various environments, such as in soils, rivers, streams, groundwaters, marine and freshwater sediments, estuaries, Oxygen Minimum Zones, etc. (Seitzinger, 1988;Seitzinger et al., 2006). Different parameters determine the occurrence of denitrification (Seitzinger et al., 2006):

- 1) The availability of NO<sub>3</sub><sup>-</sup> and of the different potential electron donors,

- 2) The  $O_2$  concentrations, since denitrification needs almost fully anoxic conditions ( $O_2$  concentrations below  $6 \mu\text{mol L}^{-1}$ ),
- 3) The competition with other processes for substrates.

Denitrification can enter in competition for  $\text{NO}_3^-$  or  $\text{NO}_2^-$  with two processes: anaerobic  $\text{NH}_4^+$  oxidation (anammox) and dissimilative reduction of  $\text{NO}_3^-$  to  $\text{NH}_4^+$  (DNRA).

### 1.2.3.2 Anammox and DNRA

Anammox is an autotrophic denitrification producing  $\text{N}_2$  from  $\text{NO}_2^-$  and  $\text{NH}_4^+$ . It has been put in evidence for the first time in a wastewater treatment system by Van de Graaf et al. (1995), and since has been shown to occur in various environments (e.g. in Danish marine sediments, Black Sea water column, Lake Tanganyika water column, Lake Rassnitzer water column, etc.; Thamdrup and Dalsgaard, 2002; Kuypers et al., 2003; Schubert et al., 2006; Hamersley et al., 2009). Its contribution in  $\text{N}_2$  production strongly differs between the different systems; for example it is estimated to contribute for 19-35 % in the Golfo Dulce, in Costa Rica (Dalsgaard et al., 2003), while its contribution in Lake Tanganyika has been estimated to only 13% (Schubert et al., 2006).

Like Anammox, the significance of DNRA strongly depends on the environment. As summarized by Burgin and Hamilton (2007), it can account between 5% and 100% of the  $\text{NO}_3^-$  removal. DNRA is an anaerobic process of  $\text{NO}_3^-$  fermentation. Contrary to anammox and denitrification, it produces  $\text{NH}_4^+$ , biologically more available, which can be used for nitrification or for biomass growth (Burgin and Hamilton, 2007). It strongly enters in competition with denitrification for  $\text{NO}_3^-$ , but it seems that DNRA is favored in environments with a high organic matter content, while denitrification is favored in environments with higher  $\text{NO}_3^-$  concentrations (Burgin and Hamilton, 2007).

Even though DNRA and anammox cannot be, at our knowledge, directly coupled to  $\text{CH}_4$  oxidation, they can be indirectly related to AOM, since they influence the occurrence of denitrification. Indeed, anammox can enter in competition with denitrification for  $\text{NO}_2^-$ , while DNRA can compete with denitrification for  $\text{NO}_3^-$ . Also, DNRA indirectly influences denitrification by producing  $\text{NH}_4^+$ , which can be used by nitrifying bacteria to produce  $\text{NO}_3^-$ , fueling denitrification in substrates.

## 1.3 Importance of freshwaters in $\text{CH}_4$ cycle

Freshwaters only represent 2.5 % of total Earth's water, and almost 70% of freshwaters are present in glaciers and ice caps (Shiklomanov, 1993). Surface freshwaters only represent 1.2% of freshwaters, and lakes and rivers represent 21 and 0.5 % of surface waters, respectively (Shiklomanov, 1993). Lakes and rivers thus represent 0.007 and 0.0002 % of total waters (Shiklomanov, 1993), and for a long time, were considered as negligible for the  $\text{CH}_4$  budget. Rivers were even consider as inert

systems, just transporting the different elements between the terrestrial and the aquatic compartments. However, we now know that this transport is not passive, and that numerous processes of transformation and degradation occur in rivers (Cole et al., 2007).

Despite their small area cover, lakes and rivers are responsible for 19 and 7 % of natural CH<sub>4</sub> emissions (Table 1). Tropical freshwaters (including lakes, rivers and reservoirs), in particular, raise great interest for CH<sub>4</sub> budgets, since they are suspected to be high emitters of greenhouse gases for the atmosphere. They are estimated to be responsible for around 50% of the freshwater's CH<sub>4</sub> emissions, while they only represent 18% of the total freshwater area (Bastviken et al., 2011). Tropical lakes, in particular, represent around 13% of the total freshwater area and are responsible for around 30% of the freshwater's CH<sub>4</sub> emissions (Bastviken et al., 2011). However, these estimations are suspected to be underestimated, since tropical areas are understudied. For example, Borges et al. (2015a) studied greenhouse gases emissions from 12 rivers in Africa, and obtained CH<sub>4</sub> emissions 5 times higher than those reported in the study of Bastviken et al. (2011), which concern all tropical rivers.

Freshwaters thus play a significant role in CH<sub>4</sub> emissions and are thus important contributors to global warming. Tropical freshwaters, in particular, are hotspots of biological activity, mainly due to permanent high water temperatures (Lewis Jr, 1987). These environments are thus highly productive and great amounts of organic matter are usually degraded, conducting to high CH<sub>4</sub> production rates. Even if a part of this CH<sub>4</sub> is oxidized, a great part reaches the atmosphere.

## **1.4 Description of the study sites**

This study focuses on the AOM in Lake Kivu, a tropical great lake and a lake located in a former stone quarry in Belgium, allowing to also study AOM in a temperate lake.

### *1.4.1 Lake Kivu*

Lake Kivu is an African Great Lake located at the border between the Rwanda and the Democratic Republic of the Congo (Figure 3). It is a deep (maximum and mean depths of 485 and 245 m, respectively) meromictic tropical lake characterized by huge amounts of dissolved gases (CO<sub>2</sub> and CH<sub>4</sub>) and nutrients in the anoxic bottom waters. It is divided into three basins and two bays: the main basin or Northern Basin, the Kalehe Basin or Western Basin, the Ishungu Basin or Southern Basin, Bukavu Bay in the south and Kabuno Bay in the north. Kabuno Bay, in particular, presents a so unique structure that it can be considered as an individual lake.

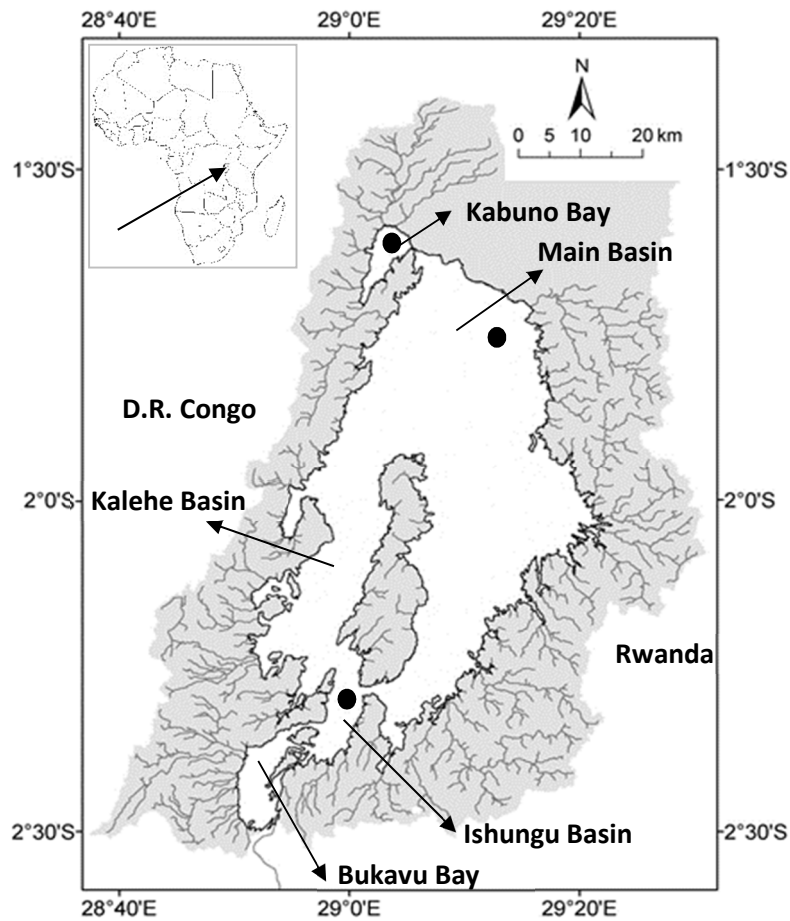


**Figure 3:** Map of Lake Kivu and the different sampling sites

This study focused on the main Basin and Kabuno Bay, and at a lower extent on the Ishungu Basin. The main basin and Ishungu basins share a similar vertical structure. The only difference between both basins is that the Ishungu Basin is smaller and more closely surrounded by lands. Biogeochemical processes can thus be potentially more influenced by allochthonous inputs. Anyway, the water column of both basins can be divided into two main compartments: the mixolimnion and the monimolimnion (Figure 4; Schmid and Wüest, 2012).

The mixolimnion is a narrow zone comprised between the surface to ~65 m depth and influenced by the seasonality. In rainy season, a stratification takes place, with waters anoxic from ~40 m depth. During the dry season, enhanced lake evaporation and changes in solar radiation induce a cooling of surface waters (Thiery et al., 2014b), causing a mixing until ~65 m depth. A part of the nutrients trapped in anoxic waters is made available for microorganisms, especially phytoplankton, which proliferates. Sedimentation of organic matter from the surface sustains a microbial foodweb, especially nitrifying bacteria, which impoverishes the water column in ammonia ( $\text{NH}_4^+$ ) and in oxygen

and enriches the water column in  $\text{NO}_3^-$ , conducting to the establishment of the rainy season's stratification and  $\text{NO}_3^-$  accumulation zone (nitracline). The mixolimnion thus presents intense biological activity and is consequently called "biozone" (Schmid and Wüest, 2012).

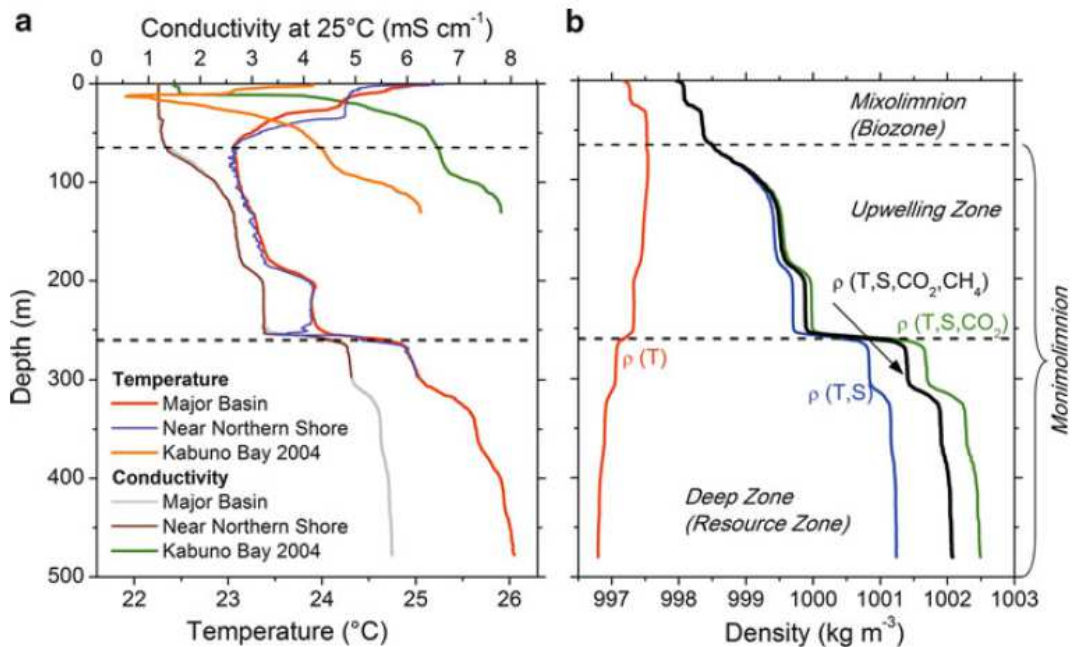


**Figure 4:** Vertical structure of Lake Kivu in the main Basin and in Kabuno Bay. From Schmid and Wüest (2012).

Below ~65 m depth, no seasonal influence is observed; the water is permanently anoxic. The monimolimnion can be itself divided into two compartments, the upwelling zone and the resource zone, separated by a strong chemocline located between 255 and 262 m depth, which is maintained by subaquatic springs entering in the lake at 255 m depth (Schmid and Wüest, 2012). The upwelling zone owes its name to the upwelling generated by the subaquatic springs, while the resource zone is the zone containing the part of  $\text{CH}_4$  which can be exploited to produce electricity (Schmid and Wüest, 2012).

#### 1.4.2 Kabuno Bay

The water column structure of Kabuno Bay is quite different. Kabuno Bay is shallower (maximum depth of 110 m) and permanently anoxic below ~11 m depth (Borges et al., 2011; Borges et al., 2012; Schmid and Wüest, 2012). Higher conductivities (around 6000  $\mu\text{S cm}^{-1}$  at 50 m, versus ~1500 in the main basin) and higher dissolved gases ( $\text{CO}_2$  and  $\text{CH}_4$ ) concentrations in surface waters are observed. The stratification is not influenced by seasonality, because Kabuno Bay is smaller and less exposed to wind, and thus surface waters' heat loss is less significant. Also, the strong chemocline

observed at ~11 m depth maintains the stratification, and is due to a larger contribution of subaquatic springs to the water column, since Kabuno Bay is shallower and only communicates with the main basin by a narrow connection (Borges et al., 2012).

Great differences between the main basin and Kabuno Bay are observed in terms of chemical composition. The surface waters of the main basin are rich in  $\text{SO}_4^{2-}$ , poor in Fe, Mn and  $\text{NO}_2^-$ , and presents a nitracline of  $\sim 10 \mu\text{mol L}^{-1}$  during the rainy season. The anoxic waters are rich in sulfide ( $\text{HS}^-$ ) and  $\text{NH}_4^+$  and poor in the other elements. On the contrary, Kabuno Bay is considered as a ferruginous basin due to the high dissolved Fe concentrations (up to  $500 \mu\text{mol L}^{-1}$ ) present in the anoxic waters. Contrary to the main basin, its anoxic waters are depleted in  $\text{HS}^-$ , and its surface waters rarely exhibit a nitracline.

#### 1.4.3 *The Dendre Lake*

The Dendre Lake is a small water body ( $0.032 \text{ km}^2$ ) located in a former stone quarry, at Maffle, in Belgium. It is relatively deep (maximum depth of 30 m), eutrophic and meromictic, with waters permanently anoxic below 20 m depth. Above 20 m depth, stratification is influenced by seasonality, with waters anoxic from ~5 m depth in summer and with a mixing until 20 m depth in winter.

Anoxic waters are rich in  $\text{CH}_4$ , nutrients ( $\text{NH}_4^+$  and phosphate ( $\text{PO}_4^{3-}$ )),  $\text{HS}^-$  and dissolved Fe and Mn. Significant peaks of  $\text{NO}_3^-$  and  $\text{NO}_2^-$  concentrations (up to  $\sim 80$  and  $\sim 20 \mu\text{mol L}^{-1}$ , respectively) are often observed at the oxic-anoxic interfaces. The Dendre stone pit lake is surrounded by trees, which supply the water column in organic matter, and thus contribute to the eutrophic status of the lake. Also, the Dendre Lake is a place of recreation (diving and fishing activities), and fish feeding is practiced, supplying additional organic matter to the water column. A large part of the organic matter which is not aerobically degraded is thus trapped into the anoxic waters, where fermentation occurs and leads to a significant  $\text{CH}_4$  production ( $\text{CH}_4$  concentrations up to  $\sim 600 \mu\text{mol L}^{-1}$  were observed).

### 1.5 Objectives and outlines of the thesis

This study focused on AOM in three distinct environments: main basin of Lake Kivu, Kabuno Bay and Dendre stone pit lake. The main objectives of this work can be summarized as follows:

- 1) Putting in evidence and quantifying AOM and processes associated in the water columns of the three lakes,
- 2) Identifying the different potential electron acceptors for AOM involved,
- 3) Evaluating the potential importance of AOM in the reduction of  $\text{CH}_4$  fluxes to the atmosphere,
- 4) Determining the environmental factors influencing AOM.

In addition to this chapter 1, this manuscript is divided into 6 chapters, whose 5 chapters correspond to papers submitted in international journals.

**Chapter 2**, entitled "Nitrous oxide and methane seasonal variability in the epilimnion of a large tropical meromictic lake (Lake Kivu, East-Africa)" (Roland et al., 2016), sets the foundations of the study. It reports the results of a nearly 2-year sampling in Ishungu Basin (southern basin), which focused on N<sub>2</sub>O and CH<sub>4</sub> concentrations vertical profiles. This study revealed that Lake Kivu is a poor emitter of CH<sub>4</sub> and N<sub>2</sub>O for the atmosphere throughout the year. It also showed that CH<sub>4</sub> concentrations in oxic surface waters were higher during the rainy season, when the stratification is well established, and suggested that it could be due to a higher integrated CH<sub>4</sub> oxidation.

**Chapter 3**, entitled "Anaerobic methane oxidation in an East African great lake (Lake Kivu)", goes into the heart of the matter, with the measurements of CH<sub>4</sub> oxidation during 6 field campaigns in the main basin of Lake Kivu. This study also attempted to identify the potential electron acceptors, with a focus on SO<sub>4</sub><sup>2-</sup>.

**Chapter 4**, entitled "Anaerobic methane oxidation in a ferruginous tropical lake (Kabuno Bay, East Africa)", is the counterpart of the chapter 3 in Kabuno Bay. As in the previous chapter, we attempted to identify the potential electron acceptors for AOM, but with a focus on Fe.

The two previous chapters thus showed the occurrence of AOM in the water column of Lake Kivu and Kabuno Bay. If AOM in Kabuno Bay was most probably linked to Fe, it was not so clear in the main basin of Lake Kivu. It could be linked to SO<sub>4</sub><sup>2-</sup> reduction, since concentrations were high, but could also be linked, at a lower extent, to denitrification. **Chapter 5**, entitled "Denitrification, anaerobic ammonium oxidation and dissimilatory nitrate reduction to ammonium in an East African Great Lake (Lake Kivu)", focuses on the anaerobic nitrogen cycle in order to determine if it is well developed in the water column of Lake Kivu.

As described previously, despite the tropical Lake Kivu, we also studied the temperate Lake Dendre. **Chapter 6**, entitled "Emission and oxidation of methane in a meromictic, eutrophic and temperate lake (Dendre, Belgium)" (Roland et al., 2017), shows the results of AOM measurements during the four seasons in the lake Dendre. The CH<sub>4</sub> fluxes to the atmosphere were also calculated based on CH<sub>4</sub> concentrations and wind velocities.

Finally, **chapter 7** presents a general discussion, the perspectives and the conclusion.



---

## Chapter 2: Nitrous oxide and methane seasonal variability in the epilimnion of a large tropical meromictic lake (Lake Kivu, East-Africa)

---

**Adapted from:** *Fleur A. E. Roland, François Darchambeau, Cédric Morana and Alberto V. Borges (2016) Nitrous oxide and methane seasonal variability in the epilimnion of a large tropical meromictic lake (Lake Kivu, East-Africa), Aquatic Sciences, DOI:10.1007/s00027-016-0491-2*

### 2.1 Abstract

We report a data-set of monthly vertical profiles obtained from January 2012 to October 2013, from the surface to 70 m depth of nitrous oxide ( $\text{N}_2\text{O}$ ) and dissolved methane ( $\text{CH}_4$ ) in Lake Kivu, a large and deep meromictic tropical lake (East Africa). Vertical variations of  $\text{N}_2\text{O}$  were modest, with ranges of 6-9  $\text{nmol L}^{-1}$  and 0-16  $\text{nmol L}^{-1}$  in surface and bottom waters, respectively, and occasionally peaks of  $\text{N}_2\text{O}$  (up to 58  $\text{nmol L}^{-1}$ ) were observed at the oxic-anoxic interface. On the contrary, steep vertical gradients of  $\text{CH}_4$  were observed with values changing several orders of magnitude from surface (19-103  $\text{nmol L}^{-1}$ ) to 70 m (~113,000-520,000  $\text{nmol L}^{-1}$ ). Seasonal variations of  $\text{CH}_4$  were caused by annual cycles of mixing and stratification, during the dry and rainy seasons, respectively. This mixing allowed the establishment of a thick oxic layer (maximum 65 m deep), leading to decreased  $\text{CH}_4$  concentrations (minimum of 8  $\text{nmol L}^{-1}$ ), presumably due to bacterial  $\text{CH}_4$  oxidation. During the stratification period, the oxic mixed layer was thinner (minimum 25 m deep), and an increase of  $\text{CH}_4$  concentrations in surface waters was observed (maximum of 103  $\text{nmol L}^{-1}$ ), probably due to a lower integrated  $\text{CH}_4$  oxidation on the water column. Lake Kivu seasonally alternated between a source and a sink for atmospheric  $\text{N}_2\text{O}$ , but on an annual scale was a small source of  $\text{N}_2\text{O}$  to the atmosphere (on average 0.43  $\mu\text{mol m}^{-2} \text{d}^{-1}$ ), while it was a small source of  $\text{CH}_4$  to the atmosphere throughout the year (on average 86  $\mu\text{mol m}^{-2} \text{d}^{-1}$ ). Vertical and seasonal variations of  $\text{N}_2\text{O}$  are discussed in terms of nitrification and denitrification, although from the present data-set it is not possible to unambiguously identify the main drivers of  $\text{N}_2\text{O}$  production.

### 2.2 Introduction

Methane ( $\text{CH}_4$ ) and nitrous oxide ( $\text{N}_2\text{O}$ ) are two important greenhouse gases whose global warming potential are respectively 34 and 298 times higher on a 100-year time frame than carbon dioxide ( $\text{CO}_2$ ) (IPCC, 2013). Additionally,  $\text{N}_2\text{O}$  depletes stratospheric ozone. The concentrations of  $\text{CH}_4$  and  $\text{N}_2\text{O}$  in the atmosphere have significantly increased during the 20<sup>th</sup> century due to human activities, agriculture in particular.

N<sub>2</sub>O in aquatic systems is mainly produced by nitrification and denitrification with optimal temperature estimated to be in the 25–30°C range (Saad and Conrad, 1993). Hence, an increase of these processes can be expected with increasing temperatures, but N<sub>2</sub>O emissions are also strongly linked to nitrogen and oxygen availability. In this sense, the highest N<sub>2</sub>O emissions from inland waters are reported from systems enriched by fertilizer use in catchment areas or wastewaters (Zhang et al., 2010; Baulch et al., 2011). Indeed, African rivers have been recently shown to be lower N<sub>2</sub>O emitters compared to their temperate counterparts, presumably due to the different agricultural practices (i.e., traditional versus fertilizer-intensive) (Borges et al., 2015a).

CH<sub>4</sub> in aquatic systems is mostly produced in the anoxic layers of sediments and is transported to the surface by diffusion, mixing, and ebullition. Aerobic and anaerobic CH<sub>4</sub> oxidation can take place during the transport, and the fraction that is not oxidized is emitted to the atmosphere. Natural wetlands are known to be the major natural source of CH<sub>4</sub> for the atmosphere (175–217 Tg CH<sub>4</sub> y<sup>-1</sup>), as well as inland waters (lakes and rivers), since the latter were estimated to emit between 40 Tg CH<sub>4</sub> y<sup>-1</sup> (Kirschke et al., 2013) and 103 Tg CH<sub>4</sub> y<sup>-1</sup> (Bastviken et al., 2011). Furthermore, higher emissions of CH<sub>4</sub> are expected in tropical inland waters than in temperate and boreal counterparts, in accordance with recent reports (Sawakuchi et al., 2014; Borges et al., 2015a), due to the strong dependence of CH<sub>4</sub> production on temperature (Marotta et al., 2014; Yvon-Durocher et al., 2014). Within the tropical aquatic environments, the Amazon wetlands are the best studied in terms of CH<sub>4</sub> dynamics and fluxes (Bartlett et al., 1990; Devol et al., 1990; Engle and Melack, 2000; Melack et al., 2004; Bastviken et al., 2010; Borges et al., 2015b). These wetlands consist of flooded forest, floating macrophytes and permanent or temporary floodplain lakes that emit large amounts of CH<sub>4</sub> to the atmosphere. Comparatively, tropical upland lakes are much less studied for CH<sub>4</sub> and N<sub>2</sub>O dynamics. In addition, data are particularly scarce in large lakes (Holgerson and Raymond, 2016). Furthermore, seasonal variations of CH<sub>4</sub> and N<sub>2</sub>O fluxes have seldom been described in lakes, and mostly in boreal systems (e.g. Kankaala et al., 2013, Miettinen et al., 2015). Eddy-covariance allows the direct measurement of CH<sub>4</sub> and N<sub>2</sub>O fluxes to the atmosphere in lakes (e.g. Podgrajsek et al., 2014; Xiao et al., 2014), although fluxes are usually computed from dissolved concentrations in surface waters using estimates of the gas transfer velocity (e.g. Schubert et al., 2010, Kankaala et al., 2013, Miettinen et al., 2015).

In this study, we report a two-year time series of monthly measurements of CH<sub>4</sub>, N<sub>2</sub>O and nitrate (NO<sub>3</sub><sup>-</sup>) concentrations in a large tropical lake (Lake Kivu, East Africa). Lake Kivu is a deep (maximum 485 m) meromictic lake characterized by anoxic deep waters rich in dissolved CH<sub>4</sub> and nutrients (Degens et al., 1973; Schmid et al., 2005; Tassi et al., 2009). Surface waters are oligotrophic and are characterized by relatively low primary production ranging between 143 and 278 g C m<sup>-2</sup> yr<sup>-1</sup> (Darchambeau et al., 2014; Morana et al., 2014), and have been shown to be net autotrophic (Morana

et al., 2014), yet they emit carbon dioxide (CO<sub>2</sub>) to the atmosphere due to geogenic CO<sub>2</sub> inputs from deep waters (Borges et al., 2014). A first study of CH<sub>4</sub> dynamics in Lake Kivu showed very low CH<sub>4</sub> concentrations in surface waters (Borges et al., 2011), presumably due to intense CH<sub>4</sub> oxidation as CH<sub>4</sub> is transported upwards (Borges et al., 2011; Pasche et al., 2011; Morana et al., 2015a). The first study of CH<sub>4</sub> in surface waters (Borges et al., 2011) was based on a coarse seasonal coverage (only 4 cruises), focused on surface waters and did not describe the vertical variability of CH<sub>4</sub> in the top 100 m. While most previous studies have focused on carbon cycling in Lake Kivu, nitrogen cycling has received much less attention. The aim of this study is to describe seasonal variations of CH<sub>4</sub> and N<sub>2</sub>O in the epilimnion of a tropical lake and attempt to unravel the underlying processes. Moreover, as a large scale industrial extraction of CH<sub>4</sub> from the deep layers of Lake Kivu is planned (Nayar, 2009), it is important to establish the baseline of ecological and biogeochemical settings to monitor, understand and quantify the consequences of this industrial extraction of CH<sub>4</sub>. Information on the temporal variability of the vertical structure in the top 100 m is required to achieve a comprehensive description of base-line conditions of CH<sub>4</sub> in Lake Kivu prior to industrial extraction.

The present study focuses on one station in the Southern Basin of the lake (Ishungu station), and thus provides temporally resolved data compared to previous reports of CH<sub>4</sub> concentrations focusing on spatial variations in surface waters by Borges et al. (2011). The present paper also complements the work of Morana et al. (2015b) based on the same two-year sampling at Ishungu, which mainly focused on the biogeochemistry of organic matter.

## **2.3 Material and methods**

### *2.3.1 Study site*

Lake Kivu is located at the border between Rwanda and Democratic Republic of the Congo (DRC) [2.50°S 1.59°S 29.37°E 28.83°E]. Sampling was carried out every month from late January 2012 to October 2013, at one station in the Southern Basin of the Lake (Ishungu station; -2.3374°N, 28.9775°E; Figure 3).

### *2.3.2 Physico-chemical parameters and sampling*

Vertical profiles of temperature, conductivity and oxygen (O<sub>2</sub>) were obtained with a Hydrolab DS4 multiparameter probe. Water was collected with a vertical 7L Niskin bottle (Hydro-Bios) every 5 m from the surface to 70 m.

### 2.3.3 Water column chemical analyses

Samples for N<sub>2</sub>O and CH<sub>4</sub> concentrations were collected in 50 mL glass serum bottles from the Niskin bottle through a silicon tube connected to the outlet, left to overflow, poisoned with 100 µL of saturated HgCl<sub>2</sub> and immediately sealed with butyl stoppers and aluminium caps. CH<sub>4</sub> and N<sub>2</sub>O concentrations were determined via the headspace equilibration technique (20 mL N<sub>2</sub> headspace in 50 mL serum bottles) and measured by gas chromatography (GC) (Weiss, 1981) with electron capture detection (ECD) for N<sub>2</sub>O and with flame ionization detection (FID) for CH<sub>4</sub>. The SRI 8610C GC-ECD-FID was calibrated with certified CH<sub>4</sub>:CO<sub>2</sub>:N<sub>2</sub>O:N<sub>2</sub> mixtures (Air Liquide, Belgium) of 1, 10, 30 and 509 ppm CH<sub>4</sub> and of 0.2, 2.0 and 6.0 ppm N<sub>2</sub>O. Concentrations were computed using the solubility coefficients of Yamamoto et al. (1976) and Weiss and Price (1980), for CH<sub>4</sub> and N<sub>2</sub>O, respectively. The precision of measurements was ±3.9% and ±3.2% for CH<sub>4</sub> and N<sub>2</sub>O, respectively.

When preparing the headspaces, excess water was collected to quantify NO<sub>3</sub><sup>-</sup> and NH<sub>4</sub><sup>+</sup> concentrations by spectrophotometry. NO<sub>3</sub><sup>-</sup> were determined after vanadium reduction to nitrite (NO<sub>2</sub><sup>-</sup>) and quantified under this form with a Multiskan Ascent Thermo Scientific multi-plates reader (APHA, 1998; Miranda et al., 2001). NH<sub>4</sub><sup>+</sup> were quantified according to the dichloroisocyanurate-salicylate-nitroprussiate colorimetric method (Westwood, 1981), using a 5-cm light path on a spectrophotometer Thermo Spectronic Genesys 10vis. The detection limits for these methods were 0.15 µmol L<sup>-1</sup> and 0.3 µmol L<sup>-1</sup> for NO<sub>3</sub><sup>-</sup> and NH<sub>4</sub><sup>+</sup>, respectively.

### 2.3.4 CH<sub>4</sub> and N<sub>2</sub>O flux calculations

CH<sub>4</sub> and N<sub>2</sub>O fluxes with respect to the atmosphere were calculated based on temperature, CH<sub>4</sub> and N<sub>2</sub>O concentrations, and the gas transfer velocity computed from wind speed according to the Cole and Caraco (1998) relationship. By convention, a positive flux value corresponds to a gas transfer from the water to the atmosphere, and, conversely, a negative flux corresponds to a gas transfer from the atmosphere to the water. Wind speeds were obtained from the National Centers for Environmental Prediction (NCEP) gridded daily product (grid point -0.952°N, 30.000°E). These values were adjusted to fit field measurements from a meteorological station of the Institut Supérieur Pédagogique (ISP) of Bukavu. The ISP wind values were adjusted by the addition of 2 m s<sup>-1</sup> to account for differences in wind speed between lake and inland where the station is located as suggested by Thiery et al. (2014b).

### 2.3.5 Schmidt Stability Index calculations

Schmidt Stability Index (SSI) defines the thermal stability of the water column over a certain depth and expresses the amount of energy needed for its full mixing over that depth (Schmidt, 1928).

SSI from the surface to 65 m was calculated from density vertical gradients according to Schmidt (1928), and density was computed from temperature and salinity derived from conductivity according to Schmid and Wüest (2012).

## 2.4 Results

For both years, SSI (Figure 5a) and temperature variability (Figure 5b) showed one mixing period, from July to October (dry season), with a maximum mixing in September, while the water column was stratified the rest of the year (rainy season). Mixing periods did not co-occur with higher wind speeds (Figure 5a), which were observed a few weeks before the mixing. The location of the oxycline (Figure 5c) followed the seasonal cycling of mixing and stratification, and ranged from 35 to 70 m depth during the rainy and dry seasons, respectively. Deep waters (from 70 m) remained anoxic throughout the year, while surface waters (at 5 m) were well oxygenated (oxygen concentrations range: 122 to 243  $\mu\text{mol L}^{-1}$ ).  $\text{N}_2\text{O}$  profiles showed on various occasions higher concentration peaks (maximum peak of 52  $\text{nmol L}^{-1}$ ) in the oxycline, while concentrations remained relatively low in surface waters (from 6.6 to 9.3  $\text{nmol L}^{-1}$ , at 5 m) and at 70 m (from 0.1 to 16.4  $\text{nmol L}^{-1}$ ) (Figure 5d). The maximum peaks of  $\text{N}_2\text{O}$  were usually observed below the maximum peaks of  $\text{NO}_3^-$  concentrations (Figure 5e), and sometimes with a time delay. Three  $\text{NO}_3^-$  accumulation zones (nitraclines) were observed: from late January to June 2012, from late August to late December 2012, and from late August to September 2013. Maximum  $\text{NO}_3^-$  concentrations associated to these nitraclines ranged between 7 and 10  $\mu\text{mol L}^{-1}$ .  $\text{NH}_4^+$  concentrations tended to be higher in anoxic waters, with concentrations up to 110  $\mu\text{mol L}^{-1}$  at 70 m depth (Figure 5f). In oxic surface waters (at 5 m),  $\text{CH}_4$  concentrations (Figure 5g) remained low throughout the year and ranged between 19 and 103  $\text{nmol L}^{-1}$ . At 70 m,  $\text{CH}_4$  concentrations were higher and ranged from  $\sim 113,000$  to 520,000  $\text{nmol L}^{-1}$ .

$\text{N}_2\text{O}$  concentrations at 5 m depth showed no correlation to SSI (Figure 6a). The seasonal variations of  $\text{NO}_3^-$  concentrations and SSI were linked (Figure 6b): when vertical mixing occurred (low SSI; August and September 2012 and 2013),  $\text{NO}_3^-$  concentrations began to increase to reach their maximum 1-2 months later. Contrary to  $\text{N}_2\text{O}$ ,  $\text{CH}_4$  concentrations in surface waters followed the pattern of the SSI (Figure 6c) and were significantly correlated ( $R^2 = 0.23$ ,  $p < 0.01$ ,  $n = 29$ ); minima of  $\text{CH}_4$  concentrations co-occurred with SSI minima.

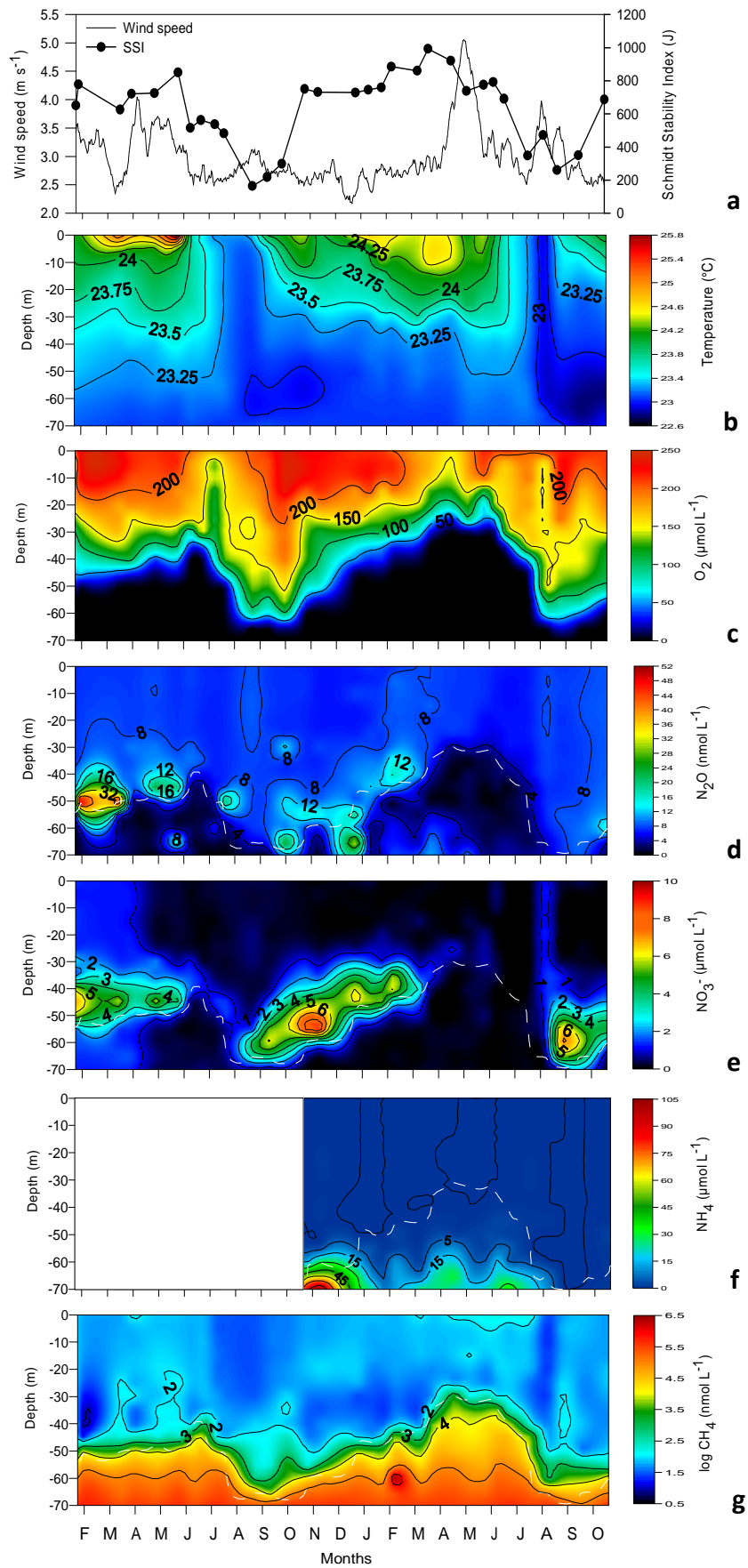


**Figure 5:** Seasonal profiles of (a) wind speed ( $\text{m s}^{-1}$ ) and Schmidt Stability Index (SSI; J), and seasonal and vertical depth profiles of (b) temperature ( $^{\circ}\text{C}$ ), (c)  $\text{O}_2$  ( $\mu\text{mol L}^{-1}$ ), (d)  $\text{N}_2\text{O}$  ( $\text{nmol L}^{-1}$ ), (e)  $\text{NO}_3^-$  ( $\mu\text{mol L}^{-1}$ ), (f)  $\text{NH}_4^+$  ( $\mu\text{mol L}^{-1}$ ) and (g)  $\log \text{CH}_4$  ( $\text{nmol L}^{-1}$ ) from late January 2012 to October 2013, from late October 2012 to October 2013. White dotted line is the oxic-anoxic transition zone.

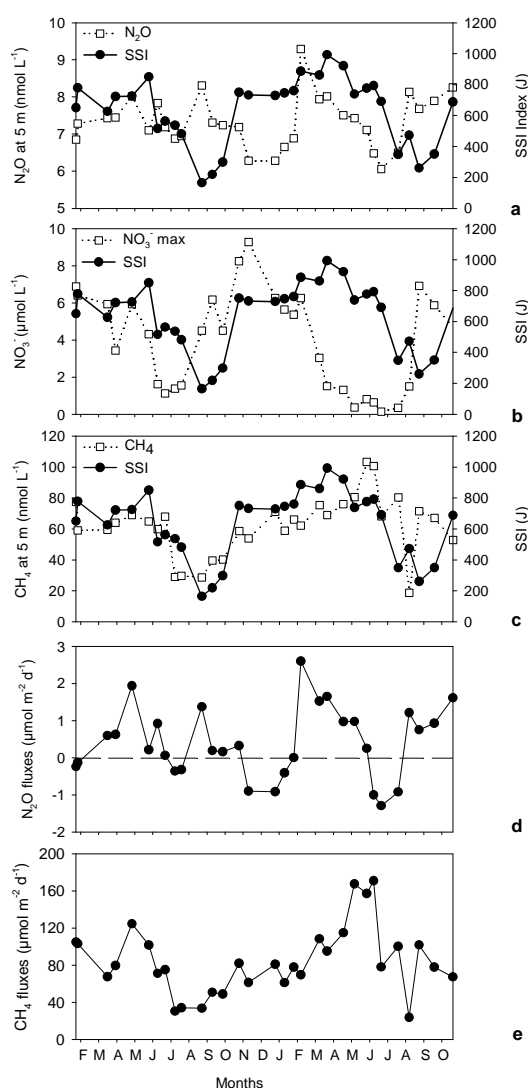


**Figure 6:** (a), (b) and (c) Comparison between Schmidt Stability Index (SSI; J; black circles) and  $\text{N}_2\text{O}$  concentrations ( $\text{nmol L}^{-1}$ ; white squares) at 5 m depth, maximum  $\text{NO}_3^-$  concentrations ( $\mu\text{mol L}^{-1}$ ; white squares) and  $\text{CH}_4$  concentrations ( $\text{nmol L}^{-1}$ ; white squares) at 5 m depth, respectively; (d) and (e) Atmospheric  $\text{N}_2\text{O}$  and  $\text{CH}_4$  fluxes ( $\mu\text{mol m}^{-2} \text{d}^{-1}$ ), respectively, from late January 2012 to October 2013.

$\text{N}_2\text{O}$  fluxes (Figure 6d) showed large fluctuations during the studied period. Negative fluxes were observed in January 2012, July-August 2012, November 2012-January 2013 and June-August 2013 (ranging between  $-2.2$  and  $-0.001 \mu\text{mol m}^{-2} \text{d}^{-1}$ ). The rest of the year,  $\text{N}_2\text{O}$  fluxes were positive, with a maximum flux of  $3.5 \mu\text{mol m}^{-2} \text{d}^{-1}$  in February 2013. The average  $\text{N}_2\text{O}$  flux for both years of sampling was  $0.4 \mu\text{mol m}^{-2} \text{d}^{-1}$ . The highest  $\text{CH}_4$  flux to the atmosphere was in June 2013 ( $222 \mu\text{mol m}^{-2} \text{d}^{-1}$ ) and the lowest was in August 2013 ( $24 \mu\text{mol m}^{-2} \text{d}^{-1}$ ) (Figure 6e). The average  $\text{CH}_4$  flux for the two

years of sampling was  $85 \mu\text{mol m}^{-2} \text{d}^{-1}$ . The seasonal differences in  $\text{CH}_4$  fluxes were very low (rainy season mean flux of  $96 \mu\text{mol m}^{-2} \text{d}^{-1}$  and dry season mean flux of  $64 \mu\text{mol m}^{-2} \text{d}^{-1}$ ).

## 2.5 Discussion

The alternation between stratification of the water column in rainy season and mixing events in dry season is a typical behavior for Lake Kivu (Schmid and Wüest, 2012). Mixing periods did not co-occur with higher wind speeds, which were observed a few weeks before the mixing. This strongly suggests that wind stress is not the main factor for the mixing of the water column in Lake Kivu contrary to what is reported for the nearby Lake Tanganyika (Thiery et al., 2014b). Indeed, increased heat fluxes due to evaporation related to changes in solar radiation and air humidity is the main driver of mixing during the dry season in Lake Kivu (Thiery et al., 2014b).

$\text{N}_2\text{O}$  fluxes fluctuated widely during the two-year sampling, and we observed both positive and negative fluxes, indicating that Lake Kivu acted as a sink and a source for atmospheric  $\text{N}_2\text{O}$ .  $\text{N}_2\text{O}$  fluxes are driven by nitrification/denitrification processes in the water column. Nitrification is considered as an important source of  $\text{N}_2\text{O}$ , while denitrification, by consuming  $\text{N}_2\text{O}$  to produce  $\text{N}_2$ , is often considered as a sink. However, in the oxic-anoxic transition zone, when  $\text{O}_2$  level is low (below  $6 \mu\text{mol L}^{-1}$ ), the last step of denitrification, i.e.  $\text{N}_2\text{O}$  reduction to  $\text{N}_2$ , can be inhibited while the  $\text{NO}_3^-$  reduction to  $\text{N}_2\text{O}$  step can still occur leading to a net  $\text{N}_2\text{O}$  production (Seitzinger et al., 2006). A few factors allow us to suggest the occurrence of these two processes in the water column of Lake Kivu.  $\text{N}_2\text{O}$  profiles, showed on some occasions concentrations peaks in the oxycline, a common feature for meromictic lakes (Mengis et al., 1997). Nitrification was evidenced by the presence of  $\text{NO}_3^-$  accumulation zones (nitraclines) during the rainy season, which in turn can sustain denitrification in the anoxic water column. Nitraclines are the result of vertical mixing of superficial waters occurring during the dry season. During this vertical mixing event, oxygen penetrated deep in the water column, down to the bottom of the mixolimnion, where reduced species such as  $\text{NH}_4^+$  are abundant.  $\text{NH}_4^+$  thus became available for phytoplankton and nitrifying bacteria and archaea growth. Accordingly, nitrification led to the establishment of a nitracline that appeared with some delay after the initial mixing event that brought  $\text{NH}_4^+$  in contact with oxic waters. The fact that maximums of  $\text{NO}_3^-$  concentrations were observed 1-2 months after the mixing event (reflected by SSI) can be explained by the time required for the nitrifier community to develop and for  $\text{NO}_3^-$  to accumulate in the water column.

In late January 2012, high  $\text{N}_2\text{O}$  values were observed in oxic waters (e.g., 47.5 m) corresponding to maximum  $\text{NO}_3^-$  values. The presence of higher abundances of a  $\text{NO}_2^-$ -oxidizing bacteria (*Nitrospira*) (İnceoğlu et al., 2015a) at those depths strongly suggests the occurrence of nitrification. Nitrification rates in Lake Kivu have never been directly quantified, but the study of Llíros et al. (2010) showed the



presence of a nitrifying archaeal community in the oxycline, suggesting a potentially important role of archaeal nitrification. In late January 2012, a diversified archaeal community was also observed (İnceoğlu et al., 2015a). The *Marine Group I (Thaumarcheota)*, which are ammonia oxidizing archaea (AOA), was well represented in the superficial oxic waters, where they represented the whole archaeal community at some depths. AOA are thought to be dominant over ammonia oxidizing bacteria (AOB) in most environments (Stieglmeier et al., 2014), and they seem to be predominant in oligotrophic environments (Stahl and De La Torre, 2012), such as the oxic waters of Lake Kivu (Llirós et al., 2010; İnceoğlu et al., 2015a). However, some N<sub>2</sub>O peaks were clearly located in anoxic waters, as in late January 2012 which suggest the involvement of other processes in N<sub>2</sub>O production, such as denitrification. Pyrosequencing data obtained by İnceoğlu et al. (2015a) showed the presence of *Betaproteobacteria*, which were highly abundant at the oxic-anoxic interface. This class includes in particular two well-known denitrifiers, *Denitratisoma* sp. and *Thiobacillus* sp., which can potentially be responsible for denitrification in Lake Kivu, and some bacterial nitrifiers, such as *Nitrosomonas* sp. As nitrification, denitrification has never been quantified in Lake Kivu, but conditions for the occurrence of this process are present in rainy season, since non-negligible NO<sub>3</sub><sup>-</sup> concentrations are often observed at the oxic-anoxic interface.

Deep isoclines of CH<sub>4</sub> concentrations followed the bottom of the oxycline, strongly suggesting the occurrence of CH<sub>4</sub> oxidation in the water column of Lake Kivu, as recently evidenced by mass balance (Borges et al., 2011; Pasche et al., 2011) or stable isotopic signature and processes measurement studies (Morana et al., 2015b; Morana et al., 2015a). İnceoğlu et al. (2015a) observed the presence of an important community of aerobic and anaerobic methanotrophs (mainly *Methylomonas*-related operational taxonomic units and anaerobic methanotrophic archaea (ANME), respectively) in the Southern Basin (Ishungu Basin) of Lake Kivu, giving support to the occurrence of intense CH<sub>4</sub> oxidation in the water column. They also observed archaeal methanogens which suggested that methanogenesis could occur in the water column, whereas previous research on CH<sub>4</sub> dynamics assumed that sediments were the only source of CH<sub>4</sub> in Lake Kivu Pasche et al. (2011). In aquatic environments, CH<sub>4</sub> is mainly produced in sediments but some studies also reported CH<sub>4</sub> production in anoxic waters (e.g. Winfrey and Zeikus, 1979; Iversen et al., 1987; Borrel et al., 2011; Crowe et al., 2011).

During our study, CH<sub>4</sub> concentrations at 5 m were significantly correlated with SSI and were higher during the rainy season (high SSI) than during the dry season (low SSI). During the rainy season, the oxic layer became thinner and anoxic waters rich in CH<sub>4</sub> were closest to the surface, limiting CH<sub>4</sub> losses by aerobic oxidation. On the contrary, during the dry season the oxic layer deepened and integrated aerobic CH<sub>4</sub> oxidation on the oxic water column might be higher leading to lower CH<sub>4</sub> concentrations in surface waters. In general, the seasonal amplitude of CH<sub>4</sub> concentrations in surface

waters was low (84 nmol L<sup>-1</sup>) compared to higher latitude lakes (range: 100–65,000 nmol L<sup>-1</sup>; Table 3). This might be explained by the large CH<sub>4</sub> accumulation during winter below the frozen lake surface and by more frequent lake overturn which mixes deep and surface waters, a typical process in holomictic lakes unlike Lake Kivu which is permanently stratified. Seasonal changes in oxic and anoxic conditions also contribute to seasonal amplitudes, as anoxia can develop through the water column below frozen lake surface leading to very high CH<sub>4</sub> concentrations. Seasonal variations of oxic layer thickness was highlighted in the present case of Lake Kivu as the driver of seasonal variations.

**Table 3:** Seasonal amplitudes of CH<sub>4</sub> concentrations (nmol L<sup>-1</sup>) in the surface waters of lakes from literature compared with Lake Kivu. Please note that the values in the table are the differences between the annual maximum and minimum, and not the annual mean value.

Seasonal CH <sub>4</sub> amplitude in surface waters (nmol L <sup>-1</sup> )	Lake name	Country	Reference
525	Kuivajärvi	Finland	Miettinen et al. (2015)
19,400	Mekkojärvi	Finland	Kankaala et al. (2013)
8,900	Nimetön	Finland	Kankaala et al. (2013)
300	Tavilampi	Finland	Kankaala et al. (2013)
810	Horkkajärvi	Finland	Kankaala et al. (2013)
320	Valkea-Kotinen	Finland	Kankaala et al. (2013)
350	Onkimajärvi	Finland	Kankaala et al. (2013)
70	Alinen Autjärvi	Finland	Kankaala et al. (2013)
90	Ekojärvi	Finland	Kankaala et al. (2013)
6	Pääjärvi	Finland	Kankaala et al. (2013)
10	Kuohijärvi	Finland	Kankaala et al. (2013)
1,120	Rotsee	Switzerland	Schubert et al. (2010)
65,000	Crystal Bog	Wisconsin (USA)	Riera et al. (1999)
40,000	Trout Bog	Wisconsin (USA)	Riera et al. (1999)
800	Crystal Lake	Wisconsin (USA)	Riera et al. (1999)
1,750	Sparkling Lake	Wisconsin (USA)	Riera et al. (1999)
285	Long Lake	Colorado (USA)	Smith and Lewis Jr (1992)
1,000	Pass Lake	Colorado (USA)	Smith and Lewis Jr (1992)
3,570	Rainbow Lake	Colorado (USA)	Smith and Lewis Jr (1992)
4,000	Dillon Lake	Colorado (USA)	Smith and Lewis Jr (1992)
84	Kivu	Rwanda/DRC	<b>This study</b>

The importance of CH<sub>4</sub> oxidation in the water column of Lake Kivu may explain low CH<sub>4</sub> fluxes observed. Only diffusive CH<sub>4</sub> fluxes are reported here, since ebullitive fluxes are supposed to be negligible due to the deepness of Lake Kivu and absence of extensive shallow zones (Borges et al., 2011), that according to Natchimuthu et al. (2015) contribute to strong spatial heterogeneity in CH<sub>4</sub> emissions from small shallow lakes. It should be noted that the parameterization used in the present work (Cole and Caraco, 1998) might underestimate the computations of gas transfer velocities due to the large size (Read et al., 2012; Schilder et al., 2013) and diurnal temperature variations (Polsenaere

et al., 2013; Podgrajsek et al., 2014) in Lake Kivu which have been reported to be large (Borges et al., 2012). Anyway, the Southern Basin of Lake Kivu was a source of CH<sub>4</sub> for the atmosphere throughout the year, but was a very small source of CH<sub>4</sub> for the atmosphere compared to other lakes globally, by an order of magnitude. The overall CH<sub>4</sub> emission for lakes is 3,281 μmol m<sup>-2</sup> d<sup>-1</sup> globally, and 7,779 μmol m<sup>-2</sup> d<sup>-1</sup> for tropical systems according to Bastviken et al. (2011), whereas the value for Lake Kivu was 85 μmol m<sup>-2</sup> d<sup>-1</sup>. Besides CH<sub>4</sub> oxidation, the low CH<sub>4</sub> emission can also be linked to the morphometric characteristics of Lake Kivu: large, deep and meromictic. Indeed, despite the fact that deep waters of Lake Kivu are extremely rich in CH<sub>4</sub> (60 km<sup>3</sup> of CH<sub>4</sub> are dissolved in deep waters; Schmid et al., 2005), the stratification of the water column (especially the main chemocline located at 250 m; Pasche et al., 2009) prevents the upward rise of this CH<sub>4</sub> towards surface waters. CH<sub>4</sub> from the upper part of the monimolimnion can only rise to surface waters by slow diffusion throughout the year, and by seasonal mixing of the epilimnion, which erodes the upper part of the monimolimnion (Borges et al., 2011; Pasche et al., 2011). Thus, due to this water column structure and an important bacterial CH<sub>4</sub> oxidation, surface waters of Lake Kivu have extremely low CH<sub>4</sub> concentrations when compared with bottom waters, which limits the CH<sub>4</sub> emissions to the atmosphere. Accordingly, the seasonal variations of CH<sub>4</sub> fluxes were estimated to be very low (rainy season mean flux of 96 μmol m<sup>-2</sup> d<sup>-1</sup> and dry season mean flux of 64 μmol m<sup>-2</sup> d<sup>-1</sup>).

This study focused on one station in the Southern Basin of Lake Kivu. However, due to the large size of Lake Kivu, some spatial heterogeneity can be observed. Numerous studies underline the importance of spatial variations of CH<sub>4</sub> emissions (e.g. Bastviken et al., 2004, Hofmann, 2013, Schilder et al., 2013, Natchimuthu et al., 2015). During our study, 5 profiles were collected in the Northern Basin of the lake, which has a larger surface and is more exposed to wind. Available data (Figure 7) suggest that the station of Ishungu, in the Southern Basin, is not representative of the whole lake, since large differences in stratifications can be observed. Indeed, the Northern Basin showed deeper mixings and more pronounced gradients, which clearly influence vertical profiles of CH<sub>4</sub> and N<sub>2</sub>O. The differences between the depths of the oxyclines impacted CH<sub>4</sub> concentrations in deep waters, and N<sub>2</sub>O profiles were also quite different. Stratification clearly influences bacterial and archaeal communities; for example, Inceoğlu et al. (2015a) estimated that the relative abundances of *Betaproteobacteria* were 28% and 46% for the Northern and Southern Basins, respectively. Moreover, due to the large size of the lake, we cannot expect that wind velocities in the Northern Basin are the same as those in the Southern Basin.

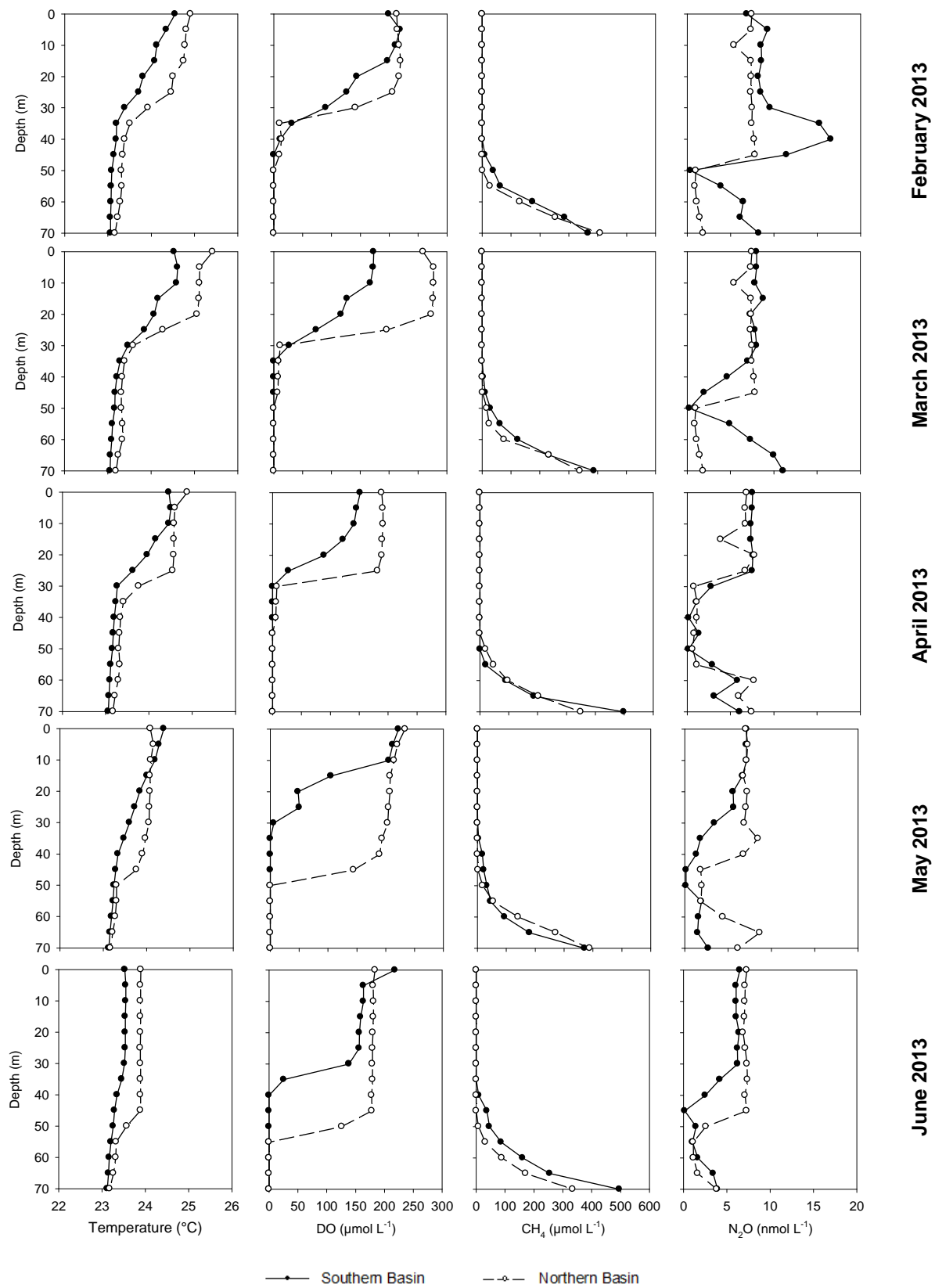


**Figure 7:** Temperature ( $^{\circ}\text{C}$ ), dissolved oxygen (DO;  $\mu\text{mol L}^{-1}$ ),  $\text{CH}_4$  concentrations ( $\mu\text{mol L}^{-1}$ ) and  $\text{N}_2\text{O}$  concentrations ( $\text{nmol L}^{-1}$ ) in the Southern Basin and in the Northern Basin from February to June 2013. The position of the Northern Basin station is shown in Figure 8.

However, CH<sub>4</sub> concentrations in surface waters (at 5 m) were quite similar in both stations ( $R^2 = 0.625$ ), and means of N<sub>2</sub>O concentrations in surface waters were 7 and 8 nmol L<sup>-1</sup> in the Northern and Southern Basins, respectively. This suggests that CH<sub>4</sub> and N<sub>2</sub>O fluxes in the Northern Basin are probably of the same order of magnitude as in the Southern Basin. Also, based on O<sub>2</sub> and temperature vertical profiles data obtained from March 2007 to April 2009 at 9 stations in the lake (Borges et al., 2011), we can assume that the station of Ishungu is well representative of the Southern Basin, and even of the Western Basin and of the south part of the Eastern Basin (Figure 8 and Table 4).

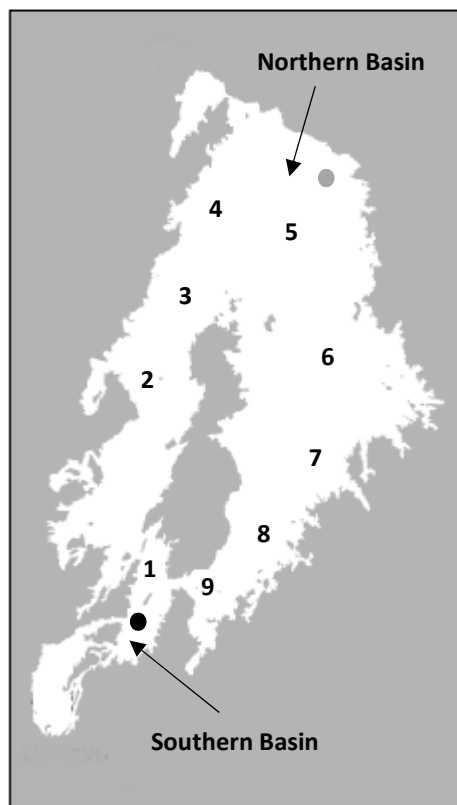


**Figure 8:** Map of Lake Kivu, showing the 9 stations sampled in March 2007, June 2008 and April 2009 (Borges et al., 2011). The black dot is the station of Ishungu and the grey dot is the station in the Northern Basin described in Figure 7.

**Table 4:** Regression coefficients ( $R^2$ ) of dissolved oxygen (DO) and temperature between the station of Ishungu and 9 stations in the lake (Figure 8), in March 2007, June 2008 and April 2009, for vertical profiles from 0 to 60 m depth, with 10 m-interval. For the three campaigns, the station of Ishungu is well correlated with stations 1 (Southern Basin), 2 (Western Basin), 8 and 9 (south part of the Eastern Basin) for both parameters.

Station	DO	Temperature
<i>March 2007</i>		
1	0.968	0.870
2	0.943	0.935
3	0.886	0.571
4	0.658	0.409
5	0.865	0.743
6	0.889	0.722
7	0.900	0.754
8	0.882	0.670
9	0.953	0.804
<i>June 2008</i>		
1	0.924	0.612
2	0.708	0.707
3	0.294	0.155
4	0.518	0.695
5	0.594	0.612
6	0.364	0.660
7	0.564	0.214
8	0.677	0.747
9	0.677	0.747
<i>April 2009</i>		
1	0.982	0.891
2	0.935	0.888
3	0.822	0.903
4	0.639	0.819
5	0.853	0.931
6	0.775	0.877
7	0.740	0.814
8	0.880	0.914
9	0.847	0.909

This study is, to our knowledge, the first one to report detailed data and long time-series of CH<sub>4</sub> and N<sub>2</sub>O in a large tropical lake. Our data confirms that Lake Kivu has a very low CH<sub>4</sub> emission to the atmosphere despite having extremely large quantities of CH<sub>4</sub> in the bottom waters. Yet, CH<sub>4</sub> in surface waters showed seasonal variations that relate mixing events and deepening of the mixolimnion. The emissions of N<sub>2</sub>O to the atmosphere were also modest although vertical profiles of N<sub>2</sub>O show dynamic patterns with marked sources and sinks of N<sub>2</sub>O in the water column. We were not able to determine from vertical profiles of N<sub>2</sub>O concentrations if nitrification or denitrification or a combination of both was the process leading to N<sub>2</sub>O accumulation in the water column that occurred at the oxic-anoxic interface. This suggests that process orientated studies quantifying denitrification and nitrification are required to further unravel C and N dynamics in this large meromictic tropical lake, as well as additional data on bacterial diversity and activity that are limited to two samplings (Inceoğlu et al., 2015b; Inceoğlu et al., 2015a). The present data-set is the first to give a detailed description of the seasonal variations of the vertical distribution of CH<sub>4</sub> and N<sub>2</sub>O in upper Lake Kivu (<100 m). Any deviation from the reported patterns will be indicative of changes in CH<sub>4</sub> and N<sub>2</sub>O cycling and potential emission to the atmosphere related to the CH<sub>4</sub> extraction (Nayar, 2009). Once the CH<sub>4</sub> is extracted in surface plants, the water is re-injected above the extraction point (to avoid diluting the resource). This re-injection could lead to the enrichment in NH<sub>4</sub><sup>+</sup> and changes in N cycling which could enhance N<sub>2</sub>O emissions to the atmosphere. The water re-injection might lead to changes in water column stratification that as we have shown allows an effective removal of upward diffusing CH<sub>4</sub> by bacterial CH<sub>4</sub> oxidation. A decrease in this water column CH<sub>4</sub> sink would lead to enhanced CH<sub>4</sub> emissions to the atmosphere.

---

## Chapter 3: Anaerobic methane oxidation in an East African great lake (Lake Kivu)

---

**Adapted from:** Fleur A. E. Roland, François Darchambeau, Cédric Morana, Sean A. Crowe, Bo Thamdrup, Jean-Pierre Descy and Alberto V. Borges (submitted) *Anaerobic methane oxidation in an East African great lake (Lake Kivu)*, *Journal of Great Lakes Research*

### 3.1 Abstract

This study investigates methane (CH<sub>4</sub>) oxidation in the water column of Lake Kivu, a deep meromictic tropical lake containing large quantities of CH<sub>4</sub> in the anoxic deep waters. Depth profiles of dissolved gases (CH<sub>4</sub> and nitrous oxide (N<sub>2</sub>O)) and of the different potential electron acceptors for anaerobic methane oxidation (AOM) (nitrate, sulfate, iron and manganese) were determined during six field campaigns between June 2011 and August 2014. Denitrification measurements based on stable isotopes were performed twice. Incubation experiments were performed to quantify CH<sub>4</sub> oxidation and nitrate consumption rates, with a focus on AOM, without and with an inhibitor of sulfate-reducing bacteria activity (molybdate). Nitrate consumption rates were measured in these incubations during all field campaigns, and sulfate consumption rates were measured in August 2014. CH<sub>4</sub> production was also measured in parallel incubations by addition of picolinic acid, an inhibitor of CH<sub>4</sub> oxidation, during three field campaigns, with rates up to 370 nmol L<sup>-1</sup> d<sup>-1</sup>. Substantial CH<sub>4</sub> oxidation activity was observed in oxic and anoxic waters, and in the upper anoxic waters of Lake Kivu, CH<sub>4</sub> is a major electron donor to sustain anaerobic metabolic processes coupled to AOM. The maximum aerobic and anaerobic CH<sub>4</sub> oxidation rates were estimated to 27 ± 2 and 16 ± 8 μmol L<sup>-1</sup> d<sup>-1</sup>, respectively. We observed a decrease of AOM rates when molybdate was added for half of the measurements, strongly suggesting the occurrence of AOM linked to sulfate reduction, but an increase of AOM rates was observed for the other half. Nitrate reduction rates and dissolved manganese production rates tended to be higher with the addition of molybdate, but the maximum rates of 0.6 ± 0.02 and 11 ± 2 μmol L<sup>-1</sup> d<sup>-1</sup>, respectively, were not high enough to explain AOM rates observed at the same depths. We also put in evidence a difference in the relative importance of aerobic and anaerobic CH<sub>4</sub> oxidation between the seasons, with a higher importance of aerobic oxidation when the oxygenated layer was thicker (in the dry season).



### 3.2 Introduction

Due to its potential impact in global warming and its increase due to human activities, the biogeochemical cycle of methane ( $\text{CH}_4$ ) raises great interest, and methanogenesis and methanotrophy have been widely studied in a large variety of environments. In natural environments,  $\text{CH}_4$  is produced anaerobically by methanogenic archaea. Recent studies also suggest that  $\text{CH}_4$  can be produced in oxic conditions, by oxygen tolerant methanogenic archaea coupled to phytoplankton activity (Grossart et al., 2011; Bogard et al., 2014; Tang et al., 2014; Tang et al., 2016). The total  $\text{CH}_4$  emission has been recently estimated to 553 Tg  $\text{CH}_4 \text{ yr}^{-1}$  for the period 2000-2009, from which 64 % is emitted by tropical areas (Kirschke et al., 2013; Saunio et al., 2016). Decadal variations in the annual atmospheric  $\text{CH}_4$  growth rate have also been attributed to changes in emissions from tropical wetlands (Nisbet et al., 2016). Previous studies estimated that 9.5% of  $\text{CH}_4$  is released from tropical freshwaters and the rest from non-tropical freshwaters (13.5%), marine ecosystems (3%), human activities (63%), plants (6%), gaseous hydrates (2%) and termites (3%) (Conrad, 2009; Bastviken et al., 2011). The real amount of  $\text{CH}_4$  produced in these systems is higher, but a significant percentage is biologically oxidized (aerobically or anaerobically) before reaching the atmosphere (Bastviken et al., 2002). Anaerobic  $\text{CH}_4$  oxidation (AOM) has been widely observed in marine environments, where it is mainly coupled to sulfate ( $\text{SO}_4^{2-}$ ) reduction (e.g. Iversen and Jørgensen, 1985; Boetius et al., 2000; Jørgensen et al., 2001). Comparatively, in situ AOM has been less frequently measured in freshwaters environments (e.g. in Lake Rotsee; Schubert et al., 2010), and is often considered as negligible compared to aerobic  $\text{CH}_4$  oxidation due to lower  $\text{SO}_4^{2-}$  concentrations than in seawater (Rudd et al., 1974). However, other potential electron acceptors for AOM, such as nitrate ( $\text{NO}_3^-$ ), iron (Fe) and manganese (Mn) (Borrel et al., 2011; Cui et al., 2015), can be found in non-negligible concentrations in freshwater environments. AOM coupled to  $\text{NO}_3^-$  reduction (NDMO) has been exclusively observed in laboratory environments (e.g. Raghoebarsing et al., 2006; Ettwig et al., 2010; Hu et al., 2011; Haroon et al., 2013; Norði and Thamdrup, 2014), and its natural significance is still unknown. Also, AOM coupled to Fe and Mn reduction has been proposed to occur in some freshwater environments (e.g. in lakes Matano and Kinneret; Crowe et al., 2011; Sivan et al., 2011; Norði et al., 2013) and marine sediments (Beal et al., 2009), but to our best knowledge, no in situ measurements have been reported in the literature.

Lake Kivu is a deep (maximum depth: 485 m) meromictic lake characterized by a high amount of  $\text{CH}_4$  (60 km<sup>3</sup> at 0°C and 1 atm) dissolved in its deep anoxic waters. Paradoxically, this lake is a very low emitter of  $\text{CH}_4$  to the atmosphere due to intense  $\text{CH}_4$  oxidation (Borges et al., 2011; Roland et al., 2016). It is divided in different basins and bays. In the water column of the main basin,  $\text{SO}_4^{2-}$  concentrations are relatively high (100-200  $\mu\text{mol L}^{-1}$ ; Morana et al., 2016) and a large  $\text{SO}_4^{2-}$ -reducing bacteria (SRB) community is present and co-occurs with methanotrophic archaea (İnceoğlu et al.,

2015a). The data based on 16S rRNA strongly suggest the occurrence of AOM coupled to  $\text{SO}_4^{2-}$  reduction (SDMO), although it remains to be demonstrated in a direct way and quantified. Also, a  $\text{NO}_3^-$  accumulation zone (nitracline) is often present during the rainy season at the oxic-anoxic interface (Roland et al., 2016), and can potentially contribute to AOM. Based on these observations, we hypothesize that  $\text{SO}_4^{2-}$  could be the unique electron acceptor involved in AOM during the dry season, while AOM coupled with  $\text{NO}_3^-$  reduction (NDMO) could also contribute during the rainy season at a lower extent. Potential AOM linked to Fe and Mn reduction will also be investigated. In order to fully investigate  $\text{CH}_4$  cycle in the water column of Lake Kivu, we also measured  $\text{CH}_4$  production in the oxic compartment.

### 3.3 Material and methods

#### 3.3.1 Sampling sites

Lake Kivu is an East African great lake located at the border between Rwanda and the Democratic Republic of the Congo (Figure 3). It is divided into one main basin, two small basins and two bays: Northern Basin (or main basin), Southern Basin (or Ishungu Basin), Western Basin (or Kalehe Basin), the bay of Kabuno in the north and the bay of Bukavu in the South.

Six field campaigns were conducted in the main basin (the Northern Basin off Gisenyi; - 1.72504°N, 29.23745°E) in June 2011 (early dry season), February 2012 (rainy season), October 2012 (late dry season), May 2013 (late rainy season), September 2013 (dry season) and August 2014 (dry season).

#### 3.3.2 Physico-chemical parameters and sampling

Vertical profiles of temperature, conductivity, pH and oxygen were obtained with a Yellow Springs Instrument 6600 V2 multiparameter probe. Water was collected with a 7L Niskin bottle (Hydro-Bios) every 2.5 m in a ~10 m zone centered at the oxic-anoxic interface.

#### 3.3.3 Chemical analyses

Samples for  $\text{CH}_4$  and  $\text{N}_2\text{O}$  concentrations, and  $\text{CH}_4$  oxidation measurements were collected in 60 ml glass serum bottles, filled directly from the Niskin bottle with tubing, left to overflow, and sealed with butyl stoppers and aluminium caps. Two bottles were directly poisoned with 200  $\mu\text{l}$  of  $\text{HgCl}_2$  injected through the septum with a syringe. Ten other bottles were incubated in the dark and at constant temperature close to in situ temperature (~23°C). Five of them received 250  $\mu\text{l}$  of a solution of sodium molybdate, an inhibitor of sulfate-reducing bacteria activity (1 mol  $\text{L}^{-1}$ ; hence a final concentration of 4 mmol  $\text{L}^{-1}$ ), and five received no treatment. In May 2013, September 2013 and August 2014, five supplementary bottles received 500  $\mu\text{l}$  of a solution of picolinic acid, an inhibitor of

CH<sub>4</sub> oxidation (6 mmol L<sup>-1</sup>; final concentration of 0.1 mmol L<sup>-1</sup>). The bacterial activity of these ten bottles was stopped at 12, 24, 48, 72 and 96h by the addition of 200 µl of a saturated solution of HgCl<sub>2</sub>. CH<sub>4</sub> and N<sub>2</sub>O concentrations were determined via the headspace equilibration technique (20 mL N<sub>2</sub> headspace in 50 mL serum bottles, for samples of the main basin) and measured by gas chromatography (GC) (Weiss, 1981) with electron capture detection (ECD) for N<sub>2</sub>O and with flame ionization detection (FID) for CH<sub>4</sub>, as described by (Borges et al., 2015a). The SRI 8610C GC-ECD-FID was calibrated with certified CH<sub>4</sub>:CO<sub>2</sub>:N<sub>2</sub>O:N<sub>2</sub> mixtures (Air Liquide, Belgium) of 1, 10, 30 and 509 ppm CH<sub>4</sub> and of 0.2, 2.0 and 6.0 ppm N<sub>2</sub>O. Concentrations were computed using the solubility coefficients of Yamamoto et al. (1976) and Weiss and Price (1980), for CH<sub>4</sub> and N<sub>2</sub>O, respectively. The precision of measurements was ±3.9% and ±3.2% for CH<sub>4</sub> and N<sub>2</sub>O, respectively.

Samples for nutrients analyses were collected in 50 ml plastic vials after being filtered through a 0.22 µm syringe filter. 200 µl of H<sub>2</sub>SO<sub>4</sub> 5N were added at each vial for preservation. Samples were then frozen. NO<sub>2</sub><sup>-</sup> and NO<sub>3</sub><sup>-</sup> concentrations were estimated by spectrophotometry. NO<sub>2</sub><sup>-</sup> concentrations were determined by the sulfanilamide coloration method (APHA 1998), using a 5-cm light path on a spectrophotometer Thermo Spectronic Genesys 10vis. NO<sub>3</sub><sup>-</sup> concentrations were determined after vanadium reduction to NO<sub>2</sub><sup>-</sup> and quantified under this form with a Multiskan Ascent Thermo Scientific multi-plates reader (APHA, 1998; Miranda et al., 2001). The detection limits for these methods were 0.03 and 0.15 µmol L<sup>-1</sup> for NO<sub>2</sub><sup>-</sup> and NO<sub>3</sub><sup>-</sup>, respectively. When making the headspaces for CH<sub>4</sub> measurements as described above, the excess water was collected and used to quantify the evolution of NO<sub>3</sub><sup>-</sup> concentrations in the incubations (reported as NO<sub>3</sub><sup>-</sup> consumption rates), according to the method previously described.

Samples for sulfide (HS<sup>-</sup>) concentrations were collected in 50 ml plastic vials, after being filtered on a 0.22 µm syringe filter. Samples were preserved with 200 µl of 20% zinc acetate (ZnAc) and were stored frozen. HS<sup>-</sup> concentrations were quantified using a 5-cm light path on a spectrophotometer, according to the method described by Cline (1969). Samples for SO<sub>4</sub><sup>2-</sup> analyses were filtered through a 0.22 µm syringe filter and collected in 5 ml Cryotube vials. Samples were preserved with 20 µl of 20% ZnAc and were stored frozen. SO<sub>4</sub><sup>2-</sup> concentrations were determined by ion chromatography (Dionex ICS-1500, with an autosampler Dionex AS50, a guard column Dionex AG22 and an analytical column Dionex IonPac AS22). The detection limits of these methods were 0.25 and 0.5 µmol L<sup>-1</sup> for HS<sup>-</sup> and SO<sub>4</sub><sup>2-</sup>, respectively. In August 2014, the decrease of SO<sub>4</sub><sup>2-</sup> concentrations in CH<sub>4</sub> incubations was measured by spectrophotometry, using a 5-cm light path on a spectrophotometer Thermo Spectronic Genesys 10vis, according to the nephelometric method described by Rodier et al. (1996), after precipitation of barium sulfate in an acid environment. The detection limit of this method was 52 µmol L<sup>-1</sup>.

**Table 5:** Depth (m) where CH<sub>4</sub> oxidation was observed, presence (+) or absence (-) of oxygen (O<sub>2</sub>), CH<sub>4</sub> oxi = maximum CH<sub>4</sub> oxidation rates (μmol L<sup>-1</sup> d<sup>-1</sup>) calculated based on a linear regression, [CH<sub>4</sub>]<sub>in</sub> = initial CH<sub>4</sub> concentrations (μmol L<sup>-1</sup>) from which the linear regression begins, % CH<sub>4</sub> = percentage of initial CH<sub>4</sub> consumed, and time (h) required for this consumption (time lapse during which the linear regression was applied to calculate CH<sub>4</sub> oxidation rates), without and with molybdate added (- Mo and + Mo, respectively), for all field campaigns. N.d. = not determined.

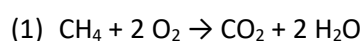
Depth (m)	O <sub>2</sub>	CH <sub>4</sub> oxi (μmol L <sup>-1</sup> d <sup>-1</sup> )		[CH <sub>4</sub> ] <sub>in</sub> (μmol L <sup>-1</sup> )		% CH <sub>4</sub>		Time (h)	
		- Mo	+ Mo	- Mo	+ Mo	- Mo	+ Mo	- Mo	+ Mo
<i>June 2011</i>									
42.5	+	0.3 ± 0.0	N.d.	0.3 ± 0	N.d.	90 ± 0	N.d.	24	N.d.
45	+	2.0 ± 0.0	N.d.	2 ± 0	N.d.	97 ± 0	N.d.	24	N.d.
47.5	-	0.8 ± 0.0	N.d.	18 ± 0	N.d.	23 ± 0	N.d.	96	N.d.
50	-	0.4 ± 0.1	N.d.	21 ± 0	N.d.	10 ± 0	N.d.	96	N.d.
<i>February 2012</i>									
45	-	0.3 ± 0.0	0.1 ± 0.0	1 ± 0	1 ± 0	73 ± 0	66 ± 0	72	72
50	-	7.7 ± 0.4	3.0 ± 0.3	8 ± 0	8 ± 0	64 ± 1	27 ± 2	16	16
55	-	4.0 ± 0.2	4.3 ± 0.0	21 ± 0	21 ± 0	12 ± 1	13 ± 0	16	16
60	-	1.2	0.4	115	105	4	3	72	96
<i>October 2012</i>									
53	+	10.2 ± 0.4	9.3 ± 0.4	10 ± 0	10 ± 0	98 ± 0	97 ± 0	24	24
55	+	0.4 ± 0.7	16.1 ± 5.4	78 ± 4	78 ± 4	2 ± 6	18 ± 5	96	24
57.5	-	0.2 ± 0.5	1.2 ± 0.5	65 ± 3	65 ± 3	4 ± 5	10 ± 5	96	96
60	-	0.0 ± 0.0	2.0 ± 2.6	129 ± 17	129 ± 17	0 ± 0	10 ± 12	96	96
70	-	0.0 ± 0.0	1.2 ± 1.6	344 ± 11	344 ± 11	0 ± 0	2 ± 3	96	96
80	-	0.0 ± 0.0	23.3 ± 0.4	538 ± 2	538 ± 2	0 ± 0	26 ± 0	96	96
<i>May 2013</i>									
40	+	0.1 ± 0.0	N.d.	0.4 ± 0	N.d.	45 ± 2	N.d.	96	N.d.
45	+	0.1 ± 0.0	N.d.	0.7 ± 0	N.d.	63 ± 1	N.d.	72	N.d.
47.5	+	0.6 ± 0.0	0.6 ± 0.0	2 ± 0	2 ± 0	75 ± 1	75 ± 1	48	48
50	+	1.5 ± 0.2	3.3 ± 1.3	20 ± 1	20 ± 1	31 ± 4	18 ± 5	96	72
52.5	+	0.5 ± 0.1	0.2 ± 0.0	25 ± 0	25 ± 0	7 ± 1	7 ± 1	72	96
55	-	1.2	3.8 ± 4.2	45	45 ± 4	8	8 ± 7	96	24
60	-	1.0	5.3 ± 5.6	115	113 ± 4	4	4 ± 4	96	24
65	-	3.2	17.2	227	223	6	6	96	24
70	-	1.5 ± 0.3	1.2 ± 0.0	410 ± 3	410 ± 3	2 ± 1	2 ± 1	120	120
<i>September 2013</i>									
40	+	0.07	N.d.	0.2	N.d.	37	N.d.	48	N.d.
45	+	0.02 ± 0.0	0.0 ± 0.0	0.1 ± 0	0.1 ± 0	73 ± 3	0 ± 0	96	96
47.5	+	13.4 ± 0.3	9.8 ± 0.3	13 ± 0	13 ± 0	93 ± 0	75 ± 1	24	24
50	+	13.9 ± 0.0	10.8 ± 0.0	27 ± 0	27 ± 0	17 ± 0	16 ± 0	12	12
52.5	+	0.2 ± 0.0	0.9 ± 0.0	50 ± 0	50 ± 0	2 ± 0	11 ± 0	96	96
55	-	0.5 ± 0.0	9.2 ± 0.5	90 ± 0	90 ± 0	2 ± 0	4 ± 0	72	12
57.5	-	0.3 ± 0.0	8.1 ± 0.4	99 ± 0	99 ± 0	3 ± 0	3 ± 0	96	12
65	-	3.5 ± 0.3	2.1 ± 0.3	215 ± 1	215 ± 1	6 ± 1	5 ± 1	72	72
<i>August 2014</i>									
55	+	27.1 ± 1.6	17.5 ± 1.6	42 ± 2	42 ± 2	68 ± 1	46 ± 3	24	24
57.5	+	2.1	1.2	69	69	6	4	48	48
60	-	0.0 ± 0.0	4.6	167 ± 20	167 ± 20	0 ± 0	6	96	48
65	-	5.1 ± 0.9	1.2 ± 0.9	275 ± 1	275 ± 1	6 ± 2	3 ± 2	96	96
67.5	-	6.8 ± 7.8	0.0 ± 0.0	358 ± 6	358 ± 6	16 ± 12	0 ± 0	96	96
70	-	3.3 ± 1.3	0.0 ± 0.0	445 ± 10	445 ± 10	6 ± 2	0 ± 0	96	96
75	-	16.0 ± 8.2	0.0 ± 0.0	689 ± 58	689 ± 58	3 ± 8	0 ± 0	96	96

In May 2013, September 2013 and August 2014, samples for Fe and Mn measurements were collected into 50 ml-plastic syringes directly from the Niskin bottle. Water was rapidly transferred from the syringe to the filtration set and was passed through 25 mm glass fiber filters. Filters were collected in 2 ml Eppendorf vials and preserved with 1 ml of a HNO<sub>3</sub> 2% solution, while filtrates were collected into four 2 ml Eppendorf vials and preserved with 20 µl of a HNO<sub>3</sub> 65% solution. The filters, for particulate Fe and Mn determination, were mineralized in specific Teflon bombs into a microwave digestion labstation (Ethos D, Milestone Inc.), after digestion with nitric acid. They were finally diluted into milli-Q water to the volume of 50 ml. Filtrates were directly diluted into milli-Q water to the volume of 50 ml. In August 2014, dissolved Mn and Fe concentrations were also determined in CH<sub>4</sub> incubations in order to measure the evolution of concentrations through time. Fe and Mn concentrations were determined by inductively coupled plasma mass spectrometry (ICP-MS) using dynamic reaction cell (DRC) technology (ICP-MS SCIEX ELAN DRC II, PerkinElmer inc.). Analytical accuracy was verified by a certified reference material (BCR 715, Industrial Effluent Wastewater).

### 3.3.4 CH<sub>4</sub> oxidation and production, NO<sub>3</sub><sup>-</sup> and SO<sub>4</sub><sup>2-</sup> consumption and Mn<sup>2+</sup> production rates calculations

CH<sub>4</sub> oxidation and production, NO<sub>3</sub><sup>-</sup> and SO<sub>4</sub><sup>2-</sup> consumption and Mn<sup>2+</sup> production rates were calculated as a linear regression of CH<sub>4</sub>, NO<sub>3</sub><sup>-</sup>, SO<sub>4</sub><sup>2-</sup> and Mn<sup>2+</sup> concentrations over time during the course of the incubation. Rates reported here are maximum rates, as they were calculated based on the maximum slopes. Table 5 shows standard deviations, initial CH<sub>4</sub> concentrations, percentage of CH<sub>4</sub> consumed and the time laps during which the CH<sub>4</sub> oxidation rates were calculated for each depth. Table 6 shows standard deviations for NO<sub>3</sub><sup>-</sup> and SO<sub>4</sub><sup>2-</sup> consumption and Mn<sup>2+</sup> production rates.

CH<sub>4</sub> oxidation rates with molybdate were corrected taking into account the oxygen supplied by the addition of the solution, which was not anoxic. As molybdate solution was at saturation with respect to O<sub>2</sub>, we considered here that 1.25 µmol L<sup>-1</sup> of O<sub>2</sub> were added to each bottle (250 µl of the solution were added to 60 ml of water). The O<sub>2</sub> concentration required to be responsible for each CH<sub>4</sub> oxidation rate was calculated according to the following stoichiometric equation (Eq. 1):



The part of each oxidation rate due to O<sub>2</sub> was then calculated according to Eq. (2):

$$(2) \text{Ro} = \text{Rm} * (\text{O}_{2r}/\text{O}_{2a})$$

where Ro is the part of each oxidation rate due to O<sub>2</sub> supply, Rm is the measured oxidation rate, O<sub>2r</sub> is the O<sub>2</sub> concentration required to be responsible for the measured CH<sub>4</sub> oxidation rate and O<sub>2a</sub> is the O<sub>2</sub> concentration added by the molybdate solution.

The final CH<sub>4</sub> oxidation rates with molybdate were obtained by subtraction (Eq. 3):

$$(3) \text{ Final CH}_4 \text{ oxidation rate with Mo} = R_m - R_o$$

All rates with molybdate reported here are final CH<sub>4</sub> oxidation rates.

**Table 6:** Anoxic depths (m), NO<sub>3</sub><sup>-</sup> and SO<sub>4</sub><sup>2-</sup> consumption and Mn<sup>2+</sup> production rates (μmol L<sup>-1</sup> d<sup>-1</sup>) and their standard deviation, without and with molybdate added (- Mo and + Mo, respectively), for all campaigns. N.d. = not determined. All rates were calculated based on a linear regression of concentrations through time. Fe<sup>2+</sup> production rates were measured at the same depths than Mn<sup>2+</sup> production rates, but were always equal to zero and are not reported here.

Depth (m)	NO <sub>3</sub> <sup>-</sup> consumption (μmol L <sup>-1</sup> d <sup>-1</sup> )		SO <sub>4</sub> <sup>2-</sup> consumption (μmol L <sup>-1</sup> d <sup>-1</sup> )		Mn <sup>2+</sup> production (μmol L <sup>-1</sup> d <sup>-1</sup> )	
	- Mo	+ Mo	- Mo	+ Mo	- Mo	+ Mo
<i>February 2012</i>						
45	0.01 ± 0.01	0.0 ± 0.0	N.d.	N.d.	N.d.	N.d.
50	0.37 ± 0.07	0.56 ± 0.02	N.d.	N.d.	N.d.	N.d.
55	0.21 ± 0.02	0.0 ± 0.0	N.d.	N.d.	N.d.	N.d.
60	0.01 ± 0.0	0.33 ± 0.0	N.d.	N.d.	N.d.	N.d.
<i>October 2012</i>						
57.5	0.0 ± 0.0	0.0 ± 0.0	N.d.	N.d.	N.d.	N.d.
60	0.0	0.02	N.d.	N.d.	N.d.	N.d.
65	0.0	0.04	N.d.	N.d.	N.d.	N.d.
70	0.0	0.04	N.d.	N.d.	N.d.	N.d.
<i>May 2013</i>						
55	0.0 ± 0.0	0.0 ± 0.0	N.d.	N.d.	N.d.	N.d.
60	0.07	0.0	N.d.	N.d.	N.d.	N.d.
65	0.0 ± 0.0	0.0 ± 0.0	N.d.	N.d.	N.d.	N.d.
70	0.03 ± 0.01	0.25 ± 0.05	N.d.	N.d.	N.d.	N.d.
<i>September 2013</i>						
55	0.0 ± 0.0	0.0 ± 0.0	N.d.	N.d.	N.d.	N.d.
57.5	0.0 ± 0.0	0.0 ± 0.0	N.d.	N.d.	N.d.	N.d.
65	0.0 ± 0.0	0.04 ± 0.01	N.d.	N.d.	N.d.	N.d.
<i>August 2014</i>						
60	0.0 ± 0.0	0.0 ± 0.0	1.0 ± 0.5	N.d.	0.0 ± 0.0	0.0 ± 0.0
62.5	0.0 ± 0.0	0.0 ± 0.0	0.7 ± 0.3	N.d.	0.0 ± 0.0	0.5 ± 0.2
65	0.0 ± 0.0	0.0 ± 0.0	0.0 ± 0.0	N.d.	0.0 ± 0.0	0.0 ± 0.0
67.5	0.0 ± 0.0	0.0 ± 0.0	1.5 ± 0.6	N.d.	0.0 ± 0.0	10.6 ± 1.6
70	0.0 ± 0.0	0.0 ± 0.0	7.5 ± 0.0	N.d.	0.0 ± 0.0	8.1 ± 0.1
75	0.0 ± 0.0	0.0 ± 0.0	0.3 ± 0.03	N.d.	0.0 ± 0.0	0.0 ± 0.0

### 3.3.5 N stable isotope labelling experiments

In May and September 2013, parallel denitrification experiments were conducted in order to link this process with CH<sub>4</sub> oxidation. Water was collected in duplicate in amber 250 ml borosilicate bottles from the Niskin bottle with tubing, left to overflow, and sealed with Teflon-coated screw caps. Before the injection of <sup>15</sup>N-labeled solutions, a 12h pre-incubation period in the dark and at 25°C was

observed in order to allow the consumption of oxygen eventually introduced in the bottles during sampling.

N stable isotope labelling experiments were based on Thamdrup and Dalsgaard (2002). Heterotrophic denitrification was determined by the injection of a  $\text{Na}^{15}\text{NO}_3$  solution in amber bottles, through the stopper (final concentration of  $5 \mu\text{mol L}^{-1}$ ). Six 12 ml vials (Labco Exetainer) were then filled from each of the duplicate bottles and placed in the dark in an incubator at ambient temperature ( $24^\circ\text{C}$ ), which was close to the in situ temperature ( $\sim 23^\circ\text{C}$ ). Microbial activity in two Exetainers was immediately arrested through the addition of  $500 \mu\text{l}$  20% ZnAc. A time course was established by arresting two further Exetainers at 6, 12, 18, 24 and 48 h. While injecting ZnAc solution to stop the incubations of the Exetainers, the excess water was collected in 2 ml-Eppendorf vials, and stored frozen, to determine the evolution of the  $\text{NO}_x^-$  concentrations through time.  $\text{NO}_x^-$  were then analyzed by chemiluminescence, after reduction with vanadium chloride ( $\text{VCl}_3$ ), with an  $\text{NO}_2^-$ ,  $\text{NO}_3^-$  and  $\text{NO}_x$  analyzer (Thermo Environmental Instruments), according to the method described by Braman and Hendrix (1989) (detection limit: 2-3 ng  $\text{NO}_x$ ).

$^{29}\text{N}_2$  and  $^{30}\text{N}_2$  concentrations in the Exetainers were measured with a gas source isotope ratio mass spectrometer (Delta V Plus, ThermoScientific) after creating a 2 ml helium headspace (volume injected in the mass spectrometer:  $50 \mu\text{l}$ ). Potential denitrification rates (detection limits of  $2.7 \text{ nmol L}^{-1} \text{ h}^{-1}$ ) in the incubations with  $^{15}\text{NO}_3^-$  were calculated according to Eq. (4) (Thamdrup and Dalsgaard, 2002):

$$(4) \text{ Potential } \text{N}_2 \text{ denitrification} = {}^{15}\text{N}^{15}\text{N}_{\text{excess}} * (\text{F}_{\text{NO}_3})^{-2}$$

where  $\text{N}_2 \text{ denitrification}$  is the production of  $\text{N}_2$  by denitrification during the incubations with  $^{15}\text{NO}_3^-$ .  ${}^{15}\text{N}^{15}\text{N}_{\text{excess}}$  is the production of excess  ${}^{15}\text{N}^{15}\text{N}$  and  $\text{F}_{\text{NO}_3}$  is the fraction of  $^{15}\text{NO}_3^-$  added in the  $\text{NO}_x^-$  pool.  $\text{NO}_x^-$  concentrations of the  $\text{NO}_x^-$  pool were measured in the incubations as described above.  ${}^{15}\text{N}^{15}\text{N}$  is the excess relative to the mass 30: mass 28 ratio in the time zero gas samples.

Only natural denitrification rates are reported here. Natural denitrification rates were calculated on the base on potential denitrification rates, according to Eq. (5):

$$(5) \text{ Natural } \text{N}_2 \text{ denitrification} = \text{Potential } \text{N}_2 \text{ denitrification} * (1 - \text{F}_{\text{NO}_3}),$$

which assumes that the rate obeys 1<sup>st</sup> order kinetics with respect to  $\text{NO}_3^-$ .

### 3.3.6 Pigment analysis

In May 2013, September 2013 and August 2014, samples for pigments analyses were collected on Whatman GF/F 47 mm glass fiber filters (filtration volumes: 3L). Filters were preserved

in 5 ml Cryotube vials and stored frozen until pigment extraction in 4 ml of 90% HPLC grade acetone. Two 15-min sonications separated by an overnight period at 4°C in dark were applied, and extracts were stored in 2 ml-amber borosilicate vials. HPLC analyses were carried out as described by Sarmento et al. (2006).

### 3.4 Results

#### 3.4.1 Physico-chemical characteristics of the water column

Vertical profiles of physico-chemical variables differed strongly between stations and campaigns (Figure 9). In the dry season, the water column was anoxic from 47.5, 57.5, 55 and 60 m in June 2011, October 2012, September 2013 and August 2014, respectively. During the rainy season, it was anoxic from 45 and 55 m in February 2012 and May 2013, respectively. At each date, the thermocline and chemocline (based on specific conductivity and pH) mirrored the oxycline and temperature at the oxic-anoxic interface averaged  $23.5 \pm 0.2^\circ\text{C}$  (mean  $\pm$  standard deviation).

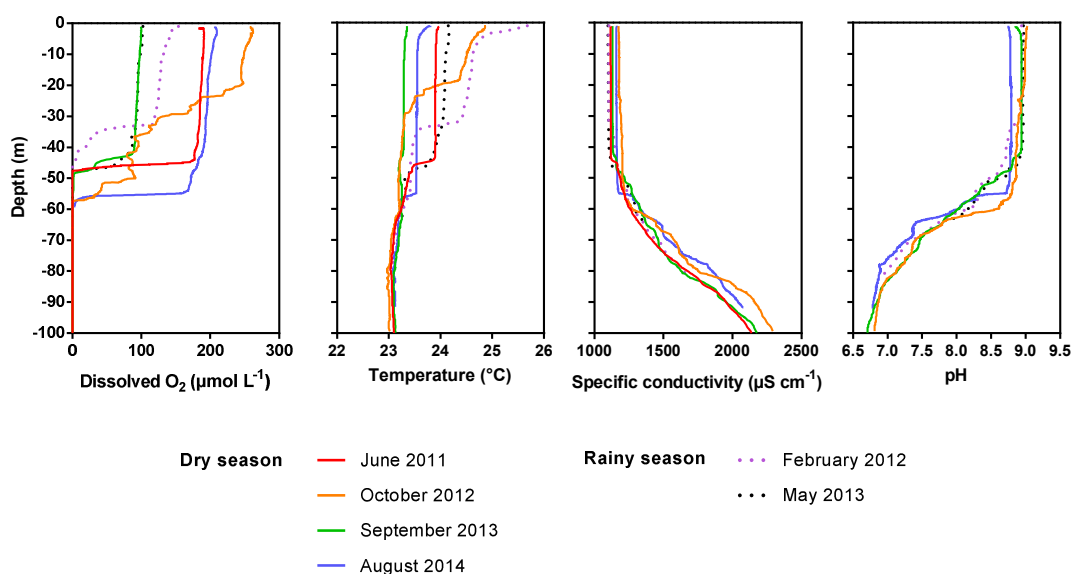


**Figure 9:** Vertical profiles of dissolved oxygen ( $\mu\text{mol L}^{-1}$ ), temperature ( $^\circ\text{C}$ ), specific conductivity ( $\mu\text{S cm}^{-1}$ ) and pH for the six field campaigns.



CH<sub>4</sub> concentrations were low ( $0.3 \pm 0.5 \mu\text{mol L}^{-1}$ ) from the surface to 45-55 m where they started to increase; at 70 m, CH<sub>4</sub> concentrations were  $385 \pm 43 \mu\text{mol L}^{-1}$  (Figure 10). For all campaigns, N<sub>2</sub>O concentrations were higher in oxic waters ( $7.0 \pm 0.4 \text{ nmol L}^{-1}$  from 0-40 m) than in anoxic waters ( $1.3 \pm 0.8 \text{ nmol L}^{-1}$  below 60 m depth). In February 2012 and September 2013, peaks of N<sub>2</sub>O up to 15 nmol L<sup>-1</sup> were observed at 50 m (anoxic waters) and at 45 m (oxic waters), respectively.

NO<sub>x</sub> profiles also reflected the seasonal variations of the water column characteristics. A zone of NO<sub>x</sub> accumulation (nitracline) was not observed in June 2011 and May 2013, and a small one (<2  $\mu\text{mol L}^{-1}$  at 52.5 m) was observed in August 2014. In February 2012, October 2012 and September 2013, NO<sub>x</sub> maxima of 3  $\mu\text{mol L}^{-1}$  (at 50 m), 4  $\mu\text{mol L}^{-1}$  (at 50 m) and 4  $\mu\text{mol L}^{-1}$  (at 47.5 m), respectively, were observed. SO<sub>4</sub><sup>2-</sup> and H<sub>2</sub>S concentrations did not show high fluctuations between the different campaigns. The mean of SO<sub>4</sub><sup>2-</sup> concentrations in oxic waters (from 0 to 50 m depth) was  $153 \pm 21 \mu\text{mol L}^{-1}$ , while the mean of H<sub>2</sub>S concentrations in anoxic waters (at 70 m depth) was  $42 \pm 25 \mu\text{mol L}^{-1}$ . SO<sub>4</sub><sup>2-</sup> concentrations strongly decreased in the anoxic zone (until  $\sim 0 \mu\text{mol L}^{-1}$  at 80 m depth), while HS<sup>-</sup> concentrations increased.

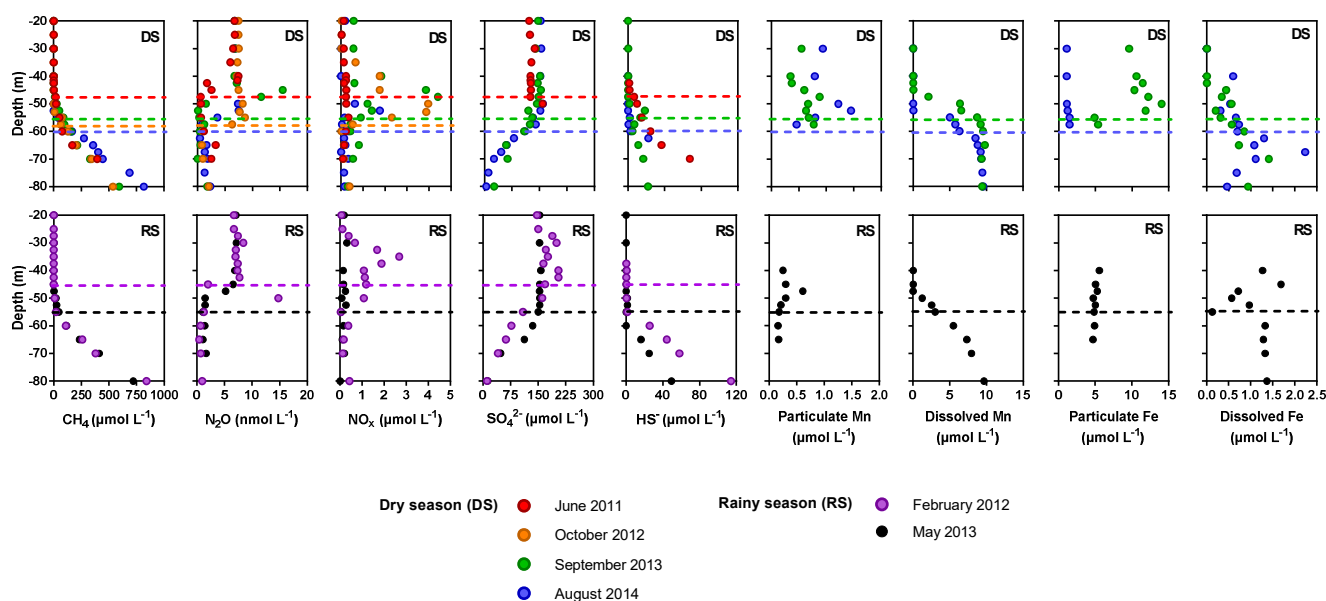


**Figure 10:** Vertical profiles of CH<sub>4</sub> ( $\mu\text{mol L}^{-1}$ ), N<sub>2</sub>O ( $\text{nmol L}^{-1}$ ), NO<sub>x</sub> ( $\mu\text{mol L}^{-1}$ ), SO<sub>4</sub><sup>2-</sup> ( $\mu\text{M}$ ), HS<sup>-</sup> ( $\mu\text{mol L}^{-1}$ ), particulate Mn and Fe ( $\mu\text{mol L}^{-1}$ ) and dissolved Mn and Fe ( $\mu\text{mol L}^{-1}$ ) concentrations for the six field campaigns. Horizontal dashed lines represent the anoxic layer for each season (same color code).

While particulate Fe concentrations were up to  $15 \mu\text{mol L}^{-1}$  in oxic waters, in September 2013, dissolved Fe concentrations were very low (less than  $2.5 \mu\text{mol L}^{-1}$  all along the vertical profiles, during the three field campaigns). On the contrary, particulate Mn concentrations were low (less than  $2 \mu\text{mol L}^{-1}$

L<sup>-1</sup>), with a maximum concentration peak located just above the oxic-anoxic interface, for the three campaigns, and dissolved Mn concentrations increased with depth, until maximum concentrations of 10 μmol L<sup>-1</sup> in anoxic waters.

### 3.4.2 Microbial process rate measurements

CH<sub>4</sub> oxidation was detected during all field campaigns (Figure 11). Aerobic CH<sub>4</sub> oxidation rates tended to be faster than anaerobic ones, since aerobic CH<sub>4</sub> oxidation consumed on average 0.9 % of initial CH<sub>4</sub> per hour, while anaerobic CH<sub>4</sub> oxidation consumed 0.2 % of initial CH<sub>4</sub> per hour. With molybdate added, 0.2 % of initial CH<sub>4</sub> concentrations were also consumed per hour on average.

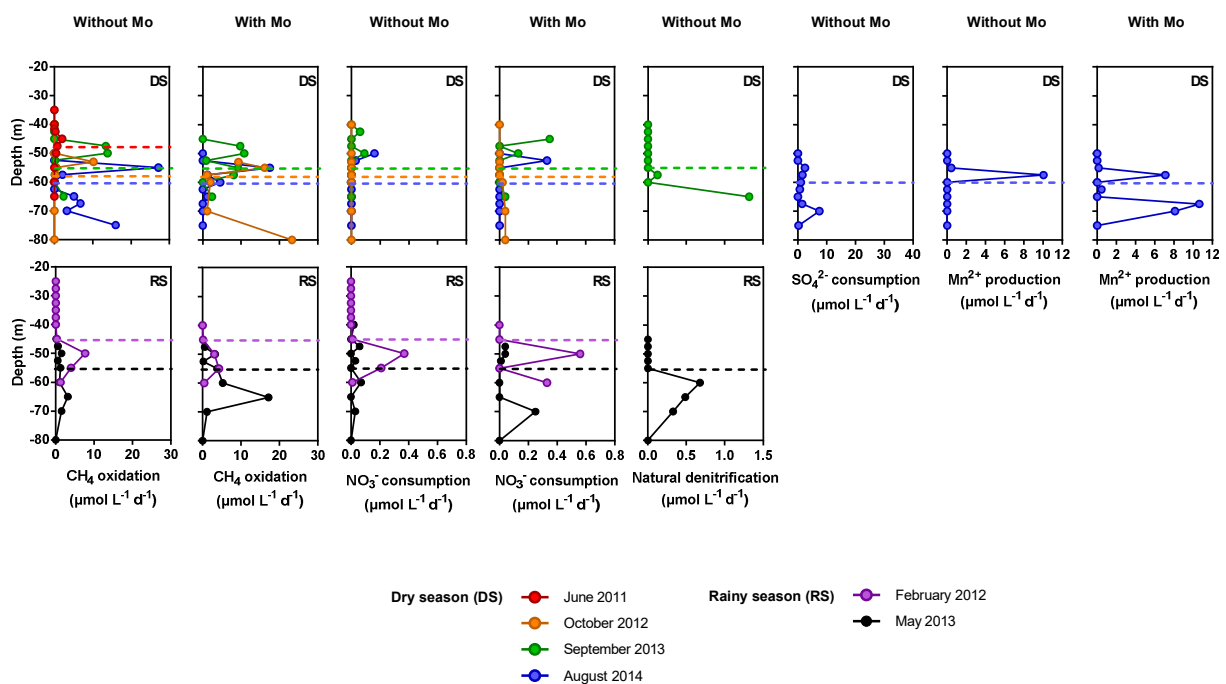


**Figure 11:** Process rates (CH<sub>4</sub> oxidation, NO<sub>3</sub><sup>-</sup> consumption, Natural denitrification, SO<sub>4</sub><sup>2-</sup> consumption and dissolved Mn production; μM/d) without and with molybdate (Mo) added, during the six field campaigns (DS: dry season; RS: rainy season). Horizontal dashed lines represent the anoxic layer for each season (same color code).

The dry season was characterized by higher maximum CH<sub>4</sub> oxidation rates in oxic waters compared to anoxic waters. The maximum oxic and anoxic oxidation rates were observed in August 2014 and were 27 ± 2 (at 55 m) and 16 ± 8 (at 75 m) μmol L<sup>-1</sup> d<sup>-1</sup>, respectively. A high SO<sub>4</sub><sup>2-</sup> consumption rate of 7.5 ± 0.0 μmol L<sup>-1</sup> d<sup>-1</sup> was observed near this region of high CH<sub>4</sub> oxidation rate, at 70 m depth. During the other field campaigns, maximum oxic CH<sub>4</sub> oxidation rates were 2 ± 0.04 and 13.9 ± 0.0 μmol L<sup>-1</sup> d<sup>-1</sup>, while maximum anoxic rates were 0.8 ± 0.01 (at 47.5 m) and 3.5 ± 0.3 (at 65 m) μmol L<sup>-1</sup> d<sup>-1</sup>, in June 2011 and September 2013, respectively. In October 2012, the CH<sub>4</sub> oxidation rate (0.2 μmol L<sup>-1</sup> d<sup>-1</sup>

<sup>1</sup>) observed in anoxic waters was negligible compared with the high rate of  $10.2 \pm 0.4 \mu\text{mol L}^{-1} \text{d}^{-1}$  observed in oxic waters.  $\text{NO}_3^-$  consumption rates tended to be low during all the campaigns, but a non-negligible natural denitrification rate of  $1.5 \mu\text{mol L}^{-1} \text{d}^{-1}$  was observed at 65 m in September 2013, in parallel incubations.

During the rainy season, maximum  $\text{CH}_4$  oxidation rates in anoxic waters were higher than in oxic waters. In February 2012, the maximum anoxic  $\text{CH}_4$  oxidation rate of  $7.7 \pm 0.4 \mu\text{mol L}^{-1} \text{d}^{-1}$  was observed at 50 m and co-occurred with the maximum  $\text{NO}_3^-$  consumption rate of  $0.4 \pm 0.1 \mu\text{mol L}^{-1} \text{d}^{-1}$ . In May 2013, the maximum anoxic  $\text{CH}_4$  oxidation rate of  $3.2 \mu\text{mol L}^{-1} \text{d}^{-1}$  was observed at 65 m, which was close to a  $\text{NO}_3^-$  consumption rate of  $0.03 \pm 0.01 \mu\text{mol L}^{-1} \text{d}^{-1}$  observed at 70 m depth. Also, higher rates of natural denitrification (based on  $^{15}\text{N}$ ) were observed between 60 and 70 m depth, with a maximum of  $0.7 \mu\text{mol NO}_3^- \text{L}^{-1} \text{d}^{-1}$  at 60 m depth. No oxic  $\text{CH}_4$  oxidation rate was observed in February 2012, while a maximum rate of  $1.5 \pm 0.2 \mu\text{mol L}^{-1} \text{d}^{-1}$  was observed in May 2013.

When molybdate was added, different profiles were observed. In February 2012 and August 2014,  $\text{CH}_4$  oxidation rates decreased when molybdate was added, while rates tended to increase when molybdate was added during the other field campaigns. In October 2012 and May 2013 in particular,  $\text{CH}_4$  oxidation rates strongly increased when molybdate was added, from  $0 \pm 0$  to  $23 \pm 0.4 \mu\text{mol L}^{-1} \text{d}^{-1}$  (at 80m) and from 3 to  $17 \mu\text{mol L}^{-1} \text{d}^{-1}$  (at 65 m), respectively. In September 2013,  $\text{CH}_4$  oxidation rates increased when molybdate was added up to  $9 \pm 0.5 \mu\text{mol L}^{-1} \text{d}^{-1}$  at 55 m. In August 2014, the addition of molybdate was also accompanied by a strong increase of dissolved Mn ( $\text{Mn}^{2+}$ ) production rates.  $\text{NO}_3^-$  consumption rates also tended to increase when molybdate was added during all field campaigns. No dissolved Fe ( $\text{Fe}^{2+}$ ) production was observed with or without molybdate added (data not shown).

$\text{CH}_4$  production was observed in oxic waters during the three sampled campaigns, with rates up to  $371 \text{ nmol L}^{-1} \text{d}^{-1}$  in August 2014 (Figure 12). For the three campaigns, the highest  $\text{CH}_4$  production peaks were located at the basis of the zones with high chlorophyll a content, just above the oxic-anoxic interface.

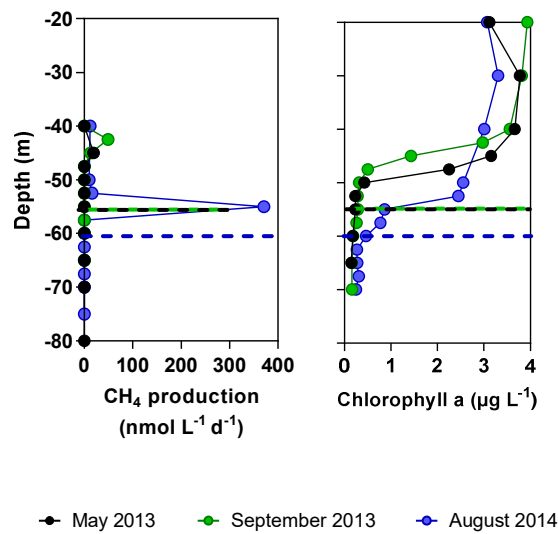


**Figure 12:** Vertical profiles of CH<sub>4</sub> production (nmol L<sup>-1</sup> d<sup>-1</sup>) and chlorophyll a concentration (µg L<sup>-1</sup>) in May 2013 (black), September 2013 (green) and August 2014 (blue). The horizontal dashed lines represent the anoxic layer for each season (same color code).

### 3.5 Discussion

High CH<sub>4</sub> oxidation rates were observed in oxic and anoxic waters (maximum  $27 \pm 2$  and  $16 \pm 8$  µmol L<sup>-1</sup> d<sup>-1</sup>, respectively). Aerobic CH<sub>4</sub> oxidation rates were sometimes very high when considering the initial CH<sub>4</sub> concentrations (Table 5). For example, the maximum aerobic CH<sub>4</sub> oxidation rate of  $27 \pm 2$  µmol L<sup>-1</sup> d<sup>-1</sup> observed at 55 m depth in August 2014 occurred at CH<sub>4</sub> concentrations of  $42 \pm 2$  µmol L<sup>-1</sup>. However, as shown in Table 5, this rate applied on a period of 24h, and 68 % of the initial CH<sub>4</sub> was consumed after 24h. The same observation is made, for example, in June 2011 (at 42.5 and 45 m), February 2012 (at 50 m) and October 2012 (at 53 m).

**Table 7:** Depth-integrated CH<sub>4</sub> oxidation rates (µmol m<sup>-2</sup> d<sup>-1</sup>) in Lake Kivu and the percent related to anaerobic oxidation of methane (AOM).

	Integration depth interval (m)	CH <sub>4</sub> oxidation (µmol m <sup>-2</sup> d <sup>-1</sup> )	% AOM
<i>Dry season</i>			
June 2011	1-65	9	30
October 2012	1-80	27	1
September 2013	1-65	81	15
August 2014	1-75	162	55
<i>Rainy season</i>			
February 2012	1-60	63	99
May 2013	1-80	44	81

A great variability in oxidation rates was observed between the different campaigns. The main pathway of CH<sub>4</sub> oxidation was aerobic in June 2011, October 2012 and September 2013 (dry season) and anaerobic in February 2012 and May 2013 (rainy season) (Table 7). In August 2014, aerobic and anaerobic oxidation rates were quite equivalent. As shown by Figure 13, aerobic oxidation rates tended to depend on the oxygenated layer depth. Aerobic CH<sub>4</sub> oxidation rates tended to be higher when the mixed layer was deeper, as usually observed during the dry season. This observation confirms hypothesis by Roland et al. (2016) who suggested, based on the seasonal evolution with depth of CH<sub>4</sub> concentrations, that during the dry season, the oxic layer deepens and integrated aerobic CH<sub>4</sub> oxidation on the oxic water column is higher. On the contrary, during the rainy season, the oxic layer is thinner, and a greater amount of CH<sub>4</sub> can be anaerobically oxidized before reaching the oxic part of the water column. While aerobic CH<sub>4</sub> oxidation is probably limited by CH<sub>4</sub> concentrations, AOM is probably limited by the availability of electron acceptors due to competition with more favorable processes (such as heterotrophic denitrification, sulfate reduction etc.). Also episodic fluctuations in water column characteristics influence bacterial communities and small variations in the water column structure may influence the abundance and/or distribution of bacterial communities, and thus contribute to the differences observed. Anyway, the relatively high aerobic and anaerobic CH<sub>4</sub> oxidation rates measured during this study and estimated from <sup>13</sup>C-CH<sub>4</sub> production by Morana et al. (2015b) explain the low air-water CH<sub>4</sub> fluxes observed throughout the year in Lake Kivu (Borges et al., 2011; Roland et al., 2016).

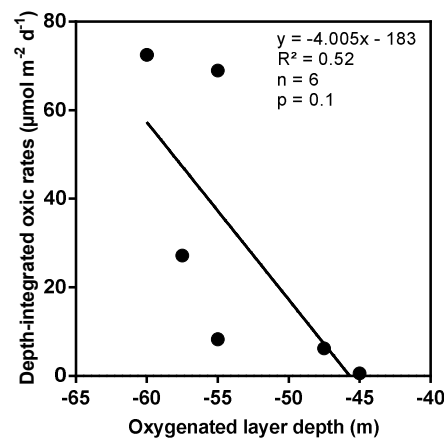


**Figure 13:** Depth-integrated aerobic CH<sub>4</sub> oxidation rates (µmol m<sup>-2</sup> d<sup>-1</sup>) compared to the oxygenated layer depth (m), for all field campaigns.

Aerobic and anaerobic CH<sub>4</sub> oxidation rates are also high compared with most other lakes (Table 8). Large differences observed can be easily explained by the different characteristics of the environments, such as vertical structure of the water column, CH<sub>4</sub> concentrations, O<sub>2</sub> and other electron acceptors concentrations, or water temperature. Lake Kivu is a tropical lake, so high water temperatures enhance bacterial activity, contrary to temperate and boreal lakes. Also, the water column of Lake Kivu allows the accumulation of high CH<sub>4</sub> concentrations in anoxic waters, which can slowly diffuse to the oxic compartment, allowing the occurrence of both aerobic and anaerobic CH<sub>4</sub> oxidation. It was presently assumed that all the CH<sub>4</sub> present in the water column of Lake Kivu was produced in anoxic sediments, by acetoclastic and hydrogen reduction methanogenesis (Pasche et al., 2011). However, we show here that a part of CH<sub>4</sub> present in oxic waters can come from aerobic CH<sub>4</sub> production. Aerobic CH<sub>4</sub> production has been recently studied (Grossart et al., 2011; Bogard et al., 2014; Tang et al., 2014; Tang et al., 2016), and different mechanisms have been proposed to explain it, among which a link with phytoplankton that produces methylated compounds (e.g. dimethylsulfoniopropionate (DMSP)), H<sub>2</sub> or acetate, which could then be used by oxygen tolerant methanogenic bacteria to produce CH<sub>4</sub> (Jarrell, 1985; Angel et al., 2011; Grossart et al., 2011). Alternatively, phytoplankton could directly produce CH<sub>4</sub> itself (Lenhart et al., 2016). During our study, the aerobic CH<sub>4</sub> production peaks were always located at the basis of the zones of high Chlorophyll a content. This location may be due to a spatial coupling between the presence of substrates produced by phytoplankton and the presence of oxygen tolerant methanogenic archaea. Inceoğlu et al. (2015a) revealed the presence of methanogenic archaea in the anoxic waters and at the oxic-anoxic interface of Lake Kivu, among which *Methanosarcinales*. Angel et al. (2011) showed that some archaea belonging to *Methanosarcinales* are capable to perform methanogenesis under oxic conditions, at lower rates than in anoxic conditions.

**Table 8:** Aerobic and anaerobic CH<sub>4</sub> oxidation rates ( $\mu\text{mol L}^{-1} \text{d}^{-1}$ ) in Lake Kivu and other lakes in literature.

Lake	Aerobic CH <sub>4</sub> oxidation ( $\mu\text{mol L}^{-1} \text{d}^{-1}$ ) (CH <sub>4</sub> concentrations; $\mu\text{mol L}^{-1}$ )	AOM ( $\mu\text{mol L}^{-1} \text{d}^{-1}$ ) (CH <sub>4</sub> concentrations; $\mu\text{mol L}^{-1}$ )	Source
<b>Kivu</b>	0.02-27 (0.2-42)	0.2-16 (65-689)	This study
<b>Kivu</b>	0.62 (3.6)	1.1 (54)	Pasche et al. (2011)
<b>Pavin (France)</b>	0.006-0.046 (0.06-0.35)	0.4 (285-785)	Lopes et al. (2011)
<b>Big Soda (US)</b>	0.0013 (0.1)	0.060 (50)	Iversen et al. (1987)
<b>Marn (Sweden)</b>	0.8 (10)	2.2 (55)	Bastviken et al. (2002)
<b>Tanganyika</b>	0.1-0.96 (<10)	0.24-1.8 (~10)	Rudd (1980)
<b>Matano (Indonesia)</b>	0.00036-0.0025 (0.5)	4.2-117 (12-484)	Sturm et al. (2016)

Very high AOM rates observed in Lake Matano compared with Lake Kivu may be explained by higher CH<sub>4</sub> concentrations in anoxic waters and greater concentrations of the highly favorable electron acceptor Fe (Sturm et al., 2016). Pasche et al. (2011) reported lower aerobic and anaerobic CH<sub>4</sub> oxidation rates than those we measured, but their CH<sub>4</sub> oxidation measurements were only made during one field campaign, as although we demonstrated during this study that a great seasonal variability in CH<sub>4</sub> oxidation rates can be observed.

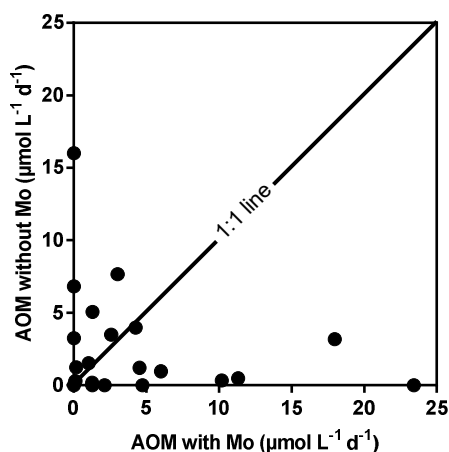
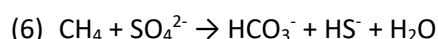


**Figure 14:** Comparison between AOM rates ( $\mu\text{mol L}^{-1} \text{d}^{-1}$ ) measured without and with molybdate (Mo) added, during all field campaigns.

Different depth profile patterns were observed when molybdate, the inhibitor of sulfate-reducing bacteria activity, was added. About half of the measurements gave lower rates with molybdate added, and the other half gave higher rates (Figure 14). In February 2012 and August 2014, AOM rates were lower with molybdate, suggesting the occurrence of AOM coupled with SO<sub>4</sub><sup>2-</sup> reduction. Measurement of the SO<sub>4</sub><sup>2-</sup> consumption rate during the incubations were performed in August 2014. The highest rate of SO<sub>4</sub><sup>2-</sup> consumption ( $18 \pm 6 \mu\text{mol L}^{-1} \text{d}^{-1}$ ) was observed at 70 m, what was close to the higher AOM peak of  $16 \pm 8 \mu\text{mol L}^{-1} \text{d}^{-1}$  observed at 75 m depth. In terms of stoichiometry, Figure 15a shows that one AOM peak can be easily explained by the SO<sub>4</sub><sup>2-</sup> reduction rate, since 1 mole of SO<sub>4</sub><sup>2-</sup> is needed to oxidize 1 mole of CH<sub>4</sub>, according to Eq. (6):



SO<sub>4</sub><sup>2-</sup> consumption rates were calculated from the change in time of SO<sub>4</sub><sup>2-</sup> concentrations measured with the nephelometric method, which might not be precise enough, since the detection limit was 52  $\mu\text{mol L}^{-1}$ . So, due to this high detection limit, we might have missed or underestimated some SO<sub>4</sub><sup>2-</sup>

consumption rates, which could potentially be linked to AOM. Vertical profiles of  $\text{SO}_4^{2-}$  concentrations, measured by ion chromatography (detection limit of  $0.5 \mu\text{mol L}^{-1}$ ), show that  $\text{SO}_4^{2-}$  is present in enough quantity to explain AOM rates observed, for all campaigns (Table 9).

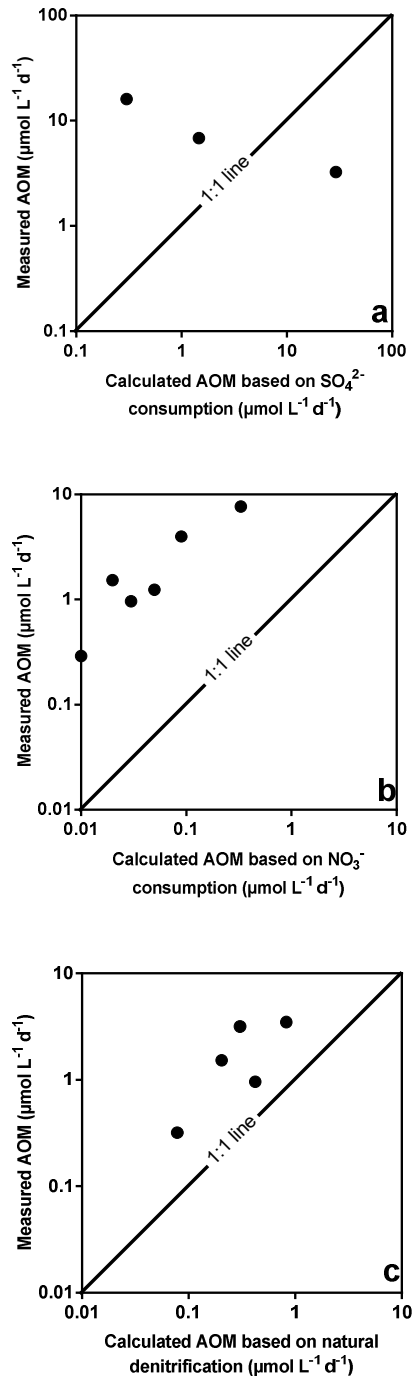


**Figure 15:** Comparison between measured and calculated AOM rates ( $\mu\text{mol L}^{-1} \text{d}^{-1}$ ) based on (a)  $\text{SO}_4^{2-}$  consumption rates, (b)  $\text{NO}_3^-$  consumption rates and (c) Natural denitrification, for all field campaigns. Note the log scales.

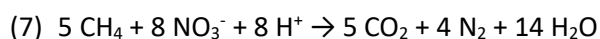


**Table 9:**  $\text{SO}_4^{2-}$ ,  $\text{NO}_x$ ,  $\text{Mn}^{2+}$ ,  $\text{MnO}_2$ ,  $\text{Fe}^{2+}$  and  $\text{Fe}(\text{OH})_3$  concentrations ( $\mu\text{mol L}^{-1}$ ) and potential anaerobic  $\text{CH}_4$  oxidation (%) based on these concentrations for all campaigns, for each depth where AOM rates were observed. N.d. = not determined.

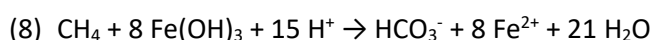
Field campaign	Depth (m)	$[\text{SO}_4^{2-}]$ ( $\mu\text{mol L}^{-1}$ ) (%)	$[\text{NO}_x]$ ( $\mu\text{mol L}^{-1}$ ) (%)	$[\text{Mn}^{2+}]$ ( $\mu\text{mol L}^{-1}$ ) (%)	$[\text{MnO}_2]$ ( $\mu\text{mol L}^{-1}$ ) (%)	$[\text{Fe}^{2+}]$ ( $\mu\text{mol L}^{-1}$ ) (%)	$[\text{Fe}(\text{OH})_3]$ ( $\mu\text{mol L}^{-1}$ ) (%)
<b>June 2011</b>	47.5	126 (100)	0.23 (4)	N.d.	N.d.	N.d.	N.d.
	50	159 (100)	0.24 (6)	N.d.	N.d.	N.d.	N.d.
<b>February 2012</b>	45	169 (100)	1.18 (84)	N.d.	N.d.	N.d.	N.d.
	50	161 (100)	1.08 (13)	N.d.	N.d.	N.d.	N.d.
	55	108 (100)	0.04 (1)	N.d.	N.d.	N.d.	N.d.
	60	77 (100)	0.38 (5)	N.d.	N.d.	N.d.	N.d.
<b>October 2012</b>	57.5	N.d.	0.53 (46)	N.d.	N.d.	N.d.	N.d.
<b>May 2013</b>	55	150 (100)	0.04 (1)	3.0 (16)	0.2 (1)	0.1 (0)	4.8 (13)
	60	135 (100)	0.15 (2)	5.5 (29)	0.2 (1)	1.3 (3)	4.9 (13)
	65	112 (100)	0.11 (0)	7.3 (12)	0.2 (0)	1.3 (1)	4.7 (4)
	70	48 (100)	0.2 (2)	8.0 (26)	N.d.	1.3 (2)	N.d.
<b>September 2013</b>	55	131 (100)	0.91 (41)	8.7 (100)	0.7 (13)	0.3 (3)	4.9 (47)
	57.5	124 (100)	0.43 (22)	9.2 (100)	0.8 (16)	0.6 (6)	5.4 (56)
	65	59 (100)	0.81 (5)	9.8 (25)	N.d.	0.9 (3)	N.d.
<b>August 2014</b>	65	61 (100)	0.20 (1)	8.8 (11)	N.d.	1.1 (1)	N.d.
	67.5	46 (100)	0.00 (0)	9.2 (9)	N.d.	2.2 (1)	N.d.
	70	26 (100)	0.33 (2)	9.3 (18)	N.d.	1.1 (1)	N.d.
	75	11 (18)	0.13 (0)	9.4 (4)	N.d.	0.7 (0)	N.d.

In February 2012, the maximum AOM peak of  $7.7 \pm 0.4 \mu\text{mol L}^{-1} \text{d}^{-1}$  co-occurred with the maximum  $\text{NO}_3^-$  consumption peak of  $0.4 \pm 0.1 \mu\text{mol L}^{-1} \text{d}^{-1}$ , at 50 m depth, suggesting that a part of AOM might have been due to  $\text{NO}_3^-$  reduction.  $\text{NO}_3^-$  consumption rates do not clearly determine if denitrification occurs in Lake Kivu, since the  $\text{NO}_3^-$  consumption recorded during the incubations might reflect the incorporation of N into the biomass, or reduction to ammonium. However, in a companion paper, we showed that natural denitrification occurred in the Northern Basin in 2011 and 2012, at rates ranging between 1.2 and 2232  $\text{nmol NO}_3^- \text{L}^{-1} \text{d}^{-1}$ , during the same field campaigns, at depths close to those where we observed AOM rates (Chapter 5). Moreover, in May and September 2013, we also observed natural denitrification rates in parallel incubations, and higher denitrification rates co-occurred with higher AOM rates. Figure 15b and 15c show AOM rates calculated based on the  $\text{NO}_3^-$  consumption rates measured in the incubations and based on natural denitrification rates measured in parallel

incubations (only in May and September 2013), respectively, and according to the stoichiometry of Eq. (7), where 8 moles of  $\text{NO}_3^-$  are needed for 5 moles of  $\text{CH}_4$  (Raghoebarsing et al., 2006):

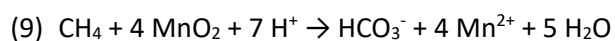


All AOM rates cannot be solely explained by  $\text{NO}_3^-$  consumption rates. Even natural denitrification rates are not sufficient to explain AOM rates observed. This discrepancy suggests that  $\text{NO}_3^-$  is not an important electron acceptor for AOM in Lake Kivu, which is not surprising when considering low natural  $\text{NO}_3^-$  concentrations. Indeed, the majority of AOM rates observed cannot be explained by the  $\text{NO}_x$  concentrations (Table 9). Only very low AOM rates can be fully explained by  $\text{NO}_x$  concentrations. Also, it seems that Fe cycling in the water column of Lake Kivu is not well developed, since while particulate Fe concentrations were up to  $15 \mu\text{mol L}^{-1}$ , dissolved Fe concentrations were very low (Figure 10), suggesting that Fe reduction is a limited process. While particulate Fe concentrations were high enough to explain up to 56 % of the small AOM rates observed (Table 9), dissolved Fe concentrations can only explain up to 6 % of the small AOM rates, and only 0-2 % of higher AOM rates, according to Eq. (8) (Beal et al., 2009):



Moreover, in August 2014, no  $\text{Fe}^{2+}$  production rate was observed in the incubations, without and with molybdate added, which tends to support the low occurrence of Fe reduction in the water column of Lake Kivu. It is thus likely that Fe does not play a significant role for AOM.

$\text{MnO}_2$  and  $\text{Mn}^{2+}$  concentrations were also measured in May 2013, September 2013 and August 2014 (Figure 10). AOM can occur with  $\text{MnO}_2$  as electron acceptor, and produce  $\text{Mn}^{2+}$  according to Eq. (9) (Beal et al., 2009):



According to this relationship, 1 mole of  $\text{CH}_4$  consumes 4 moles of  $\text{MnO}_2$  and produces 4 moles of  $\text{Mn}^{2+}$ . In September 2013, we can see that  $\text{MnO}_2$  can significantly contribute to AOM at depths near the oxic-anoxic interface (Table 9). Particulate Mn concentrations were very low compared to dissolved Mn concentrations, with a peak located just above the oxic-anoxic interface, for each campaign. Jones et al. (2011) showed the same profile in Lake Matano, and concluded that Mn is recycled at least 15 times before sedimentation.  $\text{Mn}^{2+}$  is probably oxidized in presence of small quantities of  $\text{O}_2$ , precipitates and is directly reduced in anoxic waters. The same profile is probably observed in Lake Kivu, and  $\text{MnO}_2$  can thus probably significantly contribute to AOM only at depths close to the oxic-anoxic interface. A significant part of AOM could be due to  $\text{MnO}_2$  reduction for depths

near the oxic-anoxic interface if we take into account  $\text{Mn}^{2+}$  concentrations (Table 9), and considering two hypotheses: 1) All the  $\text{Mn}^{2+}$  measured at each depth come from the reduction of precipitated  $\text{MnO}_2$ , and 2) all the  $\text{Mn}^{2+}$  come from  $\text{MnO}_2$  reduction with  $\text{CH}_4$ . However, these hypotheses are unlikely, since  $\text{Mn}^{2+}$  present at each depth can come from diffusion from upper depths, and  $\text{MnO}_2$  can be reduced by other electron donors than  $\text{CH}_4$ . Also, for  $\text{SO}_4^{2-}$  and  $\text{NO}_x$ , other processes such as  $\text{SO}_4^{2-}$  reduction with organic matter and heterotrophic denitrification can take place. The percentages of AOM reported in Table 9 and the calculated AOM rates reported in Figure 15 are thus potential maximum percentages and rates. Nevertheless,  $\text{CH}_4$  has the potential to be the major electron donor in anoxic waters of Lake Kivu based on consideration of the standing stocks and fluxes of carbon. Indeed,  $\text{CH}_4$  concentration at 70 m is  $\sim 385 \mu\text{mol L}^{-1}$  which is distinctly higher than typical dissolved organic carbon concentrations of  $142 \mu\text{mol L}^{-1}$  that is very refractory anyway (Morana et al., 2014; 2015b) and particulate organic carbon (POC) concentrations in anoxic waters typically lower than  $30 \mu\text{mol L}^{-1}$  (Morana et al., 2015a). In terms of supply of carbon, the  $\text{CH}_4$  vertical flux of  $9.4 \text{ mmol m}^{-2} \text{ d}^{-1}$  (Morana et al., 2015b) is also higher compared to the downward flux of POC from the mixed layer of  $5.2 \pm 1.7 \text{ mmol m}^{-2} \text{ d}^{-1}$  (average value of 24 month-deployment of sediment traps in the Northern Basin from November 2012 to November 2014, unpublished data). This is in general agreement with the high methanotrophic production in Lake Kivu ( $8.2 - 28.6 \text{ mmol m}^{-2} \text{ d}^{-1}$ ) estimated by a parallel study (Morana et al., 2015b).

Considering the very high  $\text{SO}_4^{2-}$  concentrations compared with other potential electron acceptors (mean of 103, 0.40, 0.42 and  $4.9 \mu\text{mol L}^{-1}$  for  $\text{SO}_4^{2-}$ ,  $\text{NO}_x$ , particulate Mn and particulate Fe, respectively, at depths where AOM was observed), it is likely that AOM in Lake Kivu is mainly coupled to  $\text{SO}_4^{2-}$  reduction. Moreover, half of the measurements showed that the inhibition of SRB activity by molybdate induced a decrease of AOM rates. However, the other half of the measurements showed that AOM rates were higher when molybdate was added. These results are surprising and difficult to explain. We firstly considered if we artificially induced aerobic oxidation by injecting molybdate, since the solution was not anoxic. As described in Sect. 3.3.4, we calculated the impact of  $\text{O}_2$  supply for each  $\text{CH}_4$  oxidation rate, which was clearly limited, since the median value of relative standard deviations (between rates with molybdate and rates with molybdate if no  $\text{O}_2$  was added) was 6.8 %, and thus did not strongly influence  $\text{CH}_4$  oxidation rates. Even if a significant artificially-induced aerobic oxidation can be ruled out, the  $\text{O}_2$  supply could potentially induce  $\text{NO}_3^-$ , particulate Fe and Mn production, and thus increase AOM linked to these electron acceptors. However, no increased concentrations of these elements was observed during the incubations with molybdate (data not shown). We were not able to directly measure the  $\text{SO}_4^{2-}$  concentrations in incubations with molybdate with the nephelometric method, due to a reaction between molybdate and reagents inducing absorbance higher than the

maximum absorbance measurable for the specific wavelength. Since  $\text{HS}^-$  oxidation is very fast (Canfield et al., 2005), it is very likely that the artificially introduced  $\text{O}_2$  was directly consumed by this way, and thus that  $\text{SO}_4^{2-}$  concentrations were higher in incubations with molybdate. However, the increase of AOM in presence of molybdate cannot be due to the increase of  $\text{SO}_4^{2-}$  concentrations, since molybdate inhibit  $\text{SO}_4^{2-}$  reduction.

We can thus hypothesize that a modification in competitive relationships among the bacterial community in presence of molybdate, such as a decrease of competition between denitrifying bacteria and/or Mn-reducing bacteria and SRB, would explain the higher  $\text{NO}_3^-$  consumption rates observed with molybdate added. Also,  $\text{Mn}^{2+}$  production rates increased with molybdate in August 2014. Competitive relationships for electron donors among bacterial communities have already been observed in literature (e.g. Westermann and Ahring, 1987, Achtnich et al., 1995). In Lake Kivu, it is unlikely that the strong increase in AOM rates was only due to a change in competition between SRB and denitrifying bacteria and/or SRB and Mn-reducing bacteria, since  $\text{NO}_3^-$  and  $\text{MnO}_2$  concentrations are in any way insufficient to be responsible for all AOM rates. However, with the present dataset, this hypothesis cannot be definitively ruled out, and further studies are required to really understand the influence of molybdate on the bacterial communities. The measurement of the bacterial communities' evolution in the incubations, without and with molybdate added, would be really interesting.

### **3.6 Conclusions**

We put in evidence a diversified  $\text{CH}_4$  cycle, with the occurrence of AOM and aerobic  $\text{CH}_4$  production, and their seasonal variability, in the water column of a meromictic tropical lake. Presently,  $\text{CH}_4$  oxidation in Lake Kivu was superficially measured by Jannasch (1975), and was estimated on the base on mass balance and comparison to fluxes (Borges et al., 2011; Pasche et al., 2011). It was also supposed to occur based on pyrosequencing results (İnceoğlu et al., 2015a; Zigah et al., 2015), which put in evidence the presence of sulfate-reducing bacteria and methanotrophic archaea in the water column and suggested that AOM could be coupled to  $\text{SO}_4^{2-}$  reduction. Morana et al. (2015b) made isotopic composition analysis which revealed the occurrence of aerobic and anaerobic  $\text{CH}_4$  oxidation in the water column of Lake Kivu, and concluded that aerobic  $\text{CH}_4$  oxidation was probably the main pathway of  $\text{CH}_4$  removal. Finally, important  $\text{CH}_4$  oxidation was also supposed to be responsible for small  $\text{CH}_4$  fluxes to the atmosphere observed throughout the year (Borges et al. 2011; Roland et al., 2016). However, any of these studies directly put in evidence and measured aerobic and anaerobic oxidation rates and, nothing was known about seasonal and spatial variability of  $\text{CH}_4$  oxidation in Lake Kivu, nor the different potential electron acceptors for AOM. We were not able to clearly identify the main electron acceptor of AOM based on this dataset, but considering the high  $\text{SO}_4^{2-}$  concentrations,

it is likely that AOM could be mainly coupled to  $\text{SO}_4^{2-}$  reduction. A seasonal variability in the respective importance of aerobic and anaerobic  $\text{CH}_4$  oxidation rates was observed, with a higher importance of aerobic oxidation in dry season and of AOM in rainy season. This can be linked to the position of the oxygenated layer depth, which is located deeper during the dry season, due to the seasonal mixing of the mixolimnion. At this period of the year, the oxic-anoxic interface is located close to the chemocline, below which the  $\text{CH}_4$  concentrations are typically 5 orders of magnitude larger than in the upper part of the mixolimnion. By contrast, during the rainy season, when the thermal stratification within the mixolimnion is well established, the volume of the oxic compartment is smaller than the volume of the anoxic compartment, and hence  $\text{CH}_4$  can only reach the oxic waters by diffusion, after that a significant fraction of the  $\text{CH}_4$  upward flux has been oxidized by AOM, which limit the aerobic  $\text{CH}_4$  oxidation.

---

## Chapter 4: Anaerobic methane oxidation in a ferruginous tropical lake (Kabuno Bay, East Africa)

---

**Adapted from:** Fleur A.E. Roland, François Darchambeau, Cédric Morana, Jean-Pierre Descy and Alberto V. Borges (submitted) *Anaerobic methane oxidation in a ferruginous tropical lake (Kabuno Bay, East Africa)*, *Journal of Geophysical Research:Biogeosciences*

### 4.1 Abstract

We studied methane (CH<sub>4</sub>) oxidation in the water column of a ferruginous tropical lake (Kabuno Bay, sub-basin of Lake Kivu, East Africa), with a focus on anaerobic CH<sub>4</sub> oxidation (AOM). The Kabuno Bay is characterized by a strong and permanent stratification starting at 10 m depth, anoxic below 11.25m, and rich in dissolved iron (Fe) and CH<sub>4</sub>. Due to these features, we tested the hypothesis that AOM occurs in the water column of Kabuno Bay, and investigated potential electron acceptors (Fe, manganese (Mn), sulfate (SO<sub>4</sub><sup>2-</sup>) or nitrate (NO<sub>3</sub><sup>-</sup>)), with the hypothesis that Fe was the main electron acceptor. We measured the change of CH<sub>4</sub> concentrations in incubations without and with an inhibitor of sulfate-reducing bacteria (SRB) activity (molybdate), and with an inhibitor of CH<sub>4</sub> oxidation (picolinic acid) during three field campaigns (in May 2013 – rainy season, September 2013 – dry season and August 2014 – dry season). We put in evidence high AOM rates (up to 75 ± 5 μmol L<sup>-1</sup> d<sup>-1</sup>) without molybdate added. With molybdate added, AOM rates tended to decrease in May 2013, and strongly increased (up to 269 ± 15 μmol L<sup>-1</sup> d<sup>-1</sup>) during the two other field campaigns. Particulate Mn and NO<sub>x</sub> concentrations were too low (less than 2 and 10 μmol L<sup>-1</sup>, respectively) to be considered as important potential electron acceptors for AOM, while SO<sub>4</sub><sup>2-</sup> and particulate Fe concentrations were higher (up to 600 and 40 μmol L<sup>-1</sup>, respectively). However, HS<sup>-</sup> concentrations in anoxic waters were very low (less than 1 μmol L<sup>-1</sup>), suggesting a low occurrence of SO<sub>4</sub><sup>2-</sup> reduction. These results strongly suggest that Fe is the main electron acceptor for AOM in the water column. We also put in evidence the occurrence of methanogenesis in the oxic water column with rates up to 48 nmol L<sup>-1</sup> d<sup>-1</sup>.

### 4.2 Introduction

Lake Kivu is an East African great lake located at the border between Rwanda and the Democratic Republic of the Congo. It is very rich in dissolved gases (methane (CH<sub>4</sub>) and carbon dioxide (CO<sub>2</sub>)) and is divided into one main basin, two small basins and two bays: Northern Basin (or main basin), Southern Basin (or Ishungu Basin), Western Basin (or Kalehe Basin), the Kabuno Bay in the north

and the bay of Bukavu in the South (Figure 16). Kabuno Bay is a sub-basin only connected to the main basin by a narrow and shallow connection limiting water circulation. Due to the combined effect of limited exchanges, sub-aquatic springs rich in salts entering the bay and the small size of the bay limiting the effect of wind, a strong stratification is established throughout the year, with waters usually anoxic below ~11 m depth (Borges et al., 2011). This strong stratification is responsible for very high CH<sub>4</sub> and iron (Fe) concentrations, Kabuno Bay being considered as a ferruginous anoxic basin. Also, anoxic waters of Kabuno Bay are characterized by low sulfide (HS<sup>-</sup>) concentrations (Llirós et al., 2015).

Inland waters and wetlands are major sources of CH<sub>4</sub> to atmosphere (Bastviken et al., 2011; Borges et al., 2015a; Stanley et al., 2016). While progress has been made in refining the evaluation of the CH<sub>4</sub> emission rates (e.g. Saunio et al., 2016), less attention has been given to evaluate the underlying production and loss terms, methanogenesis and methane oxidation. In marine sediments, most of the methane removal is due to anaerobic CH<sub>4</sub> oxidation (AOM) using SO<sub>4</sub><sup>2-</sup> as electron acceptor, by a consortium of methanogens and sulfate-reducing bacteria (e.g. Iversen and Jørgensen, 1985; Boetius et al., 2000; Jørgensen et al., 2001). However, AOM can occur with other electron acceptors such as nitrate (NO<sub>3</sub><sup>-</sup>), manganese (Mn) and Fe (Borrel et al., 2011; Cui et al., 2015). In the ocean, AOM coupled to SO<sub>4</sub><sup>2-</sup>-reduction dominates because SO<sub>4</sub><sup>2-</sup> is more abundant than any other electron acceptor by several orders of magnitude. In freshwaters on the other hand, SO<sub>4</sub><sup>2-</sup> is usually not abundant.

The water column of Kabuno Bay is anoxic, rich in Fe and CH<sub>4</sub>, and poor in HS<sup>-</sup>. These features are rarely encountered in modern environments, Lake Matano in Indonesia being one of the few (Crowe et al., 2011; Sturm et al., 2016), while they were widespread in Archean Oceans (Konhauser et al., 2005). Llirós et al. (2015) showed an efficient Fe cycling in Kabuno Bay, with the occurrence of pelagic photoferrotrophy (anaerobic oxidation of Fe coupled to light), which is suggested to have played a significant role in the biosphere of early Earth. Numerous studies also raise the possibility of a coupling between anaerobic CH<sub>4</sub> oxidation (AOM) and Fe reduction, in marine sediments (Beal et al., 2009) and freshwater environments (e.g. Konhauser et al., 2005; Caldwell et al., 2008; Crowe et al., 2011; Sturm et al., 2016). In this study, we measured CH<sub>4</sub> oxidation rates in the water column of Kabuno Bay, and investigated the potential importance of Fe as a terminal electron acceptor for AOM. We hypothesized that NO<sub>3</sub><sup>-</sup> should not be an important electron acceptor for AOM, since previous measurements showed that NO<sub>3</sub><sup>-</sup> concentrations in Kabuno Bay are generally very low (< 1 μmol L<sup>-1</sup>). On the contrary, we hypothesized that Fe could be the main electron acceptor for AOM. In order to provide further insights on CH<sub>4</sub> cycle in the water column of Kabuno Bay, we also investigated the

possible occurrence of pelagic CH<sub>4</sub> production, as recently reported in oxic layers of productive lakes (Grossart et al., 2011; Bogard et al., 2014; Tang et al., 2014).

### 4.3 Material and methods

#### 4.3.1 Sampling and physico-chemical parameters

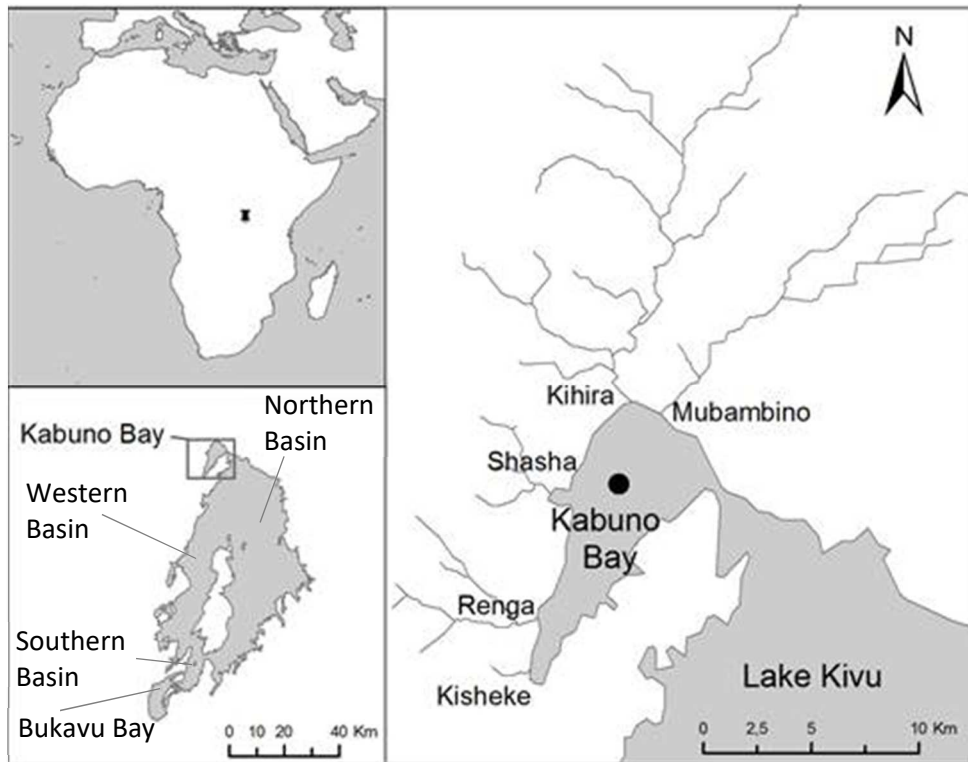


**Figure 16:** Map of Lake Kivu, showing the different basins and bays, and focus on Kabuno Bay, showing the sampling site (black plot) and the five main rivers entering the lake.

The Kabuno Bay (-1.6216°N, 29.0497°E; Figure 16) was sampled in May 2013 (late rainy season), September 2013 (dry season) and August 2014 (dry season). Vertical profiles of temperature, conductivity, pH and oxygen were obtained with a Yellow Springs Instrument (YSI) 6600 V2 multiparameter probe. Because of high amounts of dissolved gases (in particular CO<sub>2</sub>) in superficial waters of Kabuno bay, a home-made sampler (Figure 17) was constructed to avoid losses of CH<sub>4</sub> when samples were brought to the surface. Sealed N<sub>2</sub>-flushed 60 ml borosilicate serum bottles were fixed on a two-meter high plate, every 0.25 m. Thin needles equipped with non-return valves (valves allowing the water to fill in the bottles but preventing gases to escape from the bottles) penetrated the butyl stoppers. The non-turn valves were sealed by butyl caps. A string was connected to caps in series (all caps were connected at the same string). The plate was immersed at right depths and caps were removed from the non-turn valves by pulling on the string, and allowing water to enter the bottles through the needle. The system was left under water 10 minutes to fill the serum bottles. Once



the sampling device was brought back to the surface, the needles were removed from the butyl stoppers and further processed as described below. Serum bottles were half-filled with water, and the other half was a N<sub>2</sub> headspace.

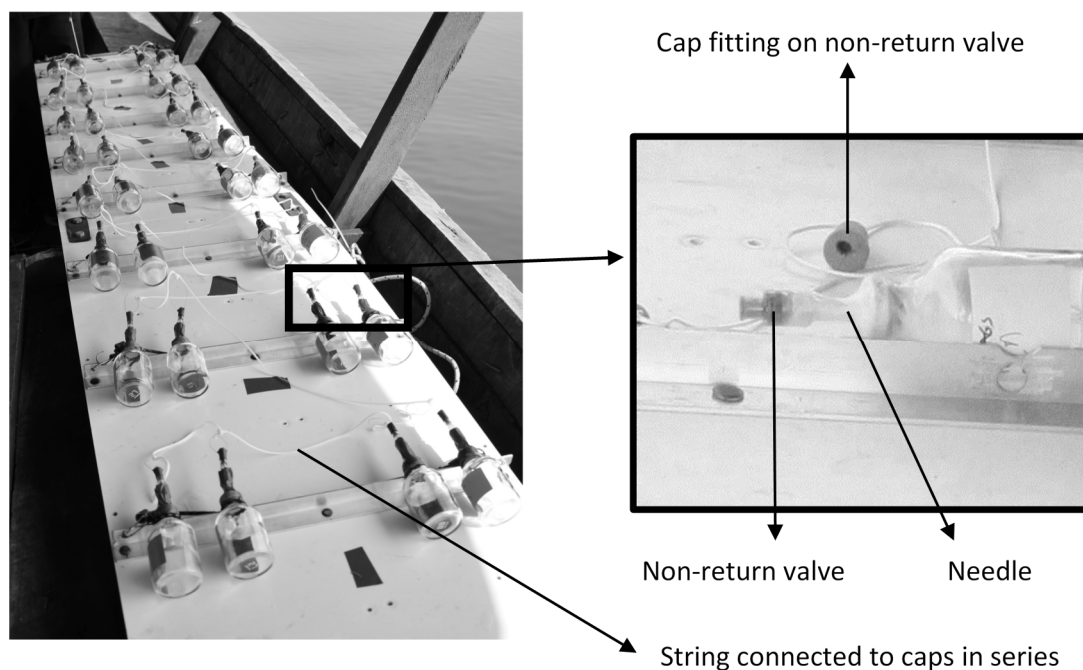


**Figure 17:** Specifically designed sampler for sampling of the water column of Kabuno Bay.

#### 4.3.2 Chemical analyses

Samples were collected for the measurement of CH<sub>4</sub>, N<sub>2</sub>O, nutrients, SO<sub>4</sub><sup>2-</sup>, HS<sup>-</sup>, Fe and Mn concentrations, and for the determination of CH<sub>4</sub> oxidation.

Samples for CH<sub>4</sub> concentrations and CH<sub>4</sub> incubations were collected in sealed (with butyl stoppers and aluminium caps) N<sub>2</sub>-flushed 60 ml glass serum bottles, as described above. The same sampling methodology as widely described in Chapter 3 has been applied here. Briefly, two bottles were directly poisoned with 200 µl of HgCl<sub>2</sub>, five bottles received an inhibitor of sulfate-reducing bacteria (sodium molybdate), five received an inhibitor of aerobic methane oxidation (picolinic acid) and five received no treatment. The bottles were incubated in dark and at constant temperature close to in situ temperature (~23°C), and the biological activity was stopped at ~12, 24, 48, 72 and 96h by the addition of 200 µl of HgCl<sub>2</sub>. CH<sub>4</sub> concentrations were determined via the headspace equilibration technique and measured by gas chromatography (GC) (Weiss, 1981), as described by Borges et al. (2015a). The precision of measurements was ±3.9%.

**Table 10:** Depth (m) where CH<sub>4</sub> oxidation was observed, presence (+) or absence (-) of oxygen (O<sub>2</sub>), CH<sub>4</sub> oxi = maximum CH<sub>4</sub> oxidation rates (μmol L<sup>-1</sup> d<sup>-1</sup>) calculated based on a linear regression, [CH<sub>4</sub>]<sub>in</sub> = initial CH<sub>4</sub> concentrations (μmol L<sup>-1</sup>) from which the linear regression begins, %CH<sub>4</sub> = percentage of initial CH<sub>4</sub> consumed, and time (h) required for this consumption (time lapse during which the linear regression was applied to calculate CH<sub>4</sub> oxidation rates), without and with molybdate added (- Mo and + Mo, respectively), for all field campaigns. -/+ Mo = without and with Mo.

Depth (m)	O <sub>2</sub>	CH <sub>4</sub> oxi (μmol L <sup>-1</sup> d <sup>-1</sup> )		[CH <sub>4</sub> ] <sub>in</sub> (μmol L <sup>-1</sup> )	%CH <sub>4</sub>		Time (h)	
		-Mo	+Mo	-/+ Mo	-Mo	+Mo	-Mo	+Mo
<i>May 2013</i>								
9	+	0.03 ± 0.0	0 ± 0	0.5 ± 0	37 ± 1	0 ± 0	120	120
9.5	+	0.14 ± 0.03	0 ± 0	0.8 ± 0.1	54 ± 8	42 ± 11	72	72
10	+	0.04	0 ± 0	0.7	40	34	120	120
10.5	+	0.0 ± 0.0	0 ± 0	0.6 ± 0	24 ± 0	30 ± 0	120	120
11	+	0 ± 0	0 ± 0	0.6 ± 0	0 ± 0	29 ± 9	120	120
11.5	-	23.9 ± 4.7	2.3 ± 3.3	139 ± 33	45 ± 13	31 ± 17	120	120
12	-	6.6 ± 0.6	4.5 ± 0.6	200 ± 4	16 ± 2	10 ± 2	120	120
13	-	4.0 ± 0.6	0.8 ± 0.6	209 ± 4	4 ± 2	3 ± 2	120	120
<i>September 2013</i>								
11.5	-	11.1 ± 1.6	15.9 ± 1.6	132 ± 11	82 ± 2	80 ± 2	120	120
12	-	1.6 ± 0.7	5.9 ± 0.7	151 ± 5	15 ± 3	24 ± 3	120	120
13	-	8.1 ± 0.3	69.4 ± 2.4	174 ± 1	18 ± 1	21 ± 1	72	12
<i>August 2014</i>								
9.25	+	0.1 ± 0.0	0 ± 0	0.4 ± 0	27 ± 8	23 ± 8	24	72
10	+	0.1 ± 0.0	0 ± 0	0.5 ± 0	17 ± 1	26 ± 1	72	72
10.25	+	0.2 ± 0.0	0 ± 0	1 ± 0	30 ± 1	48 ± 1	48	24
10.5	+	0.1 ± 0.0	0 ± 0	1 ± 0	32 ± 6	50 ± 4	48	48
11	+	0 ± 0	0 ± 0	1 ± 0	0 ± 0	47 ± 3	72	48
11.25	-	1.0 ± 0.2	0 ± 0	2 ± 0	37 ± 11	55 ± 8	24	72
11.5	-	0 ± 0	12.8 ± 1.3	5 ± 0	0 ± 0	79 ± 1	72	6
11.75	-	47.2	205.8	43 ± 20	93 ± 3	95 ± 2	24	6
12	-	75.3 ± 5.3	269.0 ± 14.5	130 ± 7	35 ± 3	92 ± 0	24	12

Samples for nutrients analyses were collected into 250 ml borosilicate bottles, with the same sampling method as described above. Water was then collected from the bottles with a 50 ml-syringe, filtered through a 0.22 μm syringe filter, preserved with 200 μl of H<sub>2</sub>SO<sub>4</sub> 5N, and stored frozen. NO<sub>2</sub><sup>-</sup> and NO<sub>3</sub><sup>-</sup> concentrations were estimated by spectrophotometry as described in Chapter 3. The concentrations are reported here as NO<sub>x</sub> concentrations (NO<sub>3</sub><sup>-</sup> + NO<sub>2</sub><sup>-</sup>).

Samples for  $\text{SO}_4^{2-}$  and sulfide ( $\text{HS}^-$ ) concentrations were collected in  $\text{N}_2$ -flushed 60 ml serum bottles, by the same sampling method as described above. Water was rapidly filtered after collection through a  $0.22 \mu\text{m}$  syringe filter, and collected in 5 ml Cryotube vials and 50 ml plastic vials for  $\text{SO}_4^{2-}$  and  $\text{HS}^-$ , respectively. Samples were preserved with  $20 \mu\text{l}$  of 20% zinc acetate (ZnAc), for  $\text{SO}_4^{2-}$  and  $200 \mu\text{l}$  of ZnAc for  $\text{HS}^-$ ; both samples were then stored frozen.  $\text{SO}_4^{2-}$  and  $\text{HS}^-$  concentrations were determined as described in Chapter 3. The detection limits were  $0.5$  and  $0.25 \mu\text{mol L}^{-1}$  for  $\text{SO}_4^{2-}$  and  $\text{HS}^-$ , respectively.

Samples for Fe and Mn measurements were collected into sealed  $\text{N}_2$ -flushed 60 ml glass serum bottles, with the sampler described above. Water was rapidly transferred from the bottles to the filtration set with a syringe equipped with a tube, and was passed through  $25 \text{ mm}$  glass fiber filters. Filters were collected in 2 ml Eppendorf vials and preserved with 1 ml of a  $\text{HNO}_3$  2% solution, while filtrates were collected into four 2 ml Eppendorf vials and preserved with  $20 \mu\text{l}$  of a  $\text{HNO}_3$  65% solution. Fe and Mn concentrations were determined by inductively coupled plasma mass spectrometry (ICP-MS) as described in Chapter 3.

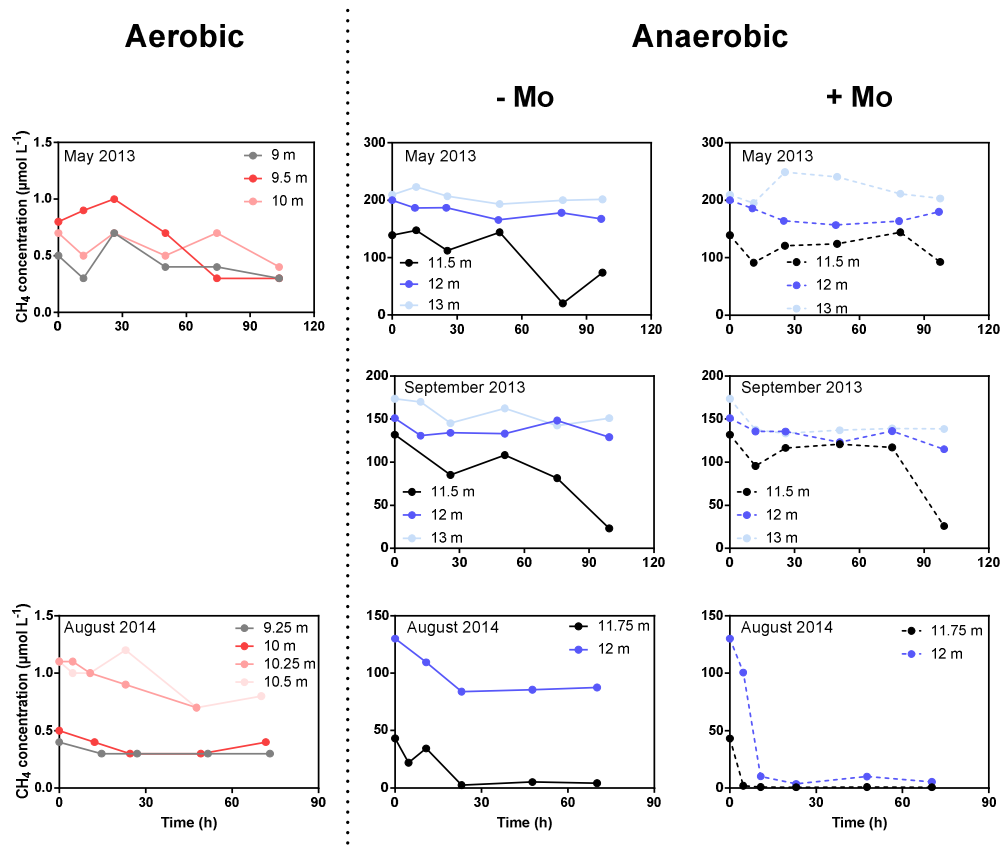


**Figure 18:** Time profiles of  $\text{CH}_4$  concentrations ( $\mu\text{mol L}^{-1}$ ) in the incubations, without and with molybdate added (-Mo and +Mo, respectively), for aerobic and anaerobic depths where visible  $\text{CH}_4$  oxidation was measured, for the three field campaigns.

#### 4.3.3 CH<sub>4</sub> oxidation and production rates calculations

CH<sub>4</sub> oxidation and production rates were calculated as a linear regression of CH<sub>4</sub> concentrations over time during the course of the incubation. Rates reported here are maximum rates, as they were calculated based on the maximum slopes. Table 10 shows standard deviations, initial CH<sub>4</sub> concentrations, percentage of CH<sub>4</sub> consumed and the time laps during which the CH<sub>4</sub> oxidation rates were calculated for each depth. Incubations profiles for depths where detectable CH<sub>4</sub> oxidation and CH<sub>4</sub> production was measured are shown in Figure 18 and Figure 19, respectively.

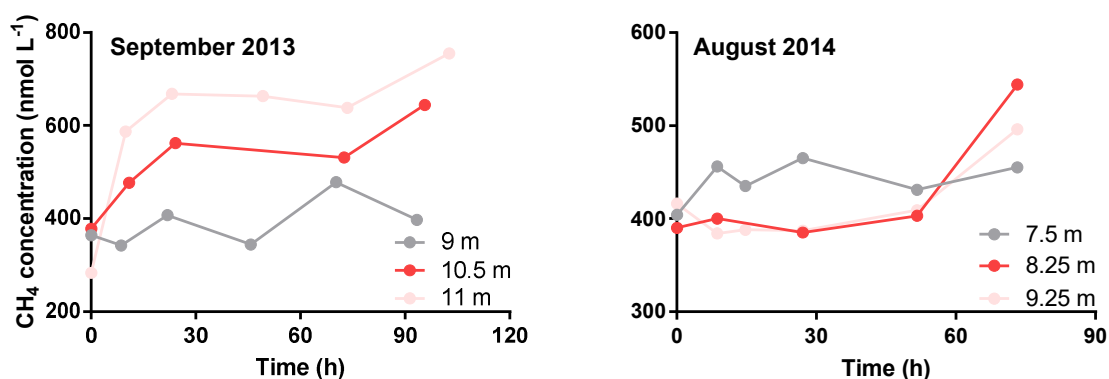


**Figure 19:** Time profiles of CH<sub>4</sub> concentrations (nmol L<sup>-1</sup>) in the incubations with picolinic acid added, for depths where visible CH<sub>4</sub> production was measured, for the campaigns of September 2013 and August 2014.

The molybdate solution was not anoxic, and a correction of the CH<sub>4</sub> oxidation rates has been applied taking into account the oxygen supply. We considered that 2.5 μmol L<sup>-1</sup> of O<sub>2</sub> were added to each bottle (250 μl of the solution were added to 30 ml of water). The calculations are detailed in Chapter 3.

#### 4.3.4 Pigment analyses

Samples for pigments analyses were collected every 0.25 m, from 9 to 13 m depth in September 2013, and from 8 to 12 m depth in August 2014. Water was collected with the sampler described above, and filtered through Whatman GF/F 47 mm diameter filters. The filtration volume depended on the depth sampled, but was on average 0.3 L. Filters were preserved and extracted as described in Chapter 3, and HPLC analyses were carried out as described by Sarmento et al. (2006).

## 4.4 Results

### 4.4.1 Physico-chemical parameters and CH<sub>4</sub> concentrations

The water column was undoubtedly anoxic from 11.25 m during all seasons (Figure 20). Chemoclines and thermoclines were located at 10.75 m, 10.5 m and 10.25 m in May 2013, September 2013 and August 2014, respectively.

CH<sub>4</sub> concentrations were low (0.1-1.1 μmol L<sup>-1</sup>) in oxic waters and very high in anoxic waters. In May 2013 and September 2013, they strongly increased from 11.25 m, up to ~200 μmol L<sup>-1</sup> at 13 m depth. In August 2014, CH<sub>4</sub> concentrations strongly increased at 11.75 m, up to 130 μmol L<sup>-1</sup> at 12 m.

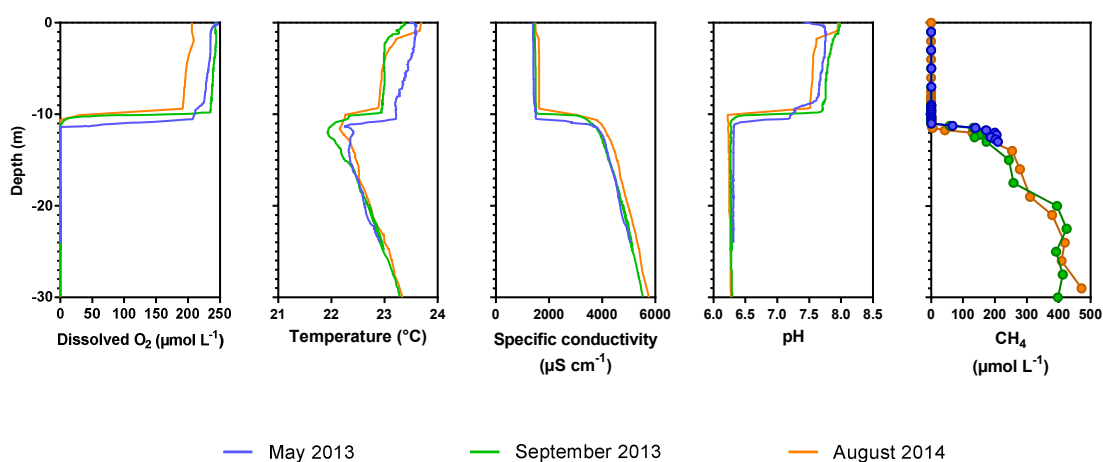


**Figure 20:** Vertical profiles of dissolved oxygen (μmol L<sup>-1</sup>), temperature (°C), specific conductivity (μS cm<sup>-1</sup>), pH and CH<sub>4</sub> concentrations (μmol L<sup>-1</sup>) in the water column of Kabuno Bay, in May 2013 (blue), September 2013 (green) and August 2014 (orange).

### 4.4.2 CH<sub>4</sub> oxidation and production rates

CH<sub>4</sub> oxidation rates in oxic waters were very low, with the maximum rate of  $0.14 \pm 0.03$  μmol L<sup>-1</sup> d<sup>-1</sup> observed in May 2013 (Figure 21). High CH<sub>4</sub> oxidation rates were observed during all field campaigns in anoxic waters. The maximum CH<sub>4</sub> oxidation rate of  $75 \pm 5$  μmol L<sup>-1</sup> d<sup>-1</sup> was observed in August 2014, in anoxic waters (at 12 m depth). High rates were also observed in May 2013 and September 2013, with maximums of  $24 \pm 5$  and  $11 \pm 2$  μmol L<sup>-1</sup> d<sup>-1</sup>, respectively, also in anoxic waters (both at 11.5 m).

When molybdate was added, CH<sub>4</sub> oxidation rates decreased in May 2013. On the contrary, rates strongly increased in September 2013 and August 2014. The maximum rates observed were  $72 \pm 2$  and  $285$  μmol L<sup>-1</sup> d<sup>-1</sup> in September 2013 (at 13 m depth) and August 2014 (at 12 m depth), respectively.

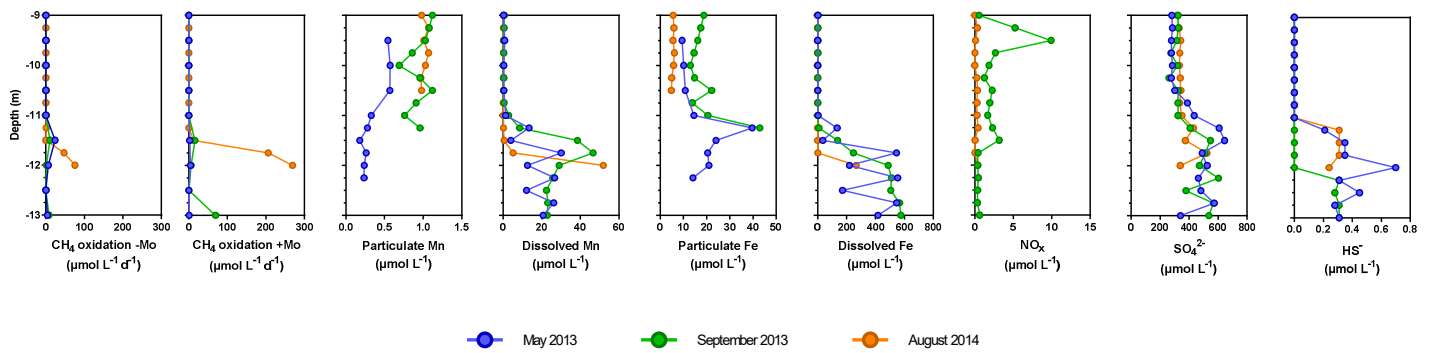


**Figure 21:** CH<sub>4</sub> oxidation ( $\mu\text{mol L}^{-1} \text{d}^{-1}$ ) without and with molybdate added (-Mo and +Mo, respectively), particulate Mn, dissolved Mn, particulate Fe, dissolved Fe, NO<sub>x</sub>, SO<sub>4</sub><sup>2-</sup> and HS<sup>-</sup> concentrations ( $\mu\text{mol L}^{-1}$ ) in the water column of Kabuno Bay, in May 2013 (blue), September 2013 (green) and August 2014 (orange).

No CH<sub>4</sub> production was observed in May 2013, while rates up to 48 nmol L<sup>-1</sup> d<sup>-1</sup> and 28 nmol L<sup>-1</sup> d<sup>-1</sup> were observed in September 2013 and August 2014, respectively (Figure 22). In September 2013, this higher peak was observed near the oxic-anoxic interface (at 11 m depth), but two peaks were also observed in oxic waters (at 9 and 10.5 m depth). In August, the three CH<sub>4</sub> production peaks were observed in oxic waters. For both campaigns, CH<sub>4</sub> production was only observed in oxic waters and in the zone of higher chlorophyll a concentration.

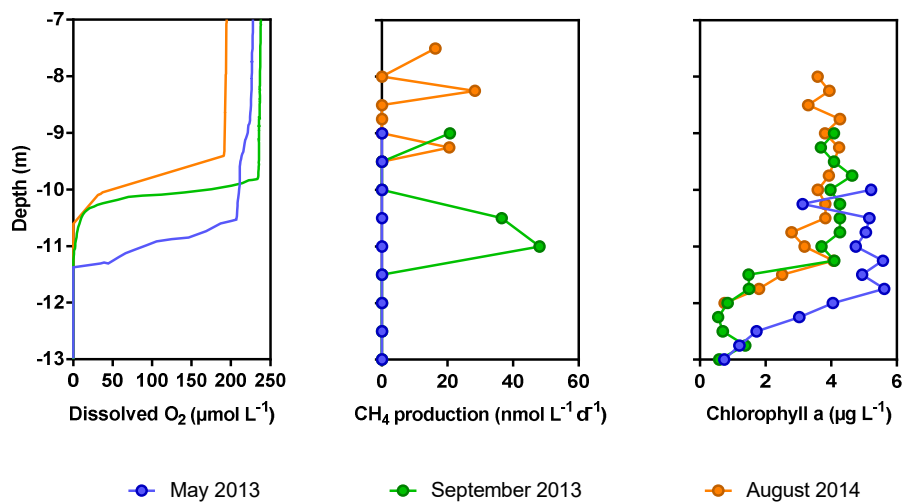


**Figure 22:** Dissolved O<sub>2</sub> concentrations ( $\mu\text{mol L}^{-1}$ ), CH<sub>4</sub> production rates ( $\text{nmol L}^{-1} \text{d}^{-1}$ ) and Chlorophyll a concentration ( $\mu\text{g L}^{-1}$ ) in May 2013 (blue), September 2013 (green) and August 2014 (orange).

#### 4.4.3 Potential electron acceptors concentrations

Particulate Mn and Fe concentrations were low (less than 1.5 and 50  $\mu\text{mol L}^{-1}$ , respectively) compared to dissolved Mn and Fe concentrations (up to 55 and 600  $\mu\text{mol L}^{-1}$ , respectively).  $\text{NO}_x$  concentrations were very low (less than 1  $\mu\text{mol L}^{-1}$ ) through the vertical profile in August 2014, while a peak of 10  $\mu\text{mol L}^{-1}$  was observed at 9.5 m depth in September 2013.  $\text{SO}_4^{2-}$  concentrations were high (up to 600  $\mu\text{mol L}^{-1}$ ) through the vertical profiles, during all field campaigns. On the contrary,  $\text{HS}^-$  concentrations were low (less than 1  $\mu\text{mol L}^{-1}$ ) all along the vertical profiles, during all campaigns.

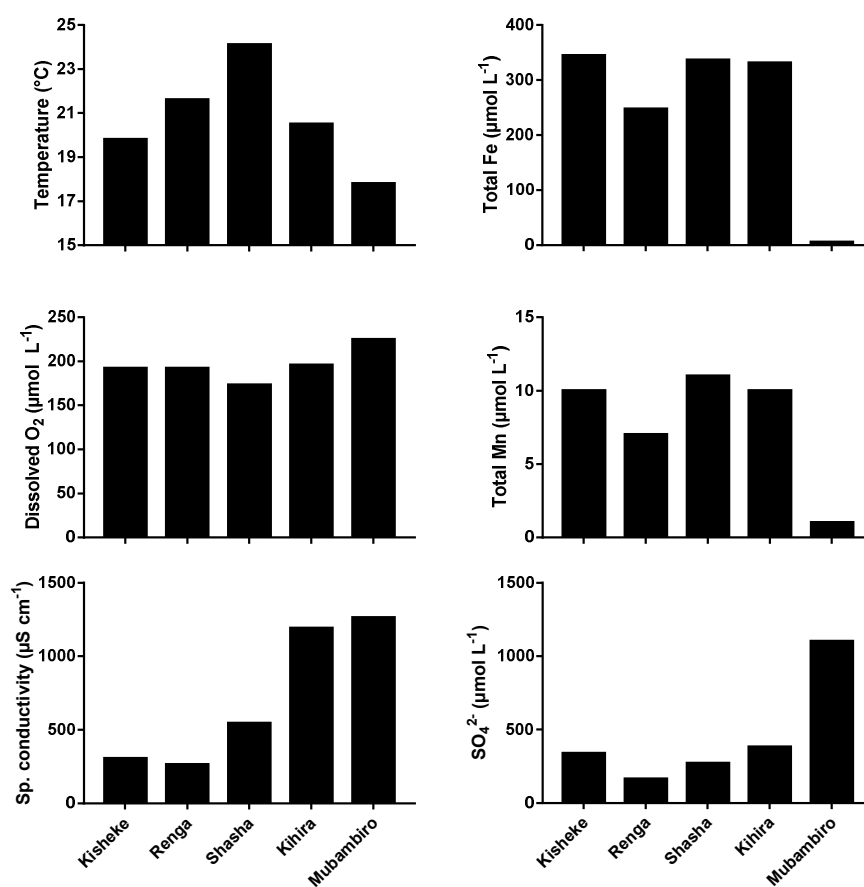


**Figure 23:** Average of the physico-chemical parameters (temperature ( $^{\circ}\text{C}$ ), dissolved oxygen ( $\mu\text{mol L}^{-1}$ ) and specific conductivity ( $\mu\text{S cm}^{-1}$ )), and the total Fe, total Mn and  $\text{SO}_4^{2-}$  concentrations ( $\mu\text{mol L}^{-1}$ ) in the five main rivers flowing into the Kabuno Bay. The average was calculated on the sampled period (from November 2013 to June 2014).

## 4.5 Discussion

The water column of Kabuno Bay is very rich in  $\text{SO}_4^{2-}$  and Fe. These elements can come from different potential sources: rivers, groundwaters, wet and dry atmospheric deposition. Five main rivers flow to Kabuno Bay (Figure 16). Figure 23 shows the mean of physico-chemical parameters and  $\text{SO}_4^{2-}$ , total Mn and total Fe concentrations, in these five rivers, during 8 months (from November 2013 to June 2014).  $\text{NO}_3^-$  concentrations were previously measured by Balagizi et al. (2015). All the rivers were relatively rich in total Fe and  $\text{SO}_4^{2-}$ , while total Mn concentrations were low. Balagizi et al. (2015) showed that these rivers were also rich in  $\text{NO}_3^-$  (25-140  $\mu\text{mol L}^{-1}$ ). Since the rivers were well oxygenated, it is likely that Fe and Mn were mostly present under their particulate forms since these both elements precipitate quickly in presence of small quantities of  $\text{O}_2$ . The rivers can thus be an important source of particulate Fe,  $\text{SO}_4^{2-}$  and  $\text{NO}_3^-$  for the epilimnion of Kabuno Bay. Wet and dry deposition contribute substantially to the chemical composition of Kabuno Bay, especially because it is located in a volcanic area (Jolley et al., 2008). However, comparison of the specific conductivity in the rivers and the water column of Kabuno Bay show that specific conductivity is higher in Kabuno Bay, epilimnion included (<1500 and  $\sim 1800 \mu\text{S cm}^{-1}$  in the rivers and in Kabuno Bay, respectively). In the anoxic waters, the specific conductivity is even higher than  $4000 \mu\text{S cm}^{-1}$ . This much higher value suggests that a great part of the salts present in the water column of Kabuno Bay comes from deep water inputs, most probably from deep springs, as also observed in the main basin of Lake Kivu (Ross et al., 2015). Balagizi et al. (2015) showed that the north part of the Kabuno Bay is composed of basalt/volcanic ash, which is known to be generally rich in Fe. The erosion of the rock (by rivers, groundwaters or the lake itself) can thus also supply the water column in the different elements. However, the high concentrations of the different elements do not necessarily reflect their importance for the water column of the lake. For example,  $\text{NO}_3^-$  concentrations were high in the rivers (Balagizi et al., 2015) and are known to be high in wet and dry atmospheric deposits in volcanic regions (Jolley et al., 2008), but they were very low in Kabuno Bay's water column, suggesting that a great part can be directly and rapidly incorporated into the biomass or denitrified, for example, and is thus not available for biogeochemical processes. Also,  $\text{SO}_4^{2-}$  concentrations were high in rivers and in the water column of Kabuno Bay all along the vertical profiles, even in anoxic waters, but  $\text{HS}^-$  concentrations were very low, strongly suggesting a limited S cycle in Kabuno Bay ( $\text{SO}_4^{2-}$  reduction does not seem to be an important process). On the contrary, non-negligible particulate Fe concentrations and high dissolved Fe concentrations were observed, suggesting that a complete Fe cycle can occur in the water column, as also suggested by the study of Llorós et al. (2015).

Nearly no aerobic  $\text{CH}_4$  oxidation rates were observed during all the seasons. Table 11 shows integrated  $\text{CH}_4$  oxidation rates on the water column. AOM accounted for minimum 99.5 % of the total



**Table 11:** Depth-integrated CH<sub>4</sub> oxidation rates ( $\mu\text{mol m}^{-2} \text{d}^{-1}$ ) in Kabuno Bay and the percentage related to anaerobic oxidation of methane (% AOM).

	<b>Integration depth interval (m)</b>	<b>CH<sub>4</sub> oxidation (<math>\mu\text{mol m}^{-2} \text{d}^{-1}</math>)</b>	<b>% AOM</b>
<i>May 2013</i>	1.25-13.25	35	99.5
<i>September 2013</i>	1.25-13.25	21	100
<i>August 2014</i>	1.25-13.25	77	99.9

CH<sub>4</sub> oxidation observed. This can be linked to the small size of the oxic compartment. Indeed, independently of the season, the water column of Kabuno Bay was only clearly anoxic from 11.25 m, and was poorly oxygenated from ~10.25 m depth. So, a large part of the CH<sub>4</sub> produced in anoxic waters can be removed by AOM before reaching the oxic compartment. Moreover, the chemocline is strong (specific conductivity rapidly increases from 1500 to 4000  $\mu\text{S cm}^{-1}$ ) and thus strongly slows down the diffusion of CH<sub>4</sub> to the oxic compartment. This can explain the much lower aerobic CH<sub>4</sub> oxidation rates in Kabuno Bay compared to the main basin of Lake Kivu, studied in Chapter 3 (Table 12). The water column of the main basin is stratified deeper and, contrary to Kabuno Bay, is strongly influenced by the season. The stratification deepens during the dry season, allowing a higher input of CH<sub>4</sub> from anoxic waters to oxic waters by turbulent mixing, and thus higher aerobic CH<sub>4</sub> oxidation rates.

**Table 12:** Aerobic and anaerobic CH<sub>4</sub> oxidation rates ( $\mu\text{mol L}^{-1} \text{d}^{-1}$ ) in Kabuno Bay, Lake Kivu (companion paper) and other lakes in literature.

<b>Lake</b>	<b>Aerobic CH<sub>4</sub> oxidation (<math>\mu\text{mol L}^{-1} \text{d}^{-1}</math>) (CH<sub>4</sub> concentrations; <math>\mu\text{mol L}^{-1}</math>)</b>	<b>AOM (<math>\mu\text{mol L}^{-1} \text{d}^{-1}</math>) (CH<sub>4</sub> concentrations; <math>\mu\text{mol L}^{-1}</math>)</b>	<b>Source</b>
<b>Kabuno Bay</b>	0.03-0.14 (0.5-0.8)	0.1-75 (1-130)	This study
<b>Kivu</b>	0.02-27 (0.2-42)	0.2-16 (65-689)	Chapter 3
<b>Pavin (France)</b>	0.006-0.046 (0.06-0.35)	0.4 (285-785)	Lopes et al. (2011)
<b>Big Soda (US)</b>	0.0013 (0.1)	0.06 (50)	Iversen et al. (1987)
<b>Marn (Sweden)</b>	0.8 (10)	2.2 (55)	Bastviken et al. (2002)
<b>Tanganyika</b>	0.1-0.96 (<10)	0.24-1.8 (~10)	Rudd (1980)
<b>Matano (Indonesia)</b>	0.00036-0.0025 (0.5)	4.2-117 (12-484)	Sturm et al. (2016)

Contrary to aerobic CH<sub>4</sub> oxidation, AOM rates in Kabuno Bay were high without and with molybdate added. Without molybdate added, the maximum AOM rate was estimated to 75 ± 5 μmol L<sup>-1</sup> d<sup>-1</sup>, at 13 m depth in August 2014. When comparing with the main basin of Lake Kivu, and with other lakes in literature, AOM rates in Kabuno Bay are generally higher (except for Lake Matano) (Table 12). If we take into account CH<sub>4</sub> concentrations related to these AOM rates, bacterial communities in Kabuno Bay are capable to consume, per day, on average 10-58 % of the CH<sub>4</sub> present. In the main basin of Lake Kivu and in Lake Matano, they are able to consume on average 0.3-2 % and 24-35 %, respectively. AOM in Kabuno Bay can thus be more efficient than in Lake Matano, and lower rates observed are due to lower CH<sub>4</sub> concentrations present at depths where AOM occurred. Although the vertical structures of the water column strongly influence the oxidation rates, as explained above, the concentrations of the potential electron acceptors also play an important role. In the main basin of Lake Kivu, it is likely that AOM mainly occurs with SO<sub>4</sub><sup>2-</sup> as electron acceptor, since NO<sub>3</sub><sup>-</sup>, Fe and Mn concentrations are low compared to SO<sub>4</sub><sup>2-</sup> concentrations (Chapter 3). In Kabuno Bay, Fe concentrations are much higher, and it is known that AOM coupled to Fe reduction is thermodynamically more favorable (Crowe et al., 2011).

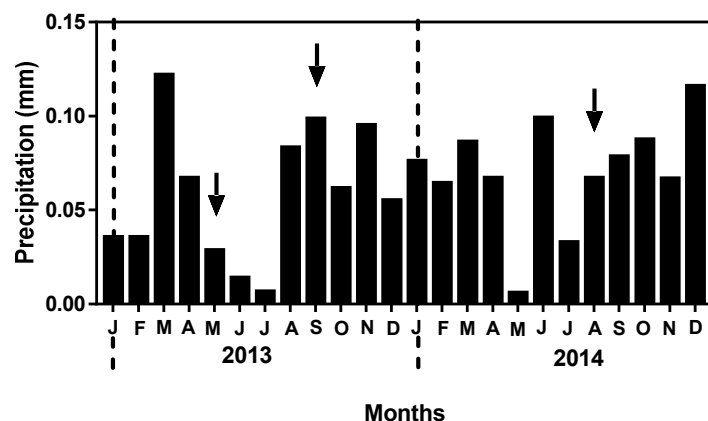
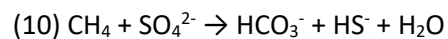


**Figure 24:** Recorded precipitations (mm) from January 2013 to December 2014. Dashed lines represent the beginning of the years and arrows our three field campaigns (May 2013, September 2013 and August 2014). Data from Thiery et al., 2014b; Thiery et al., 2014a.

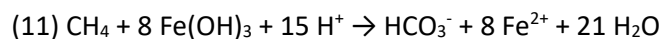
When molybdate was added, AOM rates decreased in May 2013 and strongly increased during the other two field campaigns. The rainfall pattern was very different just before May 2013 compared to the other two field campaigns, with very high precipitations inducing a water level 1 m higher (Figure 24). As we can see in Figure 20, the physico-chemical parameters in May 2013 were quite different than the other two seasons, since the oxycline, thermocline and chemocline were located deeper. Also,

the water column temperature was higher in May 2013. These features may influence the bacterial communities and induce the differences observed.

In September 2013 and August 2014, AOM strongly increased with molybdate, until a rate of  $269 \pm 15 \mu\text{mol L}^{-1} \text{d}^{-1}$  at 13 m depth in August 2014. This profile strongly suggests that  $\text{SO}_4^{2-}$  reduction is not the main pathway of AOM in Kabuno Bay. As described above,  $\text{HS}^-$  concentrations were very low in the anoxic waters (less than  $1 \mu\text{mol L}^{-1}$ ), despite high  $\text{SO}_4^{2-}$  concentrations (which would allow to fuel AOM at 100 % for all depths where AOM was observed, according to Eq. 10; Table 13), which suggests that  $\text{SO}_4^{2-}$  reduction is not an important process in the water column.



Indeed, Llíros et al. (2015) showed that  $\text{SO}_4^{2-}$  reduction was ~24 times lower than Fe reduction. They also showed that an important Fe-related bacterial community was present in the water column of Kabuno Bay, among which *Chlorobium ferrooxidans*, a Green Sulfur Bacteria (GSB) capable of Fe oxidation. Despite this Fe-oxidative bacteria, GSB community also comprises Fe-reducers,  $\text{SO}_4^{2-}$  reducers, methanotrophs and methanogens (Llíros et al., 2015). Measurements of particulate Fe concentrations showed, when available, that particulate Fe can account for up to 12 % of the AOM observed (based on Eq. 11, according to which 8 moles of particulate Fe are required to oxidize 1 mole of  $\text{CH}_4$ ; Crowe et al., 2011), which is not negligible.



However, for very high rates observed in deep anoxic waters (13 m depth), it is unlikely that particulate Fe concentrations are high enough to explain them. But it is known that Fe and Mn can be recycled many times, and thus that the same molecule of Fe and Mn can be used several times by the bacterial community (Jones et al., 2011). This recycling can be abiotic or biotic. Abiotic recycling can be due to small oxygen incursion in anoxic waters (for example, due to a small destabilization of the water column structure next to higher wind speed), which causes the oxidation of reduced Fe to particulate Fe, which can thus be used again by oxidizers. Biotic recycling can be due to photoferrotrophy, which oxidizes reduced Fe into particulate Fe and fixes  $\text{CO}_2$ . Llíros et al. (2015) and Morana et al. (2016) showed that photoferrotrophy was an important process in the water column of Kabuno Bay. This process can thus indirectly support AOM by producing particulate Fe, which can be next reduced, creating a microbial loop. The increase of AOM observed when molybdate was added may be due to a higher availability of particulate Fe when SRB activity is inhibited. Indeed, when  $\text{SO}_4^{2-}$  reduction occurs,  $\text{HS}^-$  produced can react with particulate Fe, conducting to abiotic Fe reduction, and particulate Fe is thus less available for bacteria.

**Table 13:**  $\text{SO}_4^{2-}$ ,  $\text{NO}_3^-$ , Particulate Fe ( $\text{Fe}_p$ ), Dissolved Fe ( $\text{Fe}_d$ ), Particulate Mn ( $\text{Mn}_p$ ) and Dissolved Mn ( $\text{Mn}_d$ ) concentrations ( $\mu\text{mol L}^{-1}$ ) and potential anaerobic  $\text{CH}_4$  oxidation (%) based on these concentrations for all campaigns, for each depth where AOM rates were observed. N.d. = not determined.

Field campaign	Depth (m)	$[\text{SO}_4^{2-}]$ ( $\mu\text{mol L}^{-1}$ ) (%)	$[\text{NO}_3^-]$ ( $\mu\text{mol L}^{-1}$ ) (%)	$[\text{Fe}_p]$ ( $\mu\text{mol L}^{-1}$ ) (%)	$[\text{Fe}_d]$ ( $\mu\text{mol L}^{-1}$ ) (%)	$[\text{Mn}_p]$ ( $\mu\text{mol L}^{-1}$ ) (%)	$[\text{Mn}_d]$ ( $\mu\text{mol L}^{-1}$ ) (%)
<b>May</b>	11.5	645 (100)	N.d.	24 (3)	36 (5)	0.18 (0.0)	4 (1)
	12	524 (100)	N.d.	21 (10)	220 (100)	0.24 (0.2)	13 (12)
	13	340 (100)	N.d.	N.d.	418 (100)	N.d.	21 (32)
<b>September</b>	11.5	547 (100)	3 (4)	43 (12)	139 (38)	1 (0.5)	38 (21)
	12	472 (100)	0.3 (3)	N.d.	506 (100)	N.d.	22 (87)
	13	536 (100)	0.5 (1)	N.d.	576 (100)	N.d.	23 (22)
<b>August</b>	11.75	522 (100)	0 (0)	N.d.	1 (0.3)	N.d.	5 (4)
	12	329 (100)	0.3 (0.3)	N.d.	267 (46)	N.d.	52 (18)

Therefore, data indicates that AOM in Kabuno Bay mainly occurs with Fe as electron acceptor. On the contrary, particulate and dissolved Mn concentrations were low, and particulate Mn concentrations can account for maximum 0.5 % of the AOM observed (Table 13). Also,  $\text{NO}_x$  concentrations in Kabuno Bay are usually very low (less than  $1 \mu\text{mol L}^{-1}$ ), and cannot thus significantly contribute to very high AOM rates, such as those observed at 13 m depth in September 2013 and August 2014. However, in September 2013,  $\text{NO}_x$  concentrations can contribute for 4 % to the AOM at 11.5 m depth, which is not negligible. These potential contributions are maximum contributions, since we consider here that all the  $\text{NO}_x$ ,  $\text{SO}_4^{2-}$  and particulate Fe and Mn are used for AOM, which is unlikely. As described above,  $\text{SO}_4^{2-}$  reduction seems to be a minor process in the water column of Kabuno Bay, and thus all the  $\text{SO}_4^{2-}$  present are not reduced. Also,  $\text{NO}_x$  can be used for other processes, such as denitrification or reduction into  $\text{NH}_4^+$ , which are two processes thermodynamically more favorable. During a study conducted in 2012, Michiels et al. (in press) showed that denitrification and DNRA occurred with reduced Fe as electron donor in the water column of Kabuno Bay.

Also, we show in Table 13 the potential contribution of dissolved Fe and Mn, if we consider that all the Fe and Mn present at those depths come from the reduction of particulate Fe and Mn, respectively, with AOM, what is clearly unlikely. Fe and Mn present at one depth can be due to precipitation and can thus come from the reduction of particulate Fe and Mn from other depths above, or can also be due to inputs by groundwaters. However, these results show the important potential

contribution of Fe cycling in AOM in Kabuno Bay. We must also note that AOM rates reported here are maximum rates, since the maximum slope was used to calculate the rates. This explains why rates can be very high compared with CH<sub>4</sub> concentrations, such as rates with molybdate added observed at 12.75 and 13 m in August 2014. As shown in Table 10, almost all the CH<sub>4</sub> was depleted after 6 and 12h, respectively, so very rapidly compared to rates without molybdate added. So, at these depths, CH<sub>4</sub> became rapidly limiting for AOM when molybdate was added.

Despite availability of electron acceptors and abundance and activity of the bacterial community, aerobic and anaerobic CH<sub>4</sub> oxidation also depends on CH<sub>4</sub> concentrations. Methanogenesis is commonly assumed to occur in anoxic sediments. Recently, it has also been suggested to occur in aerobic waters (Grossart et al., 2011; Bogard et al., 2014; Tang et al., 2014; Tang et al., 2016), which could explain the "ocean CH<sub>4</sub> paradox". These studies suggest that CH<sub>4</sub> production in oxic waters could be linked to phytoplankton activity that produces methylated substrates, H<sub>2</sub> or acetate which can be used by methanogens, or alternatively the CH<sub>4</sub> could be produced by the phytoplankton itself (Lenhart et al., 2016). Moreover, some methanogenic bacteria are known to be oxygen tolerant (Jarrell, 1985; Angel et al., 2011). As the study of Llirós et al. (2015) showed that methanogenic bacteria was present in the water column of Kabuno Bay, we used picolinic acid, known to be an inhibitor of CH<sub>4</sub> oxidation in soils (Bronson and Mosier, 1994), in order to identify CH<sub>4</sub> production. In September 2013, CH<sub>4</sub> production was observed in oxic waters and near the oxic-anoxic interface, while it was clearly observed in oxic waters in August 2014 (the sampling was not deep enough to identify if production also occurred in anoxic waters). The maximum production rates were 28-48 nmol L<sup>-1</sup> d<sup>-1</sup>, so in the same order of magnitude than those reported by Grossart et al. (2011) in Lake Stechlin (43-58 nmol L<sup>-1</sup> d<sup>-1</sup>). During this study, CH<sub>4</sub> production was present in the zones where chlorophyll a content was high, suggesting that it may be linked to phytoplankton activity. However, with the present dataset, it is impossible to clearly identify the mechanisms involved in CH<sub>4</sub> production in the oxic waters of Kabuno Bay. We must also note that our production rates may be underestimated, since according to Bronson and Mosier (1994), CH<sub>4</sub> oxidation is not fully inhibited (31%) by the addition of picolinic acid. The efficiency of this inhibitor for CH<sub>4</sub> oxidation has not been tested in freshwaters.

In conclusion, we put in evidence very high AOM rates in this ferruginous basin, which would be coupled with Fe reduction, since S cycling is not very developed in this sub-basin, and NO<sub>x</sub> and Mn concentrations are usually low. AOM is also probably linked to the activity of Green Sulfur Bacteria, which are capable of photoferrotrophy and can thus produce particulate Fe that can fuel AOM coupled with Fe reduction. Moreover, we also put in evidence the occurrence of CH<sub>4</sub> production in aerobic waters. We thus show that CH<sub>4</sub> cycling can be very important and diversified in a Fe rich environment. This type of environments are not widespread nowadays, but these conditions (high Fe concentrations

and low oxygen concentrations) were widespread in the Archean Oceans. By analogy, this study thus allows to show that methanotrophs might play an important role in Fe cycling in the ancient oceans, as previously suggested by Konhauser et al. (2005).

---

## Chapter 5: Denitrification, anaerobic ammonium oxidation and dissimilatory nitrate reduction to ammonium in an East African Great Lake (Lake Kivu)

---

**Adapted from:** Fleur A. Roland, François Darchambeau, Alberto V. Borges, Loreto De Brabandere, Cédric Morana, Pierre Servais, Bo Thamdrup and Sean Crowe (under review) *Denitrification, anaerobic ammonium oxidation and dissimilatory nitrate reduction to ammonium in an East African Great Lake (Lake Kivu)*, *Limnology and Oceanography*

### 5.1 Abstract

We investigated anaerobic nitrogen cycling in the water column of Lake Kivu, a deep meromictic tropical lake. Data were collected at one station in the Northern Basin and one in the Southern Basin, during two sampling campaigns (June 2011 - dry season, and February 2012 - rainy season). Short-term incubations of sulfide-free water with  $^{15}\text{N}$ -labeled substrates revealed high potential denitrification and dissimilatory nitrate reduction to ammonium (DNRA) rates (up to 350 and 36  $\text{nmol N produced L}^{-1} \text{ h}^{-1}$ , respectively), while anaerobic ammonium oxidation (anammox) was relatively low (up to 3.3  $\text{nmol N produced L}^{-1} \text{ h}^{-1}$ ). However, anammox rates achieved 44  $\text{nmol N produced L}^{-1} \text{ h}^{-1}$  when  $^{15}\text{NH}_4^+$  was added at depths where  $\text{NH}_4^+$  concentrations were very low ( $< 1 \mu\text{mol L}^{-1}$ ). With the addition of 5  $\mu\text{mol L}^{-1}$  of  $^{15}\text{NO}_3^-$  and 10  $\mu\text{mol L}^{-1}$  of  $\text{H}_2\text{S}$ , we showed that denitrification and anammox were stimulated in the Northern Basin, while the increase of DNRA rates was less notable. In the Southern Basin, the addition of  $\text{H}_2\text{S}$  decreased denitrification rates, probably because of competition with DNRA, which increased, while no effect was observed on anammox. This study thus puts in evidence the co-occurrence of denitrification, anammox and DNRA, for the first time in a great tropical lake, and underlines the spatial heterogeneity of these processes. Contrary to widespread believe, we show that anammox can significantly occur in presence of  $\text{H}_2\text{S}$ , suggesting that the contribution of anammox in nitrogen cycle may be underestimated.

### 5.2 Introduction

As an element required for life, the availability of nitrogen (N) can limit biological growth and ecosystem productivity. N is cycled through the biosphere via a number of microbial-mediated processes including biological fixation of  $\text{N}_2$  gas, nitrification, denitrification, anaerobic ammonium oxidation (anammox), and dissimilatory nitrate reduction to ammonium (DNRA). Human activities, notably the use of fertilizers and farming of N-fixing crops (e.g. soybeans), have disrupted the pre-human N-cycle by increasing total global fixed N pools as well as nitrous oxide ( $\text{N}_2\text{O}$ ) emissions to the

atmosphere. N<sub>2</sub>O is both a potent greenhouse gas and an ozone depleting agent, and in 2011, estimates suggested that atmospheric N<sub>2</sub>O concentrations had risen 20% since pre-industrial times (IPCC, 2013). Effective prediction and management of ecosystem responses to perturbations of the N-cycle requires detailed knowledge of the processes responsible for N-cycling and the ultimate removal of fixed N back to the atmosphere.

Three anaerobic metabolisms are responsible for nitrate (NO<sub>3</sub><sup>-</sup>) or nitrite (NO<sub>2</sub><sup>-</sup>) reduction, canonical denitrification, anaerobic ammonium oxidation (anammox), and dissimilatory reduction of nitrate to ammonium (DNRA). These three processes have markedly different impacts on the N-cycle; denitrification and anammox lead to N<sub>2</sub> production and ecosystem N-loss; denitrification produces N<sub>2</sub>O as an intermediate; and DNRA leads to N retention as NH<sub>4</sub><sup>+</sup>, possibly promoting N recycling. Knowledge on the regulation of these competing processes is crucial for predicting, modeling, and managing the N-cycle.

Canonical denitrification is commonly observed in rivers, streams, marine and estuarine sediments, and in anoxic lake waters (Seitzinger, 1988). It can be heterotrophic, with organic matter as electron donor, or chemolithotrophic with iron, sulfur compounds, methane, or hydrogen as electron donors (Kirchman et al., 2008). While heterotrophic denitrification is generally assumed to operate ubiquitously in anoxic marine and freshwater sediments, observation of chemolithotrophic denitrification with H<sub>2</sub>S come mostly from marine sediments (Jensen et al., 2009; Lavik et al., 2009; Canfield et al., 2010) and some marine oxygen minimum zones such as Chilean upwelling system and Baltic Sea (Canfield et al., 2010; Dalsgaard et al., 2013). Nevertheless, studies suggest that chemolithotrophic denitrification could account for 25-40 % of the N loss from freshwaters (streams, wetlands and lakes; Burgin and Hamilton, 2008), and though direct measurements of the process exist (e.g. Lake Lugano; Wenk et al., 2013), they are to date limited. While denitrification has been widely described, the co-occurrence and regulation of denitrification and other anaerobic metabolisms, such as anammox and DNRA, remains uncertain across many environments. Anammox is an autotrophic process, which constitutes a competitive advantage compared to heterotrophic denitrification (Hulth et al., 2005), and is known to be more oxygen tolerant (Kuyppers et al., 2005; Jensen et al., 2008), allowing it to occur in a wider variety of environments. However, the efficiency of the process is reduced, since anammox bacteria are known to have a slow growth rate (Jetten et al., 1998; Jetten et al., 2001; Hulth et al., 2005). DNRA competes with denitrification for NO<sub>3</sub><sup>-</sup>, with DNRA expected to dominate in environments with a high organic matter:fixed N ratio, whereas higher NO<sub>3</sub><sup>-</sup> concentrations may favor denitrification (Kelso et al., 1997; Silver et al., 2001; Dong et al., 2011). As anaerobic processes, the three processes are regulated by O<sub>2</sub> concentrations. Also, the availability of



different substrates (organic matter,  $\text{NO}_2^-$ ,  $\text{NO}_3^-$ ,  $\text{NH}_4^+$ ,  $\text{HS}^-$ ) regulates their occurrence, and determine the occurrence of potential competitive relationships.

Denitrification, anammox and DNRA are all known to be enhanced at high temperatures (Saad and Conrad, 1993; Van Hulle et al., 2010; Dong et al., 2011). Tropical lakes represent only a small areal fraction of lakes globally (Lewis Jr, 2000) but are characterized by high mean annual temperatures that may support a disproportionately large role in global biogeochemical cycling (Lewis Jr, 1987). The N-cycle in tropical freshwaters, and in particular in tropical great lakes, however, remains understudied. The co-occurrence of denitrification, anammox and DNRA, and their regulation have been poorly examined. We investigated one of the East-African Great Lakes, Lake Kivu, located at the border between Rwanda and the Democratic Republic of Congo. Lake Kivu is characterized by deep waters rich in  $\text{NH}_4^+$ , carbon dioxide, and methane (Schmid et al., 2005). Compared to temperate lakes, tropical lakes exhibit minimal seasonality of their physico-chemical parameters. In Lake Kivu, the dry season (from June to September) is accompanied by a deeper mixing of the oxygenated surface waters (i.e. the epilimnion), compared to the rainy season. During the rainy season,  $\text{NO}_3^-$  accumulates at the base of the mixed-layer, forming a nitrogenous zone (also described as a nitracline) (Llirós et al., 2010; Pasche et al., 2011) where  $\text{N}_2\text{O}$  accumulates (Roland et al., 2016), indicating active N-cycling. A zone of sulfate ( $\text{SO}_4^{2-}$ ) reduction is present below the oxic-anoxic interface, leading to  $\text{HS}^-$  accumulation to concentrations up to  $200 \mu\text{mol L}^{-1}$  in the anoxic waters (Pasche et al., 2011; Morana et al., 2016). Fluxes of  $\text{HS}^-$  from these deeper waters into the nitrogenous zone could support denitrification coupled to  $\text{HS}^-$  oxidation. Furthermore, as the deep waters of Lake Kivu are also rich in  $\text{NH}_4^+$ , fluxes of  $\text{NH}_4^+$  into the nitrogenous zone could fuel anammox. To test these hypothesis, and bring new data and knowledge on N-cycling in tropical lakes, we conducted a suite of process rate measurements, as well as geochemical and microbiological analyses over two seasons and at two stations in Lake Kivu. Our results reveal that all three  $\text{NO}_3^-$  and  $\text{NO}_2^-$  reduction processes operate in Lake Kivu, supporting  $\text{N}_2$  and  $\text{N}_2\text{O}$  production as well as N retention and recycling.

## 5.3 Material and methods

### 5.3.1 Sampling sites

Sampling campaigns were conducted during the dry season (June 2011) and rainy season (February 2012). Sampling was conducted at two stations; one in the Northern Basin ( $-1.72504^\circ\text{N}$ ,  $29.23745^\circ\text{E}$ ) and one in the Southern Basin ( $-2.3374^\circ\text{N}$ ,  $28.9775^\circ\text{E}$ ) (Figure 3).

### 5.3.2 Physico-chemical parameters and sampling

Water was collected with a vertical 7L Niskin-type bottle (Hydro-Bios) at 5 m intervals from the surface to 80 m for chemical water analyses. For N stable isotope labeling experiments, water was collected with a higher spatial resolution (at 2.5 m intervals) in a 10 m zone, located 5 m above and 5 m below the oxic-anoxic interface.

Vertical profiles of temperature, conductivity, pH and oxygen were obtained with a Yellow Springs Instrument 6600 V2 multiparameter probe. The pH probe malfunctioned in June 2011. Therefore, the pH data presented for this campaign were measured with a portable pH meter and a Metrohm pH electrode on water sampled from the Niskin bottles.

### 5.3.3 N stable isotope labeling experiments

Water was collected in duplicate in amber 250 ml borosilicate bottles from the Niskin bottle with tubing, left to overflow three times the bottle volume, and sealed with Teflon-coated screw caps. Before the injection of  $^{15}\text{N}$ -labeled solutions, a 12h pre-incubation period in dark and at 25°C was observed in order to allow the consumption of oxygen inadvertently introduced to the bottles during sampling.

N stable isotope labeling experiments were based on Thamdrup and Dalsgaard (2002). Denitrification, anammox and DNRA were determined by amending water with  $^{15}\text{NO}_3^-$  to a final concentration of 5  $\mu\text{mol L}^{-1}$ . In the rainy season, anammox was also determined by amendment with  $^{15}\text{NH}_4^+$  to a final concentration of 5  $\mu\text{mol L}^{-1}$ . Amendments were made by injecting stock label solutions (concentration of 2.5  $\text{mmol L}^{-1}$ ) through the septa of the amber glass vials. Six 12 ml vials (Labco Exetainer) were then filled from each of the duplicate bottles and placed in the dark in an incubator at ambient temperature (25°C), which was close to the in situ temperature (~24°C). Exetainers were overfilled to avoid exposure to oxygen. Microbial activity in two Exetainers was immediately arrested through the addition of 500  $\mu\text{l}$  20% zinc acetate (ZnAc). A time course was established by arresting two further Exetainers at 6, 12, 18, 24 and 48 h. In order to test the effect of  $\text{HS}^-$  on N transformations, experiments were conducted with the supplementary addition of  $\text{HS}^-$  to amber bottles with  $^{15}\text{NO}_3^-$  (for final concentration of 10  $\mu\text{mol L}^{-1}$ , in rainy season only). In the Northern Basin, in rainy season,  $^{15}\text{NO}_3^-$  enrichment experiments were also conducted at 55, 60 and 65 m, with  $^{15}\text{NO}_3^-$  final concentrations of 0.5, 1, 2, 5 and 10  $\mu\text{mol L}^{-1}$ . These experiments were conducted on water collected three days after the other labeling experiments.

$^{29}\text{N}_2$  and  $^{30}\text{N}_2$  concentrations in the Exetainers were measured with a gas source isotope ratio mass spectrometer (delta V plus, ThermoScientific) after creating a 1 ml helium headspace (volume

injected in the mass spectrometer: 50 µl). Denitrification and anammox rates (detection limits of 2.7 and 0.07 nmol L<sup>-1</sup> h<sup>-1</sup>, respectively) in the incubations with <sup>15</sup>NO<sub>3</sub><sup>-</sup> were calculated according to Eq. (12) and (13), and anammox rates in the incubation with <sup>15</sup>NH<sub>4</sub><sup>+</sup> were calculated according to Eq. (14) (Thamdrup and Dalsgaard, 2002; Thamdrup et al., 2006):

$$(12) N_2 \text{ denitrification } ^{15}\text{NO}_3 = ^{15}\text{N}^{15}\text{N}_{\text{excess}} * (F_{\text{NO}_3})^{-2}$$

$$(13) N_2 \text{ anammox } ^{15}\text{NO}_3 = (F_{\text{NO}_3})^{-1} * (^{14}\text{N}^{15}\text{N}_{\text{excess}} + 2 * (1 - (F_{\text{NO}_3})^{-1}) * ^{15}\text{N}^{15}\text{N}_{\text{excess}})$$

$$(14) N_2 \text{ anammox } ^{15}\text{NH}_4 = ^{15}\text{N}^{14}\text{N}_{\text{excess}} * (F_{\text{NH}_4})^{-2}$$

where  $N_2 \text{ denitrification } ^{15}\text{NO}_3$  and  $N_2 \text{ anammox } ^{15}\text{NO}_3$  are the production of N<sub>2</sub> by denitrification and anammox, respectively, during the incubations with <sup>15</sup>NO<sub>3</sub><sup>-</sup> and  $N_2 \text{ anammox } ^{15}\text{NH}_4$  is the production of N<sub>2</sub> by anammox in the incubations with <sup>15</sup>NH<sub>4</sub><sup>+</sup>. <sup>15</sup>N<sup>15</sup>N<sub>excess</sub> is the production of excess <sup>15</sup>N<sup>15</sup>N, <sup>14</sup>N<sup>15</sup>N<sub>excess</sub> is the production of excess <sup>14</sup>N<sup>15</sup>N, F<sub>NO<sub>3</sub></sub> is the fraction of <sup>15</sup>NO<sub>3</sub><sup>-</sup> in the NO<sub>x</sub> pool and F<sub>NH<sub>4</sub></sub> is the fraction of <sup>15</sup>NH<sub>4</sub><sup>+</sup> in the NH<sub>4</sub><sup>+</sup> pool. <sup>15</sup>N<sup>15</sup>N and <sup>14</sup>N<sup>15</sup>N excess is the excess relative to mass 30 and 29, respectively, in the time zero gas samples.

<sup>29</sup>N<sub>2</sub>O and <sup>30</sup>N<sub>2</sub>O concentrations were also measured in the incubations with the mass spectrometer. N<sub>2</sub>O peaks appeared after their respective N<sub>2</sub> peaks. Total N<sub>2</sub>O production rates in the incubations were calculated by the sum of the <sup>15</sup>N<sup>15</sup>N<sub>excess</sub> and the <sup>14</sup>N<sup>15</sup>N<sub>excess</sub>.

DNRA was only measured in rainy season and was determined as the accumulation of <sup>15</sup>N<sub>excess</sub> from NO<sub>3</sub><sup>-</sup> into the NH<sub>4</sub><sup>+</sup> pool. Measurements of <sup>15</sup>N-NH<sub>4</sub><sup>+</sup> were conducted by first converting NH<sub>4</sub><sup>+</sup> to N<sub>2</sub> following oxidation by hypobromite, as previously described by Knowles and Blackburn (1993). N<sub>2</sub> was then analyzed as described above.

$$(15) \text{NH}_4^+ \text{ DNRA} = ^{15}\text{NH}_4^+ \text{ excess} * (F_{\text{NO}_3})$$

While injecting ZnAc solution to stop the incubations of the Exetainers, the excess water was collected in 2 ml-Eppendorf vials, and stored frozen, to determine the evolution of the NO<sub>x</sub> concentrations through time. NO<sub>x</sub> were then analyzed by chemiluminescence, after reduction with vanadium chloride (VCl<sub>3</sub>), with an NO<sub>2</sub><sup>-</sup>, NO<sub>3</sub><sup>-</sup> and NO<sub>x</sub> analyzer (Thermo Environmental Instruments), according to the method described by Braman and Hendrix (1989) (detection limit: 2-3 ng).

### 5.3.4 Water-column chemical analyses

Samples for determination of vertical profiles of NO<sub>x</sub> concentrations were collected in 2 ml-Eppendorf vials, stored frozen and analyzed as described above.

Samples for determination of NH<sub>4</sub><sup>+</sup>, NO<sub>3</sub><sup>-</sup> and NO<sub>2</sub><sup>-</sup> concentrations in vertical profiles were collected in 50 ml plastic vials after being filtered through a 0.22 µm syringe filter. 200 µl of H<sub>2</sub>SO<sub>4</sub> (5N)

were added to each vial for preservation, and samples were stored frozen.  $\text{NH}_4^+$  and  $\text{NO}_2^-$  concentrations were quantified by spectrophotometry, using a 5-cm light path on a spectrophotometer Thermo Spectronic Genesys 10vis, according to the dichloroisocyanurate-salicylate-nitroprussiate colorimetric method (Westwood, 1981) and the sulfanilamide coloration method (APHA, 1998), respectively.  $\text{NO}_3^-$  concentrations were determined after vanadium reduction to  $\text{NO}_2^-$  and quantified with a Multiskan Ascent Thermo Scientific multi-plates reader (APHA, 1998; Miranda et al., 2001). The detection limits for these methods were 0.3, 0.03 and 0.15  $\mu\text{mol L}^{-1}$ , for  $\text{NH}_4^+$ ,  $\text{NO}_2^-$  and  $\text{NO}_3^-$ , respectively.

Samples for  $\text{H}_2\text{S}$  concentrations were collected directly from the Niskin-type bottle in plastic syringes. Water was filtered through a 0.22  $\mu\text{m}$  syringe filter in 50 ml plastic vials, and was rapidly preserved with 200  $\mu\text{l}$  of 20% ZnAc. Samples were stored frozen.  $\text{H}_2\text{S}$  concentrations were quantified using a 1-cm light path on a spectrophotometer, according to the method described by Cline (1969) (detection limit: 0.25  $\mu\text{mol L}^{-1}$ ). Samples for  $\text{SO}_4^{2-}$  concentrations were filtered through a 0.22  $\mu\text{m}$  syringe filter and collected in 5 ml cryotube. Samples were preserved with 20  $\mu\text{l}$  of 20 % ZnAc and were stored frozen.  $\text{SO}_4^{2-}$  concentrations were determined by ion chromatography (Dionex ICS-1500, with an autosampler Dionex AS50, a guard column Dionex AG22 and an analytical column Dionex IonPac AS22; detection limit: 0.5  $\mu\text{mol L}^{-1}$ ).

Samples for determination of  $\text{N}_2\text{O}$  concentrations in vertical profiles were collected in 50 ml borosilicate serum bottles from the Niskin bottle with a tube, left to overflow, poisoned with 100  $\mu\text{l}$  of saturated  $\text{HgCl}_2$  and sealed with butyl stoppers and aluminum caps. Concentration of  $\text{N}_2\text{O}$  was determined via the headspace equilibration technique and measured by gas chromatography as described by Borges et al. (2015a).

## **5.4 Results and discussion**

### *5.4.1 Physico-chemical parameters and Lake Kivu vertical structure description*

Lake Kivu is a large (2370  $\text{km}^2$ ) and deep meromictic lake with permanent anoxic waters below 70 m, but with fluctuations in the depth of the oxycline between the dry and the rainy season (oxygen is mixed to deeper waters in the dry season). It can be divided into a Southern Basin that is smaller and shallower (maximum depth of 180 m) than the Northern Basin (also called main basin, 485 m deep) and both are connected at a depth of 130 m (Descy et al., 2012). Due to its smaller size, the Southern Basin is less influenced by wind driven mixing. Episodic fluctuations of the stratification are thought to be less frequent in the Southern basin due to sheltering by the surrounding hills (Darchambeau et al., 2014). During our study, we observed differences in the vertical structure of the water column between the Northern and Southern basins (Figure 25). In the Northern Basin, during the dry season,

the water column was anoxic below 47.5 m, while it was anoxic below 45 m during the rainy season. In the Southern Basin, the water column was anoxic below 45 m in dry season and below 50 m in rainy season. Primary thermoclines in the Northern Basin strongly differed between seasons and were coincident with the oxycline. In the Southern Basin, the difference between the thermocline between seasons was less notable.

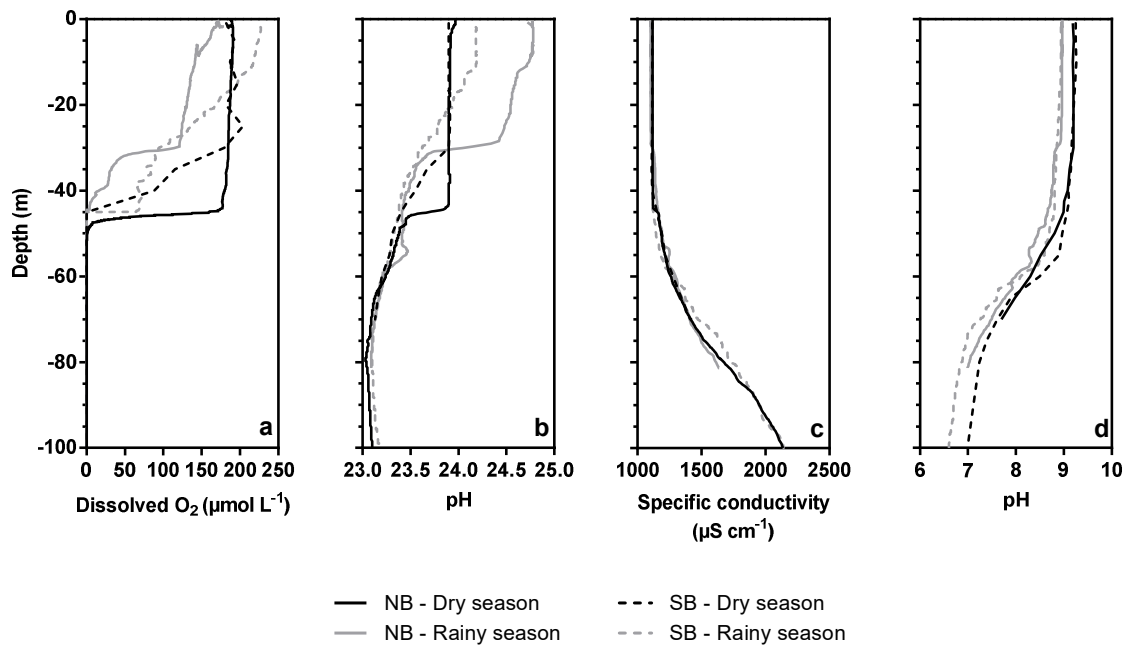


**Figure 25:** Physico-chemical parameters in the Northern Basin (NB; a, b, c, d) and Southern Basin (SB; e, f, g, h), during the dry season (June 2011, black lines) and rainy season (February 2012, grey lines).

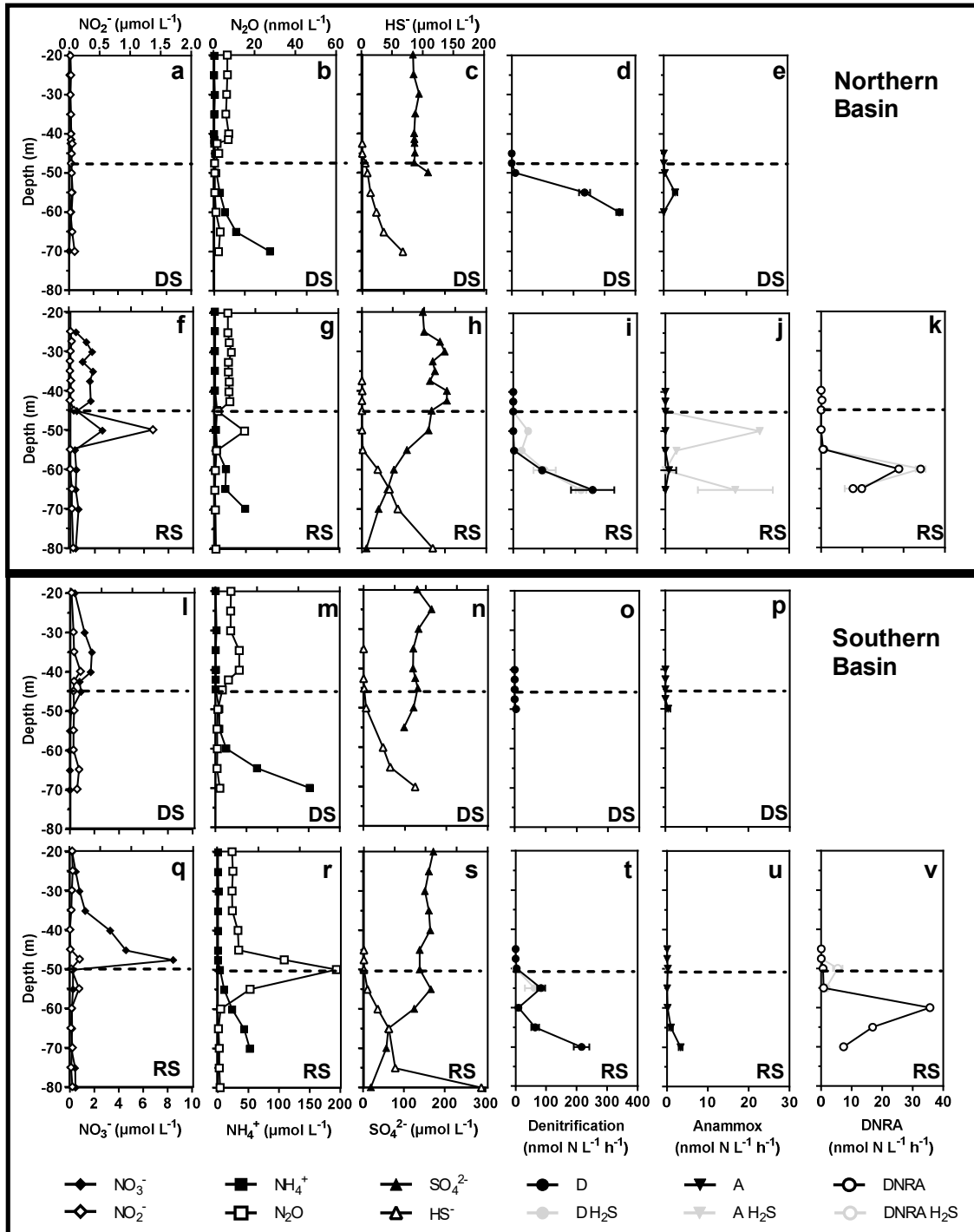


**Figure 26:** Vertical profiles of  $\text{NO}_3^-$ ,  $\text{NO}_2^-$ ,  $\text{NH}_4^+$ ,  $\text{N}_2\text{O}$ ,  $\text{SO}_4^{2-}$  and  $\text{HS}^-$  concentrations, and rates of Denitrification (D), Anammox (A) and DNRA ( $\text{nmol N produced L}^{-1} \text{h}^{-1}$ ) without (D, A, and DNRA, respectively) and with (D  $\text{H}_2\text{S}$ , A  $\text{H}_2\text{S}$  and DNRA  $\text{H}_2\text{S}$ , respectively)  $\text{H}_2\text{S}$  added, during both seasons (RS: Rainy season; DS: Dry season) and in both stations.

$\text{NH}_4^+$  concentrations reflected the thermal structure in both basins and were low ( $< 2 \mu\text{mol L}^{-1}$ ) in the oxic waters, increasing to concentrations up to  $90 \mu\text{mol L}^{-1}$  and  $152 \mu\text{mol L}^{-1}$  at 70 m, in the Northern and Southern Basins, respectively (Figure 26). The accumulation of  $\text{NH}_4^+$  in anoxic waters reflects ammonification during the degradation of the organic matter and a lack of nitrification in the absence of  $\text{O}_2$ .  $\text{HS}^-$  concentrations were also higher in anoxic waters, while  $\text{SO}_4^{2-}$  concentrations were relatively high ( $100\text{--}200 \mu\text{mol L}^{-1}$ ) in oxic waters and decreased in the top part of the anoxic waters, where  $\text{HS}^-$  increased.

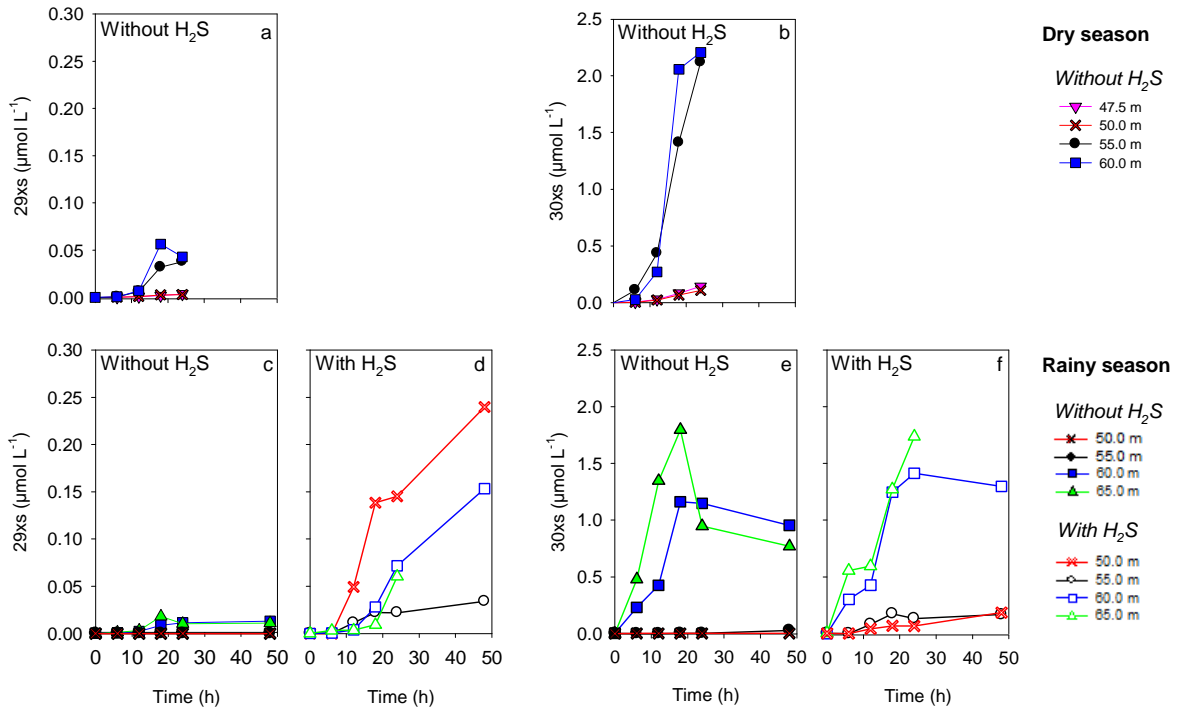
$\text{NO}_2^-$  and  $\text{NO}_3^-$  concentrations were low throughout most of the water column, for both seasons and both stations, but accumulation up to  $1.5 \mu\text{mol L}^{-1}$  (in the Northern Basin) and  $8 \mu\text{mol L}^{-1}$  (in the Southern Basin), respectively, was observed during the rainy season in proximity to the boundary between oxic and anoxic waters.  $\text{NO}_3^-$  and  $\text{NO}_2^-$  accumulation generally co-occurred with peaks in  $\text{N}_2\text{O}$  concentrations ( $15 \text{ nmol L}^{-1}$  in the Southern Basin, and  $58 \text{ nmol L}^{-1}$  in the Northern Basin). Low oxygen concentrations within these depth intervals suggest redox conditions favorable both to denitrification and to high  $\text{N}_2\text{O}$  yields (Codispoti et al., 1992). In dry season,  $\text{N}_2\text{O}$  concentrations were higher in oxic waters (around  $10 \text{ nmol L}^{-1}$ ) than in anoxic waters (below  $5 \text{ nmol L}^{-1}$ ), at both stations.

#### 5.4.2 Denitrification, anammox and DNRA without $\text{H}_2\text{S}$ added

Results of time course incubations ( $29_{\text{excess}}$  and  $30_{\text{excess}}$  production) are reported in Figure 27. Irrespective of seasons and stations, the increase of  $29_{\text{excess}}$  and  $30_{\text{excess}}$  tended to be low at the beginning of the incubation, then strongly increased, and finally tended to stabilize at the end of the incubation. The initial time lag observed before the production of  $\text{N}_2$  could be explained by the time required for the community to restore from the perturbation of the sampling. The plateau observed at the end of the incubations could be due to a bacterial community saturation or substrates limitation ( $\text{NO}_3^-$  or organic matter).

Rate measurements reported in this section should be considered as potential rates due to the fact that the addition of the  $^{15}\text{N}$  labeled compounds increased substrate concentrations relative to their in situ values. Rates and pathways differed between seasons and stations (Figure 26). Denitrification rates were higher in the Northern Basin than in the Southern Basin for both seasons. The maximum rate of denitrification of  $348 \text{ nmol N produced L}^{-1} \text{ h}^{-1}$  was observed at 60 m depth in dry season. In the Southern Basin, the maximum rate of denitrification was  $216 \text{ nmol N produced L}^{-1} \text{ h}^{-1}$  and was observed at 70 m in rainy season. In dry season, almost no denitrification was observed in the Southern Basin, probably due to shallow sampling (denitrification seemed to start at 50 m depth, and was maybe

### Northern Basin



### Southern Basin

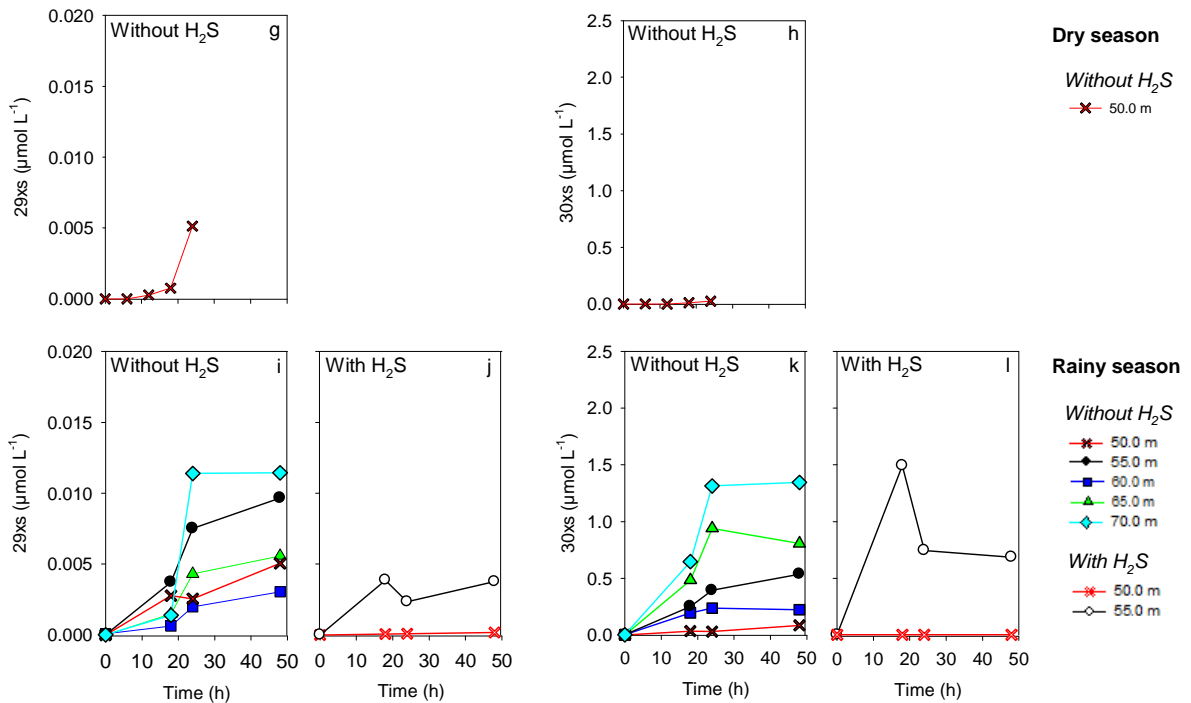


**Figure 27:** 29<sub>excess</sub> and 30<sub>excess</sub> ( $\mu\text{mol L}^{-1}$ ) production in the Northern (a-f) and Southern (g-l) basins, in dry (a, b, g and h) and rainy (c-f and i-l) seasons, with and without H<sub>2</sub>S added. Only depths with significant and visible productions are shown.



present deeper). In contrast to denitrification, rates of anammox tended to be higher in the Southern Basin. The maximum anammox rate of 3.3 nmol N produced L<sup>-1</sup> h<sup>-1</sup> was observed in the Southern Basin at 70 m in rainy season. The maximum anammox rate was less than 1% of the maximum denitrification rate, suggesting it played a small role in N<sub>2</sub> production in Lake Kivu. DNRA was also observed in the water of Lake Kivu during our study. In contrast to denitrification, but like anammox, rates of DNRA were higher in the Southern Basin, with a maximum rate of 36 nmol N produced L<sup>-1</sup> h<sup>-1</sup> observed at 60 m. In the Northern Basin, the maximum rate of DNRA was 9 nmol N produced L<sup>-1</sup> h<sup>-1</sup> at 60 m.

Schubert et al. (2006) used the same method to quantify denitrification and anammox in the water column of Lake Tanganyika. The vertical structure of Lake Tanganyika water column shares characteristics with Lake Kivu water column: anoxic waters rich in NH<sub>4</sub><sup>+</sup>, oxic surface waters depleted in nutrients, NO<sub>3</sub><sup>-</sup> accumulation (~10 μmol L<sup>-1</sup>) near the oxic-anoxic interface and very low NO<sub>2</sub><sup>-</sup> concentrations. Schubert et al. (2006) reported maximum denitrification rates of 200 nmol N produced L<sup>-1</sup> h<sup>-1</sup> - the same magnitude as the rates observed in Lake Kivu. In Lake Rassnitzer, Hamersley et al. (2009) measured maximum denitrification rates of only 6 nmol N produced L<sup>-1</sup> h<sup>-1</sup>. These two studies also measured anammox rates from <sup>15</sup>NO<sub>3</sub><sup>-</sup>-labelling experiments, and obtained rates of 20 and 1.4 nmol N produced L<sup>-1</sup> h<sup>-1</sup> in Lake Tanganyika and Rassnitzer, respectively. In marine environments, denitrification was estimated to 0-216 nmol N produced L<sup>-1</sup> h<sup>-1</sup> (Brettar and Rheinheimer, 1991; Dalsgaard et al., 2003; Kuypers et al., 2005; Thamdrup et al., 2006; Jensen et al., 2008; Dalsgaard et al., 2012; Dalsgaard et al., 2013). The high differences in denitrification and anammox rates between the different environments can be attributed to the different bacterial communities and environment characteristics, such as substrate availability, physico-chemical parameters (pH, oxygen, salinity, temperature), and the presence of inhibitors (e.g. too high concentrations of NH<sub>4</sub><sup>+</sup>, NO<sub>2</sub><sup>-</sup>, organic matter) (Jin et al., 2012). For example, temperature in Lake Rassnitzer was around 5°C at depths sampled during the study of Hamersley et al. (2009), while it was around 23°C in Lake Kivu, what strongly influences anammox and denitrification processes. Also, the abundance and diversity of bacterial communities play an important role. Currently, all anammox bacteria identified belong to the order *Planctomycetales* (Strous et al., 1999). The study of Inceoğlu et al. (2015a) focused on the identification of bacterial and archaeal communities in the water column of Lake Kivu, at the same stations and during the same field campaigns. They showed that *Planctomycetes* were present in the water column, but they were not well represented, what is consistent with low anammox rates we observed during this study. On the contrary, in Lake Tanganyika, anammox bacteria seemed to be better represented (Schubert et al., 2006), which may explain higher anammox rates observed. High denitrification rates observed in Lake Kivu can also be linked to the abundance of the denitrifying bacterial community. Indeed, Inceoğlu et al. (2015a) also revealed the presence of a diversified

community of *Proteobacteria*, among which *Betaproteobacteria*. Numerous nitrogen cycle-related bacteria belong to this class, including well-known denitrifiers, such as *Thiobacillus* sp. and *Denitratisoma* sp. (Claus and Kutzner, 1985; Tiedje, 1994; Ghosh and Dam, 2009). In addition to the presence of these bacteria, Inceoğlu et al. (2015b) also put in evidence their activity by the identification of specific genes. They thus showed the presence of functional genes involved in denitrification, strongly supporting the occurrence of denitrification in the water column of Lake Kivu.

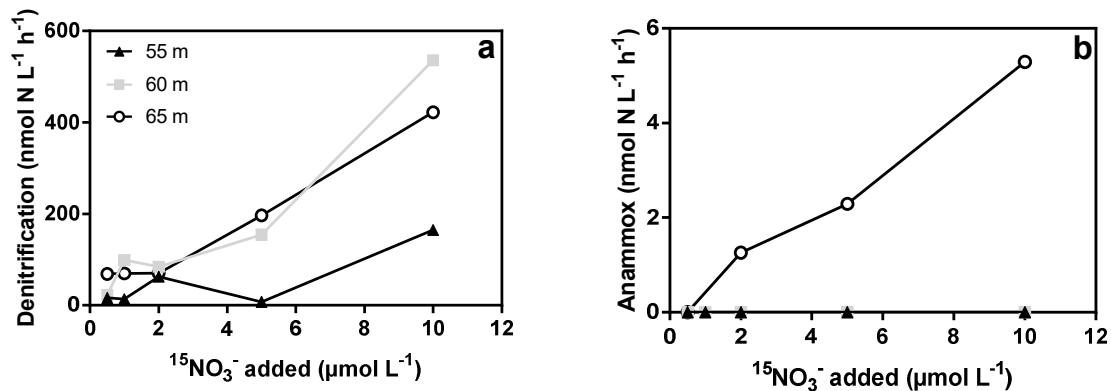


**Figure 28:** Potential denitrification (a) and anammox (b) rates (nmol N produced L<sup>-1</sup> h<sup>-1</sup>) with different  $^{15}\text{NO}_3^-$  concentrations added (0.5, 1, 2, 5 and 10 μmol L<sup>-1</sup>), in the Northern Basin, during the rainy season, at the depths of 55 (black triangles), 60 (grey squares) and 65 m (white circles). Experiments were conducted during rainy season only (February 8, 2012).

We determined the effect of substrate availability on  $\text{NO}_3^-$  reduction. In the Northern Basin, in the rainy season,  $^{15}\text{NO}_3^-$  labeling experiments were conducted with amendments of  $^{15}\text{NO}_3^-$  of different final initial concentrations. These experiments were conducted at depths of 55, 60 and 65 m (Figure 28). Rates of denitrification increased with increasing  $^{15}\text{NO}_3^-$  concentrations, at all depths measured. The maximum rate of denitrification (536 nmol N produced L<sup>-1</sup> h<sup>-1</sup>,  $\text{N}_2 + \text{N}_2\text{O}$ ) was observed at 60 m with a final  $^{15}\text{NO}_3^-$  concentration of 10 μmol L<sup>-1</sup>. No anammox was observed at the depths of 55 and 60 m, while rates of anammox increased with increasing  $^{15}\text{NO}_3^-$  concentrations up to 5.2 nmol N produced L<sup>-1</sup> h<sup>-1</sup> with 10 μmol L<sup>-1</sup>, at 65 m. These results strongly suggest that denitrification in Lake Kivu is limited by  $\text{NO}_3^-$  concentrations, and likewise, that anammox is probably limited by the supply of  $\text{NO}_2^-$ , through partial denitrification. Also, experiments amended with  $^{15}\text{NH}_4^+$  suggest that anammox in the Southern Basin is co-limited by  $\text{NH}_4^+$ . Indeed, these experiments revealed high rates of anammox in the Southern Basin (Figure 29), while no anammox was observed in the Northern Basin. Anammox rates were higher (up to 44 nmol N L<sup>-1</sup> h<sup>-1</sup>) than those measured with  $^{15}\text{NO}_3^-$ , and were located at shallower depths (at 47.5 m), where  $\text{NH}_4^+$  concentrations were very low (less than 1 μmol L<sup>-1</sup>).

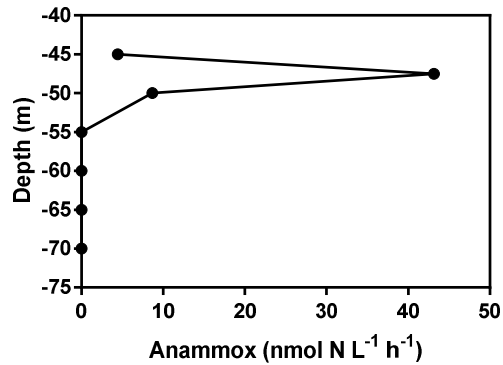


**Figure 29:** Potential anammox rates (nmol N produced L<sup>-1</sup> h<sup>-1</sup>) measured in the incubations with <sup>15</sup>NH<sub>4</sub><sup>+</sup> added, in rainy season, in the Southern Basin.

If we compare in terms of relative contribution of anammox to N<sub>2</sub> (Table 14), we estimated it to be potentially up to 13 % in Lake Kivu, exactly like in Lake Tanganyika (Schubert et al., 2006), while it was estimated to up to 50 % in Lake Rassnitzer (Hamersley et al., 2009). In the anoxic water column of Golfo Duce, anammox accounted for 19-35 % in the formation of N<sub>2</sub> (Dalsgaard et al., 2003). However, in Lake Kivu, anammox was not present in the main basin (Northern Basin), and can be thus considered as of little importance in the water column of Lake Kivu.

Denitrification, anammox, and DNRA all compete for NO<sub>3</sub><sup>-</sup>, and competition may thus appear between the different processes. During our study, we observed a competitive relationship between denitrification and DNRA, since for both stations, higher denitrification rates corresponded to the lower DNRA rates (Figure 30a). Also, competition between anammox and DNRA seemed to occur, since anammox rates tended to be lower when DNRA rates were higher (Figure 30b). Although DNRA can fuel the anammox bacterial community in NH<sub>4</sub><sup>+</sup>, they can also enter in competition for NO<sub>2</sub><sup>-</sup> and NO<sub>3</sub><sup>-</sup>. At depths where the different processes were measured, NH<sub>4</sub><sup>+</sup> was not limiting (so the supply by DNRA was not required for anammox), contrary to NO<sub>2</sub><sup>-</sup>, and NO<sub>3</sub><sup>-</sup>, what can explain the competitive relationship. On the contrary, anammox seemed to not enter in competition with denitrification for substrates, since anammox rates tended to be higher when denitrification rates were higher (Figure 30c). This suggests that anammox bacteria may gain benefit from NO<sub>2</sub><sup>-</sup> produced as intermediate during the denitrification process.

**Table 14:** Contribution (%) of denitrification and anammox in the formation of N<sub>2</sub>, in both basins and during both campaigns, with and without H<sub>2</sub>S added. N.d.: not determined, SD: standard deviation.

<b>Northern Basin</b>						
	Without H <sub>2</sub> S (%)			With H <sub>2</sub> S (%)		
	Denitrification	Anammox	SD	Denitrification	Anammox	SD
<i>Dry season</i>						
45	0	0	0	n.d	n.d	
47.5	0	0	0	n.d	n.d	
50	98	2	0	n.d	n.d	
55	99	1	0	n.d	n.d	
60	100	0	1	n.d	n.d	
<i>Rainy season</i>						
40	0	0	0	0	0	0
42.5	0	0	0	0	0	0
45	0	0	0	0	0	0
50	100	0	0	68	32	39
55	100	0	0	91	9	5
60	99	1	0	100	0	0
65	100	0	0	93	7	4
<b>Southern Basin</b>						
	Without H <sub>2</sub> S (%)			With H <sub>2</sub> S (%)		
	Denitrification	Anammox	SD	Denitrification	Anammox	SD
<i>Dry season</i>						
40	0	0	0	n.d	n.d	
45	0	0	0	n.d	n.d	
47.5	0	0	0	n.d	n.d	
50	87	13	9	n.d	n.d	
<i>Rainy season</i>						
45	0	0	0	0	0	0
47.5	100	0	0	0	0	0
50	94	6	5	100	0	0
55	100	0	0	100	0	0
60	99	1	1	n.d	n.d	
65	99	1	0	n.d	n.d	
70	98	2	0	n.d	n.d	

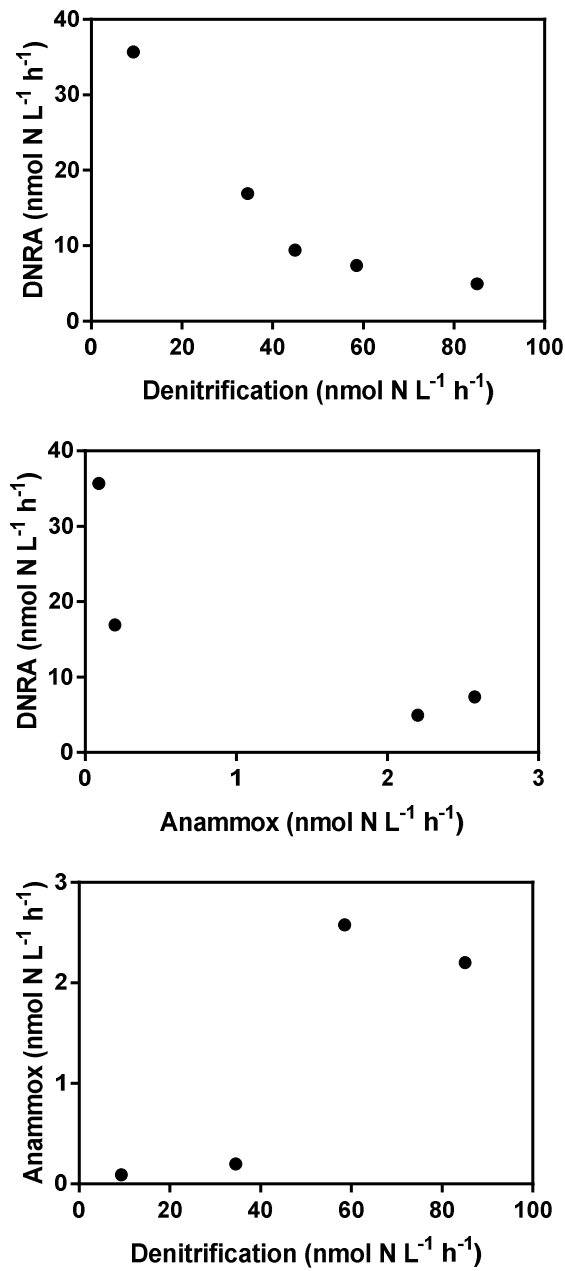


**Figure 30:** Correlation between (a) DNRA and denitrification rates, (b) DNRA and anammox rates and (c) Anammox and denitrification rates ( $\text{nmol N produced L}^{-1} \text{h}^{-1}$ ) at both stations and during both seasons.

#### 5.4.3 Denitrification, anammox and DNRA with $\text{H}_2\text{S}$ added

All rates reported in this section are also potential rates, measured in the incubations with  $^{15}\text{NO}_3^-$  and  $\text{H}_2\text{S}$  added, during the rainy season. In the Northern Basin, the addition of  $\text{H}_2\text{S}$  was followed by an increase of denitrification, anammox and DNRA rates at almost all depths measured, except at

65 m where denitrification and DNRA rates slightly decreased. In particular, anammox rate increased up to 24 nmol N produced L<sup>-1</sup> h<sup>-1</sup> at 50 m. In the Southern Basin, H<sub>2</sub>S experiments were only performed at four depths (45, 47.5, 50 and 55 m) for denitrification and anammox, and at three depths (47.5, 50 and 55 m) for DNRA. The addition of H<sub>2</sub>S tended to decrease denitrification rates, while no effect was observed on anammox rates, which remained below detection. On the contrary, the addition of H<sub>2</sub>S tended to stimulate DNRA rates.

In the Northern Basin, we showed that anammox rates were significantly stimulated by the addition of H<sub>2</sub>S. Also, its contribution to N<sub>2</sub> production reached 32 % (Table 14). Some studies have suggested an inhibitory effect of H<sub>2</sub>S on anammox (Dalsgaard et al., 2003; Jensen et al., 2008; Jensen et al., 2009). However, other studies conducted in wastewater bed reactors and in laboratory cultures showed that anammox bacteria tolerate H<sub>2</sub>S and even that H<sub>2</sub>S can stimulate anammox (Kalyuzhnyi et al., 2006; Jung et al., 2007; Russ et al., 2014). The study of Wenk et al. (2013) on Lake Lugano, which used the same incubation method, also showed that anammox was stimulated by the addition of H<sub>2</sub>S. To explain anammox activity in the presence of H<sub>2</sub>S, they suggested that anammox bacteria lived in aggregates with chemolithotrophic denitrifying bacteria and thus in the presence of lower concentrations of H<sub>2</sub>S following its consumption by the denitrifying bacteria. The latter would also produce NO<sub>2</sub><sup>-</sup>, which would in turn stimulate anammox. In our study, the addition of H<sub>2</sub>S also stimulated denitrification in the Northern Basin, suggesting the occurrence of chemolithotrophic denitrification. Production of N<sub>2</sub>O also increased with the addition of H<sub>2</sub>S (Table 15), strongly suggesting the occurrence of chemolithotrophic denitrification, which stimulates NO<sub>3</sub><sup>-</sup> and NO<sub>2</sub><sup>-</sup> reduction relative to N<sub>2</sub>O reduction, leading to a higher N<sub>2</sub>O production. Also, bacterial communities potentially capable to perform chemolithotrophic denitrification seem to be present in the water column of Lake Kivu. Indeed, İnceoğlu et al. (2015a) put in evidence the presence of *Epsilonproteobacteria* and *Gammaproteobacteria*, two classes among which bacteria capable of HS<sup>-</sup> oxidation, such as *Sulfurimonas* sp., *Sulfuricurvum* sp., *Thiothrix* sp. and *Thiomicrospira* sp., can be found (Larkin and Strohl, 1983; Eisen et al., 2002; Inagaki et al., 2003; Friedrich et al., 2005; Sievert et al., 2008; Ghosh and Dam, 2009). Also, as previously said, they showed that *Betaproteobacteria* were well represented, among which we can find *Thiobacillus* sp., which is capable to perform denitrification coupled to sulfur oxidation.

In contrast, in the Southern Basin, the addition of H<sub>2</sub>S tended to decrease denitrification rates (N<sub>2</sub> + N<sub>2</sub>O). An experimental error, such as an inhibition of denitrification by the addition of small quantities of atmospheric oxygen, seems very unlikely, since a pre-incubation period of 12h after filling the incubation vials was respected before the start of the experiment, to allow the consumption of the potential external oxygen artificially introduced. Alternatively, denitrifiers can compete for NO<sub>3</sub><sup>-</sup> and

NO<sub>2</sub><sup>-</sup> with DNRA and anammox bacteria. During our measurements, DNRA rates tended to decrease when H<sub>2</sub>S was added. The inhibition of denitrification when H<sub>2</sub>S was present has been frequently reported (e.g. Jorgensen, 1989; Joye and Hollibaugh, 1995; An and Gardner, 2002) but it is now established that denitrification can be coupled with H<sub>2</sub>S oxidation (e.g. Brettar and Rheinheimer, 1991; Burgin and Hamilton, 2008; Jensen et al., 2009). So, it seems that the apparent inhibition of denitrification (actually the inhibition of N<sub>2</sub>O reduction to N<sub>2</sub>) at high H<sub>2</sub>S concentrations could be due to a competition with DNRA for substrates. Indeed, several studies suggest that DNRA can be enhanced at high H<sub>2</sub>S concentrations (e.g. Brunet and Garcia-Gil, 1996; Rysgaard et al., 1996; Sayama et al., 2005) and becomes more competitive than denitrification. The fact that denitrification rates decreased with H<sub>2</sub>S added only in the Southern Basin could be explained by the higher importance of DNRA in the Southern Basin (reflected by higher DNRA rates in "normal" conditions, without H<sub>2</sub>S added), and so by a stronger competition.

**Table 15:** Relative contribution (% ± standard deviation) of N<sub>2</sub> production compared with N<sub>2</sub>+N<sub>2</sub>O production without and with H<sub>2</sub>S added, in rainy season, for depths with significant rates of denitrification. N.d.: not determined

	Without H <sub>2</sub> S	With H <sub>2</sub> S
<i>Northern Basin</i>		
50	100 ± 0	92 ± 6
55	100 ± 0	100 ± 0
60	96 ± 3	88 ± 5
65	99 ± 3	47 ± 24
<i>Southern Basin</i>		
47.5	100 ± 0	Not detected
50	100 ± 0	100 ± 0
55	99 ± 2	100 ± 2
60	74 ± 27	n.d
65	84 ± 2	n.d
70	94 ± 1	n.d

#### 5.4.4 Natural rates

Natural conditions for the occurrence of denitrification in the water column of Lake Kivu were present during the rainy season, since non negligible NO<sub>x</sub> concentrations and a denitrifying bacterial community were observed. Moreover, in the Northern Basin, the location of the N<sub>2</sub>O peak in the anoxic

part of the water column suggests that N<sub>2</sub>O could have been produced through denitrification. Also, the water column of Lake Kivu seems to be a favorable environment for DNRA, since *Epsilonproteobacteria*, *Deltaproteobacteria* and *Gammaproteobacteria*, among which we can find bacteria capable of DNRA, such as *Wolinella* sp., *Desulfovibrio* sp., *Geobacter* sp. or *Vibrio* sp. (Bokranz et al., 1983; Dalsgaard and Bak, 1994; Simon, 2002; Strohm et al., 2007) were well represented in the water column of Lake Kivu (Inceoğlu et al., 2015a). On the contrary, the water column of Lake Kivu first seems to be unfavorable for anammox, since *Planctomycetes* were seldom observed (Inceoğlu et al., 2015a), and low NO<sub>2</sub><sup>-</sup> concentrations and high H<sub>2</sub>S concentrations might be inhibiting for anammox. However, we showed that anammox could occur, and even be stimulated, when H<sub>2</sub>S was present, and also can occur with NO<sub>3</sub><sup>-</sup> instead of NO<sub>2</sub><sup>-</sup>.

As shown by Figure 28, the scales in our range of NO<sub>3</sub><sup>-</sup> concentrations are linear with these ones. We thus calculated natural rates (<sup>14</sup>N<sup>14</sup>N) in our incubations with <sup>15</sup>NO<sub>3</sub><sup>-</sup> added according to following equations:

$$(16) \text{ Natural N}_2 \text{ denitrification} = \text{Potential N}_2 \text{ denitrification} * (1 - F_{\text{NO}_3})$$

$$(17) \text{ Natural N}_2 \text{ anammox} = \text{Potential N}_2 \text{ anammox} * (1 - F_{\text{NO}_3})$$

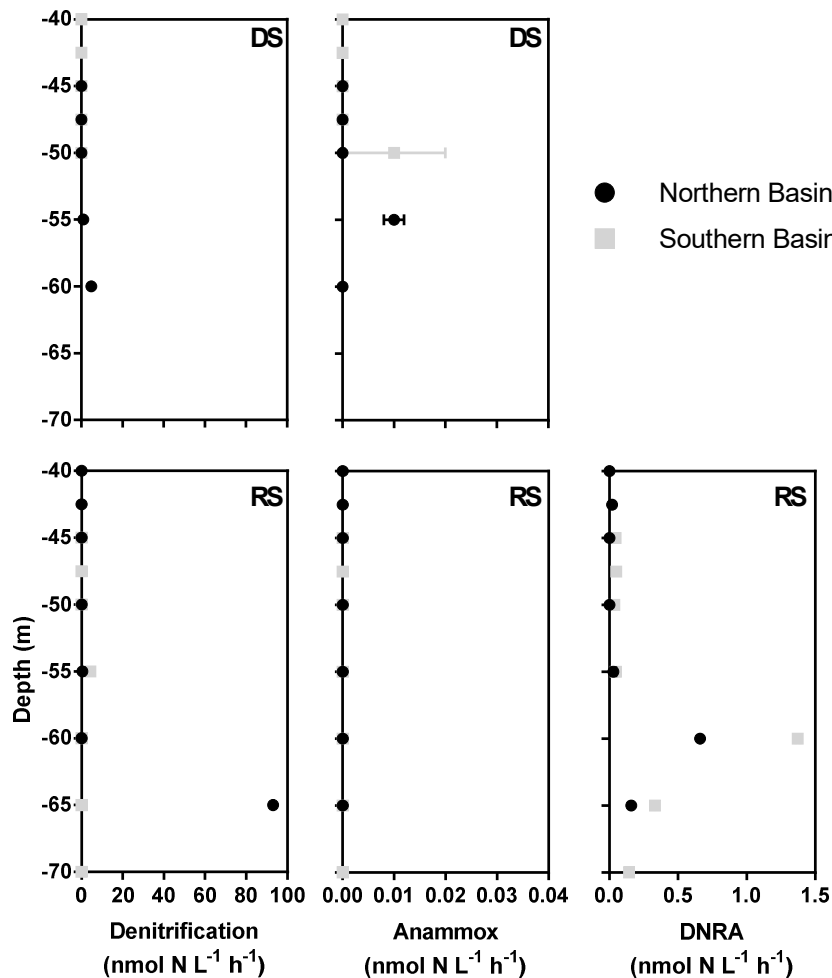
$$(18) \text{ Natural NH}_4^+ \text{ DNRA} = \text{Potential NH}_4^+ \text{ DNRA} * (1 - F_{\text{NO}_3})$$

Figure 31 reports natural rates measured in our incubations. Denitrification was naturally present in the water column of Lake Kivu, in particular in rainy season, where a maximum rate of 93 nmol N produced L<sup>-1</sup> h<sup>-1</sup> was observed at 65 m in the Northern Basin. In dry season, natural denitrification rates were lower, due to low NO<sub>3</sub><sup>-</sup> concentrations. Almost no anammox was observed (maximum rate of 0.01 nmol N produced L<sup>-1</sup> h<sup>-1</sup>), and DNRA rates were also significantly lower (maximum rate of 0.7 produced nmol N L<sup>-1</sup> h<sup>-1</sup>). We must note that when H<sub>2</sub>S was added, denitrification, anammox and DNRA rates all increased, and anammox rates achieved 9 nmol N produced L<sup>-1</sup> h<sup>-1</sup> in rainy season (data not shown).

The maximum depth-integrated natural denitrification rate was observed in the Northern Basin and can be estimated to 0.01 mmol N m<sup>-2</sup> d<sup>-1</sup>, while the depth-integrated natural DNRA rate observed in the Northern Basin was estimated to only 0.0001 mmol N m<sup>-2</sup> d<sup>-1</sup> (integration from 40 to 65 m depth). The maximum depth-integrated natural DNRA rate was observed in the Southern Basin and was estimated to 0.0002 mmol N m<sup>-2</sup> d<sup>-1</sup>. Dalsgaard et al. (2013) also calculated depth-integrated in-situ denitrification rates from their incubations, which ranged from 0.06 to 2.11 mmol N m<sup>-2</sup> d<sup>-1</sup>. Schubert et al. (2006) calculated depth-integrated denitrification rates of 2.4 mmol N m<sup>-2</sup> d<sup>-1</sup>, but their calculations were based on potential denitrification rates and they admit that their calculations should be taken with caution, since they only performed one measurement. Depth-integrated potential



denitrification rates in Lake Kivu were higher, but remained low, with a maximum of  $0.05 \text{ mmol N m}^{-2} \text{ d}^{-1}$  (in the Northern Basin).



**Figure 31:** Natural denitrification, anammox and DNRA rates ( $\text{nmol N produced L}^{-1} \text{ h}^{-1}$ ) at both stations and during both seasons. RS: Rainy season, DS: Dry season

#### 5.4.5 Spatial heterogeneity

During this study, we put in evidence important differences between the Northern and the Southern Basin of Lake Kivu. Without  $\text{H}_2\text{S}$  added, denitrification tended to be higher in the Northern Basin, while anammox and DNRA tended to be more important in the Southern Basin. The treatment with  $^{15}\text{NH}_4^+$  added also showed important potential anammox rates only in the Southern Basin.

However, differences in bacterial communities between both basins are not significant, since relative abundances of bacterial community capable of DNRA was estimated to be up to 8 and 13 %

(means of both campaigns) in the Northern and Southern Basins, respectively, while relative abundance of denitrifying community was estimated to 35 and 44 % (İnceoğlu et al., 2015a). It seems unlikely that the small difference in term of the bacterial community composition is the only factor determining the different process rates observed in the Northern and Southern Basin. As explained above, the basins are morphometrically different. The Southern Basin seems to be more stable than the Northern Basin, what may explain why anammox was more widespread in the Southern Basin, since anammox is a slow process requiring quite stable environmental conditions (Strous et al., 1999). Also, based upon  $\text{NH}_4^+$  vertical profiles, it seems that  $\text{NH}_4^+$  concentrations tend to be higher in the Southern Basin, probably linked to higher DNRA rates, what can influence anammox. However, we cannot draw definitive conclusions based on so few profiles. Concerning heterotrophic denitrification and DNRA, it is difficult to explain differences observed with available data. We can hypothesize that organic matter supply is different between both basins, with higher supply in the Southern Basin, due to its smaller size. Indeed, due to higher proximity of surrounded lands, allochthonous organic matter supplies may be higher, especially during the rainy season. This would favor DNRA over denitrification (Kelso et al., 1997; Silver et al., 2001; Dong et al., 2011).

## **5.5 Conclusion**

This study reports the occurrence of denitrification, DNRA and anammox for the first time in Lake Kivu. To our best knowledge, it is also the first study that reports such data in the water column of a large tropical lake. We showed that these three processes can coexist in the anoxic water column, even if competition for substrates seemed to occur. As Wenk et al. (2013) in Lake Lugano, we showed a co-occurrence of chemolithotrophic denitrification and anammox. Further studies are required to determine if aggregates between denitrifying bacteria and anammox bacteria are possible and if they are present in Lake Kivu, and to elucidate the competitive relationships between the three processes.

---

## Chapter 6: Emission and oxidation of methane in a meromictic, eutrophic and temperate lake (Dendre, Belgium)

---

**Adapted from:** Fleur A.E. Roland, François Darchambeau, Cédric Morana, Steven Bouillon and Alberto V. Borges (2017) *Emission and oxidation of methane in a meromictic, eutrophic and temperate lake (Dendre, Belgium)*, *Chemosphere*, DOI: 10.1016/j.chemosphere.2016.10.138

### 6.1 Abstract

We sampled the water column of the Dendre stone pit lake (Belgium) in spring, summer, autumn and winter. Depth profiles of several physico-chemical variables, nutrients, dissolved gases (CO<sub>2</sub>, CH<sub>4</sub>, N<sub>2</sub>O), sulfate, sulfide, iron and manganese concentrations and δ<sup>13</sup>C-CH<sub>4</sub> were determined. We performed incubation experiments to quantify CH<sub>4</sub> oxidation rates, with a focus on anaerobic CH<sub>4</sub> oxidation (AOM), without and with an inhibitor of sulfate reduction (molybdate). The evolution of nitrate and sulfate concentrations during the incubations was monitored. The water column was anoxic below 20 m throughout the year, and was thermally stratified in summer and autumn. High partial pressure of CO<sub>2</sub> and CH<sub>4</sub> and high concentrations of ammonium and phosphate were observed in anoxic waters. Important nitrous oxide and nitrate concentration maxima were also observed (up to 440 nmol L<sup>-1</sup> and 80 μmol L<sup>-1</sup>, respectively). Vertical profiles of δ<sup>13</sup>C-CH<sub>4</sub> unambiguously showed the occurrence of AOM. Important AOM rates (up to 14 μmol L<sup>-1</sup> d<sup>-1</sup>) were observed and often co-occurred with nitrate consumption peaks, suggesting the occurrence of AOM coupled with nitrate reduction. AOM coupled with sulfate reduction also occurred, since AOM rates tended to be lower when molybdate was added. CH<sub>4</sub> oxidation was mostly aerobic (~80% of total oxidation) in spring and winter, and almost exclusively anaerobic in summer and autumn. Despite important CH<sub>4</sub> oxidation rates, the estimated CH<sub>4</sub> fluxes from the water surface to the atmosphere were high (mean of 732 μmol m<sup>-2</sup> d<sup>-1</sup> in spring, summer and autumn, and up to 12,482 μmol m<sup>-2</sup> d<sup>-1</sup> in winter).

### 6.2 Introduction

Methane (CH<sub>4</sub>) is known to be an important natural and anthropogenic greenhouse gas. CH<sub>4</sub> concentrations in the atmosphere have increased dramatically during the 20<sup>th</sup> century to reach 1850 ppb in 2015, mainly due to human activities (agriculture, waste disposal and energy extraction and production) (IPCC, 2013;Kirschke et al., 2013;NOAA, 2015). In natural environments, CH<sub>4</sub> is anaerobically produced by methanogenic archaea. The total CH<sub>4</sub> emission to the atmosphere has been estimated to 540 Tg CH<sub>4</sub> yr<sup>-1</sup>, with a significant contribution from inland waters (Bastviken et al.,

2011;Borges et al., 2015a;Holgerson and Raymond, 2016). The actual amount of CH<sub>4</sub> produced is higher, as a significant fraction of CH<sub>4</sub> produced is biologically oxidized before reaching the atmosphere (Bastviken et al., 2002). CH<sub>4</sub> oxidation limits the flux of CH<sub>4</sub> to the atmosphere, and in inland waters can fuel a microbial based food-web (Jones and Grey, 2011).

CH<sub>4</sub> oxidation can be performed under both aerobic and anaerobic conditions. It is now commonly assumed that anaerobic CH<sub>4</sub> oxidation (AOM) can occur with different final electron acceptors: sulfate (SO<sub>4</sub><sup>2-</sup>), nitrate (NO<sub>3</sub><sup>-</sup>), nitrite (NO<sub>2</sub><sup>-</sup>), iron (Fe) and/or manganese (Mn) (Borrel et al., 2011). In seawater, NO<sub>3</sub><sup>-</sup> concentrations are low (usually < 5 μmol L<sup>-1</sup>), while SO<sub>4</sub><sup>2-</sup> concentrations are much higher (~30 mmol L<sup>-1</sup>). Also, Fe and Mn concentrations (on the order of pmol L<sup>-1</sup>) in seawater are negligible compared to SO<sub>4</sub><sup>2-</sup> concentrations. So, even if denitrification, Fe- and Mn-reduction are thermodynamically more favorable than SO<sub>4</sub><sup>2-</sup> reduction, the latter remains the main anaerobic pathway for the degradation of organic matter in the oceans, including the degradation of CH<sub>4</sub>. While AOM is thus generally coupled to SO<sub>4</sub><sup>2-</sup> reduction (SDMO) in marine waters and sediments (e.g. Iversen and Jørgensen, 1985;Boetius et al., 2000;Jørgensen et al., 2001), other electron acceptors of AOM have been much less frequently studied in freshwater systems. Due to low the SO<sub>4</sub><sup>2-</sup> concentrations usually observed in freshwaters environments, AOM is often considered to be negligible compared to aerobic CH<sub>4</sub> oxidation (Rudd et al., 1974). However, AOM in freshwaters can also be coupled to NO<sub>2</sub><sup>-</sup> and NO<sub>3</sub><sup>-</sup> reduction (NDMO), which is thermodynamically much more favorable than SDMO (free Gibbs energy of -928, -765 and -17 kJ mol<sup>-1</sup> CH<sub>4</sub>, with NO<sub>2</sub><sup>-</sup>, NO<sub>3</sub><sup>-</sup> and SO<sub>4</sub><sup>2-</sup> reduction, respectively; Raghoebarsing et al., 2006;Borrel et al., 2011). NDMO has been observed in experimental environments with enrichment of bacteria of interest (e.g. Ettwig et al., 2010;Hu et al., 2011;Haroon et al., 2013), or in sediments cultures with electron acceptors added (e.g. Deutzmann and Schink, 2011;á Norđi and Thamdrup, 2014). Despite numerous laboratory observations, the significance of NDMO in natural environments is still largely unknown. Although AOM coupled with Fe- and Mn-reduction (FDMO and MDMO, respectively) has been proposed to occur in various freshwater environments (e.g. ferruginous lakes Matano and Kinneret; Crowe et al., 2011;Sivan et al., 2011;á Norđi et al., 2013), to our knowledge no direct rate measurements have been reported in the literature.

In this study, we investigated biogeochemistry of the water column of Dendre stone pit lake (Belgium), a relatively deep (maximum depth 30 m) but small (0.032 km<sup>2</sup>) water body in a former limestone quarry, with a focus on quantifying AOM rates and related electron acceptors. This lake was chosen to be an ideal system for studying AOM dynamics because it is known to be meromictic (waters anoxic below 20 m depth throughout the year) and rich in both organic matter (eutrophic) and sulfide (HS<sup>-</sup>) in the anoxic layers. The lake is fed by springs at 7 and 18 m depth, providing potentially NO<sub>3</sub><sup>-</sup> rich groundwater due to generalized fertilizer contamination that is common in Belgium (SPW-DGO3,

2015). We thus hypothesized that high organic matter supply and bottom layer anoxia sustain high methanogenesis rates, and that CH<sub>4</sub> production is removed by SDMO and/or NDMO based on occurrence of high HS<sup>-</sup> concentrations, and potentially high NO<sub>3</sub><sup>-</sup> concentrations.

## 6.3 Material and methods

### 6.3.1 Physico-chemical parameters and sampling

Sampling in the Dendre stone pit lake (50.6157°N, 3.7949°E) was carried out in spring (May 2014), summer (August 2014), winter (February 2015) and autumn (October 2015). Depth profiles of dissolved oxygen (O<sub>2</sub>) concentrations, temperature, pH and specific conductivity were obtained with Yellow Springs Instrument 6600 V2 and Hydrolab DS5 multiparameter probes. The conductivity, pH and oxygen probes were calibrated the day before each sampling using the protocols and standards recommended by the manufacturer.

### 6.3.2 CH<sub>4</sub> oxidation measurements and water column chemical analyses

At each depth of interest, duplicate samples for N<sub>2</sub>O and CH<sub>4</sub> concentration analyses were collected in 60 mL glass serum bottles from a Niskin bottle through a silicon tube connected to the outlet, left to overflow, poisoned with 200 µL of a saturated HgCl<sub>2</sub> solution and immediately sealed with butyl stoppers and aluminium caps. Ten other bottles per depth were incubated in the dark and constant temperature (close to in-situ temperature): five of them received 250 µL of a solution of molybdate (1 mol L<sup>-1</sup>, hence a final concentration of 4 mmol L<sup>-1</sup>), an inhibitor of sulfur-reducing bacteria and five received no treatment. The biological activity of two incubated bottles (one from each treatment) was stopped at 12, 24, 48, 72 and 96h by the addition of a saturated 200 µL HgCl<sub>2</sub> solution. CH<sub>4</sub> and N<sub>2</sub>O concentrations were determined via the headspace equilibration technique (20 mL N<sub>2</sub> headspace in 60 mL serum bottles) and measured by gas chromatography (GC) with electron capture detection (ECD) for N<sub>2</sub>O and with flame ionization detection (FID) for CH<sub>4</sub> (Weiss, 1981). The SRI 8610C GC-ECD-FID was calibrated with certified CH<sub>4</sub>:CO<sub>2</sub>:N<sub>2</sub>O:N<sub>2</sub> mixtures (Air Liquide, Belgium) of 1, 10, 30 and 509 ppm CH<sub>4</sub> and of 0.2, 2.0 and 6.0 ppm N<sub>2</sub>O. Concentrations were computed using the solubility coefficients of Yamamoto et al. (1976) and Weiss and Price (1980), for CH<sub>4</sub> and N<sub>2</sub>O, respectively. The precision of measurements was ±3.9% and ±3.2% for CH<sub>4</sub> and N<sub>2</sub>O, respectively. CH<sub>4</sub> oxidation rates were calculated based on the decrease of CH<sub>4</sub> concentrations in the incubations.

In autumn, triplicate samples for the determination of the partial pressure of CO<sub>2</sub> (pCO<sub>2</sub>) were collected in 60 ml plastic syringes directly from the Niskin. The pCO<sub>2</sub> was measured with an infra-red gas analyzer (Licor Li-840) after headspace equilibration in the syringe (Abril et al., 2015; Borges et al.,

2015a). The Li-840 was calibrated with N<sub>2</sub> and certified CO<sub>2</sub>:N<sub>2</sub> mixtures (Air Liquide, Belgium) of 388, 813, 3788 and 8300 ppm CO<sub>2</sub>. The precision of measurements was ±4.1%.

Water extracted for creating the headspace in the serum bottles was used to quantify SO<sub>4</sub><sup>2-</sup>, NH<sub>4</sub><sup>+</sup>, NO<sub>2</sub><sup>-</sup>, NO<sub>3</sub><sup>-</sup>, Mn and Fe concentrations. SO<sub>4</sub><sup>2-</sup>, NO<sub>2</sub><sup>-</sup> and NH<sub>4</sub><sup>+</sup> concentrations were quantified colorimetrically using a 5-cm optical path and a Genesys 10vis spectrophotometer (Thermo Spectronic). SO<sub>4</sub><sup>2-</sup> concentrations were determined by the nephelometric method according to Rodier et al. (1996), after being precipitated in barium sulfate in an acid environment. NH<sub>4</sub><sup>+</sup> concentrations were determined using the dichloroisocyanurate-salicylate-nitroprussiate colorimetric method (Westwood, 1981), and NO<sub>2</sub><sup>-</sup> concentrations were determined by the sulfanilamide coloration method (APHA, 1998). NO<sub>3</sub><sup>-</sup> concentrations were determined after vanadium reduction to NO<sub>2</sub><sup>-</sup> and quantified with a Multiskan Ascent Thermo Scientific multi-plates reader (APHA, 1998; Miranda et al., 2001). The detection limits for these methods were 52, 0.3, 0.15 and 0.03 μmol L<sup>-1</sup>, for SO<sub>4</sub><sup>2-</sup>, NH<sub>4</sub><sup>+</sup>, NO<sub>3</sub><sup>-</sup> and NO<sub>2</sub><sup>-</sup>, respectively.

The samples for total Fe and Mn determination were digested and mineralized in nitric acid, using specific Teflon bombs in a microwave digestion labstation (Ethos D, Milestone Inc.). They were finally diluted into milli-Q water to a volume of 50 ml. The total Fe and Mn concentrations were determined by inductively coupled plasma mass spectrometry (ICP-MS) using dynamic reaction cell (DRC) technology (ICP-MS SCIEX ELAN DRC II, PerkinElmer inc.). Analytical accuracy was verified by a certified reference material (BCR 715, Industrial Effluent Wastewater).

Additional samples to determine vertical profiles of NO<sub>3</sub><sup>-</sup>, NH<sub>4</sub><sup>+</sup>, NO<sub>2</sub><sup>-</sup>, PO<sub>4</sub><sup>3-</sup> and SO<sub>4</sub><sup>2-</sup> concentrations were collected in 50 ml plastic vials after being filtered through a 0.22 μm syringe filter, and stored frozen. NO<sub>3</sub><sup>-</sup>, NO<sub>2</sub><sup>-</sup>, NH<sub>4</sub><sup>+</sup> and SO<sub>4</sub><sup>2-</sup> concentrations were determined according to respective methods described above. PO<sub>4</sub><sup>3-</sup> concentrations were determined colorimetrically with a 5-cm optical path, in a spectrophotometer Thermo Spectronic Genesys 10vis, using the ammonium molybdate-potassium antimonyl tartrate method (APHA, 1998). The detection limit of this method was 0.03 μmol L<sup>-1</sup>.

Samples to determine vertical profiles of H<sub>2</sub>S concentrations were collected in 60 ml biological oxygen demand bottles after being filtered through a 0.22 μm syringe filter, and preserved with 2 ml of 1 mol L<sup>-1</sup> zinc acetate. Concentrations were determined colorimetrically as described above, using the analytical method described by Cline (1969).

In summer and autumn, an additional 60 mL glass serum bottle per depth was collected and preserved as described above in order to measure the δ<sup>13</sup>C values of CH<sub>4</sub> (δ<sup>13</sup>C-CH<sub>4</sub>). δ<sup>13</sup>C-CH<sub>4</sub> was then determined by a custom developed technique (Morana et al. 2015), whereby a 5 ml helium headspace

was first created and CH<sub>4</sub> was flushed out through a double-hole needle. CO<sub>2</sub> and H<sub>2</sub>O were first removed with a CO<sub>2</sub> trap (soda lime) and a water trap (magnesium perchlorate) and then the non-methane volatile organic molecules were trapped and hence removed from the gas stream in a loop immersed in liquid nitrogen. The CH<sub>4</sub> was converted to CO<sub>2</sub> in an online combustion column similar to that in an Elemental Analyzer. The resulting CO<sub>2</sub> was subsequently preconcentrated by immersion of a stainless steel loop in liquid nitrogen passed through a micropacked GC column (HayeSep Q 2m, 0.75mm ID ; Restek), and finally measured on a Thermo DeltaV Advantage isotope ratio mass spectrometer. CO<sub>2</sub> produced by acidification (H<sub>3</sub>PO<sub>4</sub>) of certified reference standards for  $\delta^{13}\text{C}$  analysis (IAEA-CO1 and LSVEC) was used to calibrate  $\delta^{13}\text{C}$ -CH<sub>4</sub> data. Reproducibility estimated based on duplicate injection of a selection of samples was typically better than  $\pm 0.5$  ‰.

### 6.3.3 CO<sub>2</sub>, CH<sub>4</sub> and N<sub>2</sub>O fluxes calculations

CO<sub>2</sub>, CH<sub>4</sub> and N<sub>2</sub>O fluxes to the atmosphere were calculated from the dissolved concentration at 1 m depth from which was computed the concentration gradient across the air-water interface of CO<sub>2</sub>, CH<sub>4</sub> and N<sub>2</sub>O, and the gas transfer velocity computed from wind speed according to the Cole and Caraco (1998) relationship. A positive flux value corresponds to a net gas transfer from the water to the atmosphere, while a negative flux corresponds to a net gas transfer from the atmosphere to the water. Wind speeds were obtained from the National Centers for Environmental Prediction (NCEP) gridded daily product (grid point: 50.4752°N, 3.7500°E).

## 6.4 Results

### 6.4.1 Physico-chemical parameters

The position of thermoclines and chemoclines (specific conductivity and pH) strongly differed between seasons (Figure 32). The water column was well stratified during the sampling in spring, summer and autumn, with thermoclines located in the upper part of the water column (first 10 m), while in winter, the water column was mixed from surface to 20 m. Surface temperatures were higher in spring and summer (maximum 18°C at 1 m depth), lowest in winter (5°C at 1 m depth), and intermediate in autumn (14°C at 1 m depth).

During winter, when the water column was almost entirely mixed, the oxycline was located at the bottom of the lake (20 m) (Figure 32). However, the oxycline moved upward following the establishment of the thermal stratification in spring, to reach 7 m and 8.5 m in summer and autumn, respectively. In spring, summer and winter, significant N<sub>2</sub>O concentration peaks were observed, with a maximum of 440 nmol L<sup>-1</sup> recorded at 14 m in summer. In autumn, the distribution of N<sub>2</sub>O was more uniform than during the other seasons, with highest N<sub>2</sub>O concentrations of 35 nmol L<sup>-1</sup>. Except during

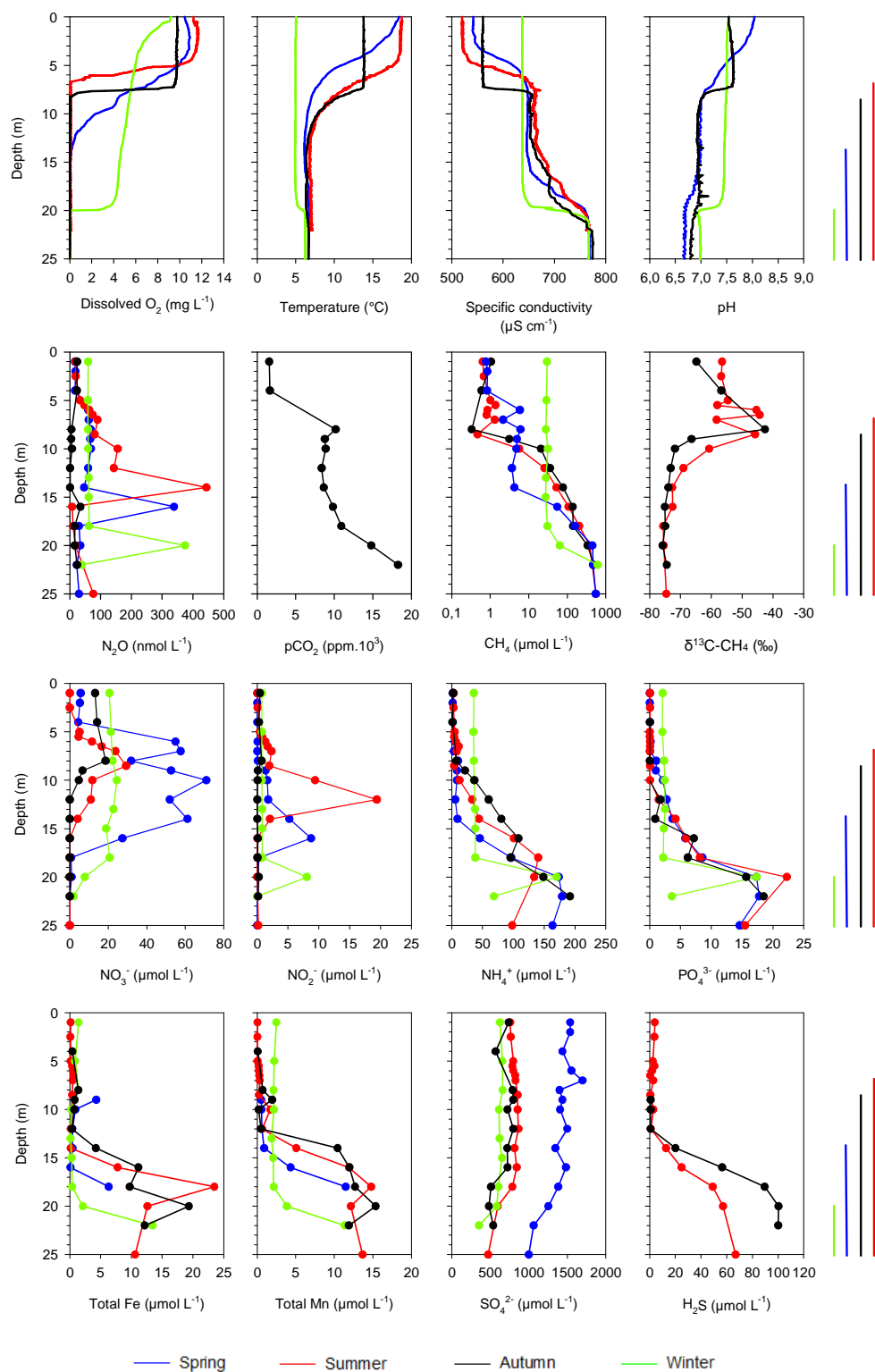


**Figure 32:** Vertical profiles of dissolved oxygen (mg L<sup>-1</sup>), temperature (°C), specific conductivity (μS cm<sup>-1</sup>), pH, N<sub>2</sub>O concentrations (nmol L<sup>-1</sup>), pCO<sub>2</sub> (ppm.10<sup>3</sup>), CH<sub>4</sub> concentrations (μmol L<sup>-1</sup>), δ<sup>13</sup>C-CH<sub>4</sub> (‰), nutrients (NO<sub>3</sub><sup>-</sup>, NO<sub>2</sub><sup>-</sup>, NH<sub>4</sub><sup>+</sup>, PO<sub>4</sub><sup>3-</sup>), total Fe, total Mn, SO<sub>4</sub><sup>2-</sup> and H<sub>2</sub>S concentrations (μmol L<sup>-1</sup>) in spring (blue), summer (red), autumn (black) and winter (green). Vertical lines to the right represent the anoxic layer for each season (same color code). Note the X log scale for CH<sub>4</sub> concentrations.



winter when the peak was observed at the oxic-anoxic interface, N<sub>2</sub>O peaks were observed below the oxycline, in anoxic waters during the other three seasons. The pCO<sub>2</sub> value in autumn (1560 ppm at 1 m depth) was well above the atmospheric equilibrium (390 ppm) in oxic surface waters and strongly increased in anoxic waters to reach ~18,000 ppm. The CH<sub>4</sub> concentrations strongly increased in anoxic waters (up to 618 μmol L<sup>-1</sup>) but were also quite important in oxic waters, especially in winter (up to 30 μmol L<sup>-1</sup> at 1 m depth), and ranged between 0.6 and 1 μmol L<sup>-1</sup> at 1 m depth during the other three seasons. During summer, δ<sup>13</sup>C-CH<sub>4</sub> were stable in bottom waters (~ -75 ‰) but started to gradually increase at 10 m, slightly below the base of the oxycline, to reach a maximum of -45 ‰ between 8.5 and 6 m. In autumn, similarly low δ<sup>13</sup>C-CH<sub>4</sub> (-75 ‰) were measured in bottom waters but the increase near the oxic-anoxic interface was more abrupt.

Vertical profiles of NO<sub>3</sub><sup>-</sup> and NO<sub>2</sub><sup>-</sup> strongly differed between seasons (Figure 32). Important NO<sub>3</sub><sup>-</sup> accumulation zones (nitraclines) were observed in both oxic and anoxic waters in spring and at the oxic-anoxic interface in summer. The maximum NO<sub>3</sub><sup>-</sup> concentration was 70 and 30 μmol L<sup>-1</sup> in spring and summer, respectively. In autumn and winter, no nitracline was observed, but instead NO<sub>3</sub><sup>-</sup> concentrations were quite stable throughout the oxic part of the water column (around 15 and 20 μmol L<sup>-1</sup> in autumn and winter, respectively), and decreased down to 1 μmol L<sup>-1</sup> in anoxic waters. Except in autumn where NO<sub>2</sub><sup>-</sup> concentrations remained low (below 1 μmol L<sup>-1</sup>) throughout the water column, important NO<sub>2</sub><sup>-</sup> concentrations peaks were also observed. In spring and summer, the maximum peaks of 10 and 20 μmol L<sup>-1</sup>, respectively, were located in anoxic waters. In winter, maximum peak was slightly lower (8 μmol L<sup>-1</sup>) and was located at the oxic-anoxic interface. For each season, deep anoxic waters were rich in NH<sub>4</sub><sup>+</sup> and PO<sub>4</sub><sup>3-</sup> (up to 190 and 22 μmol L<sup>-1</sup>, respectively), while oxic waters were depleted in these nutrients. However, higher concentrations were observed in oxic waters in winter than in other seasons. Indeed NH<sub>4</sub><sup>+</sup> and PO<sub>4</sub><sup>3-</sup> concentrations were around 35 and 2 μmol L<sup>-1</sup>, respectively, all along the oxic part of the water column in winter, while NH<sub>4</sub><sup>+</sup> concentrations were below 5 μmol L<sup>-1</sup> and PO<sub>4</sub><sup>3-</sup> concentrations below detection in other seasons.

For each season, total Fe and Mn concentrations were quite high in anoxic waters. The maximum Fe concentration peak of 23 μmol L<sup>-1</sup> was observed in summer, while the maximum Mn concentration peak of 15 μmol L<sup>-1</sup> was observed in autumn. SO<sub>4</sub><sup>2-</sup> concentrations were high all along the vertical profiles (ranging between 354 and 1537 μmol L<sup>-1</sup>), but tended to decrease in deep anoxic waters, co-occurring with an increase of H<sub>2</sub>S concentrations (Figure 32).

#### 6.4.2 CH<sub>4</sub> oxidation

CH<sub>4</sub> oxidation was observed during all seasons (Figure 33). In spring, important rates were observed in both oxic and anoxic waters, without Mo added, up to 4 and 3 μmol L<sup>-1</sup> d<sup>-1</sup>, respectively.

In summer, no CH<sub>4</sub> oxidation was observed in oxic waters. However, important CH<sub>4</sub> oxidation rates were observed in anoxic waters, without and with Mo added. Without Mo added, the two maximum peaks of 9 and 6 μmol L<sup>-1</sup> d<sup>-1</sup> were observed at 14 and 18 m depth, respectively. These peaks co-occurred with important NO<sub>3</sub><sup>-</sup> and SO<sub>4</sub><sup>2-</sup> consumption peaks, up to 2 and 20 μmol L<sup>-1</sup> d<sup>-1</sup>, respectively. A NO<sub>2</sub><sup>-</sup> consumption peak of 0.4 μmol L<sup>-1</sup> d<sup>-1</sup> was also observed at 14 m, and another one was also observed in oxic waters. With Mo added, oxidation peaks were observed at the same depths, but rates were lower than without Mo. Important NO<sub>3</sub><sup>-</sup> consumption peaks were also observed at 14 and 18 m, up to 5.5 μmol L<sup>-1</sup> d<sup>-1</sup>, so higher than without Mo added.

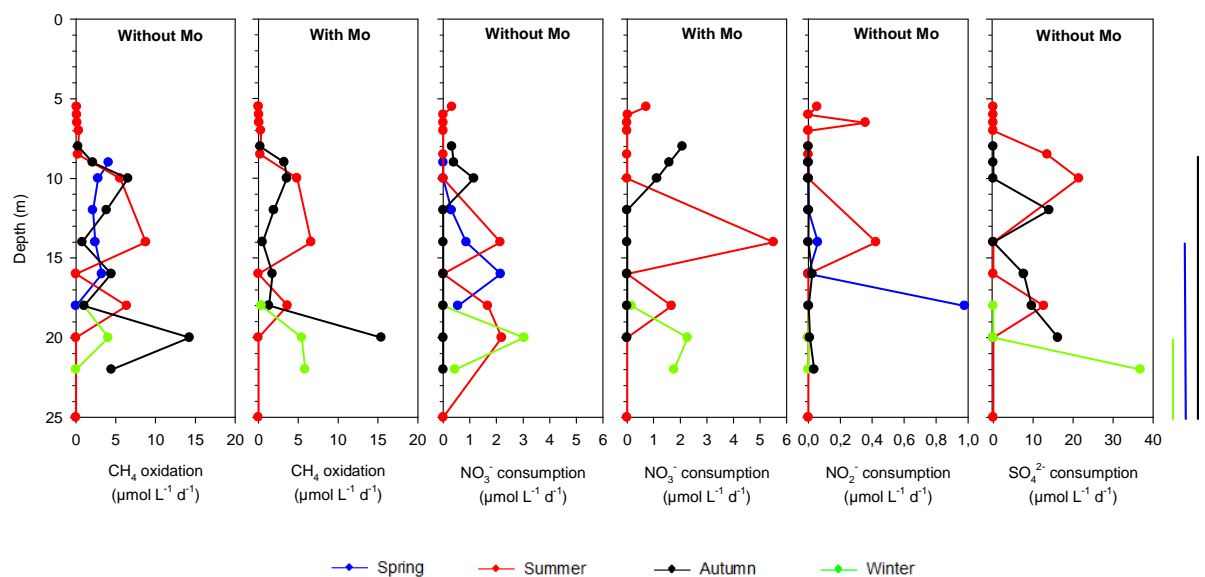


**Figure 33:** Vertical profiles of CH<sub>4</sub> oxidation rates (μmol L<sup>-1</sup> d<sup>-1</sup>) without and with molybdate (Mo) added, NO<sub>3</sub><sup>-</sup> consumption rates (μmol L<sup>-1</sup> d<sup>-1</sup>) without and with Mo added, NO<sub>2</sub><sup>-</sup> and SO<sub>4</sub><sup>2-</sup> consumption rates (μmol L<sup>-1</sup> d<sup>-1</sup>) without Mo added, in spring (blue), summer (red), autumn (black) and winter (green). Vertical lines to the right represent the anoxic layer for each season (same color code).

In autumn, important oxidation rates were measured throughout the anoxic zone, while no CH<sub>4</sub> oxidation was observed in oxic waters. The maximum oxidation rate of ~15 μmol L<sup>-1</sup> d<sup>-1</sup> was observed at 20 m, with and without Mo added. Except at 20 m where CH<sub>4</sub> oxidation rate with Mo was slightly higher than without Mo, CH<sub>4</sub> oxidation rates were always lower with Mo added. Without Mo added, only one peak of NO<sub>3</sub><sup>-</sup> consumption was observed, at 10 m, and thus co-occurred with the first oxidation peak. One SO<sub>4</sub><sup>2-</sup> consumption peak of 14 μmol L<sup>-1</sup> d<sup>-1</sup> was observed at 12 m. Below 14 m, SO<sub>4</sub><sup>2-</sup> consumption linearly increased. No measurable NO<sub>2</sub><sup>-</sup> consumption was observed. With Mo added, NO<sub>3</sub><sup>-</sup> consumption was observed just below the oxic-anoxic interface and linearly decreased in anoxic waters, following the same pattern than CH<sub>4</sub> oxidation until 12 m depth. In winter, an aerobic oxidation

rate of  $1 \mu\text{mol L}^{-1} \text{d}^{-1}$  was observed at 18 m. Without Mo added, the maximum oxidation peak of  $4 \mu\text{mol L}^{-1} \text{d}^{-1}$  was observed at the oxic-anoxic interface, and no oxidation was observed below 20 m. A  $\text{NO}_3^-$  consumption rate of  $3 \mu\text{mol L}^{-1} \text{d}^{-1}$  was observed at the same depth, and  $\text{SO}_4^{2-}$  consumption strongly increased below 20 m (until  $37 \mu\text{mol L}^{-1} \text{d}^{-1}$ ). No  $\text{NO}_2^-$  consumption was observed. With Mo added, no aerobic  $\text{CH}_4$  oxidation was observed. Also, the  $\text{CH}_4$  oxidation peak observed at 20 m was slightly higher ( $5 \mu\text{mol L}^{-1} \text{d}^{-1}$ ) and an oxidation peak of  $6 \mu\text{mol L}^{-1} \text{d}^{-1}$  was observed at 22 m depth.  $\text{NO}_3^-$  consumption was lower than without Mo at 20 m depth, but was higher at 22 m.

#### 6.4.3 $\text{CH}_4$ , $\text{N}_2\text{O}$ and $\text{CO}_2$ fluxes

$\text{CH}_4$  and  $\text{N}_2\text{O}$  air-water fluxes were estimated during the four seasons, and  $\text{CO}_2$  air-water flux was estimated for autumn (Table 16). The maximum  $\text{CH}_4$  flux of  $12,482 \mu\text{mol m}^{-2} \text{d}^{-1}$  was observed in winter, while  $\text{CH}_4$  fluxes were similar in spring, summer and autumn (mean of  $641 \mu\text{mol m}^{-2} \text{d}^{-1}$ ).  $\text{N}_2\text{O}$  fluxes were quite constant all along the year (mean of  $17 \mu\text{mol m}^{-2} \text{d}^{-1}$  for summer, autumn and winter), except in spring where the flux was distinctly lower ( $5 \mu\text{mol m}^{-2} \text{d}^{-1}$ ). The  $\text{CO}_2$  flux in autumn was  $67,000 \mu\text{mol m}^{-2} \text{d}^{-1}$ .

**Table 16:**  $\text{CH}_4$ ,  $\text{N}_2\text{O}$  and  $\text{CO}_2$  fluxes ( $\mu\text{mol m}^{-2} \text{d}^{-1}$ ) to the atmosphere during the different seasons. Nd: not determined.

	$\text{CH}_4$ fluxes	$\text{N}_2\text{O}$ fluxes	$\text{CO}_2$ fluxes
Spring	633	5	Nd
Summer	1,000	18	Nd
Autumn	564	13	67,000
Winter	12,482	19	Nd

## 6.5 Discussion

Physico-chemical parameters (temperature, specific conductivity, pH and oxygen) showed that the mixed layer depth varied according to the season, but that the deepest part of the water column (below 20 m) was anoxic throughout the year. Oxygen concentrations in surface waters were also higher in summer and spring, which can be linked with higher temperatures and irradiance favoring phytoplankton activity, and oxygen production through photosynthesis.

Higher water temperatures also enhance bacterial activity, and denitrification and nitrification, which both produce  $\text{N}_2\text{O}$ , are known to be enhanced when temperature increases (Saad and Conrad, 1993; Van Hulle et al., 2010; Dong et al., 2011). High  $\text{N}_2\text{O}$  concentrations were observed in summer and

spring. In spring, the maximum N<sub>2</sub>O peak was located at 16 m, and co-occurred with the maxima in NO<sub>2</sub><sup>-</sup> concentration and NO<sub>3</sub><sup>-</sup> consumption rate. In summer, the maximum N<sub>2</sub>O peak was observed at 14 m depth, and also co-occurred with the maximum NO<sub>3</sub><sup>-</sup> consumption rate. Altogether, these observations reflect the occurrence of denitrification in the anoxic water of the lake. Heterotrophic denitrification requires organic matter and NO<sub>3</sub><sup>-</sup> supply. The higher NO<sub>3</sub><sup>-</sup> concentrations were observed in spring, when nitrification is favored by higher temperatures and abundant NH<sub>4</sub><sup>+</sup> following winter-time mixing.

Denitrification can be heterotrophic, with organic matter as electron donor, but can also be autotrophic with other electron donors. One of these electron donors can be CH<sub>4</sub>. AOM coupled with NO<sub>3</sub><sup>-</sup> reduction (NDMO) is still poorly understood. However, it is thermodynamically highly favorable (Borrel et al., 2011) and can thus be of great importance in anoxic environments with high NO<sub>3</sub><sup>-</sup> concentrations. During this study, we investigated CH<sub>4</sub> oxidation using two different approaches. The first one was the measurement of the δ<sup>13</sup>C of dissolved CH<sub>4</sub> along the depth profile in summer and autumn. While δ<sup>13</sup>C-CH<sub>4</sub> values in deep waters were very low (~65 ‰), significant increases of δ<sup>13</sup>C-CH<sub>4</sub> values were observed between 6 and 8.5 m depth in summer (at the oxic-anoxic interface and in anoxic waters, until -44 ‰), and at 8 m depth in autumn (also at the oxic-anoxic interface, until -43 ‰). During microbial processes, isotopic fractionation occurs, since organisms preferentially use the lighter isotopes. Therefore, during CH<sub>4</sub> oxidation, bacteria preferentially use <sup>12</sup>C-CH<sub>4</sub> and the residual CH<sub>4</sub> pool is then enriched in <sup>13</sup>C. For both seasons, the increases of δ<sup>13</sup>C-CH<sub>4</sub> values co-occurred with a strong decrease of CH<sub>4</sub> concentrations, at the oxic-anoxic interfaces. Hence, the vertical profiles of δ<sup>13</sup>C-CH<sub>4</sub> strongly suggest that a large part of CH<sub>4</sub> was oxidized within a 5 m depth interval, in summer and autumn. In autumn, it also co-occurred with a strong increase in pCO<sub>2</sub>. In autumn and summer, δ<sup>13</sup>C-CH<sub>4</sub> decreased from the base of the oxic layer towards surface waters, by ~22 and ~12 ‰, respectively. Such a decrease cannot be related to exchange with the atmosphere since the atmospheric δ<sup>13</sup>C-CH<sub>4</sub> is close to -47 ‰ (Quay et al., 1999). A possible explanation would be CH<sub>4</sub> production in oxic conditions related to primary production by pathways that remain elusive (Tang et al., 2016) as recently reported in several lakes (Grossart et al., 2011; Bogard et al., 2014; Tang et al., 2014). Such an explanation is consistent with the eutrophic nature of the Dendre Lake and should be further investigated in future.

The fraction of the CH<sub>4</sub> flux oxidized in a given depth interval was calculated according to the following equation (Coleman et al., 1981):

$$(19) \ln(1-f) = \ln \left( \frac{(\delta^{13}\text{C-CH}_{4t} + 1000)}{(\delta^{13}\text{C-CH}_{4b} + 1000)} \right) / \left( \frac{1}{\alpha} - 1 \right)$$

where  $f$  is the fraction of CH<sub>4</sub> oxidized in the depth interval,  $\delta^{13}\text{C-CH}_{4t}$  and  $\delta^{13}\text{C-CH}_{4b}$  are the  $\delta^{13}\text{C-CH}_4$  values at the top and at the bottom of the depth interval, respectively, and  $\alpha$  is the isotope fractionation factor.

**Table 17:** Depth-integrated CH<sub>4</sub> oxidation rates ( $\mu\text{mol m}^{-2} \text{d}^{-1}$ ) through all the water column, and percentages of aerobic and anaerobic CH<sub>4</sub> oxidation, for the four seasons.

	Depth-integrated oxidation rates ( $\mu\text{mol m}^{-2} \text{d}^{-1}$ )	Aerobic oxidation (%)	Anaerobic oxidation (%)
Spring	48	79	21
Summer	67	1	99
Autumn	70	3	97
Winter	27	77	23

Coleman et al. (1981) showed that  $\alpha$  was dependent on temperature. Bastviken et al. (2002) determined a  $\alpha$  of  $1.0196 \pm 0.002$  for three Swedish lakes, whose temperature profiles are closer to what we observed. Based on this approach, we computed that in the Dendre Lake in summer, a large fraction (70-73 %) of the upward flux of CH<sub>4</sub> was oxidized in a narrow depth interval (between 8.5 and 12 m; anoxic waters). The same observation is made in autumn, since 81-83 % was oxidized between 8 and 10 m depth (mostly in anoxic waters). This isotopic approach clearly shows the importance of the AOM in the water column of the pit stone lake of the Dendre.

In addition to these indirect estimations of CH<sub>4</sub> oxidation, we directly quantified CH<sub>4</sub> oxidation in incubation experiments during which the evolution of CH<sub>4</sub> concentrations was measured through time. Our incubations focused on AOM and fewer measurements were made in oxic waters. In spring, quite important aerobic CH<sub>4</sub> oxidation rates were observed. If we integrate aerobic rates over the oxic water column (from 0 to 13 m), we obtain an estimated aerobic oxidation rate of  $38 \mu\text{mol m}^{-2} \text{d}^{-1}$ . If we do the same for the anoxic water column (from 14 to 25 m), only  $10 \mu\text{mol m}^{-2} \text{d}^{-1}$  were anaerobically oxidized. These estimates suggest that aerobic CH<sub>4</sub> oxidation was the main pathway of CH<sub>4</sub> oxidation in spring, yet AOM still accounted for 21% of total CH<sub>4</sub> oxidation (Table 17). In summer, three measurements of aerobic CH<sub>4</sub> oxidation were also made at 5.5, 6 and 6.5 m depth. Very low CH<sub>4</sub> oxidation rates were observed (mean of  $0.2 \mu\text{mol L}^{-1} \text{d}^{-1}$ ) in oxic waters, while the maximum AOM rate was estimated to  $9 \mu\text{mol L}^{-1} \text{d}^{-1}$  at 14 m, in accordance with  $\delta^{13}\text{C-CH}_4$  data. In summer, AOM was clearly the main pathway of CH<sub>4</sub> oxidation, accounting for 99% of total CH<sub>4</sub> oxidation (Table 17). As shown in Figure 34, aerobic CH<sub>4</sub> oxidation highly depends on CH<sub>4</sub> concentrations, confirming a strong substrate control of CH<sub>4</sub> oxidation (e.g. Guérin and Abril, 2007). CH<sub>4</sub> concentrations in oxic waters were higher

in spring than in summer, with means of 5 and 1  $\mu\text{mol L}^{-1}$  at depths where oxidation was measured, respectively. These important differences may be explained by the mixed layer depth of the water column. In spring, the water column was anoxic deeper, so  $\text{CH}_4$  produced in anoxic waters was anaerobically oxidized over a less important depth than in summer, where the water was anoxic at 7 m. Moreover, higher water temperatures observed in summer might enhance  $\text{CH}_4$  oxidation. In spring, a greater amount of  $\text{CH}_4$  could thus reach the oxic waters, explaining higher  $\text{CH}_4$  concentrations

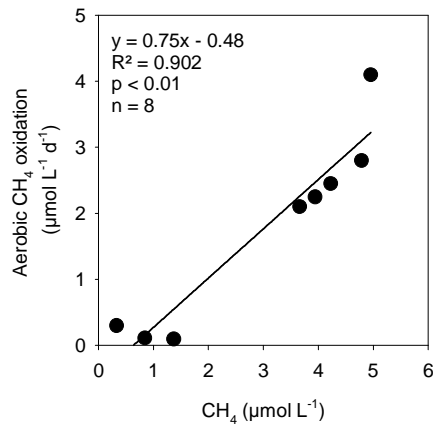
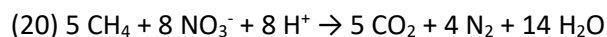


**Figure 34:**  $\text{CH}_4$  concentrations ( $\mu\text{mol L}^{-1}$ ) in oxic waters compared with aerobic  $\text{CH}_4$  oxidation rates ( $\mu\text{mol L}^{-1} \text{d}^{-1}$ ), for all seasons.

observed, and so higher aerobic  $\text{CH}_4$  oxidation rates. Figure 35a shows the dependence of depth-integrated oxidation rates with the depth of the oxygenated layer. Depth-integrated oxidation rates were lower when the oxycline was located deeper, so in winter and spring, which shows the importance of the anaerobic compartment. Also, as shown by Figure 35b, higher  $\text{CH}_4$  oxidation rates correspond to lower  $\text{CH}_4$  fluxes, illustrating the importance of  $\text{CH}_4$  oxidation to prevent  $\text{CH}_4$  emissions to the atmosphere. In correlation with Figure 35a and 35b, Figure 35c shows that a deeper oxycline is linked to higher  $\text{CH}_4$  fluxes.

Incubations also revealed important AOM rates. Because  $\text{NO}_3^-$  and  $\text{SO}_4^{2-}$  concentrations in the water column were high, we also measured the evolution of these concentrations in the incubations, in order to determine if these elements might be AOM electron acceptors. In spring, summer and winter, all the AOM peaks co-occurred with  $\text{NO}_3^-$  consumption peaks. In autumn, only the first AOM peak observed at 10 m depth co-occurred with the peak of  $\text{NO}_3^-$  consumption. These results strongly suggest the existence of a coupling between  $\text{CH}_4$  oxidation and  $\text{NO}_3^-$  reduction. However, the observed  $\text{NO}_3^-$  consumption rates are not sufficient to be responsible for the observed AOM rates (Figure 36a).

These calculations are based on stoichiometry of the following equation, according to which 8 moles of  $\text{NO}_3^-$  are needed for the oxidation of 5 moles of  $\text{CH}_4$  (Raghoebarsing et al., 2006):



The other electron acceptor present at high concentrations is  $\text{SO}_4^{2-}$ .  $\text{SO}_4^{2-}$  concentrations were high throughout all vertical profiles, and tended to decrease in anoxic waters, when  $\text{H}_2\text{S}$  concentrations increased, showing a  $\text{SO}_4^{2-}$  reduction zone. In our incubations, we observed important  $\text{SO}_4^{2-}$

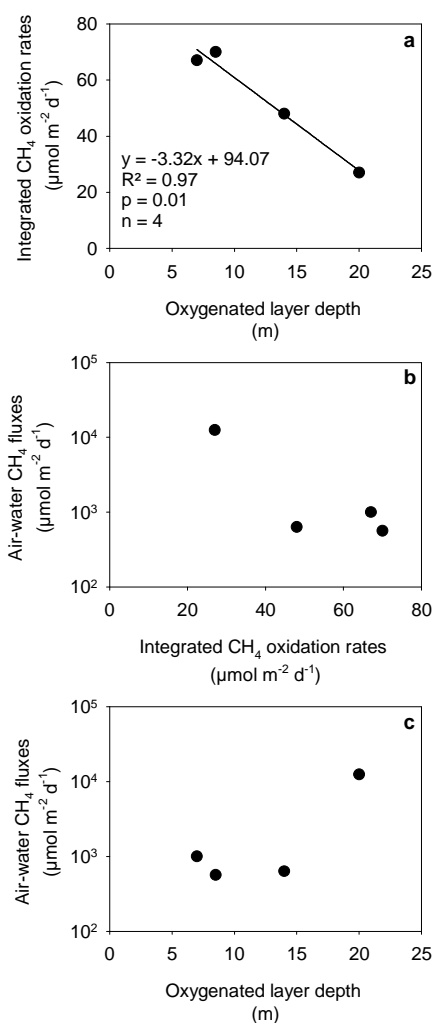


**Figure 35:** (a) Depth-integrated  $\text{CH}_4$  oxidation rates ( $\mu\text{mol m}^{-2} \text{d}^{-1}$ ) compared with depth of the oxygenated layer (m) and air-water  $\text{CH}_4$  fluxes ( $\mu\text{mol m}^{-2} \text{d}^{-1}$ ) compared with (b) depth-integrated  $\text{CH}_4$  oxidation rates ( $\mu\text{mol m}^{-2} \text{d}^{-1}$ ) and (c) depth of the oxygenated layer (m), for all seasons. Note the Y log scales for b and c.

consumption rates that can potentially contribute to the AOM. Indeed,  $\text{SO}_4^{2-}$  consumption rates are sufficient to explain AOM rates observed at some depths. Moreover, when we inhibited sulfate-reducing bacteria by the addition of Mo, we tended to observe lower AOM rates, strongly suggesting a coupling between AOM and  $\text{SO}_4^{2-}$  reduction. However, AOM was not fully inhibited, and we can invoke two different reasons to explain this. First, the specific inhibitor used (molybdate) may not be fully efficient, as suggested by Nauhaus et al. (2005) who demonstrated that the two distinct archaeal communities capable of AOM (ANME-I and ANME-II) reacted differently to molybdate, with an incomplete inhibition of ANME-I for the same concentrations of inhibitor. Because we did not perform pyrosequencing analyses in our study, we cannot determine relative community dominance. A second mechanism to explain why AOM was not fully inhibited when molybdate was added, is that SDMO is not the only AOM pathway in the water column of the Dendre stone pit lake, confirming the potential occurrence of NDMO, as described above.

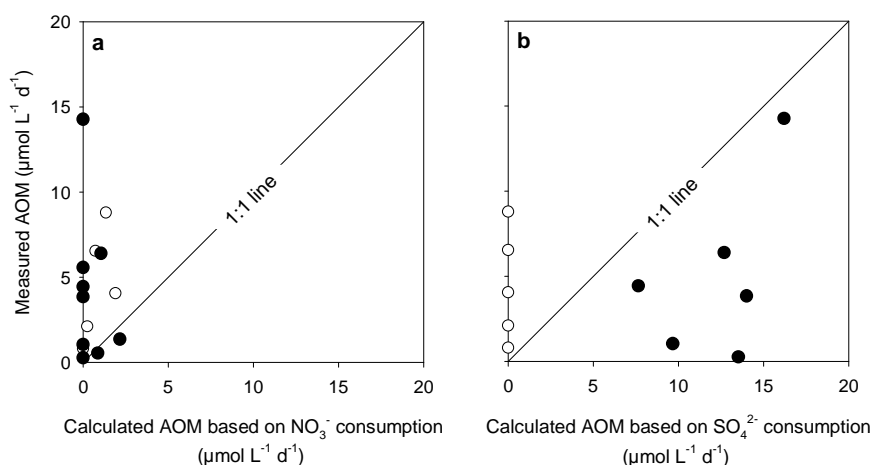


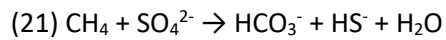
**Figure 36:** Measured AOM ( $\mu\text{mol L}^{-1} \text{d}^{-1}$ ) compared with AOM calculated on base on (a)  $\text{NO}_3^-$  and (b)  $\text{SO}_4^{2-}$  consumption rates ( $\mu\text{mol L}^{-1} \text{d}^{-1}$ ), for all seasons. White dots are AOM rates measured with no observation of  $\text{SO}_4^{2-}$  consumption.

We must note that AOM rates calculated on the basis of  $\text{NO}_3^-$  and  $\text{SO}_4^{2-}$  consumption rates are potential maximum rates, since we consider here that  $\text{NO}_3^-$  and  $\text{SO}_4^{2-}$  reduction occurs only with  $\text{CH}_4$  as electron donor, which is unlikely. Heterotrophic denitrification and  $\text{SO}_4^{2-}$  reduction with organic matter are both more favorable, especially in an environment with high organic matter supply.

We can thus hypothesize that AOM occurred with different electron acceptors in the Dendre stone pit lake. As NDMO is thermodynamically more favorable than SDMO, and as  $\text{NO}_3^-$  concentrations are relatively high, we suppose that AOM firstly occurs with  $\text{NO}_3^-$  as electron acceptor. When  $\text{NO}_3^-$  becomes depleted, AOM can occur with  $\text{SO}_4^{2-}$ , since SDMO is less favorable but  $\text{SO}_4^{2-}$  concentrations



are higher than  $\text{NO}_3^-$  concentrations. Figure 36b shows  $\text{CH}_4$  oxidation rates calculated on the basis of  $\text{SO}_4^{2-}$  consumption rates (according to stoichiometry of Eq. 21; Borrel et al., 2011) compared with measured  $\text{CH}_4$  oxidation rates.



This shows that most of the AOM must be coupled with  $\text{SO}_4^{2-}$  reduction (data points to the right side of the 1:1 line in Figure 36b), but that  $\text{SO}_4^{2-}$  is not the only electron acceptor, since some oxidation rates cannot be explained by  $\text{SO}_4^{2-}$  consumption rates alone (data points to the left side of the 1:1 line in Figure 5b). We must note that calculated AOM rates associated with  $\text{SO}_4^{2-}$  are higher than measured AOM rates, illustrating that not all the  $\text{SO}_4^{2-}$  consumption is linked to  $\text{CH}_4$  oxidation. Also, calculated AOM rates based on  $\text{NO}_3^-$  and  $\text{SO}_4^{2-}$  consumption rates are potential maximum rates, since in our calculations, we consider that all  $\text{NO}_3^-$  and  $\text{SO}_4^{2-}$  reduction occurs only with  $\text{CH}_4$  as electron donor. In any case,  $\text{NO}_3^-$  can thus be responsible for a part of the AOM not explained by  $\text{SO}_4^{2-}$  (at the left of the 1:1 line) but it is not sufficient, which means that other electron acceptors must be involved, such as Fe and Mn. Total Fe and Mn concentrations were relatively high in the water column and can thus potentially contribute to AOM. In summer and autumn in particular, higher Fe and Mn concentration peaks co-occurred with high  $\text{CH}_4$  oxidation peaks.

Regardless of the electron acceptors, AOM rates in the Dendre stone pit lake were quite high compared to other temperate or boreal lakes reported in literature (Table 18) and must thus contribute to limited atmospheric  $\text{CH}_4$  fluxes.  $\text{CH}_4$  concentrations in oxic waters were also high. In winter, in particular,  $\text{CH}_4$  concentrations in oxic waters were up to  $30 \mu\text{mol L}^{-1}$ , which can be linked to the mixing of the water column. The annual average of  $\text{CH}_4$  concentrations in surface waters was  $8.1 \mu\text{mol L}^{-1}$  which is one order of magnitude higher than the global average of lakes of the same size class ( $0.01\text{--}0.1 \text{ km}^2$ ) of  $0.7 \mu\text{mol L}^{-1}$  reported by Holgerson and Raymond (2016). The corresponding median of  $\text{CH}_4$  emission to the atmosphere ( $816 \mu\text{mol m}^{-2} \text{ d}^{-1}$ ) in the Dendre Lake is also high compared to other lakes globally, since the global median of diffusive  $\text{CH}_4$  fluxes from lakes at the same latitude reported by Bastviken et al. (2011) is  $263 \mu\text{mol m}^{-2} \text{ d}^{-1}$ , while the global flux for lakes of the same size class reported by Holgerson and Raymond (2016) is  $279 \mu\text{mol m}^{-2} \text{ d}^{-1}$ .

**Table 18:** Anaerobic CH<sub>4</sub> oxidation rates (μmol L<sup>-1</sup> d<sup>-1</sup>) from other lakes in literature.

Lake	AOM rate	Source
Dendre	Seasonal means: 2 - 5 Maximum: 15	This study
Marn (Sweden)	2.2	Bastviken et al. (2002)
Illersjoen (Sweden)	1.3 – 3.0	Bastviken et al. (2002)
Pavin (France)	0.4	Lopes et al. (2011)
Mendota (US)	5.8	Harrits and Hanson (1980)
Big Soda (US)	0.06	Iversen et al. (1987)
Mono (US)	0.08	Oremland et al. (1993)
Tanganyika (Africa)	0.24 – 1.8	Rudd et al. (1974)

Bastviken et al. (2011) also reported fluxes due to the emission of CH<sub>4</sub> stored in the water column during lake overturn. The median value of these fluxes plus the diffusive fluxes is estimated to 1,000 μmol m<sup>-2</sup> d<sup>-1</sup> (Bastviken et al., 2011) that is lower than CH<sub>4</sub> emissions estimated in the Dendre stone pit lake in winter (12,482 μmol m<sup>-2</sup> d<sup>-1</sup>). So high CH<sub>4</sub> fluxes in winter in the Dendre stone pit lake can be explained by an accumulation of CH<sub>4</sub> in anoxic waters during the stratification periods, which are mixed with the oxic waters during lake overturn, as described above. As water temperatures are low, microbial CH<sub>4</sub> oxidation in winter is reduced and does not consume the high stock of CH<sub>4</sub>, which can escape to the atmosphere. High CH<sub>4</sub> production in the water column of the Dendre Lake can be explained by a high primary production due to high nutrient availability. Indeed, high DIN (57 μmol L<sup>-1</sup>) and PO<sub>4</sub><sup>2-</sup> (2 μmol L<sup>-1</sup>) concentrations observed in surface waters (at 5 m) illustrate the eutrophic status of the lake. This is not surprising considering that this stone pit lake is mainly fed by ground waters, which are enriched in DIN from extensive fertilizer use on cropland (SPW-DGO3, 2015).

The N<sub>2</sub>O fluxes were higher in summer, autumn and winter, with a mean of 17 μmol m<sup>-2</sup> d<sup>-1</sup>. In spring, N<sub>2</sub>O flux was estimated to 5 μmol m<sup>-2</sup> d<sup>-1</sup>. Lower N<sub>2</sub>O flux, linked to lower N<sub>2</sub>O concentrations in surface waters observed in spring, might be linked to higher bacterial activity and therefore more efficient denitrification, leading to a stronger N<sub>2</sub>O consumption. Compared with fluxes reported by Huttunen et al. (2003) for five boreal lakes, N<sub>2</sub>O fluxes measured in the Dendre stone pit lake were very high, and no negative flux was observed, suggesting that the water column was a source of N<sub>2</sub>O for the atmosphere all the year. These higher N<sub>2</sub>O emissions can also be related to high DIN concentrations.

In conclusion, this study demonstrates the occurrence of AOM in the water column of a small freshwater body. Results show that AOM occurred with  $\text{SO}_4^{2-}$  as electron acceptor, but also strongly suggest that AOM also occurred with  $\text{NO}_3^-$  reduction. Further studies are nevertheless needed to clearly identify these processes, such as incubations spiked with the addition of the different potential electron acceptors for AOM and description of the microbial community composition. In this study, we also demonstrate that a flooded quarry can be a significant source of atmospheric greenhouse gases. While the majority of eutrophic agriculturally impacted lakes are net  $\text{CO}_2$  sinks (Balmer and Downing, 2011), we suggest that these systems can be extreme emitters of other potent greenhouse gases such as  $\text{CH}_4$  and  $\text{N}_2\text{O}$ , in response to nitrogen enrichment and high primary productivity.

---

## Chapter 7: General discussion, conclusions and perspectives

---

### 7.1 Comparison between two tropical lakes and a temperate lake

Table 19 compares Lake Kivu, Kabuno Bay and Lake Dendre morphometry and water column characteristics. In terms of morphometry, Lake Dendre is very small compared to Lake Kivu and Kabuno Bay, and they have contrasted water column composition. Two questions can thus be asked:

- 1) Are the systems reliable models of their respective category?
- 2) Are the systems comparable?

**Table 19:** Comparison between morphometries and water column characteristics of the main basin of Lake Kivu (Schmid and Wüest, 2012; Roland et al., 2016), Kabuno Bay (Schmid and Wüest, 2012; Llíros et al., 2015; This study-Chapter 4) and Lake Dendre (Roland et al., 2017).

	<i>Lake Kivu</i>	<i>Kabuno Bay</i>	<i>Lake Dendre</i>
<b>Morphometry</b>			
Surface area (km <sup>2</sup> )	2370	48	0.032
Maximum depth (m)	485	110	30
Mean depth (m)	245	?	20
<b>Chemical composition</b>			
Mean of CH <sub>4</sub> concentrations (μmol L <sup>-1</sup> )	380 at 70m	436 at 30m	510 at 22m
Maximum NO <sub>3</sub> <sup>-</sup> concentrations (μmol L <sup>-1</sup> )	~10	~10	~70
Maximum NO <sub>2</sub> <sup>-</sup> concentrations (μmol L <sup>-1</sup> )	~2	~0.2	~20
Maximum SO <sub>4</sub> <sup>2-</sup> concentrations (μmol L <sup>-1</sup> )	~250	~600	~1500
Maximum HS <sup>-</sup> concentrations (μmol L <sup>-1</sup> )	~80 at 70m	~12 at 15m	~100 at 22m
Maximum total Fe concentrations (μmol L <sup>-1</sup> )	~15	~600	~25
Maximum total Mn concentrations (μmol L <sup>-1</sup> )	~10	~60	~15
<b>Processes</b>			
Depth-integrated CH <sub>4</sub> oxidation rates (μmol m <sup>-2</sup> d <sup>-1</sup> )	9-162	21-77	27-70
Maximum AOM rate (μmol L <sup>-1</sup> d <sup>-1</sup> )	16	75	15
Mean of CH <sub>4</sub> flux (μmol m <sup>-2</sup> d <sup>-1</sup> )	~97	~612	~3670

### 7.1.1 *Are the systems reliable models of their respective category?*

Tropical lakes are characterized by high irradiance and water temperature throughout the year, what strongly influence stratification, dissolved O<sub>2</sub> concentrations and biological activity (Lewis Jr, 1987). In tropical lakes, the difference of temperature between the top and the bottom of the water column is less important than in a temperate lake (Lewis Jr, 1987). In theory, the consequence is that the stratification can be more rapidly influenced by small differences of temperature, such as between the day and the night (Lewis Jr, 1987). The nutrients trapped into anoxic waters can thus be released in the oxic waters more often than in a temperate lake, where nutrients are supposed to be made available solely during the complete seasonal mixing (Lewis Jr, 1987). Primary production and biogeochemical processes in tropical lakes are thus supposed to take benefit from these nutrients (Lewis Jr, 2010). The mixed layer, which is supposed to be shallower in tropical lakes than in temperate ones, also theoretically enhances primary production, since biomass is more concentrated in a thinner mixing layer (Lewis Jr, 1987). Finally, biological processes are supposed to be enhanced in tropical lakes by a better degradation of the organic matter due to higher water temperatures.

However, all these theoretical features do not apply to Lake Kivu, Kabuno Bay and Lake Dendre. Lake Kivu is so deep and large that its stratification cannot be significantly influenced by the differences in temperature observed between the day and the night, and is only disturbed during the annual seasonal mixing in dry season. Also, its stratification is strongly maintained by subaquatic springs entering in the lake at 255 m depth. The mixolimnion is thus strongly limited in nutrients during the stratification period and is considered as oligotrophic. Also, contrary to the theory, the mixed layer of Lake Kivu is very thick and the biomass is not particularly concentrated. The influence of the subaquatic springs is even more important in Kabuno Bay, since this one is smaller, conducting to the strong stratification observed, which is not influenced by seasonality. On the contrary, Lake Dendre is so small and its stratification is so shallow in summer and autumn, that differences in temperature between the day and the night may cause small destabilizations of the stratification and contribute to supply the oxic layer in nutrients. Moreover, Lake Dendre is a eutrophic system and is thus largely supplied in organic matter and nutrients by external inputs. So, even though biological processes in Lake Kivu and Kabuno Bay have the advantage of high water temperatures, they are advantageous by high nutrients supply in Lake Dendre.

In theory, as described in chapter 1, tropical lakes are also supposed to be higher emitters of CH<sub>4</sub> for the atmosphere than temperate lakes, whereas our study reported lower fluxes from Lake Kivu (chapter 2; Roland et al., 2016) than from Lake Dendre (chapter 6; Roland et al., 2017). This Lake Kivu feature had already been reported by Borges et al. (2011), and can be explained by the specific

structure of the water column, as detailed in chapter 2 (Roland et al., 2016). High CH<sub>4</sub> oxidation rates reported in Chapter 3 also contribute to low CH<sub>4</sub> emissions observed.

### 7.1.2 Are three lakes comparable?

The three systems are very different but share four main characteristics: they are meromictic, are deep compared to their surface area (and thus have a very limited littoral zone), have high CH<sub>4</sub> concentrations in their anoxic waters and non-negligible CH<sub>4</sub> oxidation rates, in particular AOM, occur in their water column. The maximum AOM rates were in the same order of magnitude in Lake Dendre and the main basin of Lake Kivu, despite the fact that CH<sub>4</sub> oxidation is influenced by temperature (Dunfield et al., 1993), while it was clearly higher in Kabuno Bay. However, as shown in Figure 37, the integrated CH<sub>4</sub> oxidation rates in Kabuno Bay were lower than in Lake Kivu and Lake Dendre, what is linked to the fact that CH<sub>4</sub> oxidation always occurs in superficial waters, and so rates are integrated on a smaller part of the water column. In Lake Dendre, despite the occurrence of high CH<sub>4</sub> oxidation rates, CH<sub>4</sub> fluxes were very high. This is linked to the mixing occurring in winter, which releases CH<sub>4</sub> from anoxic waters, and the lower CH<sub>4</sub> oxidation rates observed in winter, as explained in Chapter 6. Very high CH<sub>4</sub> emissions observed in Kabuno Bay can also be linked to a less efficient integrated CH<sub>4</sub> oxidation, due to the superficial stratification.

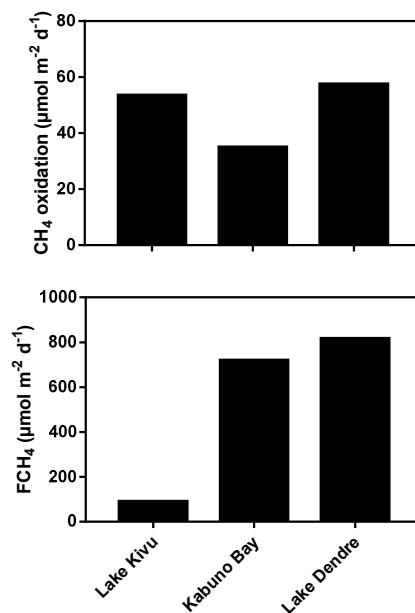


**Figure 37:** Median values of integrated CH<sub>4</sub> oxidation rates and CH<sub>4</sub> fluxes (µmol m<sup>-2</sup> d<sup>-1</sup>) in the three lakes.

CH<sub>4</sub> fluxes are also linked to the surface area of the three environments (Figure 38). Higher CH<sub>4</sub> fluxes were linked to smaller environments. Borges et al. (2011) and Holgerson and Raymond (2016) showed that smaller lakes were higher emitters of CH<sub>4</sub>. This may be linked to "*shallow waters, high sediment and edge to water volume ratios, and frequent mixing*" (Holgerson and Raymond, 2016). As explained above, Lake Dendre water column is shallower and smaller, and may be influenced by the differences in temperature between the day and the night, which may induce a shallow mixing and release CH<sub>4</sub> from the anoxic waters to the atmosphere.

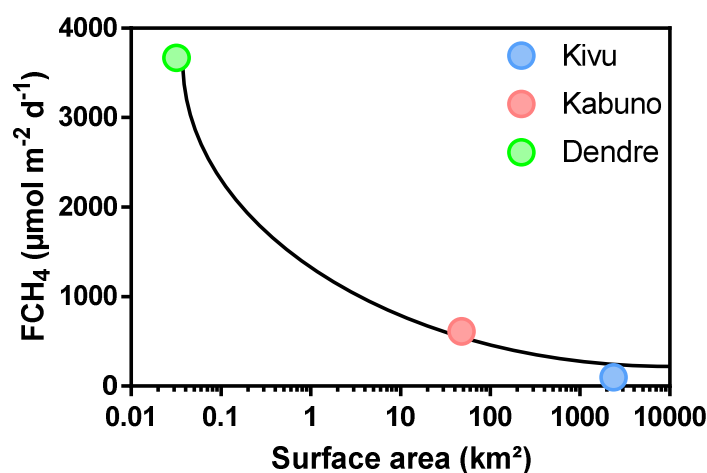


**Figure 38:** Correlation between mean values of CH<sub>4</sub> fluxes (μmol m<sup>-2</sup> d<sup>-1</sup>) and surface area (km<sup>2</sup>) of the three lakes. Note X log scale.

We can also ask at which extent CH<sub>4</sub> fluxes are dependent on CH<sub>4</sub> oxidation, and how it differs between the different lakes. Correlations were observed between integrated CH<sub>4</sub> oxidation and CH<sub>4</sub> fluxes in Lake Dendre and Lake Kivu (Figure 39a). The correlation was negative in Lake Dendre, showing that lower CH<sub>4</sub> fluxes were linked to higher integrated CH<sub>4</sub> oxidation. On the contrary, in Lake Kivu, higher CH<sub>4</sub> fluxes were linked to higher integrated CH<sub>4</sub> oxidation rates. Integrated CH<sub>4</sub> oxidation rates include aerobic and anaerobic CH<sub>4</sub> oxidation. In Lake Kivu, half of the field campaigns showed a higher contribution of aerobic CH<sub>4</sub> oxidation in total integrated CH<sub>4</sub> oxidation (Figure 39b, at the right of the 1:1 line), while the other half showed a higher AOM contribution. Figure 39c shows that aerobic CH<sub>4</sub> oxidation is the main pathway influencing CH<sub>4</sub> fluxes in Lake Kivu, since a higher contribution of aerobic CH<sub>4</sub> oxidation was associated to lower CH<sub>4</sub> fluxes. So, the positive relationship observed in Figure 39a is due to the influence of AOM rates on the total CH<sub>4</sub> oxidation. Indeed, when AOM rates are higher, it

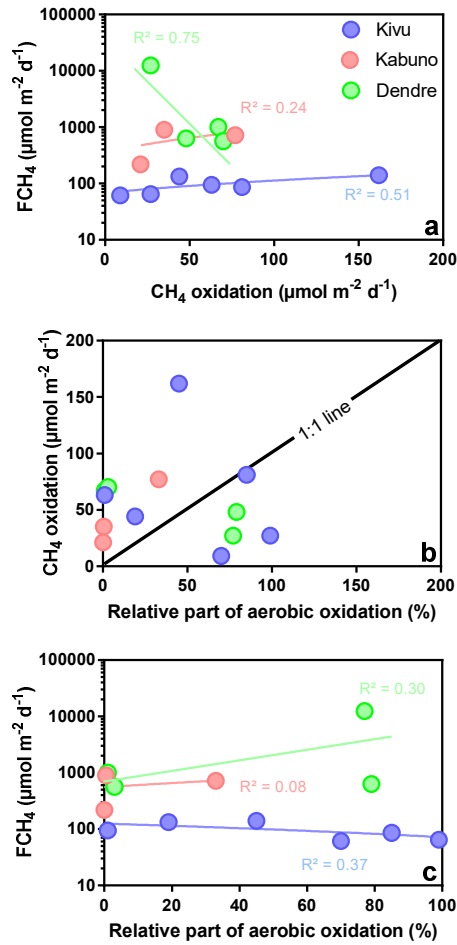


**Figure 39:** Correlation between (a) Total integrated CH<sub>4</sub> oxidation and CH<sub>4</sub> fluxes (μmol m<sup>-2</sup> d<sup>-1</sup>), (b) the part of aerobic CH<sub>4</sub> oxidation (%) and Total integrated CH<sub>4</sub> oxidation (μmol m<sup>-2</sup> d<sup>-1</sup>), (c) the part of aerobic CH<sub>4</sub> oxidation (%) and CH<sub>4</sub> fluxes (μmol m<sup>-2</sup> d<sup>-1</sup>) for all the field campaigns in the three lakes. Note Y log scales for FCH<sub>4</sub>.

means that the stratification is shallower (Chapter 3), and thus that integrated aerobic CH<sub>4</sub> oxidation is lower. As aerobic CH<sub>4</sub> oxidation is the most efficient pathway of CH<sub>4</sub> consumption, CH<sub>4</sub> fluxes increase when its relative contribution in total integrated CH<sub>4</sub> oxidation decreases.

On the contrary, in Lake Dendre, it seems that AOM is the main pathway preventing the escape of CH<sub>4</sub> in the atmosphere, since a higher contribution of aerobic CH<sub>4</sub> oxidation (and so lower integrated AOM rates) was linked to higher CH<sub>4</sub> fluxes (Figure 39c). This can be linked to the fact that the stratification is very shallow in summer, and so the oxic compartment is smaller when the water temperatures are higher. The oxic compartment is deeper when the mixing occurs, in winter, but as temperatures are strongly lower, aerobic CH<sub>4</sub> oxidizing bacteria are less active.



In Kabuno Bay, the influence of CH<sub>4</sub> oxidation on CH<sub>4</sub> fluxes is lower (Figure 39a). In particular, aerobic CH<sub>4</sub> oxidation seems to have no influence on CH<sub>4</sub> fluxes (Figure 39c). This can be linked to the shallow stratification of Kabuno Bay throughout the year. The oxic compartment is small compared to the anoxic one, and thus the relative contribution of aerobic oxidation on total CH<sub>4</sub> oxidation is low, as shown in Figure 39b. AOM was thus always the main pathway of CH<sub>4</sub> consumption in Kabuno Bay.

## 7.2 Why studying small environments such as Lake Dendre?

First, we can justify the study of small water bodies in terms of greenhouse gases emission and their potential impact on global warming. As explained above, it has been showed that smaller lakes are higher emitters of CH<sub>4</sub> for the atmosphere (per surface area) (Borges et al., 2011; Holgerson and Raymond, 2016). Moreover, Downing et al. (2006) also showed that smaller lakes were clearly more abundant than larger lakes, and thus their impact on global warming is non negligible. They recorded tens of millions lakes of the size of Lake Dendre, thousands lakes like Kabuno Bay and only hundreds lakes of the size of Kivu.

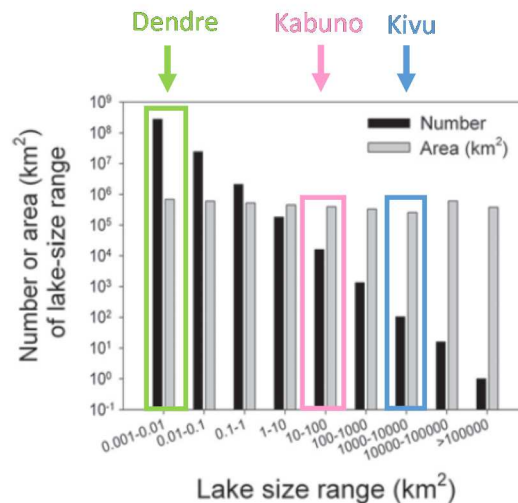


**Figure 40:** Global size distributions of numbers and land area covered by lakes, sorted in different size ranges (km<sup>2</sup>). Adapted from Downing (2010)

Secondly, former stone quarries are completely understudied. A question that can be asked is: at which extent a quarry lake is different from natural lakes? Different characteristics of quarry lakes can strongly influence biogeochemical processes occurring in their water column and sediments:

- 1) They are often very deep (depending on regional precipitations) and thus seem to be very often meromictic (Galas, 2003),
- 2) The littoral zone is limited,
- 3) They are often surrounded by "cliffs", limiting wind influence

Studying these environments would thus contribute to expand our knowledge in the field of limnology.

Thirdly, the Lake Dendre is a perfect environment for the study of CH<sub>4</sub> oxidation. It is strongly stratified during a large part of the year, has high CH<sub>4</sub> concentrations in its deep waters and presents significant concentrations of the different potential electron acceptors. Also, the last but not the least, it is located near the laboratory and thus does not require substantial financial budgets.

### 7.3 On the problem of the AOM electron acceptors

The identification of the potential electron acceptors of AOM in the three environments was one of the objectives of this thesis, but it was not so obvious. In Lake Dendre, SO<sub>4</sub><sup>2-</sup> has been identified as the main electron acceptor, and NO<sub>3</sub><sup>-</sup> has been suggested to be a second significant electron acceptor. However, when we compare AOM rates with the concentrations of the different potential electron acceptors, no significant relationship is observed (Figure 41). However, the second best relationship is observed with SO<sub>4</sub><sup>2-</sup> consumption rates, supporting the results of Chapter 6, where AOM rates were lower with the addition of the inhibitor of sulfate-reducing bacteria activity. Together, these results strongly suggest that the main electron acceptor for AOM in Lake Dendre is SO<sub>4</sub><sup>2-</sup>.

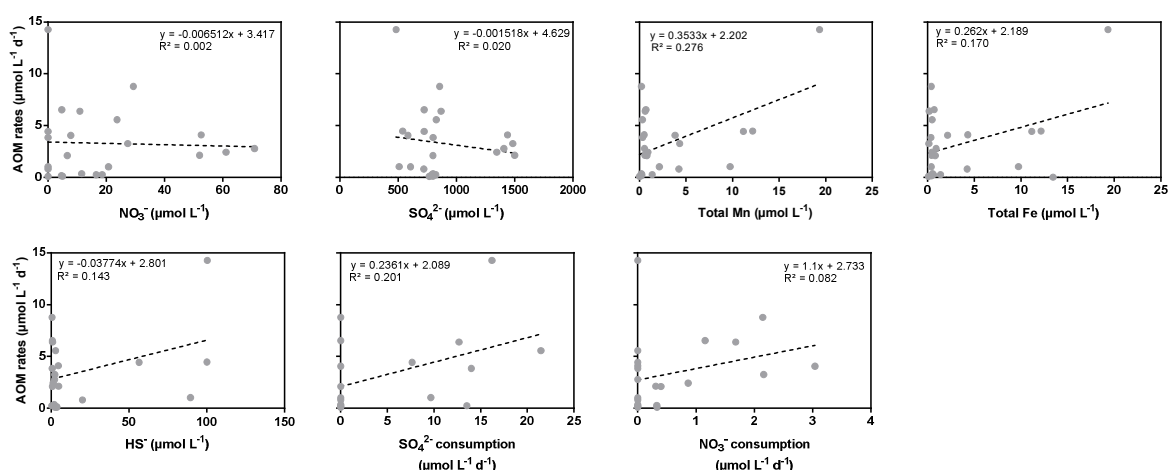


**Figure 41:** Comparison between AOM rates and NO<sub>3</sub><sup>-</sup>, SO<sub>4</sub><sup>2-</sup>, HS<sup>-</sup>, Total Mn and Fe concentrations (μmol L<sup>-1</sup>), and NO<sub>3</sub><sup>-</sup> and SO<sub>4</sub><sup>2-</sup> consumption rates (μmol L<sup>-1</sup> d<sup>-1</sup>), for all the field campaigns where these parameters have been measured in Lake Dendre.

In Kabuno Bay, like in Lake Dendre, no significant relationship between AOM rates and the concentrations of the potential electron acceptors is observed (Figure 42). Surprisingly, a negative relationship is observed with dissolved Fe concentrations, showing that AOM rates were higher when dissolved Fe concentrations were lower. Also, the best relationship observed is with particulate Mn concentrations and shows that higher AOM rates co-occur with lower concentrations, suggesting that AOM could be coupled with Mn reduction. However, the most probable electron acceptor for AOM was Fe, since Mn and  $\text{NO}_3^-$  concentrations were very low, and sulfur cycle seemed to be negligent. Low  $\text{NO}_3^-$  concentrations in Kabuno Bay can be linked to the occurrence of denitrification, as shown by Michiels et al. (in press), strongly supporting the idea that  $\text{NO}_3^-$  cannot be a significant electron acceptor for AOM in Kabuno Bay, since the competition for  $\text{NO}_3^-$  is probably too strong. Relationships established here also show that correlations between AOM rates and  $\text{NO}_3^-$ ,  $\text{SO}_4^{2-}$  and  $\text{HS}^-$  concentrations are very bad.

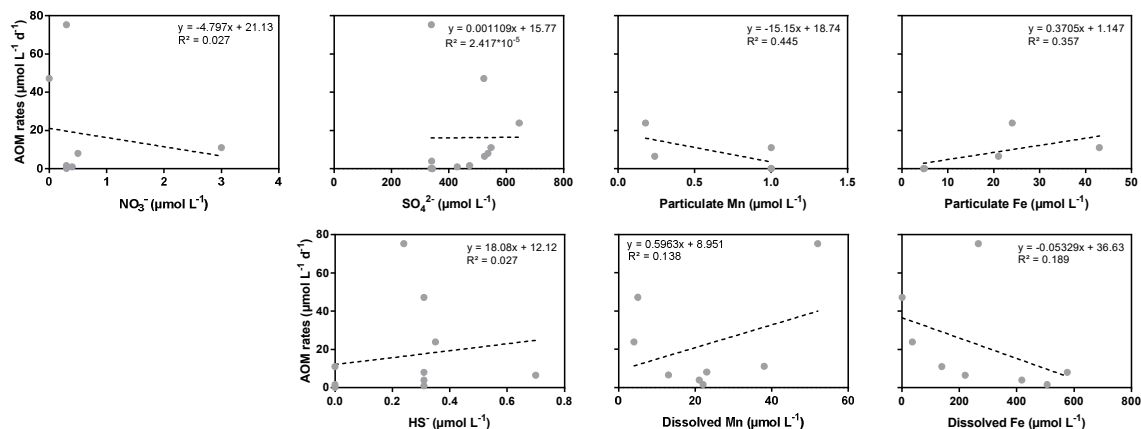


**Figure 42:** Comparison between AOM rates and  $\text{NO}_3^-$ ,  $\text{SO}_4^{2-}$ ,  $\text{HS}^-$ , Particulate and dissolved Mn and Fe concentrations ( $\mu\text{mol L}^{-1}$ ) for all the field campaigns where these parameters have been measured in Kabuno Bay.

In the main basin of Lake Kivu, high AOM rates were reported, but the definitive identification of electron acceptors involved is also still lacking. As for the two other study sites, any strong relationship is observed between AOM rates and the different potential electron acceptors (Figure 43). The better relationships are with particulate Fe, particulate Mn and  $\text{SO}_4^{2-}$ , suggesting that higher AOM rates co-occurred with the disappearance of these elements in anoxic waters, and so with their reduction. However, any relationship was observed with the reduced forms of Fe and  $\text{SO}_4^{2-}$  (dissolved Fe and  $\text{HS}^-$ , respectively), while a small correlation can be made with dissolved Mn. These correlations tend to suggest that particulate Mn could be the main electron acceptor in the main basin of Lake Kivu, but the concentrations are not high enough to support the rates observed, contrary to  $\text{SO}_4^{2-}$

concentrations. These correlations also support that  $\text{NO}_3^-$  cannot be an important electron acceptor, what may be linked to the occurrence of heterotrophic denitrification, anammox and DNRA in the water column of Lake Kivu (Chapter 5). Indeed, a strong competition for  $\text{NO}_3^-$  seems to occur, and  $\text{CH}_4$  oxidizing archaea have probably more interest in using another electron acceptor for which there is less competition, such as  $\text{SO}_4^{2-}$ .

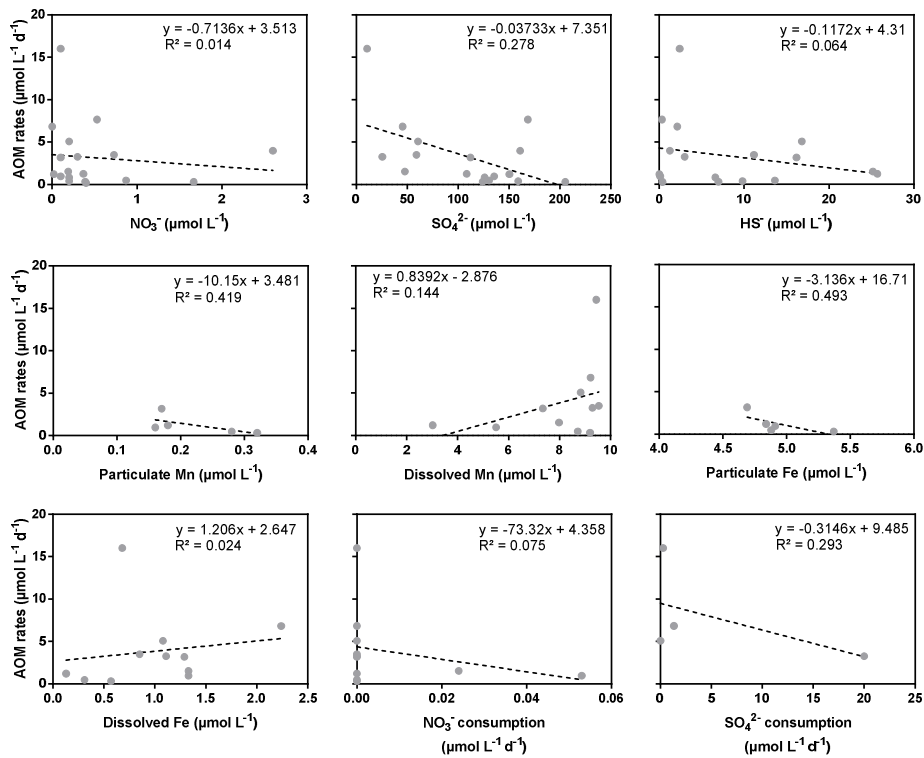


**Figure 43:** Comparison between AOM rates and  $\text{NO}_3^-$ ,  $\text{SO}_4^{2-}$ ,  $\text{HS}^-$ , Particulate Mn and Fe, Dissolved Mn and Fe concentrations (µmol L<sup>-1</sup>), and  $\text{NO}_3^-$  and  $\text{SO}_4^{2-}$  consumption rates (µmol L<sup>-1</sup> d<sup>-1</sup>), for all the field campaigns where these parameters have been measured in the main basin of Lake Kivu.

## 7.4 Conclusions and perspectives

In conclusion, this thesis put in evidence significant AOM rates in very contrasting freshwater environments. It also illustrates the complexity of this process and the competitive relationships occurring between the different biogeochemical processes. Numerous studies are still required to really elucidate the electron acceptors involved, or simply to better understand the environments.

Putting in cultures water from the water columns, with the addition of the different potential electron acceptors, would be really interesting to identify the main electron acceptors. Also, identifying

specific inhibitors for each biogeochemical process would help to identify the competitive relationships between the different processes.

Further studies are also required to better know the three environments. In Lake Dendre, which is a very interesting environment, it would be interesting to perform pyrosequencing analyses to identify the archaeal and bacterial diversity, and to measure processes such as denitrification, DNRA, anammox, N<sub>2</sub> fixation, aerobic and anaerobic CH<sub>4</sub> oxidation. Also, quantifying phytoplankton biomass and the different forms of organic matter would be useful to better characterize the system. In Lake Kivu and Kabuno Bay, numerous studies have already been made, but the quantification of two processes is still lacking: N<sub>2</sub> fixation and methanogenesis. During our study, we initiate the study of aerobic methanogenesis in the water column, but deeper investigations are required.

Finally, studying other former stone quarries would also be interesting to identify if systems like Lake Dendre are widespread or if Lake Dendre is an exception. Considering the high number of stone quarries (in Wallonia, the study of Remacle (2005) prospected 4647 quarries, and the prospection was not finished when publishing her article), it could be significant to estimate their role in greenhouse gases emissions.

---

## Bibliography

---

á Norði, K., Thamdrup, B., and Schubert, C. J.: Anaerobic oxidation of methane in an iron-rich Danish freshwater lake sediment, *Limnol. Oceanogr.*, 58, 546-554, doi:10.4319/lo.2013.58.2.0546, 2013.

á Norði, K., and Thamdrup, B.: Nitrate-dependent anaerobic methane oxidation in a freshwater sediment, *Geochim. Cosmochim. Acta*, 132, 141-150, doi:10.1016/j.gca.2014.01.032, 2014.

Abril, G., Bouillon, S., Darchambeau, F., Teodoru, C. R., Marwick, T. R., Tamooch, F., Ochieng Omengo, F., Geeraert, N., Deirmendjian, L., and Polsemaere, P.: Technical Note: Large overestimation of pCO<sub>2</sub> calculated from pH and alkalinity in acidic, organic-rich freshwaters, *Biogeosciences*, 12, 67-78, doi:10.5194/bg-12-67-2015, 2015.

Achnich, C., Bak, F., and Conrad, R.: Competition for electron donors among nitrate reducers, ferric iron reducers, sulfate reducers, and methanogens in anoxic paddy soil, *Biol. Fert. Soils*, 19, 65-72, doi:10.1007/BF00336349, 1995.

Allan, W., Struthers, H., and Lowe, D. C.: Methane carbon isotope effects caused by atomic chlorine in the marine boundary layer: Global model results compared with Southern Hemisphere measurements, *J. Geophys. Res. Atmos.*, 112, doi:10.1029/2006JD007369, 2007.

An, S., and Gardner, W. S.: Dissimilatory nitrate reduction to ammonium (DNRA) as a nitrogen link, versus denitrification as a sink in a shallow estuary (Laguna Madre/Baffin Bay, Texas), *Mar. Ecol. Prog. Ser.*, 237, 41-50, doi:10.3354/meps237041, 2002.

Angel, R., Matthies, D., and Conrad, R.: Activation of Methanogenesis in Arid Biological Soil Crusts Despite the Presence of Oxygen, *PLoS ONE*, 6, e20453, doi:10.1371/journal.pone.0020453, 2011.

APHA: Standard methods for the examination of water and wastewater, American Public Health Association, 1998.

Balagizi, C. M., Darchambeau, F., Bouillon, S., Yalire, M. M., Lambert, T., and Borges, A. V.: River geochemistry, chemical weathering, and atmospheric CO<sub>2</sub> consumption rates in the Virunga Volcanic Province (East Africa), *Geochem. Geophys. Geosyst.*, 16, 2637-2660, doi:10.1002/2015GC005999, 2015.

Balmer, M. B., and Downing, J. A.: Carbon dioxide concentrations in eutrophic lakes: undersaturation implies atmospheric uptake, *Inland Waters*, 1, 125-132, doi:10.5268/IW-1.2.366, 2011.

Bartlett, K. B., Crill, P. M., Bonassi, J. A., Richey, J. E., and Harriss, R. C.: Methane flux from the Amazon River floodplain: emissions during rising water, *J. Geophys. Res.*, 95, 16,773-716,788, doi:10.1029/JD095iD10p16773, 1990.

Bastviken, D., Ejlertsson, J., and Tranvik, L.: Measurement of methane oxidation in lakes: A comparison of methods, *Environ. Sci. Technol.*, 36, 3354-3361, doi:10.1021/es010311p, 2002.

Bastviken, D., Cole, J., Pace, M., and Tranvik, L.: Methane emissions from lakes: Dependence of lake characteristics, two regional assessments, and a global estimate, *Glob. Biogeochem. Cycles*, 18, doi:10.1029/2004GB002238, 2004.

Bastviken, D., Santoro, A. L., Marotta, H., Pinho, L. Q., Calheiros, D. F., Crill, P., and Enrich-Prast, A.: Methane emissions from pantanal, South America, during the low water season: Toward more comprehensive sampling, *Environ. Sci. Technol.*, 44, 5450-5455, doi:10.1021/es1005048, 2010.

Bastviken, D., Tranvik, L. J., Downing, J. A., Crill, P. M., and Enrich-Prast, A.: Freshwater methane emissions offset the continental carbon sink, *Science*, 331, 50, doi:10.1126/science.1196808, 2011.

Baulch, H. M., Schiff, S. L., Maranger, R., and Dillon, P. J.: Nitrogen enrichment and the emission of nitrous oxide from streams, *Glob. Biogeochem. Cycles*, 25, doi:10.1029/2011GB004047, 2011.

Beal, E. J., House, C. H., and Orphan, V. J.: Manganese- and iron-dependent marine methane oxidation, *Science*, 325, 184-187, doi:10.1126/science.1169984, 2009.

Boetius, A., Ravensschlag, K., Schubert, C. J., Rickert, D., Widdel, F., Gieseke, A., Amann, R., Jørgensen, B. B., Witte, U., and Pfannkuche, O.: A marine microbial consortium apparently mediating anaerobic oxidation of methane, *Nature*, 407, 623-626, doi:10.1038/35036572, 2000.

Bogard, M. J., del Giorgio, P. A., Boutet, L., Chaves, M. C. G., Prairie, Y. T., Merante, A., and Derry, A. M.: Oxic water column methanogenesis as a major component of aquatic CH<sub>4</sub> fluxes, *Nat. Commun.*, 5, doi:10.1038/ncomms6350, 2014.

Bokranz, M., Katz, J., Schröder, I., Robertson, A. M., and Kröger, A.: Energy metabolism and biosynthesis of *Vibrio succinogenes* growing with nitrate or nitrite as terminal electron acceptor, *Arch. Microbiol.*, 135, 36-41, doi:10.1007/BF00419479, 1983.

Borges, A. V., Abril, G., Delille, B., Descy, J. P., and Darchambeau, F.: Diffusive methane emissions to the atmosphere from Lake Kivu (Eastern Africa), *J. Geophys. Res. Biogeosci.*, 116, doi:10.1029/2011JG001673, 2011.

Borges, A. V., Bouillon, S., Abril, G., Delille, B., Poirier, D., Commarieu, M.-V., Lepoint, G., Morana, C., Champenois, W., and Servais, P.: Variability of carbon dioxide and methane in the epilimnion of Lake Kivu, in: *Lake Kivu-Limnology and biogeochemistry of a tropical great lake*, edited by: Descy, J. P., Darchambeau, F., and Schmid, M., Springer, New York London, 47-66, 2012.

Borges, A. V., Morana, C., Bouillon, S., Servais, P., Descy, J.-P., and Darchambeau, F.: Carbon Cycling of Lake Kivu (East Africa): Net Autotrophy in the Epilimnion and Emission of CO<sub>2</sub> to the Atmosphere Sustained by Geogenic Inputs, *PLoS ONE*, 9, e109500, doi:10.1371/journal.pone.0109500, 2014.

Borges, A. V., Darchambeau, F., Teodoru, C. R., Marwick, T. R., Tamoo, F., Geeraert, N., Omengo, F. O., Guérin, F., Lambert, T., and Morana, C.: Globally significant greenhouse-gas emissions from African inland waters, *Nat. Geosci.*, 8, 637-642, doi:10.1038/ngeo2486, 2015a.

Borges, A. V., Abril, G., Darchambeau, F., Teodoru, C. R., Deborde, J., Vidal, L. O., Lambert, T., and Bouillon, S.: Divergent biophysical controls of aquatic CO<sub>2</sub> and CH<sub>4</sub> in the World's two largest rivers, *Sci. Rep.*, 5, doi:10.1038/srep15614, 2015b.

Borrel, G., Jézéquel, D., Biderre-Petit, C., Morel-Desrosiers, N., Morel, J.-P., Peyret, P., Fonty, G., and Lehours, A.-C.: Production and consumption of methane in freshwater lake ecosystems, *Res. Microbiol.*, 162, 832-847, doi:10.1016/j.resmic.2011.06.004, 2011.

Braman, R. S., and Hendrix, S. A.: Nanogram nitrite and nitrate determination in environmental and biological materials by vanadium(III) reduction with chemiluminescence detection, *Anal. Chem.*, 61, 2715-2718, doi:10.1021/ac00199a007, 1989.

Brauman, A., Kane, M. D., Labat, M., and Breznak, J. A.: Genesis of acetate and methane by gut bacteria of nutritionally diverse termites, *Science*, 257, 1384-1387, doi:10.1126/science.257.5075.1384, 1992.

Brettar, I., and Rheinheimer, G.: Denitrification in the Central Baltic: evidence for H<sub>2</sub>S-oxidation as motor of denitrification at the oxic-anoxic interface, *Mar. Ecol. Prog. Ser.*, 77, 157-169, doi:10.3354/meps077157, 1991.

Bronson, K. F., and Mosier, A. R.: Suppression of methane oxidation in aerobic soil by nitrogen fertilizers, nitrification inhibitors, and urease inhibitors, *Biol. Fert. Soils*, 17, 263-268, doi:10.1007/bf00383979, 1994.

Brunet, R. C., and Garcia-Gil, L. J.: Sulfide-induced dissimilatory nitrate reduction to ammonia in anaerobic freshwater sediments, *FEMS Microbiol. Ecol.*, 21, 131-138, doi:10.1016/0168-6496(96)00051-7, 1996.

Burgin, A. J., and Hamilton, S. K.: Have we overemphasized the role of denitrification in aquatic ecosystems? A review of nitrate removal pathways, *Front. Ecol. Environ.*, 5, 89-96, doi:10.1890/1540-9295(2007)5[89:HWOTRO]2.0.CO;2, 2007.

Burgin, A. J., and Hamilton, S. K.: NO<sub>3</sub>--driven SO<sub>4</sub> 2- production in freshwater ecosystems: implications for N and S cycling, *Ecosystems*, 11, 908-922, doi:10.1007/s10021-008-9169-5, 2008.

Burgin, A. J., Yang, W. H., Hamilton, S. K., and Silver, W. L.: Beyond carbon and nitrogen: how the microbial energy economy couples elemental cycles in diverse ecosystems, *Front. Ecol. Environ.*, 9, 44-52, doi:10.1890/090227, 2011.

Caldwell, S. L., Laidler, J. R., Brewer, E. A., Eberly, J. O., Sandborgh, S. C., and Colwell, F. S.: Anaerobic Oxidation of Methane: Mechanisms, Bioenergetics, and the Ecology of Associated Microorganisms, *Environ. Sci. Technol.*, 42, 6791-6799, doi:10.1021/es800120b, 2008.

Canfield, D. E., Kristensen, E., and Thamdrup, B.: The sulfur cycle, *Adv. Mar. Biol.*, 48, 313-381, doi:10.1016/S0065-2881(05)48009-8, 2005.

Canfield, D. E., Stewart, F. J., Thamdrup, B., De Brabandere, L., Dalsgaard, T., Delong, E. F., Revsbech, N. P., and Ulloa, O.: A cryptic sulfur cycle in oxygen-minimum-zone waters off the Chilean coast, *Science*, 330, 1375-1378, doi:10.1126/science.1196889, 2010.

Claus, G., and Kutzner, H. J.: Physiology and kinetics of autotrophic denitrification by *Thiobacillus denitrificans*, *Appl. Microbiol. Biotechnol.*, 22, 283-288, doi:10.1007/bf00252031, 1985.

Cline, J. D.: Spectrophotometric determination of hydrogen sulfide in natural waters, *Limnol. Oceanogr.*, 14, 454-458, doi:10.4319/lo.1969.14.3.0454, 1969.

Codispoti, L., Elkins, J., Yoshinari, T., Friederich, G., Sakamoto, C., and Packard, T.: On the nitrous oxide flux from productive regions that contain low oxygen waters, in: *Oceanography of the Indian Ocean*, Desai BN ed., Rotterdam, The Netherlands: Balkema, 271-284, 1992.

Cole, J. J., and Caraco, N. F.: Atmospheric exchange of carbon dioxide in a low-wind oligotrophic lake measured by the addition of SF<sub>6</sub>, *Limnol. Oceanogr.*, 43, 647-656, 1998.

Cole, J. J., Prairie, Y. T., Caraco, N. F., McDowell, W. H., Tranvik, L. J., Striegl, R. G., Duarte, C. M., Kortelainen, P., Downing, J. A., Middelburg, J. J., and Melack, J.: Plumbing the Global Carbon Cycle: Integrating



Inland Waters into the Terrestrial Carbon Budget, *Ecosystems*, 10, 172-185, doi:10.1007/s10021-006-9013-8, 2007.

Coleman, D. D., Risatti, J. B., and Schoell, M.: Fractionation of carbon and hydrogen isotopes by methane-oxidizing bacteria, *Geochim. Cosmochim. Acta*, 45, 1033-1037, doi:10.1016/0016-7037(81)90129-0, 1981.

Conrad, R.: Contribution of hydrogen to methane production and control of hydrogen concentrations in methanogenic soils and sediments, *FEMS Microbiol. Ecol.*, 28, 193-202, doi:10.1111/j.1574-6941.1999.tb00575.x, 1999.

Conrad, R.: The global methane cycle: Recent advances in understanding the microbial processes involved, *Environ. Microbiol. Rep.*, 1, 285-292, doi:10.1111/j.1758-2229.2009.00038.x, 2009.

Crowe, S., Katsev, S., Leslie, K., Sturm, A., Magen, C., Nomosatryo, S., Pack, M., Kessler, J., Reeburgh, W., and Roberts, J.: The methane cycle in ferruginous Lake Matano, *Geobiol.*, 9, 61-78, doi:10.1111/j.1472-4669.2010.00257.x, 2011.

Cui, M., Ma, A., Qi, H., Zhuang, X., and Zhuang, G.: Anaerobic oxidation of methane: an "active" microbial process, *Microbiologyopen*, 4, 1-11, doi:10.1002/mbo3.232, 2015.

Curry, C. L.: Modeling the soil consumption of atmospheric methane at the global scale, *Glob. Biogeochem. Cycles*, 21, doi:10.1029/2006GB002818, 2007.

Dalsgaard, T., and Bak, F.: Nitrate reduction in a sulfate-reducing bacterium, *Desulfovibrio desulfuricans*, isolated from rice paddy soil: sulfide inhibition, kinetics, and regulation, *Appl. Environ. Microbiol.*, 60, 291-297, 1994.

Dalsgaard, T., Canfield, D. E., Petersen, J., Thamdrup, B., and Acuña-González, J.: N<sub>2</sub> production by the anammox reaction in the anoxic water column of Golfo Dulce, Costa Rica, *Nature*, 422, 606-608, doi:10.1038/nature01526, 2003.

Dalsgaard, T., Thamdrup, B., Fariás, L., and Revsbech, N. P.: Anammox and denitrification in the oxygen minimum zone of the eastern South Pacific, *Limnol. Oceanogr.*, 57, 1331-1346, doi:10.4319/lo.2012.57.5.1331, 2012.

Dalsgaard, T., De Brabandere, L., and Hall, P. O. J.: Denitrification in the water column of the central Baltic Sea, *Geochim. Cosmochim. Acta*, 106, 247-260, doi:10.1016/j.gca.2012.12.038, 2013.

Damm, E., Kiene, R. P., Schwarz, J., Falck, E., and Dieckmann, G.: Methane cycling in Arctic shelf water and its relationship with phytoplankton biomass and DMSP, *Mar. Chem.*, 109, 45-59, doi:10.1016/j.marchem.2007.12.003, 2008.

Damm, E., Helmke, E., Thoms, S., Schauer, U., Nöthig, E., Bakker, K., and Kiene, R. P.: Methane production in aerobic oligotrophic surface water in the central Arctic Ocean, *Biogeosciences*, 7, 1099-1108, doi:10.5194/bg-7-1099-2010, 2010.

Damm, E., Thoms, S., Beszczynska-Möller, A., Nöthig, E. M., and Kattner, G.: Methane excess production in oxygen-rich polar water and a model of cellular conditions for this paradox, *Polar Sci.*, 9, 327-334, doi:10.1016/j.polar.2015.05.001, 2015.

Darchambeau, F., Sarmiento, H., and Descy, J. P.: Primary production in a tropical large lake: The role of phytoplankton composition, *Sci. Total Environ.*, 473–474, 178-188, doi:10.1016/j.scitotenv.2013.12.036, 2014.

Degens, E. T., von Herzen, R. P., Wong, H.-K., Deuser, W. G., and Jannasch, H. W.: Lake Kivu: structure, chemistry and biology of an East African rift lake, *Geol. Rundsch.*, 62, 245-277, doi:10.1007/BF01826830, 1973.

Descy, J.-P., Darchambeau, F., Schmid, M., Wüest, A., Pasche, N., Muvundja, F. A., Müller, B., Borges, A. V., Bouillon, S., Abril, G., Delille, B., Poirier, D., Commarieu, M.-V., Lepoint, G., Morana, C., Champenois, W., Servais, P., Sarmiento, H., Lliros, M., Libert, X., Schmitz, M., Wimba, L., Nzavuga-Izere, A., Garcia-Armisen, T., Borrego, C., Isumbisho, M., Snoeks, J., Kaningini, B., Masilya, P., Nyina-wamwiza, L., Guillard, J., Jarc, L., and Bürgmann, H.: *Lake Kivu: Limnology and biogeochemistry of a tropical great lake*, Springer, 2012.

Deutzmann, J. S., and Schink, B.: Anaerobic oxidation of methane in sediments of Lake Constance, an oligotrophic freshwater lake, *Appl. Environ. Microbiol.*, 77, 4429-4436, doi:10.1128/AEM.00340-11, 2011.

Devol, A. H., Richey, J. E., Forsberg, B. R., and Martinelli, L. A.: Seasonal dynamics in methane emissions from the Amazon River floodplain to the troposphere, *J. Geophys. Res.*, 95, 16,417-416,426, doi:10.1029/JD095iD10p16417, 1990.

Dong, L. F., Sobey, M. N., Smith, C., Rusmana, I., Phillips, W., Stott, A., Osborn, A. M., and Nedwell, D. B.: Dissimilatory reduction of nitrate to ammonium (DNRA) not denitrification or anammox dominates benthic nitrate reduction in tropical estuaries, *Limnol. Oceanogr.*, 279-291, doi:10.4319/lo.2011.56.1.0279, 2011.

Downing, J. A., Prairie, Y. T., Cole, J. J., Duarte, C. M., Tranvik, L. J., Striegl, R. G., McDowell, W. H., Kortelainen, P., Caraco, N. F., Melack, J. M., and Middelburg, J. J.: The global abundance and size distribution of lakes, ponds, and impoundments, *Limnol. Oceanogr.*, 51, 2388-2397, doi:10.4319/lo.2006.51.5.2388, 2006.

Downing, J. A.: Emerging global role of small lakes and ponds: Little things mean a lot, *Limnetica*, 29, 9-24, 2010.

Dunfield, P., Knowles, R., Dumont, R., and Moore, T. R.: Methane production and consumption in temperate and subarctic peat soils: Response to temperature and pH, *Soil Biol. Biochem.*, 25, 321-326, doi:10.1016/0038-0717(93)90130-4, 1993.

Durisch-Kaiser, E., Klauer, L., Wehrli, B., and Schubert, C.: Evidence of Intense Archaeal and Bacterial Methanotrophic Activity in the Black Sea Water Column, *Appl. Environ. Microbiol.*, 71, doi: 10.1128/AEM.71.12.8099-8106.2005, 2005.

Dutaur, L., and Verchot, L. V.: A global inventory of the soil CH<sub>4</sub> sink, *Glob. Biogeochem. Cycles*, 21, doi:10.1029/2006GB002734, 2007.

Ehhalt, D. H.: The atmospheric cycle of methane, *Tellus*, 26, 58-70, doi:10.1111/j.2153-3490.1974.tb01952.x, 1974.

Eisen, J. A., Nelson, K. E., Paulsen, I. T., Heidelberg, J. F., Wu, M., Dodson, R. J., Deboy, R., Gwinn, M. L., Nelson, W. C., Haft, D. H., Hickey, E. K., Peterson, J. D., Durkin, A. S., Kolonay, J. L., Yang, F., Holt, I., Umayam, L. A., Mason, T., Brenner, M., Shea, T. P., Parksey, D., Nierman, W. C., Feldblyum, T. V., Hansen, C. L., Craven, M. B., Radune, D., Vamathevan, J., Khouri, H., White, O., Gruber, T. M., Ketchum, K. A., Venter, J. C., Tettelin, H., Bryant, D. A., and Fraser, C. M.: The complete genome sequence of *Chlorobium tepidum* TLS, a photosynthetic, anaerobic, green-sulfur bacterium, *PNAS*, 99, 9509-9514, doi:10.1073/pnas.132181499, 2002.

Eller, G., Känel, L., and Krüger, M.: Cooccurrence of Aerobic and Anaerobic Methane Oxidation in the Water Column of Lake Plußsee, *Appl. Environ. Microbiol.*, 71, doi: 10.1128/AEM.71.12.8925-8928.2005, 2005.

Engle, D., and Melack, J. M.: Methane emissions from an Amazon floodplain lake: Enhanced release during episodic mixing and during falling water, *Biogeochemistry*, 51, 71-90, doi:10.1023/A:1006389124823, 2000.

Ettwig, K. F., Shima, S., Van De Pas-Schoonen, K. T., Kahnt, J., Medema, M. H., Op Den Camp, H. J. M., Jetten, M. S. M., and Strous, M.: Denitrifying bacteria anaerobically oxidize methane in the absence of Archaea, *Environ. Microbiol.*, 10, 3164-3173, doi:10.1111/j.1462-2920.2008.01724.x, 2008.

Ettwig, K. F., Van Alen, T., Van de Pas-Schoonen, K. T., Jetten, M. S. M., and Strous, M.: Enrichment and Molecular Detection of Denitrifying Methanotrophic Bacteria of the NC10 Phylum, *Appl. Environ. Microbiol.*, 75, 3656-3662, doi:10.1128/AEM.00067-09, 2009.

Ettwig, K. F., Butler, M. K., Le Paslier, D., Pelletier, E., Mangenot, S., Kuypers, M. M., Schreiber, F., Dutilh, B. E., Zedelius, J., and De Beer, D.: Nitrite-driven anaerobic methane oxidation by oxygenic bacteria, *Nature*, 464, 543-548, doi:10.1038/nature08883, 2010.

Florez-Leiva, L., Damm, E., and Farías, L.: Methane production induced by dimethylsulfide in surface water of an upwelling ecosystem, *Prog. Oceanogr.*, 112–113, 38-48, doi:10.1016/j.pocean.2013.03.005, 2013.

Friedrich, C. G., Bardischewsky, F., Rother, D., Quentmeier, A., and Fischer, J.: Prokaryotic sulfur oxidation, *Curr. Opin. Microbiol.*, 8, 253-259, doi:10.1016/j.mib.2005.04.005, 2005.

Galas, J.: Limnological Study on a Lake Formed in a Limestone Quarry (Kraków, Poland). I. Water Chemistry, *Pol. J. Environ. Stud.*, 12, 297-300, 2003.

Ghosh, W., and Dam, B.: Biochemistry and molecular biology of lithotrophic sulfur oxidation by taxonomically and ecologically diverse bacteria and archaea, *FEMS Microbiol. Rev.*, 33, 999-1043, doi:10.1111/j.1574-6976.2009.00187.x, 2009.

Grossart, H.-P., Frindte, K., Dziallas, C., Eckert, W., and Tang, K. W.: Microbial methane production in oxygenated water column of an oligotrophic lake, *PNAS*, 108, 19657-19661, doi:10.1073/pnas.1110716108, 2011.

Guérin, F., and Abril, G.: Significance of pelagic aerobic methane oxidation in the methane and carbon budget of a tropical reservoir, *J. Geophys. Res. Biogeosci.*, 112, doi:10.1029/2006JG000393, 2007.

Hackley, K. C., Liu, C. L., and Coleman, D. D.: Environmental Isotope Characteristics of Landfill Leachates and Gases, *Ground Water*, 34, 827-836, doi:10.1111/j.1745-6584.1996.tb02077.x, 1996.

Hamersley, M. R., Woebken, D., Boehrer, B., Schultze, M., Lavik, G., and Kuypers, M. M. M.: Water column anammox and denitrification in a temperate permanently stratified lake (Lake Rassnitzer, Germany), *Syst. Appl. Microbiol.*, 32, 571-582, doi:10.1016/j.syapm.2009.07.009, 2009.

Haroon, M. F., Hu, S., Shi, Y., Imelfort, M., Keller, J., Hugenholtz, P., Yuan, Z., and Tyson, G. W.: Anaerobic oxidation of methane coupled to nitrate reduction in a novel archaeal lineage, *Nature*, 500, 567-570, doi:10.1038/nature12375, 2013.

Harrits, S. M., and Hanson, R. S.: Stratification of aerobic methane-oxidizing organisms in Lake Mendota, Madison, Wisconsin, *Limnol. Oceanogr.*, 25, 412-421, doi:10.4319/lo.1980.25.3.0412, 1980.

Hinrichs, K.-U., Hayes, J. M., Sylva, S. P., Brewer, P. G., and DeLong, E. F.: Methane-consuming archaeobacteria in marine sediments, *Nature*, 398, 802-805, doi:10.1038/19751, 1999.

Hinrichs, K.-U., and Boetius, A.: The Anaerobic Oxidation of Methane: New Insights in Microbial Ecology and Biogeochemistry, in: *Ocean Margin Systems*, edited by: Wefer, G., Billett, D., Hebbeln, D., Jørgensen, B. B., Schlüter, M., and van Weering, T. C. E., Springer Berlin Heidelberg, Berlin, Heidelberg, 457-477, 2003.

Hofmann, H.: Spatiotemporal distribution patterns of dissolved methane in lakes: How accurate are the current estimations of the diffusive flux path?, *Geophys. Res. Lett.*, 40, 2779-2784, doi:10.1002/grl.50453, 2013.

Holgerson, M. A., and Raymond, P. A.: Large contribution to inland water CO<sub>2</sub> and CH<sub>4</sub> emissions from very small ponds, *Nat. Geosci.*, 9, 222-226, doi:10.1038/NGEO2654, 2016.

Hu, S., Zeng, R. J., Burow, L. C., Lant, P., Keller, J., and Yuan, Z.: Enrichment of denitrifying anaerobic methane oxidizing microorganisms, *Environ. Microbiol. Rep.*, 1, 377-384, doi:10.1111/j.1758-2229.2009.00083.x, 2009.

Hu, S., Zeng, R. J., Keller, J., Lant, P. A., and Yuan, Z.: Effect of nitrate and nitrite on the selection of microorganisms in the denitrifying anaerobic methane oxidation process, *Environ. Microbiol. Rep.*, 3, 315-319, doi:10.1111/j.1758-2229.2010.00227.x, 2011.

Hulth, S., Aller, R. C., Canfield, D. E., Dalsgaard, T., Engström, P., Gilbert, F., Sundbäck, K., and Thamdrup, B.: Nitrogen removal in marine environments: recent findings and future research challenges, *Mar. Chem.*, 94, 125-145, doi:10.1016/j.marchem.2004.07.013, 2005.

Hungate, R. E.: Hydrogen as an intermediate in the rumen fermentation, *Arch. Mikrobiol.*, 59, 158-164, doi:10.1007/bf00406327, 1967.

Huttunen, J. T., Alm, J., Liikanen, A., Juutinen, S., Larmola, T., Hammar, T., Silvola, J., and Martikainen, P. J.: Fluxes of methane, carbon dioxide and nitrous oxide in boreal lakes and potential anthropogenic effects on the aquatic greenhouse gas emissions, *Chemosphere*, 52, 609-621, doi:10.1016/S0045-6535(03)00243-1, 2003.

Inagaki, F., Takai, K., Kobayashi, H., Nealson, K. H., and Horikoshi, K.: *Sulfurimonas autotrophica* gen. nov., sp. nov., a novel sulfur-oxidizing  $\epsilon$ -proteobacterium isolated from hydrothermal sediments in the Mid-Okinawa Trough, *Int. J. Syst. Evol. Microbiol.*, 53, 1801-1805, doi:10.1099/ijs.0.02682-0, 2003.

İnceoğlu, Ö., Llíros, M., García-Armisen, T., Crowe, S. A., Michiels, C., Darchambeau, F., Descy, J.-P., and Servais, P.: Distribution of bacteria and archaea in meromictic tropical Lake Kivu (Africa), *Aquat. Microb. Ecol.*, 74, 215-233, doi:10.3354/ame01737, 2015a.

İnceoğlu, Ö., Llíros, M., Crowe, S., García-Armisen, T., Morana, C., Darchambeau, F., Borges, A., Descy, J.-P., and Servais, P.: Vertical Distribution of Functional Potential and Active Microbial Communities in Meromictic Lake Kivu, *Microb. Ecol.*, 70, 596-611, doi:10.1007/s00248-015-0612-9, 2015b.

IPCC: *Climate Change 2013: The Physical Science Basis. Contribution of Working Group I to the Fifth Assessment Report of the Intergovernmental Panel on Climate Change*, Cambridge University Press, Cambridge, United Kingdom and New York, NY, USA, 1535 pp., 2013.

Iversen, N., and Jørgensen, B.: Anaerobic methane oxidation rates at the sulfate-methane transition in marine sediments from Kattegat and Skagerrak (Denmark), *Limnol. Oceanogr.*, 30, 944-955, doi:10.4319/lo.1985.30.5.0944, 1985.

Iversen, N., Oremland, R. S., and Klug, M. J.: Big Soda Lake (Nevada). 3. Pelagic methanogenesis and anaerobic methane oxidation, *Limnol. Oceanogr.*, 32, 804-814, doi:10.4319/lo.1987.32.4.0804, 1987.

Jannasch, H. W.: Methane oxidation in Lake Kivu (central Africa)1, *Limnol. Oceanogr.*, 20, 860-864, doi:10.4319/lo.1975.20.5.0860, 1975.

Jarrell, K. F.: Extreme Oxygen Sensitivity in Methanogenic Archaeobacteria, *Bioscience*, 35, 298-302, doi:10.2307/1309929, 1985.

Jensen, M. M., Kuypers, M. M. M., Lavik, G., and Thamdrup, B.: Rates and regulation of anaerobic ammonium oxidation and denitrification in the Black Sea, *Limnol. Oceanogr.*, 53, 23-36, doi:10.4319/lo.2008.53.1.0023, 2008.

Jensen, M. M., Petersen, J., Dalsgaard, T., and Thamdrup, B.: Pathways, rates, and regulation of N<sub>2</sub> production in the chemocline of an anoxic basin, Mariager Fjord, Denmark, *Mar. Chem.*, 113, 102-113, doi:10.1016/j.marchem.2009.01.002, 2009.

Jetten, M. S. M., Strous, M., van de Pas-Schoonen, K. T., Schalk, J., van Dongen, U. G. J. M., van de Graaf, A. A., Logemann, S., Muyzer, G., van Loosdrecht, M. C. M., and Kuenen, J. G.: The anaerobic oxidation of ammonium, *FEMS Microbiol. Rev.*, 22, 421-437, doi:10.1111/j.1574-6976.1998.tb00379.x, 1998.

Jetten, M. S. M., Wagner, M., Fuerst, J., van Loosdrecht, M., Kuenen, G., and Strous, M.: Microbiology and application of the anaerobic ammonium oxidation ('anammox') process, *Curr. Opin. Biotechnol.*, 12, 283-288, doi:10.1016/S0958-1669(00)00211-1, 2001.

Jin, R. C., Yang, G. F., Yu, J. J., and Zheng, P.: The inhibition of the Anammox process: A review, *Chem. Eng. J.*, 197, 67-79, doi:10.1016/j.cej.2012.05.014, 2012.

Jolley, D. W., Widdowson, M., and Self, S.: Volcanogenic nutrient fluxes and plant ecosystems in large igneous provinces: an example from the Columbia River Basalt Group, *J. Geol. Soc.*, 165, 955-966, doi:10.1144/0016-76492006-199, 2008.

Jones, C., Crowe, S. A., Sturm, A., Leslie, K. L., MacLean, L. C. W., Katsev, S., Henny, C., Fowle, D. A., and Canfield, D. E.: Biogeochemistry of manganese in ferruginous Lake Matano, Indonesia, *Biogeosciences*, 8, 2977-2991, doi:10.5194/bg-8-2977-2011, 2011.

Jones, R. I., and Grey, J.: Biogenic methane in freshwater food webs, *Freshwater Biol.*, 56, 213-229, doi:10.1111/j.1365-2427.2010.02494.x, 2011.

Jørgensen, B. B., Weber, A., and Zopfi, J.: Sulfate reduction and anaerobic methane oxidation in Black Sea sediments, *Deep-Sea Res. Pt. I*, 48, 2097-2120, doi:10.1016/S0967-0637(01)00007-3, 2001.

Jørgensen, K. S.: Annual Pattern of Denitrification and Nitrate Ammonification in Estuarine Sediment, *Appl. Environ. Microbiol.*, 55, 1841-1847, 1989.

Joye, S. B., and Hollibaugh, J. T.: Influence of sulfide inhibition of nitrification on nitrogen regeneration in sediments, *Science*, 270, 623-625, doi:10.1126/science.270.5236.623, 1995.

Kalyuzhnyi, S., Gladchenko, M., Mulder, A., and Versprille, B.: DEAMOX-New biological nitrogen removal process based on anaerobic ammonia oxidation coupled to sulphide-driven conversion of nitrate into nitrite, *Water Res.*, 40, 3637-3645, doi:10.1016/j.watres.2006.06.010, 2006.

Kampman, C., Hendrickx, T. L. G., Luesken, F. A., van Alen, T. A., Op den Camp, H. J. M., Jetten, M. S. M., Zeeman, G., Buisman, C. J. N., and Temmink, H.: Enrichment of denitrifying methanotrophic bacteria for application after direct low-temperature anaerobic sewage treatment, *J. Hazard. Mater.*, 227–228, 164-171, doi:10.1016/j.jhazmat.2012.05.032, 2012.

Kankaala, P., Huotari, J., Tulonen, T., and Ojala, A.: Lake-size dependent physical forcing drives carbon dioxide and methane effluxes from lakes in a boreal landscape, *Limnol. Oceanogr.*, 58, 1915-1930, doi:10.4319/lo.2013.58.6.1915, 2013.

Karl, D. M., and Tilbrook, B. D.: Production and transport of methane in oceanic particulate organic matter, *Nature*, 368, 732-734, doi:10.1038/368732a0, 1994.

Karl, D. M., Beversdorf, L., Björkman, K. M., Church, M. J., Martinez, A., and Delong, E. F.: Aerobic production of methane in the sea, *Nat. Geosci.*, 1, 473-478, doi:10.1038/ngeo234, 2008.

Kelso, B., Smith, R. V., Laughlin, R. J., and Lennox, S. D.: Dissimilatory nitrate reduction in anaerobic sediments leading to river nitrite accumulation, *Appl. Environ. Microbiol.*, 63, 4679-4685, 1997.

Kirchman, D. L., Sherr, E., Sherr, B., Fuhrman, J. A., Hagström, A., Moran, M. A., Bèjà, O., Suzuki, M. T., Worden, A. Z., Not, F., Nagata, T., del Giorgio, P. A., Gasol, J. M., Robinson, C., Church, M. J., Jürgens, K., Massana, R., Breitbart, M., Middelboe, M., Rohwer, F., Zehr, J. P., Paerl, H. W., Thamdrup, B., and Dalsgaard, T.: *Microbial Ecology of the Oceans*, John Wiley & Sons, New Jersey, 2008.

Kirschke, S., Bousquet, P., Ciais, P., Saunoy, M., Canadell, J. G., Dlugokencky, E. J., Bergamaschi, P., Bergmann, D., Blake, D. R., Bruhwiler, L., Cameron-Smith, P., Castaldi, S., Chevallier, F., Feng, L., Fraser, A., Heimann, M., Hodson, E. L., Houweling, S., Josse, B., Fraser, P. J., Krummel, P. B., Lamarque, J.-F., Langenfelds, R. L., Le Quere, C., Naik, V., O'Doherty, S., Palmer, P. I., Pison, I., Plummer, D., Poulter, B., Prinn, R. G., Rigby, M., Ringeval, B., Santini, M., Schmidt, M., Shindell, D. T., Simpson, I. J., Spahni, R., Steele, L. P., Strode, S. A., Sudo, K., Szopa, S., van der Werf, G. R., Voulgarakis, A., van Weele, M., Weiss, R. F., Williams, J. E., and Zeng, G.: Three decades of global methane sources and sinks, *Nat. Geosci.*, 6, 813-823, doi:10.1038/ngeo1955, 2013.

Knowles, R., and Blackburn, T. H.: *Nitrogen isotope techniques*, Academic Press, Inc., 1993.

Konhauser, K. O., Newman, D. K., and Kappler, A.: The potential significance of microbial Fe(III) reduction during deposition of Precambrian banded iron formations, *Geobiology*, 3, 167-177, doi:10.1111/j.1472-4669.2005.00055.x, 2005.

Krüger, M., Frenzel, P., and Conrad, R.: Microbial processes influencing methane emission from rice fields, *Glob. Change Biol.*, 7, 49-63, doi:10.1046/j.1365-2486.2001.00395.x, 2001.

Kuypers, M. M., Lavik, G., Woebken, D., Schmid, M., Fuchs, B. M., Amann, R., Jørgensen, B. B., and Jetten, M. S.: Massive nitrogen loss from the Benguela upwelling system through anaerobic ammonium oxidation, *PNAS*, 102, 6478-6483, doi: 10.1073/pnas.0502088102, 2005.

Kuypers, M. M. M., Silekers, A. O., Lavik, G., Schmid, M., Jørgensen, B. B., Kuenen, J. G., Sinninghe Damsté, J. S., Strous, M., and Jetten, M. S. M.: Anaerobic ammonium oxidation by anammox bacteria in the Black Sea, *Nature*, 422, 608-611, doi:10.1038/nature01472, 2003.

Larkin, J., and Strohl, W.: Beggiatoa, Thiobacillus, and Thioploca, *Annu. Rev. Microbiol.*, 37, 341-367, doi:10.1146/annurev.mi.37.100183.002013, 1983.

Lavik, G., Stührmann, T., Brüchert, V., Van Der Plas, A., Mohrholz, V., Lam, P., Mußmann, M., Fuchs, B. M., Amann, R., Lass, U., and Kuypers, M. M. M.: Detoxification of sulphidic African shelf waters by blooming chemolithotrophs, *Nature*, 457, 581-584, doi:10.1038/nature07588, 2009.

Lenhart, K., Klintzsch, T., Langer, G., Nehrke, G., Bunge, M., Schnell, S., and Keppler, F.: Evidence for methane production by the marine algae *Emiliana huxleyi*, *Biogeosciences*, 13, 3163-3174, doi:10.5194/bg-13-3163-2016, 2016.

Lewis Jr, W. M.: Tropical limnology, *Annu. Rev. Ecol. Evol. Syst.*, 18, 159-184, doi:10.1146/annurev.es.18.110187.001111, 1987.

Lewis Jr, W. M.: Basis for the protection and management of tropical lakes, *Lake Reserv. Manage.*, 5, 35-48, doi:10.1046/j.1440-1770.2000.00091.x, 2000.

Lewis Jr, W. M.: Biogeochemistry of tropical lakes, *Verh. Internat. Verein. Limnol.*, 30, 1595-1603, 2010.

Llirós, M., Gich, F., Plasencia, A., Auguet, J. C., Darchambeau, F., Casamayor, E. O., Descy, J. P., and Borrego, C.: Vertical distribution of ammonia-oxidizing crenarchaeota and methanogens in the epipelagic waters of lake kivu (Rwanda-Democratic Republic of the Congo), *Appl. Environ. Microbiol.*, 76, 6853-6863, doi:10.1128/AEM.02864-09, 2010.

Llirós, M., García-Armisen, T., Darchambeau, F., Morana, C., Triadó-Margarit, X., Inceoğlu, Ö., Borrego, C. M., Bouillon, S., Servais, P., Borges, A. V., Descy, J. P., Canfield, D. E., and Crowe, S. A.: Pelagic photoferrotrophy and iron cycling in a modern ferruginous basin, *Sci. Rep.*, 5, 13803, doi:10.1038/srep13803, 2015.

Lopes, F., Viollier, E., Thiam, A., Michard, G., Abril, G., Groleau, A., Prévot, F., Carrias, J.-F., Albéric, P., and Jézéquel, D.: Biogeochemical modelling of anaerobic vs. aerobic methane oxidation in a meromictic crater lake (Lake Pavin, France), *Appl. Geochem.*, 26, 1919-1932, doi:10.1016/j.apgeochem.2011.06.021, 2011.

Luesken, F. A., Sánchez, J., Van Alen, T., Sanabria, J., Op Den Camp, H. J. M., Jetten, M. S. M., and Kartal, B.: Simultaneous Nitrite-Dependent Anaerobic Methane and Ammonium Oxidation Processes, *Appl. Environ. Microbiol.*, 77, doi:10.1128/AEM.05539-11, 2011.

Marotta, H., Pinho, L., Gudas, C., Bastviken, D., Tranvik, L. J., and Enrich-Prast, A.: Greenhouse gas production in low-latitude lake sediments responds strongly to warming, *Nature Clim. Change*, 4, 467-470, doi:10.1038/nclimate2222, 2014.

Melack, J. M., Hess, L. L., Gastil, M., Forsberg, B. R., Hamilton, S. K., Lima, I. B. T., and Novo, E. M. L. M.: Regionalization of methane emissions in the Amazon Basin with microwave remote sensing, *Glob. Change Biol.*, 10, 530-544, doi:10.1111/j.1365-2486.2004.00763.x, 2004.

Mengis, M., Gächter, R., and Wehrli, B.: Sources and sinks of nitrous oxide (N<sub>2</sub>O) in deep lakes, *Biogeochemistry*, 38, 281-301, doi:10.1023/A:1005814020322, 1997.

Metcalf, W. W., Griffin, B. M., Cicchillo, R. M., Gao, J., Janga, S. C., Cooke, H. A., Circello, B. T., Evans, B. S., Martens-Habbena, W., Stahl, D. A., and van der Donk, W. A.: Synthesis of Methylphosphonic Acid by Marine Microbes: A Source for Methane in the Aerobic Ocean, *Science*, 337, 1104-1107, doi:10.1126/science.1219875, 2012.

Michiels, C. C., Darchambeau, F., Roland, F. A. E., Morana, C., Llíros, M., García-Armisen, T., Thamdrup, B., Borges, A. V., Canfield, D. E., Servais, P., Descy, J.-P., and Crowe, S. A.: Fe-dependent N-cycling and the nutrient status of ferruginous seas, *Nat. Geosci.*, in press.

Miettinen, H., Pumpanen, J., Heiskanen, J. J., Aaltonen, H., Mammarella, I., Ojala, A., Levula, J., and Rantakari, M.: Towards a more comprehensive understanding of lacustrine greenhouse gas dynamics -- two-year measurements of concentrations and fluxes of CO<sub>2</sub>, CH<sub>4</sub> and N<sub>2</sub>O in a typical boreal lake surrounded by managed forests, *Boreal Environ. Res.*, 20, 75-89, 2015.

Miranda, K. M., Espey, M. G., and Wink, D. A.: A rapid, simple spectrophotometric method for simultaneous detection of nitrate and nitrite, *Nitric Oxide-Biol. Ch.*, 5, 62-71, doi:10.1006/niox.2000.0319, 2001.

Morana, C., Sarmiento, H., Descy, J. P., Gasol, J. M., Borges, A. V., Bouillon, S., and Darchambeau, F.: Production of dissolved organic matter by phytoplankton and its uptake by heterotrophic prokaryotes in large tropical lakes, *Limnol. Oceanogr.*, 59, 1364-1375, doi:10.4319/lo.2014.59.4.1364, 2014.

Morana, C., Darchambeau, F., Roland, F. A. E., Borges, A. V., Muvundja, F. A., Kelemen, Z., Masilya, P., Descy, J. P., and Bouillon, S.: Biogeochemistry of a large and deep tropical lake (Lake Kivu, East Africa): insights from a stable isotope study covering an annual cycle, *Biogeosciences*, 12, 4953-4963, doi:10.5194/bg-12-4953-2015, 2015a.

Morana, C., Borges, A. V., Roland, F. A. E., Darchambeau, F., Descy, J. P., and Bouillon, S.: Methanotrophy within the water column of a large meromictic tropical lake (Lake Kivu, East Africa), *Biogeosciences*, 12, 2077-2088, doi:10.5194/bg-12-2077-2015, 2015b.

Morana, C., Roland, F. A., Crowe, S. A., Llíros, M., Borges, A. V., Darchambeau, F., and Bouillon, S.: Chemoautotrophy and anoxygenic photosynthesis within the water column of a large meromictic tropical lake (Lake Kivu, East Africa), *Limnol. Oceanogr.*, doi:10.1002/lno.10304, 2016.

Natchimuthu, S., Sundgren, I., Gålfalk, M., Klemetsson, L., Crill, P., Danielsson, Å., and Bastviken, D.: Spatio-temporal variability of lake CH<sub>4</sub> fluxes and its influence on annual whole lake emission estimates, *Limnol. Oceanogr.*, doi:10.1002/lno.10222, 2015.

Nauhaus, K., Treude, T., Boetius, A., and Krüger, M.: Environmental regulation of the anaerobic oxidation of methane: a comparison of ANME-I and ANME-II communities, *Environ. Microbiol.*, 7, 98-106, doi:10.1111/j.1462-2920.2004.00669.x, 2005.

Nayar, A.: Earth science: a lakeful of trouble, *Nature News*, 460, 321-323, doi:10.1038/460321a, 2009.

Nisbet, E. G., Dlugokencky, E. J., Manning, M. R., Lowry, D., Fisher, R. E., France, J. L., Michel, S. E., Miller, J. B., White, J. W. C., Vaughn, B., Bousquet, P., Pyle, J. A., Warwick, N. J., Cain, M., Brownlow, R., Zazzeri, G., Lanoisellé, M., Manning, A. C., Gloor, E., Worthy, D. E. J., Brunke, E. G., Labuschagne, C., Wolff, E. W., and Ganesan, A. L.: Rising atmospheric methane: 2007–2014 growth and isotopic shift, *Glob. Biogeochem. Cycles*, 30, 1356-1370, doi:10.1002/2016GB005406, 2016.

The NOAA annual greenhouse gas index (AGGI), 2015.

Oremland, R. S., Miller, L. G., Colbertson, C. W., Robinson, S., Smith, R. L., Lovley, D., Whiticar, M. J., King, G. M., Kiene, R. P., and Iversen, N.: Aspects of the biogeochemistry of methane in Mono Lake and the Mono Basin of California, in: *Biogeochemistry of global change*, Springer, 704-741, 1993.



Orphan, V. J., Ussler Iii, W., Naehr, T. H., House, C. H., Hinrichs, K. U., and Paull, C. K.: Geological, geochemical, and microbiological heterogeneity of the seafloor around methane vents in the Eel River Basin, offshore California, *Chem. Geol.*, 205, 265-289, doi:10.1016/j.chemgeo.2003.12.035, 2004.

Pasche, N., Dinkel, C., Müller, B., Schmid, M., Wuëst, A., and Wehrli, B.: Physical and biogeochemical limits to internal nutrient loading of meromictic lake kivu, *Limnol. Oceanogr.*, 54, 1863-1873, doi:10.4319/lo.2009.54.6.1863, 2009.

Pasche, N., Schmid, M., Vazquez, F., Schubert, C. J., Wüest, A., Kessler, J. D., Pack, M. A., Reeburgh, W. S., and Bürgmann, H.: Methane sources and sinks in Lake Kivu, *J. Geophys. Res. Biogeosci.*, 116, G03006, doi:10.1029/2011JG001690, 2011.

Podgrajsek, E., Sahlée, E., and Rutgersson, A.: Diurnal cycle of lake methane flux, *J. Geophys. Res. Biogeosci.*, 119, 236-248, doi:10.1002/2013JG002327, 2014.

Polsenaere, P., Deborde, J., Detandt, G., Vidal, L. O., Pérez, M. A., Marieu, V., and Abril, G.: Thermal enhancement of gas transfer velocity of CO<sub>2</sub> in an Amazon floodplain lake revealed by eddy covariance measurements, *Geophys. Res. Lett.*, 40, 1734-1740, doi:10.1002/grl.50291, 2013.

Quay, P., Stutsman, J., Wilbur, D., Snover, A., Dlugokencky, E., and Brown, T.: The isotopic composition of atmospheric methane, *Global Biogeochem. Cy.*, 13, 445-461, doi:10.1029/1998GB900006, 1999.

Raghoebarsing, A. A., Pol, A., Van de Pas-Schoonen, K. T., Smolders, A. J., Ettwig, K. F., Rijpstra, W. I. C., Schouten, S., Damsté, J. S. S., den Camp, H. J. O., and Jetten, M. S.: A microbial consortium couples anaerobic methane oxidation to denitrification, *Nature*, 440, 918-921, doi:10.1038/nature04617, 2006.

Read, J. S., Hamilton, D. P., Desai, A. R., Rose, K. C., MacIntyre, S., Lenters, J. D., Smyth, R. L., Hanson, P. C., Cole, J. J., and Staehr, P. A.: Lake-size dependency of wind shear and convection as controls on gas exchange, *Geophys. Res. Lett.*, 39, doi:10.1029/2012GL051886, 2012.

Remacle, A.: L'inventaire des carrières de Wallonie (Belgique) : présentation générale et aspects entomologiques Notes fauniques de Gembloux, 57, 73-79, 2005.

Repeta, D. J., Ferron, S., Sosa, O. A., Johnson, C. G., Repeta, L. D., Acker, M., DeLong, E. F., and Karl, D. M.: Marine methane paradox explained by bacterial degradation of dissolved organic matter, *Nature Geosci.*, 9, 884-887, doi:10.1038/ngeo2837, 2016.

Riera, J. L., Schindler, J. E., and Kratz, T. K.: Seasonal dynamics of carbon dioxide and methane in two clear-water lakes and two bog lakes in northern Wisconsin, U.S.A, *Can. J. Fish. Aquat. Sci.*, 56, 265-274, doi:10.1139/f98-182, 1999.

Rodier, J., Bazin, C., Broutin, J., Chambon, P., Champsaur, H., and Rodi, L.: L'Analyse de l'Eau (8ème édtn), Dunod, Paris: France, 1996.

Roland, F. A. E., Darchambeau, F., Morana, C., and Borges, A. V.: Nitrous oxide and methane seasonal variability in the epilimnion of a large tropical meromictic lake (Lake Kivu, East-Africa), *Aquat. Sci.*, 1-10, doi:10.1007/s00027-016-0491-2, 2016.

Roland, F. A. E., Darchambeau, F., Morana, C., Bouillon, S., and Borges, A. V.: Emission and oxidation of methane in a meromictic, eutrophic and temperate lake (Dendre, Belgium), *Chemosphere*, 168, 756-764, doi:10.1016/j.chemosphere.2016.10.138, 2017.

Ross, K. A., Gashugi, E., Gafasi, A., Wüest, A., and Schmid, M.: Characterisation of the Subaquatic Groundwater Discharge That Maintains the Permanent Stratification within Lake Kivu; East Africa, *PLoS ONE*, 10, e0121217, doi:10.1371/journal.pone.0121217, 2015.

Rudd, J. W.: Methane oxidation in Lake Tanganyika (East Africa), *Limnol. Oceanogr.*, 25, 958-963, doi:10.4319/lo.1980.25.5.0958, 1980.

Rudd, J. W. M., Hamilton, R. D., and Campbell, N. E. R.: Measurement of microbial oxidation of methane in lake water, *Limnol. Oceanogr.*, 19, 519-524, doi:10.4319/lo.1974.19.3.0519, 1974.

Russ, L., Speth, D. R., Jetten, M. S., Op den Camp, H. J., and Kartal, B.: Interactions between anaerobic ammonium and sulfur-oxidizing bacteria in a laboratory scale model system, *Environ. microbiol.*, 16, 3487-3498, doi: 10.1111/1462-2920.12487, 2014.

Rysgaard, S., Risgaard-Petersen, N., and Sloth, N. P.: Nitrification, denitrification, and nitrate ammonification in sediments of two coastal lagoons in Southern France, *Hydrobiologia*, 329, 133-141, doi:10.1007/BF00034553, 1996.

Saad, O. A. L. O., and Conrad, R.: Temperature dependence of nitrification, denitrification, and turnover of nitric oxide in different soils, *Biol. Fert. Soils*, 15, 21-27, doi:10.1007/BF00336283, 1993.

Sarmiento, H., Isumbiso, M., and Descy, J.-P.: Phytoplankton ecology of Lake Kivu (eastern Africa), *J. Plankton Res.*, 28, 815-829, doi:10.1093/plankt/fbl017, 2006.

Saunois, M., Bousquet, P., Poulter, B., Peregon, A., Ciais, P., Canadell, J. G., Dlugokencky, E. J., Etiope, G., Bastviken, D., Houweling, S., Janssens-Maenhout, G., Tubiello, F. N., Castaldi, S., Jackson, R. B., Alexe, M., Arora, V. K., Beerling, D. J., Bergamaschi, P., Blake, D. R., Brailsford, G., Brovkin, V., Bruhwiler, L., Crevoisier, C., Crill, P., Curry, C., Frankenberg, C., Gedney, N., Höglund-Isaksson, L., Ishizawa, M., Ito, A., Joos, F., Kim, H. S., Kleinen, T., Krummel, P., Lamarque, J. F., Langenfelds, R., Locatelli, R., Machida, T., Maksyutov, S., McDonald, K. C., Marshall, J., Melton, J. R., Morino, I., O'Doherty, S., Parmentier, F. J. W., Patra, P. K., Peng, C., Peng, S., Peters, G. P., Pison, I., Prigent, C., Prinn, R., Ramonet, M., Riley, W. J., Saito, M., Schroeder, R., Simpson, I. J., Spahni, R., Steele, P., Takizawa, A., Thornton, B. F., Tian, H., Tohjima, Y., Viovy, N., Voulgarakis, A., van Weele, M., van der Werf, G., Weiss, R., Wiedinmyer, C., Wilton, D. J., Wiltshire, A., Worthy, D., Wunch, D. B., Xu, X., Yoshida, Y., Zhang, B., Zhang, Z., and Zhu, Q.: The Global Methane Budget: 2000-2012, *Earth Syst. Sci. Data Discuss.*, 2016, 1-79, doi:10.5194/essd-2016-25, 2016.

Sawakuchi, H. O., Bastviken, D., Sawakuchi, A. O., Krusche, A. V., Ballester, M. V., and Richey, J. E.: Methane emissions from Amazonian Rivers and their contribution to the global methane budget, *Glob. Change Biol.*, 20, 2829-2840, doi:10.1111/gcb.12646, 2014.

Sayama, M., Risgaard-Petersen, N., Nielsen, L. P., Fossing, H., and Christensen, P. B.: Impact of bacterial NO<sub>3</sub> - transport on sediment biogeochemistry, *Appl. Environ. Microbiol.*, 71, 7575-7577, doi:10.1128/AEM.71.11.7575-7577.2005, 2005.

Schilder, J., Bastviken, D., Hardenbroek, M., Kankaala, P., Rinta, P., Stötter, T., and Heiri, O.: Spatial heterogeneity and lake morphology affect diffusive greenhouse gas emission estimates of lakes, *Geophys. Res. Lett.*, 40, 5752-5756, doi:10.1002/2013GL057669, 2013.

Schmid, M., Halbwachs, M., Wehrli, B., and Wüest, A.: Weak mixing in Lake Kivu: New insights indicate increased risk of uncontrolled gas eruption, *Geochem. Geophys. Geosyst.*, 6, doi:10.1029/2004GC000892, 2005.

Schmid, M., and Wüest, A.: Stratification, Mixing and Transport Processes in Lake Kivu, in: *Lake Kivu: Limnology and biogeochemistry of a tropical great lake*, edited by: Descy, J. P., Darchambeau, F., and Schmid, M., Springer, New York London, 2012.

Schmidt, W.: Über die Temperatur- und Stabilitätsverhältnisse von Seen, *Geografiska Annaler*, 10, 145-177, doi:10.2307/519789, 1928.

Schubert, C. J., Durisch-Kaiser, E., Wehrli, B., Thamdrup, B., Lam, P., and Kuypers, M. M. M.: Anaerobic ammonium oxidation in a tropical freshwater system (Lake Tanganyika), *Environ. Microbiol.*, 8, 1857-1863, doi:10.1111/j.1462-2920.2006.01074.x, 2006.

Schubert, C. J., Lucas, F., Durisch-Kaiser, E., Stierli, R., Diem, T., Scheidegger, O., Vazquez, F., and Müller, B.: Oxidation and emission of methane in a monomictic lake (Rotsee, Switzerland), *Aquat. sci.*, 72, 455-466, doi:10.1007/s00027-010-0148-5, 2010.

Seitzinger, S., Harrison, J. A., Böhlke, J. K., Bouwman, A. F., Lowrance, R., Peterson, B., Tobias, C., and Van Drecht, G.: Denitrification across landscapes and waterscapes: A synthesis, *Ecol. Appl.*, 16, 2064-2090, doi:10.1890/1051-0761(2006)016[2064:DALAWA]2.0.CO;2, 2006.

Seitzinger, S. P.: Denitrification in freshwater and coastal marine ecosystems: ecological and geochemical significance, *Limnol. Oceanogr.*, 33, 702-724, doi:10.4319/lo.1988.33.4part2.0702, 1988.

Shiklomanov, I. A.: World freshwater resources, in: *Water in crisis: A guide to the world's freshwater resources*, edited by: Gleick, P. H., Oxford University Press, New-York, 1993.

Sievert, S. M., Scott, K. M., Klotz, M. G., Chain, P. S., Hauser, L. J., Hemp, J., Hügler, M., Land, M., Lapidus, A., and Larimer, F. W.: Genome of the epsilonproteobacterial chemolithoautotroph *Sulfurimonas denitrificans*, *Appl. Environ. Microbiol.*, 74, 1145-1156, doi:10.1128/AEM.01844-07, 2008.

Silver, W. L., Herman, D. J., and Firestone, M. K.: Dissimilatory nitrate reduction to ammonium in upland tropical forest soils, *Ecology*, 82, 2410-2416, doi:10.2307/2679925, 2001.

Simon, J.: Enzymology and bioenergetics of respiratory nitrite ammonification, *FEMS Microbiol. Rev.*, 26, 285-309, doi:10.1111/j.1574-6976.2002.tb00616.x, 2002.

Sivan, O., Adler, M., Pearson, A., Gelman, F., Bar-Or, I., John, S. G., and Eckert, W.: Geochemical evidence for iron-mediated anaerobic oxidation of methane, *Limnol. Oceanogr.*, 56, 1536-1544, doi:10.4319/lo.2011.56.4.1536, 2011.

Smith, L. K., and Lewis Jr, W. M.: Seasonality of methane emissions from five lakes and associated wetlands of the Colorado Rockies, *Glob. Biogeochem. Cycles*, 6, 323-338, doi:10.1029/92GB02016, 1992.

SPW-DGO3: Etat des nappes d'eau souterraine de Wallonie, Belgique, 2015.

Stahl, D. A., and De La Torre, J. R.: Physiology and diversity of ammonia-oxidizing archaea, *Annu. Rev. Microbiol.*, 66, 83-101, doi:10.1146/annurev-micro-092611-150128, 2012.

Stanley, E. H., Casson, N. J., Christel, S. T., Crawford, J. T., Loken, L. C., and Oliver, S. K.: The ecology of methane in streams and rivers: patterns, controls, and global significance, *Ecol. Monogr.*, 86, 146-171, doi:10.1890/15-1027, 2016.

Stieglmeier, M., Mooshammer, M., Kitzler, B., Wanek, W., Zechmeister-Boltenstern, S., Richter, A., and Schleper, C.: Aerobic nitrous oxide production through N-nitrosating hybrid formation in ammonia-oxidizing archaea, *The ISME Journal*, 8, 1135-1146, doi:10.1038/ismej.2013.220, 2014.

Strohm, T. O., Griffin, B., Zumft, W. G., and Schink, B.: Growth yields in bacterial denitrification and nitrate ammonification, *Appl. Environ. Microbiol.*, 73, 1420-1424, doi: 10.1128/AEM.02508-06, 2007.

Strous, M., Kuenen, J. G., and Jetten, M. S.: Key physiology of anaerobic ammonium oxidation, *Appl. Environ. Microbiol.*, 65, 3248-3250, 1999.

Sturm, A., Fowle, D. A., Jones, C., Leslie, K., Nomosatryo, S., Henny, C., Canfield, D. E., and Crowe, S. A.: Rates and pathways of CH<sub>4</sub> oxidation in ferruginous Lake Matano, Indonesia, *Biogeosciences Discuss.*, 2016, 1-34, doi:10.5194/bg-2015-533, 2016.

Tang, K. W., McGinnis, D. F., Frindte, K., Brüchert, V., and Grossart, H.-P.: Paradox reconsidered: Methane oversaturation in well-oxygenated lake waters, *Limnol. Oceanogr.*, 59, 275-284, doi:10.4319/lo.2014.59.1.0275, 2014.

Tang, K. W., McGinnis, D. F., Ionescu, D., and Grossart, H.-P.: Methane Production in Oxic Lake Waters Potentially Increases Aquatic Methane Flux to Air, *Environ. Sci. Technol. Lett.*, 3, 227-233, doi:10.1021/acs.estlett.6b00150, 2016.

Tassi, F., Vaselli, O., Tedesco, D., Montegrossi, G., Darrah, T., Cuoco, E., Mapendano, M., Poreda, R., and Delgado Huertas, A.: Water and gas chemistry at Lake Kivu (DRC): geochemical evidence of vertical and horizontal heterogeneities in a multibasin structure, *Geochem. Geophys. Geosyst.*, 10, doi:10.1029/2008GC002191, 2009.

Thamdrup, B., and Dalsgaard, T.: Production of N<sub>2</sub> through anaerobic ammonium oxidation coupled to nitrate reduction in marine sediments, *Appl. Environ. Microbiol.*, 68, 1312-1318, doi:10.1128/AEM.68.3, 2002.

Thamdrup, B., Dalsgaard, T., Jensen, M. M., Ulloa, O., Farías, L., and Escribano, R.: Anaerobic ammonium oxidation in the oxygen-deficient waters off northern Chile, *Limnol. Oceanogr.*, 51, 2145-2156, doi:10.4319/lo.2006.51.5.2145, 2006.

Thiery, W., Stepanenko, V. M., Fang, X., Jöhnk, K. D., Li, Z., Martynov, A., Perroud, M., Subin, Z. M., Darchambeau, F., Mironov, D., and van Lipzig, N. P. M.: LakeMIP Kivu: evaluating the representation of a large, deep tropical lake by a set of one-dimensional lake models, *Tellus A*, doi:10.3402/tellusa.v66.21390, 2014a.

Thiery, W., Martynov, A., Darchambeau, F., Descy, J. P., Plisnier, P. D., Sushama, L., and van Lipzig, N. P. M.: Understanding the performance of the FLake model over two African Great Lakes, *Geosci. Model Dev.*, 7, 317-337, doi:10.5194/gmd-7-317-2014, 2014b.

Thornton, J. A., Kercher, J. P., Riedel, T. P., Wagner, N. L., Cozic, J., Holloway, J. S., Dubé, W. P., Wolfe, G. M., Quinn, P. K., Middlebrook, A. M., Alexander, B., and Brown, S. S.: A large atomic chlorine source inferred from mid-continental reactive nitrogen chemistry, *Nature*, 464, 271-274, doi:10.1038/nature08905, 2010.

Tiedje, J. M.: Denitrifiers, *Methods of Soil Analysis: Part 2—Microbiological and Biochemical Properties*, 245-267, 1994.

Van de Graaf, A. A., Mulder, A., De Bruijn, P., Jetten, M. S. M., Robertson, L. A., and Kuenen, J. G.: Anaerobic oxidation of ammonium is a biologically mediated process, *Appl. Environ. Microbiol.*, 61, 1246-1251, 1995.

Van Hulle, S. W. H., Vandeweyer, H. J. P., Meesschaert, B. D., Vanrolleghem, P. A., Dejans, P., and Dumoulin, A.: Engineering aspects and practical application of autotrophic nitrogen removal from nitrogen rich streams, *Chem. Eng. J.*, 162, 1-20, doi:10.1016/j.cej.2010.05.037, 2010.

Weiss, R. F., and Price, B. A.: Nitrous oxide solubility in water and seawater, *Mar. Chem.*, 8, 347-359, 1980.

Weiss, R. F.: Determinations of carbon dioxide and methane by dual catalyst flame ionization chromatography and nitrous oxide by electron capture chromatography, *J. Chromatogr. Sci.*, 19, 611-616, 1981.

Wenk, C. B., Brees, J., Zopfi, J., Veronesi, M., Bourbonnais, A., Schubert, C. J., Niemann, H., and Lehmann, M. F.: Anaerobic ammonium oxidation (anammox) bacteria and sulfide-dependent denitrifiers coexist in the water column of a meromictic south-alpine lake, *Limnol. Oceanogr.*, 58, 1-12, doi:10.4319/lo.2013.58.1.0001, 2013.

Westermann, P., and Ahring, B. K.: Dynamics of methane production, sulfate reduction, and denitrification in a permanently waterlogged alder swamp, *Appl. Environ. Microbiol.*, 53, 2554-2559, 1987.

Westwood, D.: Ammonia in waters, in: *Methods for the examination of waters and associated materials*, HMSO, London, United Kingdom, 1981.

Whiticar, M. J., Faber, E., and Schoell, M.: Biogenic methane formation in marine and freshwater environments: CO<sub>2</sub> reduction vs. acetate fermentation—Isotope evidence, *Geochim. Cosmochim. Acta*, 50, 693-709, doi:10.1016/0016-7037(86)90346-7, 1986.

Winfrey, M., and Zeikus, J.: Microbial methanogenesis and acetate metabolism in a meromictic lake, *Appl. Environ. Microbiol.*, 37, 213-221, 1979.

Xiao, W., Liu, S., Li, H., Xiao, Q., Wang, W., Hu, Z., Hu, C., Gao, Y., Shen, J., Zhao, X., Zhang, M., and Lee, X.: A Flux-Gradient System for Simultaneous Measurement of the CH<sub>4</sub>, CO<sub>2</sub>, and H<sub>2</sub>O Fluxes at a Lake–Air Interface, *Environ. Sci. Technol.*, 48, 14490-14498, doi:10.1021/es5033713, 2014.

Yamamoto, S., Alcauskas, J. B., and Crozier, T. E.: Solubility of methane in distilled water and seawater, *J. Chem. Eng. Data*, 21, 78-80, doi:10.1021/je60068a029, 1976.

Yvon-Durocher, G., Allen, A. P., Bastviken, D., Conrad, R., Gudas, C., St-Pierre, A., Thanh-Duc, N., and del Giorgio, P. A.: Methane fluxes show consistent temperature dependence across microbial to ecosystem scales, *Nature*, 507, 488-491, doi:10.1038/nature13164, 2014.

Zhang, G. L., Zhang, J., Liu, S. M., Ren, J. L., and Zhao, Y. C.: Nitrous oxide in the Changjiang (Yangtze River) Estuary and its adjacent marine area: Riverine input, sediment release and atmospheric fluxes, *Biogeosciences*, 7, 3505-3516, doi:10.5194/bg-7-3505-2010, 2010.

Zigah, P. K., Oswald, K., Brand, A., Dinkel, C., Wehrli, B., and Schubert, C. J.: Methane oxidation pathways and associated methanotrophic communities in the water column of a tropical lake, *Limnol. Oceanogr.*, 60, 553-572, doi:10.1002/lno.10035, 2015.

Zindler, C., Bracher, A., Marandino, C. A., Taylor, B., Torrecilla, E., Kock, A., and Bange, H. W.: Sulphur compounds, methane, and phytoplankton: interactions along a north–south transit in the western Pacific Ocean, *Biogeosciences*, 10, 3297-3311, doi:10.5194/bg-10-3297-2013, 2013.

---

## List of publications (peer-reviewed)

---

- Roland F.A.E., F. Darchambeau, C. Morana, S. Bouillon & A.V. Borges (2017) Emission and oxidation of methane in a meromictic, eutrophic and temperate lake (Dendre, Belgium), *Chemosphere*, 168:756-764, DOI:10.1016/j.chemosphere.2016.10.138
- Roland F.A.E., F. Darchambeau, C. Morana & A.V. Borges (2016) Nitrous oxide and methane seasonal variability in the epilimnion of a large tropical meromictic lake (Lake Kivu, East-Africa), *Aquatic Sciences*, DOI:10.1007/s00027-016-0491-2
- Roland F.A.E., F. Darchambeau, A.V. Borges, L. De Brabandere, C. Morana, B. Thamdrup & S. Crowe (under review) Denitrification, anaerobic ammonium oxidation and dissimilatory nitrate reduction to ammonium in an East African Great Lake (Lake Kivu), *Limnology and Oceanography*
- Roland F.A.E., F. Darchambeau, C. Morana, S.A. Crowe, B. Thamdrup, J.-P. Descy & A.V. Borges (submitted) Anaerobic methane oxidation in an East African great lake (Lake Kivu), *Journal of Great Lakes Research*
- Roland F.A.E., F. Darchambeau, C. Morana, J.-P. Descy & A.V. Borges (submitted) Anaerobic methane oxidation in a ferruginous tropical lake (Kabuno Bay, East Africa), *Journal of Geophysical Research:Biogeosciences*
- Michiels C.C., F. Darchambeau, F.A.E. Roland, C. Morana, M. Llorós, T. Garcia-Armisen, B. Thamdrup, A.V. Borges, D.E. Canfield, P. Servais, J.-P. Descy & S.A. Crowe (2017) Fe-dependent N-cycling and the nutrient status of ferruginous seas, *Nature Geoscience*, in press
- Morana C., F.A.E. Roland, S.A. Crowe, M. Llorós, A.V. Borges, F. Darchambeau & S. Bouillon (2016) Chemoautotrophy and anoxygenic photosynthesis within the water column of a large meromictic tropical lake (Lake Kivu, East Africa), *Limnology and Oceanography*, DOI:10.1002/lno.10304
- Morana C., F. Darchambeau, F.A.E. Roland, A.V. Borges, F. Muvundja, Z. Kelemen, P. Masilya, J.-P. Descy & S. Bouillon (2015) Biogeochemistry of a large and deep tropical lake (Lake Kivu, East Africa) : insights from a stable isotope study covering an annual cycle, *Biogeosciences*, 12, 4953-4963, DOI:10.5194/bg-12-4953-2015
- Morana C., A.V. Borges, F.A.E. Roland, F. Darchambeau, J.-P. Descy & S. Bouillon (2015) Methanotrophy within the water column of a large meromictic tropical lake (Lake Kivu, East Africa), *Biogeosciences*, 12, 2077–2088, DOI:10.5194/bg-12-2077-2015

Université  
de Liège



Faculty of Sciences  
AGO Department  
Chemical Oceanography Unit

Quartier Agora - Allée du 6 Août, 19 - 4000 Liège – Belgium

Tel.: +32 4 366 3326

Email: [froland@ulg.ac.be](mailto:froland@ulg.ac.be)

<http://www.co2.ulg.ac.be/>